Stress Transfer, Stiffness Degradation and Transverse Cracking in Composite Laminates

By
Daxu Zhang

Submitted in accordance with the requirements for the degree of PhD
The University of Leeds, School of Civil Engineering
January 2007

The candidate confirms that the work submitted is his own and that appropriate credit has been given where reference has been made to the work of others.

To my parents and my wife Xiaoyan, with love and gratitude

Acknowledgements

First and foremost, I wish to thank my supervisor, Dr J. Ye, for his insights, encouragement and support throughout the course of my PhD. Without his invaluable advice, help and suggestions, this thesis would not be completed.

I am grateful to Dr D. Lam, Dr A. Sleigh and Dr J. Forth for their help and support. I would particularly like to thank Professor H.Y. Sheng, Hefei University of Technology, China, for his help and advice. I am also grateful to Dr. L.N. McCartney, National Physical Laboratory, for the provision of his unpublished results.

I would also like to thank the other research students in the School of Civil Engineering, for their help, friendship and lively discussions; in particular, Dr J. Yang, Dr F. Fu, Dr Y. Tan, Kiran Bhagate, Abigail Hathway, Helen Bailey, Shanmugam Palaniyandi, Miller Camargo Valero, Elly van der Linde, and Katherine Roberts.

Thanks are also due to the Postgraduate Student Secretaries of the School of Civil Engineering, Ms. D. Carr and Ms. C. Hitchen for their help and administrative assistance.

The research was funded by the Overseas Research Students Awards Scheme (ORSAS), the Tetley and Lupton Scholarship and Research Scholarships from School of Civil Engineering, to whom I address my gratitude for supporting my PhD study.

Abstract

In spite of their advantages, e.g. high strength, low weight, and high stiffness, composite laminates are prone to the formation of transverse cracking during both manufacture and service. It has been well recognised that the core to this damage mode is stress singularities near transverse cracks. In addition, transverse cracking may cause degradation in the thermoelastic properties of a laminate, and meanwhile new ply cracks usually form with the increase of applied loading. As a result, the stress transfer near transverse cracks, thermoelastic property degradation due to transverse cracking, and propagation of transverse cracks are all important issues in the analysis of composite laminates.

The major contribution of this work is to develop a new semi-analytical method, the state space method, to evaluate the stress transfer near free edges and transverse cracks. On the basis of the generalised plane strain condition, the method overcomes the limitation of analytical methods in study nonsymmetric laminates. Moreover the method guarantees continuous fields of interlaminar stresses across interfaces between layers, which is one of the obstacles for conventional finite element method.

Another contribution is to apply the stress analysis to assess the thermoelastic property degradation induced by transverse cracking in general cross-ply and symmetric angle-ply laminates. The prediction is made by using the constitutive equation of laminates in the Classical Laminate Theory. The numerical results of stiffness degradation for nonsymmetric cross-ply laminates are revealed for the first time in the literature.

The final contribution of this work is to apply the stress analysis to predict propagation of transverse cracking in general composite laminates. An energy-based cracking criterion is used to predict the crack multiplication process. The predictions for nonsymmetric laminates and the effects of shearing to transverse cracking are believed to be the first solutions in the literature.

Table of Contents

List of Figures

List of Tables

Chapter 1. Introduction

In this thesis, a systematic investigation on the stress distribution near free edges and transverse cracks, material property degradation induced by transverse cracking, and propagation of transverse cracking in composite laminates is presented. All these problems are long standing issues in the literature. Here, a novel method, the state space method, combined with composite mechanics and fracture mechanics, is used to tackle the complexity of the problems.

In this chapter, the motivation behind this research is introduced, in which the problems of free edge effect and transverse cracking are described. Then the research objectives are set corresponding to the existing problems. Contributions of this research are also stated, along with the application scope of the present study. Finally the layout of the work presented in this thesis is given.

1.1. Motivation behind This Research

Composite materials are broadly used in a variety of engineering fields, including aerospace, automotive, and civil engineering, as well as in electronic circuit boards, and sports equipment. Except the advantages such as low weight, high stiffness, high strength, low thermal expansion, corrosion resistance and retention of properties at high temperature, today laminated composites are often the choice of designers because they can be tailored to meet the specific demands of each particular application.

A composite laminate is a perfectly bonded assembly of individual plies of a unidirectional composite for which the fibres embedded in matrix are parallel in a direction that defines the orientation of the ply within the laminate. Fig. 1.1 shows a cross-ply laminate having separated individual plies (McCartney, 2001).

In spite of their many advantages, laminated composites are prone to the formation of damages when subjected to mechanical and thermal loading during both manufacture and service. It is widely recognised that free edge and internal delamination as well as

transverse ply cracking in composite laminates are the most commonly observed types of damage. An immediate effect of this damage is to cause a degradation of thermoelastic constants, such as changes in Young's modulus, Poisson's ratio and the thermal expansion coefficients. A secondary effect of these matrix dominated failure modes is that they nucleate other forms of damage, such as fibre pull out or fibre break, and provide pathways for moisture or other corrosive agents. Thus fully understanding the damage mechanism and its effect, and making the most use of composite laminates is the motivation behind the research work described in this thesis.

It has been well recognised that the core to understand the damage mechanism is stress transfer near material discontinuities in composite laminates. Both free edge and transverse cracks are material discontinuities where stress singularities usually exist. Therefore it is a prerequisite to understand the stress characteristics near these zones. In the following part, brief background descriptions are given about free edge effects and transverse cracking.

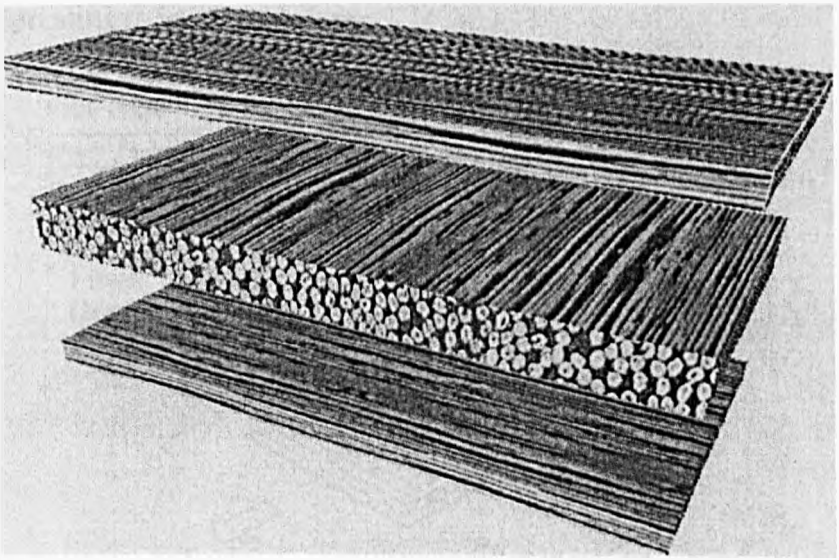

Fig. 1.1 Computer image of the structure of a cross-ply laminate

1.1.1. Free Edge

A typical composite laminate with free edges is shown in Fig. 1.2 (Pipes and Pagano, 1970). It has the form of a tensile coupon of thickness h and width L and lies within the x-y plane of the Cartesian x-y-z coordinate system. Due to the mismatch of material properties of bonded adjacent layers and the presence of gradients in the in-

plane stresses, uniaxial tension in the y-direction may give rise to high localised interlaminar stresses σ_{zz}, σ_{xz} and σ_{yz}. Then the plane stress assumption used in the Classical Laminate Theory (CLT) is no longer valid. The stress state is three dimensional, in order to satisfy the traction free boundary conditions (Becker, 1993). Interlaminar normal and shear stresses, σ_{zz}, σ_{xz} and σ_{yz}, some of which exhibit singular behaviour, are present in a boundary layer region along the free edges of composite laminates.

Interlaminar stresses not only exit in anisotropic materials, but may be present in any layered material with free edges. For isotropic layers made of the same material, there is no mismatch in material properties and interlaminar stresses are ignored in most applications. In contrast to isotropic materials, composite laminae exhibit a very broad range of properties as a function of fibre orientation. The mismatch in Poisson's ratios, shear coupling coefficients, and thermal expansion coefficients can lead to very large interlaminar stresses. These interlaminar stresses are of critical concern to designers because they can lead to delamination type failures at loads well below those corresponding to in-plane failure.

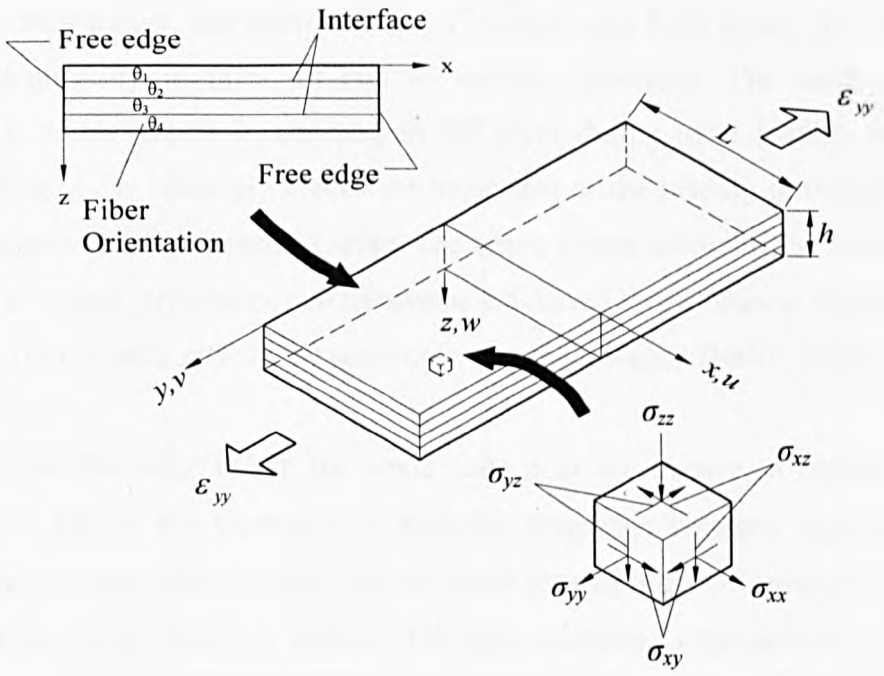

Fig. 1.2 Nomenclature of a finite width laminated coupon under an axial tension

Interlaminar stresses near free edges can be controlled to some extent through the choice of materials, fibre orientations, stacking sequence and layer thickness.

However, they can be eliminated totally only through the use of homogeneous materials. They must be considered whenever laminated composite materials are used in the design of a structure which has free edges. They are present at all free edges of laminated composites including holes and cutouts (Herakovich, 1989). A full understanding of the mechanism of the free edge effect is essential for a safe and reliable design.

1.1.2. Transverse Cracking

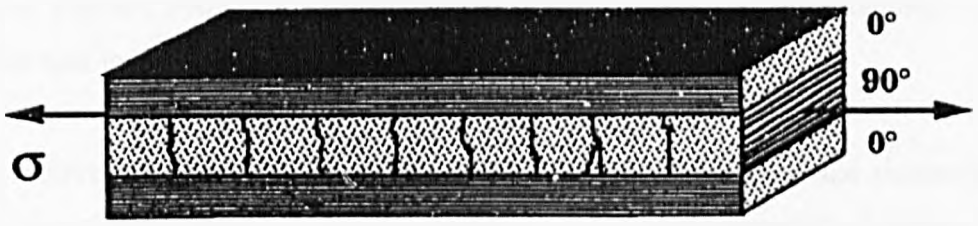

Fig. 1.3 A symmetric [0°/90°/0°] laminate with transverse cracks in 90° ply

The first form of damage in composite laminates is usually matrix cracking, which are intralaminar or ply cracks that traverse the thickness of the ply and run parallel to the fibres in that ply. Ply cracks can be observed during tensile loading, fatigue loading, changes in temperature, and thermocycling. Ply cracks can form in any plies, but they form predominantly in plies off-axis to loading directions. The most common observation of ply cracks is cracking in 90^{o} plies during axial loading in the 0^{o} direction (Fig. 1.3). These ply cracks are transverse to the loading direction and are thus sometimes called transverse cracks. The terms matrix microcracks, microcracks, intralaminar cracks, ply cracks, and transverse cracks are found often in the composite literature. They usually refer to the same cracking phenomenon (Nairn, 2000).

Similar to the free edge effect, the stress state near the transverse cracks is three dimensional due to the mismatch of material properties between layers and the interlaminar stresses often exhibit singular behaviour in order to satisfy the traction free condition along the crack surface. The stress transfer is redistributed when the laminate was damaged. The loads that such plies were carrying, when the laminate was undamaged, are transferred to neighbouring plies.

Transverse cracking in composites generally does not lead directly to failure. For all laminates, there are no transverse cracks until approaching certain onset stress or strain that corresponds to the initiation of transverse cracking. After the initial matrix crack, the crack density typically increases very rapidly. At high crack density, the transverse cracking slows down and approaches a saturation damage state. The fibres and adjacent plies serve as obstructions to crack propagation, preventing a dominant crack from forming as in monolithic materials. It can, however, facilitate other damage modes. For example, transverse cracks can induce delamination, cause fibre break or provide pathways for the entry of corrosive liquids. Such damage modes could in turn lead to laminate failure.

More importantly, transverse cracking may cause degradation in the thermoelastic properties of the laminate including changes in all effective moduli, Poisson ratios, and thermal expansion coefficients. The structure will subsequently respond differently to future loads. If a given design cannot tolerate ply cracking induced degradation in properties, then the formation of ply cracks constitutes failure of the design.

As a result the stress transfer at the transverse cracks, the effects they have on laminate properties, and the processes by which they form and develop are all important problems in the analysis of failure of composite laminates.

1.2. Objectives of This Research

The general objective of this research is to develop an analytical methodology to study the effects of the free edge and transverse cracking in composite laminates. The specific objectives chosen for investigation in this research are:

- To develop a new analytical model to investigate the stress transfer near free edges and transverse cracks in composite laminates under both mechanical and thermal loading;

- To apply the stress analysis to assess the degradation of the thermoelastic properties due to transverse cracking; and

- To apply the stress analysis to predict the propagation of transverse cracking in composite laminates, considering the residual thermal stresses.

The purpose of the stress analysis is to seek interlaminar stress solutions with high accuracy. To this end, a novel method, the state space method, is derived in both cross-ply and angle-ply laminates. On the basis of these stress solutions, the effective thermoelastic constants of a cracked laminate, which are functions of the crack density, are predicted using the constitutive equation in the Classical Laminate Theory (CLT). Furthermore, the stress solutions, combined with an energy theory, are employed to predict the development of transverse cracking in laminates, taking account of the thermal residual stresses induced in manufacture. The applications of the methodology are shown by numerical examples and are compared with numerical results from other models and experimental data in the literature.

The stress transfer model is developed under the generalised plane strain condition. It is reasonable for the present analysis to make such a hypothesis. An important application of the theoretical analysis is to simulate actual material property tests, where most test specimens are designed to subject to a very simple stress state, e.g. plane strain or plane stress condition. An accurate theoretical or numerical simulation can be used to replace these expensive tests and establish a 'virtual' laboratory.

1.3. Contributions of This Research

The major contribution of this research focuses on the area of computational modelling that is specifically applicable to the damaged composite laminates. These include:

- Successful application of the state space method to evaluate interlaminar stress singularities near free edges and transverse cracks in general composite laminates, subjected to both mechanical and thermal loading. This method overcomes the limitation of analytical methods in study nonsymmetric laminates and guarantees continuous fields of interlaminar stresses across interfaces between layers, which are obstacles for conventional finite element method (FEM);

- Successful assessment of the thermoelastic property degradation induced by transverse cracking in general cross-ply and symmetric angle-ply laminates. The prediction is made by using the constitutive equation of laminates in the Classical Laminate Theory in conjunction with the stress analysis; and

- Successful prediction of transverse cracking propagation in general composite laminates, considering the residual thermal stresses and the effects of shearing. An energy-based cracking criterion and the energy release rate due to transverse cracking are used to predict the crack multiplication process.

Under the generalised plane strain condition, the numerical results of interlaminar stress distribution, thermoelastic property degradation and transverse cracking propagation in nonsymmetric laminates are revealed for the first time in the literature.

1.4. Layout of This Thesis

The rest of this thesis is organized as follows:

Chapter 2 presents a literature review on the investigations of two types of material discontinuities in composite materials, i.e. free edges and transverse cracks. For the free edge effects, published work was focused on evaluating the interlaminar stress singularities in the vicinity of free edges. For transverse cracking problem, the issues about stress transfer, property degradation and transverse crack propagation are extensively reviewed. The stress transfer is a fundamental concern to understand the damage mechanism in composite laminates. In most circumstances, the predictions of property degradation and cracking propagation are based on the stress transfer in cracked laminates.

Chapter 3 describes the basics of approaches and theories that are required for the current work. First the concept of state space and solutions of state variable equations or state equations are briefly introduced. Then equilibrium equations and stress-strain relationships of an anisotropic material under the generalised plane strain deformation are presented. After that the effective thermoelastic constants of composite laminates are derived on the basis of the Classical Laminate Theory (CLT) and the coupling features of anisotropic materials are explained through stiffness matrices. At last the

concepts and expressions of some most pertinent principles in Fracture Mechanics are discussed and derived.

Chapter 4 develops a semi-analytical method, the state space method, to evaluate the interlaminar stress singularities near free edges and transverse cracks in general cross-ply laminates. The method is based on a state space representation of the three-dimensional equations of elasticity that is applied to a generalised plane strain condition. Numerical solutions are obtained using layer refinement in the through thickness direction and Fourier series expansion in an in-plane direction. Unlike some other solutions, no major assumptions are introduced prior to the solution derivation and it takes account of all the stress components and independent material constants. Furthermore the method always guarantees continuous distributions of both displacements and interlaminar stresses across interfaces between layers. Another significant feature is that by this approach, a laminate may be composed of an arbitrary number of orthotropic layers, each of which may have different material property and thickness.

Chapter 5 extends the state space method, which has been successfully used in cross-ply laminates, to a more sophisticated one, which is capable of investigating stress transfer in general angle-ply laminates. Once again, a generalised plane strain deformation is assumed. Because the extension-shear coupling exists in the angle-ply laminates, the stress components σ_{yz} and σ_{xy} do not vanish and therefore have to be considered in the state space equations. The challenge of the new model is to find suitable displacement expressions and in-plane Fourier series expansions for all state variables, which must satisfy the boundary conditions and could be eliminated during further derivations. These difficulties are overcome by introducing new state variables associated with appropriate expressions. Comparisons with other available results are carried out to validate the present predictions. To the best of the author's knowledge, the present solutions for nonsymmetric laminates under an axial strain and for laminates under in plane shearing are revealed for the first time in the literature and can be used as benchmarks for validating new models. In fact, since the state space method for angle-ply laminates is posed in general terms it includes the state space method for cross-ply laminates as one of its particular forms.

Chapter 6 applies the stress analysis to access the thermoelastic property degradation due to transverse cracking in cross-ply and symmetric angle-ply laminates. The relationships of the overall deformation and the applied loading in cracked laminates are assumed to follow the same constitutive equations of undamaged laminates in the Classical Laminate Theory. This is a process to homogenise the effective properties of a cracked laminate into the equivalent properties of an undamaged homogeneous plate. In term of the coupling characteristics, the effective thermoelastic properties of selected laminates are defined by their corresponding compliance matrices. The compliance coefficients of selected laminates are determined by the stress analysis of specially designed loading cases. Numerical results are presented and are validated by other results and experimental data. Since there are no available results in the literature, the stiffness degradations in nonsymmetric cross-ply laminates are compared with McCartney's prediction through Dr Ye's research collaboration.

Chapter 7 applies the stress analysis to predict the propagation of transverse cracking by using an energy-based method. The energy release rate due to transverse cracking is derived by assuming that the crack density increases uniformly. Then the critical energy release rate is introduced to predict the new crack formation. Numerical examples are presented in both symmetric and nonsymmetric laminates under tension. In addition, the transverse cracking in laminates under a combination of tension and shearing is also studied. Since there are no published results in nonsymmetric laminates to date, comparisons are only made in symmetric layups with those of other models and experimental data.

Chapter 8 summaries the overall achievements in this thesis, draws some conclusions and finally suggests ideas for continued and future investigation.

Chapter 2. Literature Review

Some fundamental knowledge of free edge effect and transverse cracking in composite laminates has been briefly outlined in the previous chapter. A common feature of free edge and transverse cracking problems is that they both involve in investigating the singular stress field which is a basis to predict property degradation and cracking propagation. The research history of free edge effect and transverse cracking began in the 1970s and a variety of models have been developed. In this chapter, a review is made on the estimation of interlaminar stresses near free edge, the stress transfer near transverse cracks, the property degradation due to transverse cracking, and the transverse crack propagation in composite laminates.

2.1. Free Edge Effect in Composite Laminates

It is a well-established fact that at free edges of composite laminates, interlaminar stresses arise due to a mismatch in elastic properties between plies. Thus in this region near the free edge known as boundary layer, it has been shown that the state of stress is three-dimensional in nature and not predictable accurately by the Classical Laminate Theory (CLT). Over the past 30 years, numerous investigators have used a variety of methods to attempt to evaluate the stresses at straight free edges. These include analytical, numerical and semi-analytical methods.

2.1.1. Analytical Methods

The existence of interlaminar stresses in a boundary layer region along free edges of laminated materials has been known for more than three decades. The first publication (Puppo and Evensen, 1970) dealing with anisotropic materials appears to be a study of anisotropic layers separated by isotropic shear layers with interlaminar normal stress being neglected throughout the laminate. Other methods were also attempted to examine the problem, including approximate elasticity solution, higher order plate theory, boundary layer theory, and variational method.

2.1.1.1. Approximate Elasticity Solution

Pagano and Pipes (1971; 1973) introduced some simple approximation equations to explain the occurrence of interlaminar normal stresses in the vicinity of free edges of a tensile coupon and conducted some basic considerations toward optimum lay-ups. Pipes and Pagano (1974) investigated symmetric angle-ply laminates under uniaxial tension by approximating the displacement field with Fourier series expansions. Convergence investigations showed that a high number of series terms were needed to reach some accuracy of the results.

Hsu and Herakovich (1977) investigated free edge effects by assuming edge displacement fields in the form of trigonometric and exponential terms. Comparison with the results of other authors nevertheless showed some discrepancies (Mittelstedt and Becker, 2004).

In most methods the laminate is assumed to be sufficiently long (Fig. 1.2). Hence, due to Saint-Venant's principle, the influence of the loading point on other remote region is negligible. Within the premise of Saint-Venant's principle, Wang and Crossman (1978) presented a simplified method for calculating interlaminar stresses accomplished by smearing two or more laminae as a quasi-homogeneous lamina.

Wang and Choi (1982b; 1982a) used the Lekhnitskii's (1963) stress potential and the theory of anisotropic elasticity and were able to determine the order of stress singularities at the laminate free edges. The eigenfunction method developed by them involves the solution of a complicated and tedious eigenvalue problem and requires the use of a collocation technique at every ply interface in order to satisfy traction continuity. This limits the application of this technique to relatively thin laminate.

Valisetty and Rehfield (1985) introduced a simple methodology for the assessment of displacements and stresses in a four-ply symmetric $[0°/90°]_s$ laminate by considering layerwise equilibrium in connection with adequate kinematical assumptions, Hooke's law and the corresponding boundary and continuity conditions. Even though easily

applicable and of a reasonable accuracy, their method is within a very limited range of applicability.

2.1.1.2. Higher Order Plate Theory

Pagano (1974) employed a higher-order plate theory for estimation of transverse normal stress in a symmetric, finite-width, composite laminate subjected to an axial extension. This theory is a reasonable approach to compute the thickness distribution of transverse normal stresses. This, however, does not seem to guarantee that the edge tractions on each layer satisfy the boundary conditions.

Krishna Murty and Hari Kumar (1989) used a higher-order theory approach and modelled the laminate as an equivalent single layer by assuming polynomials through the complete laminate thickness. The method yielded stress functions in the form of trigonometric and hyperbolic terms which were in satisfactory accord with the results of other authors. Nevertheless, one major drawback of equivalent single layer approaches in general is the occurrence of discontinuous interlaminar stresses in the interfaces as long as these are computed by constitutive equations, since the assumed displacement formulations are priori defined over the complete laminate thickness (Mittelstedt and Becker, 2004).

Becker (1993; 1994) utilised a new higher order plate theory to solve the free edge problem. The model assumed a particular warp deformation mode that is induced by the free edge effect and decays rapidly towards the laminate interior. The whole analysis is easy to apply, requires minimal computational effort, and allows interlaminar stress parameter studies to be carried out simply by changing constants in the closed form relations. However the applications are only limited to symmetric laminates.

Using the first-order shear deformation theory (FSDT) of plates and a layerwise theory, Nosier and Bahrami (2006) developed analytical solutions to the free edge problem of an antisymmetric angle-ply laminate subjected to arbitrary combinations of extensional and torisonal loads. The displacement components consist of two parts: a global part and a local part. The unknown constants appearing in the global

part of the displacement field may be determined accurately from an analysis based on the FSDT. The unknown functions appearing in the local part, on the other hand, are determined from an analysis based on a layerwise theory. The advantage of the higher-order plate theory is that it can be easily applied in antisymmetric angle-ply laminates under various loading conditions, but it's very difficult for this theory to satisfy the traction free conditions at free edges.

2.1.1.3. Boundary Layer Theory

The boundary layer theory of plane stress in isotropic elasticity is extended to the laminated composites by Tang (1975) and Tang and Levy (1975). In the boundary layer region, equations are separated into two problems, i.e. torsion problem and plane strain problem. This technique provides a tool to predict all the three interlaminar stresses.

A boundary model to study the stress concentration phenomenon in the vicinity of a free edge of a laminated composite plate is suggested by Davet and Destuynder (1986). This model allows the use of an explicit formula for the transverse shear stress. The description of the singular behaviour for a plate under inplane loading is emphasised.

Lin et al. (1995) used boundary layer theory in conjunction with the method proposed by Kassapoglou and Lagace (1986; 1987) to calculate interlaminar stress distribution near the straight free edges of generally stacked laminates. All the boundary conditions for each ply and the interface traction continuity were exactly satisfied. The laminate was subdivided into interior region and boundary layer region and each stress component is determined by superposition of the interior stress and boundary layer stress. Unfortunately the numerical results of interlaminar stresses along interfaces were only given in symmetric laminates.

2.1.1.4. Variational Method

Based on assumed in-plane stresses and the use of Reissner's variational principle, Pagano (1978a; 1978b) developed an approximate theory. The only assumption required is that regarding the stresses themselves. Information concerning

displacements is a consequence of the procedure and does not require any a prior assumption. The fact that the procedure contains a built-in method to assess and regulate the quality of the approximation, by increasing the number of imaginary layers, implies a very widespread range of application as the author and other researchers demonstrated in subsequent work.

Global modes, which follow from an assumed displacement field and lead to the definition of effective (or smeared) laminate moduli, are not sufficiently accurate for stress field computation. On the other hand, local models, in which each layer is represented as a homogeneous anisotropic continuum, become intractable as the number of layers becomes even moderately large. Pagano and Soni (1983) blended these concepts into a self-consistent model which can define detailed response functions in a region of interest (local), while representing the remainder of the domain by effective properties (global). In this investigation the laminate thickness is divided into two parts. A variational principle has been used to derive the governing equations of equilibrium. For the global region of the laminate, potential energy has been utilised, while the Reissner functional has been used for the local region. The field equations are based upon an assumed thickness distribution of stress components within each layer of the local region and displacement components in the global region.

Kassapoglou and Lagace (1986; 1987) released some leading works on the analysis of free edge stresses. The Kassapoglou and Lagace (KL) solution assumed that the stresses consist of layerwise products of in-plane exponential terms and polynomials through the thickness. The thickness terms were adjusted such that they blend into CLT in the inner laminate regions and that continuity of all interlaminar stresses in the laminate interfaces is warranted. Also, the conditions for stress free laminate facings as well as traction-free edges were met exactly. Free parameters in the in-plane stress approaches were then finally determined by minimisation of the total laminate complementary potential. Since the KL solution was something of a success due to its simplicity yet its good performance even for thick laminates, it was used and refined by several other authors. Introducing the thermoelastic stress strain relations into the KL solution, Webber and Mortan (1993) presented a variational method to determine the free edge stresses due to thermal effects. Additional terms

for the consideration of the discontinuous change of the elastic material properties in the interfaces were introduced by Rose and Herakovich (1993). The additional terms took into account the local mismatches in Poisson's ratio and coefficient of mutual influence between adjacent layers. Amrutharaj et al. (1996) used a modified KL solution to predict the edge delamination of a symmetric angle-ply tension coupon laminate.

Kim and Atluri (1994) developed an approximate method based on equilibrium equations and used the principle of minimum complimentary energy to investigate the interlaminar stresses near straight free edges of beam-type laminated composite structures under out-of-plane shear/bending. The analysis includes longitudinal degrees-of-freedom in the stress distribution. The unknowns in the resulting stress expressions are obtained by solving an eigenvalue problem whose coefficients are not constants but depend on the shear loading location. The stress component is assumed to consist of two parts, namely, the far-field stress and the companion stress. By definition, only the far-field stresses exist in the central region of the laminate away from the free edge. This hypothesis not only adds much complexity to the formulation but unfortunately yields approximately results, although the stress equilibrium, compatibility and all of the boundary conditions are satisfied.

Yin (1994a; 1994b) proposed an approximate analytical method, based on the variational principle of complimentary virtual work and using polynomial stress functions in each layer. The method involved in solving an eigenvalue problem for the interfacial values of the stress functions. Later Yin (1994c) presented simple solutions containing exponential functions to approximate the stress functions. The method, though not as rigorous and accurate as the previous eigenvalue solution, was applicable to free edge problems involving non-linear elastic materials behavior. Yin (1997) further extended the eigenfunction method and applied to thermal stress problems associated with the non-uniform temperature loads.

Flanagan (1994) presented a variational method, based on expanding stress functions in terms of a harmonic series in the thickness direction and using the principle of minimum complementary energy. The merit of this method is relatively simple and

efficient from an engineering viewpoint, but the in-plane stresses are discontinuous through the thickness direction.

Zhang and Yeh (1998) used stress functions and a variational approach to the free edge effect in symmetric laminates under mechanical and thermal load. The introduced stress functions satisfied equilibrium as well as all given boundary and continuity conditions and consisted of thickness terms in the form of polynomials multiplied with unknown in-plane functions. The governing Euler–Lagrange equations for the unknown functions were derived by imposing the principle of minimum complementary potential.

Cho and Yoon (1999), Kim et al. (2000) and Cho and Kim (2000) carried out a series of studies on free edge interlaminar stress and free edge strength using an extended Kantorovich method. The Lekhnitskii stress functions are adopted to divide interlaminar stress expressions into the in-plane and out-of-plane coordinate functions. Under the principle of complementary minimum energy through eigenproblem, the in-plane and out-of-plane stress functions are improved through the iterative extended Kantorovich method. The approach is capable of considering combined mechanical loads (extension, bending and twisting) and residual thermal loads with the limitation to symmetric lay-up configurations. Cho and Rhee (2004) combined the iterative stress based method and genetic algorithms to study the strength of free edges and optimise lay-up.

Based in part on Yin's (1994a; 1994b) implementation of the minimum complementary energy principle, Suvorov and Dvorak (2001) described an analytical procedure for evaluation of the effect of release of fibre prestress, applied prior to matrix consolidation, on stress distribution in individual plies and at free edges of composite laminates. Specific results are found for cross-ply and quasi-isotropic symmetric laminates under tension.

Inspired by Pagano's (1978b) variational method, Carreira et al. (2002) developed a model, called multiparticle models of multilayered materials (M4), to evaluate the stress state in the vicinity of a free edge or microcracks in symmetric laminates. Multiparticle models are a family of models. E.g. M4_2n+1 considers the laminate as

a membranar superposition (2n equations plus a global one, with n being the number of plies in the laminate). Resultant forces in each layer as well as interlaminar shear stresses are taken into account, yet resultant moment in the layer is not. Diaz Diaz et al. (2002) applied the M4 model into software called DEILAM and took account of the inelastic strain fields in the layers and fields of displacement discontinuities at the interfaces.

2.1.2. Numerical Methods

A common feature of all analytical methods is that they can only be used for the simple geometric cases, since for thick realistic structural laminates the solution to the full 3D problem is extremely complex. Thus a variety of numerical methods have been developed to calculate these interlaminar stresses at straight free edges. In general, these numerical methods can be divided into the finite difference method and the finite element method (FEM). Concerning the FEM, it can be sort into conventional FEM (standard displacement based elements), special purpose FEM (considering singular stresses or stress continuity) and global/local FEM.

2.1.2.1. Finite Difference Method

The first complete three-dimensional analysis of interlaminar stresses in fibrous composites involved the application of finite difference techniques to the governing elasticity equations (Pipes and Pagano, 1970). They obtained solutions to the problem of a finite width laminated coupon under tensile axial load (see Fig. 1.2). Their results showed the existence of interlaminar stresses in a boundary layer region along the free edge of the coupon. Results were presented for a variety of fibre orientations and laminate stacking sequences. It was shown that the width of the boundary layer is approximately equal to the thickness of the laminate, that the interlaminar normal stress σ_{zz} and the interlaminar shear stress σ_{xz} can exhibit singular behavior at the intersection of the layer interfaces with the free edge, and that the sign and magnitude of the interlaminar stresses are functions of the laminate configuration: material, fibre orientations, layer thickness and order of stacking (Herakovich, 1989). However since they used a relatively coarse mesh in the finite difference method, the exact nature of the stress singularities at the free edges could not be ascertained.

Following the approach used by Pipes and Pagano (1970) the interlaminar stress distribution in a four layer composite laminate in bending was studied by Salamon (1978). He predicted that the magnitudes of the interlaminar normal and shear stresses, although in general relatively small, rise sharply near the free edges. This distinguishing feature was observed over a boundary region of the order of one laminate thickness inward from the free edge (Kant and Swaminathan, 2000).

Later Altus et al. (1980) presented a 3D finite difference solution for the free edge effects in angle-ply laminates. It was shown that the 3D finite difference method gave improved results as compared to 2D analytical or numerical methods used earlier. They were able to conclude that the peeling stress σ_{zz} and the longitudinal stress σ_{xx} have a dominant effect on interlaminar failure characteristics (Kant and Swaminathan, 2000).

Bauld et al. (1985) drew comparisons between the finite element method and the finite difference method by investigating several stress concentration phenomena and concluded that both methods are essentially comparable in accuracy, yet in the direct vicinity of stress singularities the application of both methods needs refinement of the applied numerical mesh densities and are cautious interpretation of the results.

Bhaskar et al. (2000) developed an approximate three-dimensional elasticity solution based on the finite difference technique for the expansion of a circular cylindrical shell of finite length, free at its ends, and subjected to an axisymmetric, uniformly distributed radial load on the inner surface. The disadvantage of Bhaskar's finite difference method is that it does not satisfy traction free condition at the free edges, although the interlaminar stress values agree very closely with those of a plate under uniform axial extension.

2.1.2.2. Conventional Finite Element Method

Due to the singular nature of stress state near free edges, the finite element methods with standard displacement-based elements require a refined meshing strategy, whereas the element mesh may be coarse in the inner regions where CLT holds true.

An early numerical investigation was released by Isakson and Levy (1971). They modeled the problem of an isotropic shear layer in the absence of interlaminar normal stresses. It was recognised that the tensile coupon problem could be formulated as a two-dimensional finite element problem because of the independence of the stress and strain states on the axial coordinate. Initially, cross-ply laminates were studied with two-dimensional finite elements (Herakovich, 1976). It was then recognised that general laminates could also be analysed using two-dimensional finite element models. Subsequently, many results have been published using the finite element technique. In addition to those of Herakovich and co-authors (Herakovich and Bargner, 1980; Herakovich *et al.*, 1979; Herakovich and O'Brien, 1979) Wang and Crossman (1977) used the same formulation as Herakovich et al., but with a finer finite element mesh. The finer mesh provided more detail in the neighborhood of the singularity. Whitcomb et al. (1982) dedicated their work to the convergence characteristics of the displacement-based FEM in the presence of singular stress fields and pronounced the need for mesh refinements in such regions. Bauld et al. (1985) examined the convergence behaviour of the finite element method in the presence of stress singularities.

Wanthal and Yang (1991) developed three finite elements for the analysis of thick laminates where the effect of transverse shear deformation was very severe. The first layer quadrilateral element (LQ1) has 16 nodes of 40 degrees of freedom (dof) with zero transverse normal strain and constant transverse shear strain. The second layer quadrilateral element (LQ2) is of 16 nodes with 48 dof and allows for a constant transverse normal strain. One of the two terms in the expression for transverse shear strain is allowed to vary linearly through the thickness. The third layer quadrilateral element (LQ3) is of 24 nodes with 64 dof and improves upon the LQ2 element by allowing both terms in the transverse shear displacement expression to vary linearly through the layer thickness. Later Yang and He (1994) used the LQ3 element for the analysis of free edge stresses in cross-ply and angle-ply laminate.

Icardi and Bertetto (1995) studied the stress singularity at the free edge interface and at corners of laminated plates using a 20 node quadratic interpolation, isoparametric brick element and a 15 node quadratic interpolation singular wedge element

generated from the 20 node brick element. The nodal parameters assumed for both elements are the three displacement components u, v, w in the x, y, z directions. A predictor corrector procedure is used to fulfill the stress contact and traction free condition. The effect of material properties and layer orientations, the slope of inclined edges and corner angles were studied.

Three-dimensional 20-node quadratic brick elements were used by Lessard et al. (1996) to analyse the free edge effect in a symmetric cross-ply laminate. A new mesh technique, named 'slice model', allows for a higher number of elements near the anticipated stress singularity regions, therefore providing higher stress magnitudes at the edge. Property degradation is possible since the slice model has the ability to change the materials properties in all directions independent of one another.

2.1.2.3. Special Purpose Finite Element Method

Because most previous finite element methods only applied approximate satisfactions of the traction free boundary conditions. Spilker and Chou (1980) presented a special purpose hybrid stress multilayer finite element in which the traction free conditions are satisfied exactly. Chen and Huang (1989) developed a new hybrid stress finite element by modifying and reformulating Spilker and Chou's (1980) model. The hybrid-stress finite element method is characterised by an assumed stress field in the element and an assumed displacement field along the interelement boundary.

Kim and Hong (1991) used a 16 node, 48 dof curved isoparametric element without a midside node in the thickness direction. They used the substructure technique and analysed a laminate with and without hole. The effect of laminate thickness and stacking sequence on the interlaminar stress near the free edges in the case of a solid laminate and near the hole boundary in the case of a laminate with a hole were studied (Kant and Swaminathan, 2000).

On the basis of Pipes and Pagano (1970)'s displacement field for laminates under a generalised plane deformation state and Schapery (1969)'s nonlinear viscoelasic constitutive relations, Yi (1997) developed a finite element procedure for the analysis

of non-linear viscoelastic interlaminar stresses in composite laminates subjected to arbitrary combinations of axial extension, bending, and twisting loads. Yi et al. (1998) also applied this method to study the interlaminar stresses in nonsymmetrical laminated composites due to axial strain and bending.

Gaudenzi et al. (1998) proposed a multi-layer higher-order finite element technique to overcome the limits of the single-layer theories that shows discontinuities of the stress field at the interfaces. The method is demonstrated to be simple and effective both for the analysis of in-plane and through thickness distributions of interlaminar stress components.

Nguyen and Caron (2006) presented a finite element model based on the Multiparticle Model of Multilayered Materials (M4) (Carreira *et al.*, 2002) to evaluate the interlaminar stresses in symmetric laminates. An eight-node isoparametric quadrilateral element with $5n$ dof at each nodal point is formulated (n is the layer's number of the laminate). The interlaminar stresses are given directly in a straight forward manner using constitutive equations without postprocessing works.

2.1.2.4. Global/local Finite Element Method

The initial approach adopted to analyse composite laminates of finite size subjected to external loads was of a 2D finite element method. Though the 2D elements can yield accurate results at locations away from the traction free edges and discontinuities, it cannot predict accurately the complex stress state near any geometric or material discontinuities or near a traction free edge. As limitations of the 2D technique became known and more powerful computers became available, 3D finite elements were used to estimate interlaminar stresses in the critical regions of laminates. However, when the number of laminae is large, the need to have sufficient elements in the through-thickness direction combined with the undesirability of using finite elements with high aspect ratios leads to requiring many elements. Hence the analysis results in a large sparse system of equations, which requires a vast amount of computer storage space and thus makes 3D finite element modeling impracticable and possibly formidable. In view of the above facts many investigators attempted global/local finite element analysis (Hirai *et al.*, 1984; Mao

and Sun, 1991; Whitcomb and Woo, 1993a, b) that perform separate analyses on the global and local region. Thomson and Griffin (1990) extended the same approach and proposed a 2D-3D global/local finite element analysis. They subdivided the entire laminate into local and global regions, the local region being the traction free edges, and the area around geometric or material discontinuities and the global region is located far away from local region. They used a simplified 2D finite element analysis on a global region and a more detailed 3D finite element analysis on a local region.

Although the global/local finite element analysis was demonstrated to yield reasonably economical solutions by achieving considerable savings in computer time and storage, the stresses derived from the displacements by using the stress-strain relationship lead to a stress field that is usually discontinuous across element boundaries, because conventional finite element analysis is based on the approximation of displacements that only guarantees the continuity of all displacement components across the element boundaries. This discontinuity can lead to inaccurate prediction of failure load and failure mode.

2.1.3. Semi-analytical Methods

Although finite element method is probably one of the most universal methods that can be applied to problems involving any cross section and lamination profile, it still requires much computation time and quite often it cannot predict accurately stress fields for free edge analysis of multi-layered laminates. Most analytical methods also are confined the applications to study laminates having regular cross sections. Consequently some semi-analytical approaches were proposed combining a certain analytical technique with FEM or a layerwise laminate theory.

In the context of Saint-Venant's principle Dong and Goetschel (1982) used a semi-analytical method, combining the finite element interpolations over the thickness with exponential decay into the plate's interior, to model the behavior of a laminate plate composed of an arbitrary number of bonded, elastic, anisotropic layers.

The state space approach was used by Wang et al. (2000) to solve problems

involving stress decay in composite laminates due to edge boundary effects. The stress and displacement distribution was defined as a linear combination of the interior stress field and the eigenstress field. The interior stress field was determined by the Classical Laminate Theory. The solution of the eigenstress field was involved in employing the state space method and principle of virtual work. A numerical layerwise method is used to ensure a good satisfaction of the edge boundary conditions. The numerical results revealed the stress singularity near free edges, however the exact nature of the singularity could not be determined numerically in their work since the interlaminar shear stress was still present. The decay rate of edge effects was also investigated by Ye (2001a; 2001b) using the state space method for cross-ply and angle-ply laminated composite cylinders with free edges.

Ye and Sheng (2003) presented a semi-analytical method, which extended the state space method that has been successfully used in analyses of laminates subjected to various load and boundary conditions without considering stress singularities (Soldatos and Hadjigeorgiou, 1990; Ye and Soldatos, 1994a, b, 1995, 1996; Ye and Soldatos, 1997; Ye, 2002), to evaluate free edge stresses in cross-ply laminated cylinders subjected to axisymmetrically distributed transverse loads. Zhang et al. (2006b) also applied this method to investigate the free edge effect in cross-ply laminated composite plates. The method was based on a state space representation (in the form of matrix differential equation) of the three-dimensional equations of an orthotropic elastic plate. The displacements and interlaminar stresses were taken as the primary state variables. The interfacial continuity conditions are satisfied by using a transfer matrix that transmits the state variables from the top to the bottom layer. Numerical solutions were obtained using a layerwise refinement technique and in-plane Fourier series expansion. Compared to Wang et al. (2000)'s results, herein the traction free boundary conditions were fully satisfied by all stress components.

A state space finite element method that combines the traditional finite element approximation and the recursive formulation of state space equation (Soldatos and Hadjigeorgiou, 1990; Fan and Ye, 1990a, b; Ye, 2002) is proposed to evaluate the stress singularities in the vicinity of free edges or localised traction free surfaces by Ye et al. (2004). By using the method, a plate is divided into finite elements in the plane of the plate, while the through thickness distributions of the displacements and

stresses are solved directly from the state space equation. Due to the use of the standard finite element procedure in the proposed analysis, it is expected that there will be a straightforward extension to apply the method to, e.g., laminated plates with nonrectangular boundaries and plate assemblies, etc.

Tahani and Nosier (2003a; 2003b; 2003c) used a layer wise continuous displacement based approach with linear interpolation between the displacement functions in the interfaces of cross-ply laminates under uniform axial extension, thermal loading, and bi-directional bending. The in-plane solutions for the displacements were determined by the solution of the governing differential equations, which were derived by the principle of minimum potential energy of the cross-ply laminate and yielded an eigenvalue problem that was solved numerically. The resultant stress fields were of a hyperbolical form and fulfilled the boundary conditions of traction-free edge in an integral sense. The method showed a good agreement with the results of several other authors. Nevertheless, a certain drawback of the described methodology is the increasing computational effort with an increasing number of plies (Mittelstedt and Becker, 2004).

Mittelstedt and Becker (2006) developed a layerwise theory for the analysis of free edge effects in thermally loaded symmetric laminates. The method is based on a discretisation of the physical laminate plies into an arbitrary number of mathematical layers through the thickness. The principle of minimum potential energy yields the governing Euler–Lagrange equations which allow for a closed-form analytical solution for the in-plane functions, thus characterising this method as a semi-analytical one. This method is proven to be a fast and reliable means of analysis for free edge effects, however the given boundary conditions of traction free laminate edges are satisfied in an averaged sense.

A review has been made of developments in different methods used for the estimation of interlaminar stresses of free edges. The literature devoted to analytical, numerical and semi-analytical methods is surveyed. Analytical methods generally provide an acceptable compromise between accuracy and economy in predicting interlaminar stresses, but they can only be used for laminates with simple geometry, loading and boundary conditions. Numerical methods, e.g. finite element methods,

can predict three-dimensional stress state in general cases, but their storage requirements due to the large number of variables and computer costs sometimes make them impracticable. Semi-analytical methods utilising the merits of both analytical and numerical methods are not only straightforward for efficient and reliable programming but versatile enough to cover all types of problems relevant to practical situations.

2.2. Transverse Cracking in Composite Laminates

When composite laminates are subjected to tensile loading, the early stage of damage is dominated by matrix cracking in the transverse plies. Thus the stress transfer near the transverse cracks, property degradation due to transverse cracking, and the initiation and propagation of matrix cracking are all important problems in the analysis and design of composite laminates. These problems have been studied extensively during the last three decades.

2.2.1. Stress Transfer in Composite Laminates

The stress transfer near transverse cracks is a fundamental concern to understand the damage mechanism in composite laminates. In most circumstances, the predictions of property degradation and cracking propagation are based on the stress analysis of the cracked laminates. Many stress transfer approaches have been reported to model the stress distribution, the thermoelastic property degradation or/and cracking propagation in composite laminates. Some of the works are briefly reviewed as follow.

2.2.1.1. Shear Lag Analysis

Shear lag models remain the most commonly used models for calculating the stress fields of cracked composite laminates because of their simple form. They are being modified and generalised to enable better description of wider classes of laminates. Most shear lag models assume that uniform through-thickness displacement and normal stresses in every layer. Shear stress exists only in a shear transfer region between layers and is uniform through thickness within that region.

Shear-lag analysis appears to have been first introduced by Garrett and Bailey (1977) to estimate the stress distribution in the cracked 90^{o} plies, and then developed in many analyses. They used a one-dimensional shear lag model to calculate the stress transferred from the cracked transverse plies to the uncracked longitudinal plies. This work played a key role in characterising the ply crack problem and emphasised the need for predictive methodologies.

Reifsnider and the coauthors (Reifsnider and Talug, 1980; Reifsnider and Jamison, 1982) devised a simple shear lag method to evaluate stiffness reduction due to cracks. This simple analysis has yielded reasonably good predictions of stiffness reduction and is of considerable conceptual value but it is not sufficiently accurate.

Flaggs (1985) presented a two-dimensional shear lag model, followed closely in spirit to the one-dimensional shear lag model used by Garrett and Bailey (1977), to predict the tensile matrix failure in composite laminates. In the normal context, shear lag is associated with the load transfer of shear stress to normal stress or vice-versa. In his formulation, however, shear lag will also be used as the load transfer mechanism for in-plane shear as well as the normal stress.

Lim and Hong (1989) formulated a modified shear lag analysis, taking into account the concept of interlaminar shear layer, to evaluate the effect of transverse cracks on the thermoelastic property degradation. The mutual interaction of transverse cracks was considered in their analysis as the transverse crack spacing becomes small.

Lee and Daniel (1990) employed a simplified shear lag analysis to develop a progressive damage scheme for cross-ply composite laminates. Closed form solutions are given for the transverse crack density, stress distributions and reduced stiffness of damage plies as well as the entire laminate as a function of applied load and lamina properties. For progressive transverse cracking, the approach assumes that the next set of cracks occurs when the maximum axial stress in those plies reaches the transverse strength of the layer.

Fan and Zhang (1993) proposed a two dimensional shear lag analysis where the out-of-plane shear stresses vary linearly across the whole thickness of constraining layer.

Zhang et al. (1992) further improved this model to permit partial linear variation of out of plane shear stresses. The stiffness reduction due to matrix cracking was then predicted using an equivalent constraint model (ECM). The ECM laminate consists of the cracked lamina itself, the nearest ply groups and the stiffness-equivalent homogeneous layers lumped from the rest of the plies. The effect of non-uniform transverse cracking was also examined. On the basis of the ECM of the damaged laminae, Kashtalyan and Soutis (2000) used an improved 2-D shear lag analysis to determine the in-plane stresses of the ECMs and stiffness degradation in cross-ply laminates with matrix cracking both in the 0° and 90° layers. Although the ECM is verified to be a reliable method to predict stiffness reduction in cracked composite materials, the nature of this model does not allow the real interlaminar stress distributions to be evaluated.

A modified one-dimensional shear-lag approach (Xu, 1995), suitable for cross-ply laminates of various stacking sequences, is based on the assumption that longitudinal displacement is independent of the 0° ply thickness and width and is a power function of the thickness co-ordinate and indeterminate function of the length co-ordinate in the 90° piles. The stiffness reduction and matrix cracking propagation were demonstrated by numerical results. In comparison with the experimental data, this method can only provide reasonable predictions, but far from accurate.

A parabolic shear-lag analysis was developed by Berthelot et al. (1996) to investigate the stress distributions and stiffness reduction in cross-ply laminates, subjected to uniaxial tensile loading. The model assumed a parabolic variation of longitudinal displacement in the 0° and 90° layers. An extended approach of the parabolic shear-lag analysis was proposed by Berthelot (1997), in which an indeterminate variation of the longitudinal displacement across the thickness of 0 ° layer is assumed. These two approaches neglect the variations of the transverse displacement with the longitudinal coordinate. This assumption leads to a unreliable evaluation of the shear stress in the vicinity of the crack.

Smith and Ogin (1999) obtained estimates of the reduced flexural modulus as a function of crack density based on the one-dimensional shear-lag approach. The

solution is shown to agree well with a more sophisticated stress transfer model (McCartney and Pierse, 1997b) in the literature.

The shear-lag model provides a basic understanding of the load transfer process in laminates with matrix cracks in the transverse plies. However there are many shortcomings related to its basic assumptions. The shear transfer region is assumed to be restricted to the interface alone thereby introducing a shear discontinuity into the model. The assumption of uniform through-thickness displacement and normal stresses in every layer does not take account of the crack tip effects. In summary, the shear lag method is an extensively used model because of its simple mechanical principle, but it usually gives non-accurate predictions.

2.2.1.2. Variational Approaches

Variational approaches are developed on the basis of the principle of minimum complementary energy. Complementary energy is defined through thermo-mechanical stresses in layers. Different models assume different form of stress distribution in layers that satisfy the equilibrium equations. A minimisation procedure is used to find the best solution in the context of this principle. The final form of the complementary energy therefore varies according to the complexity of the model (Joffe and Varna, 1999).

Hashin (1985) was the first to use variational approach to determine the stress distribution and stiffness reduction of cracked cross-ply laminates. The analysis entailed the assumption, as is common to most shear lag theories, that the axial stress perturbation within each group of plies is a function of the axial coordinate and is independent of the thickness coordinate. The complementary energy principle was invoked to derive a strict lower bound on the effective stiffness (Praveen and Reddy, 1998). Hashin (1988) extended this method to evaluate the effective thermal expansion coefficients (TEC) of cross-ply laminates with transverse cracks.

On the basis of Hashin's variational approach Nairn (1989)) presented a new variational solution to determine the two dimensional thermoelastic stress state in cross-ply laminates of type $[0_m/90_n]_s$ and $[90_m/0_n]_s$. The stress analysis was used to

calculate the energy release rate due to formation of a new ply crack. The analysis accurately includes the effect of residual thermal stresses. The variational solution was also used to get an analytical expression for the longitudinal expansion coefficient of the cracked cross-ply laminate as a function of crack density.

Varna and Berglund (1991; 1994) compared different variational models to evaluate the thermo-elastic properties of cross-ply laminates with transverse cracks. Non-uniform stress distributions are included through the thickness of both the 0° and the 90° layers. Joffe and Varna (1999) derived closed-form expressions relating stiffness changes to the transverse crack density. The variational approach was used to calculate the stress-perturbation function in the closed-form expressions.

Within the same frame of Hashin (1985)'s model, Gudmundson and Zang (1993) presented a more refined analysis. Crack interaction was taken into account, and the complete extensional stiffness and thermal expansion for a composite laminate of arbitrary lay-up configurations were derived in closed forms. However only average ply stresses and strains can be determined by this model. Adolfsson and Gudmundson (1997) predicted thermoelastic property degradation of composite laminates with matrix cracks in all plies. Because the two-dimensional laminate theory was adopted as the theoretical basis, the analysis can be only limited in thin laminates.

Schoeppner and Pagano (1998) used a variational theorem by Reissner (1950) to study the elastic stress fields in large radius axisymmetric cylinders. The variational theorem has been shown by Pagano (1978a; 1978b) to accurately describe stress fields in flat laminates. Models based on this approach have been shown to accurately describe stress fields in the vicinity of stress risers and the axisymmetric model has been shown to provide accurate predictions of energy release rates. In addition, the models have the capability to provide improvements in the accuracy of the predicted stress fields by subdividing physical layers into sub-layers.

Praveen and Reddy (1998) employed an energy-based variational method to derive and upper bound on the effective axial stiffness of cross-ply laminates with transverse cracks. The model is complementary to Hashin (1985)'s lower bound one.

The displacement perturbations are assumed in terms of the displacements of the layerwise laminate theory of Reddy (1987). The stress transfer due to the presence of matrix cracks was also examined in detail and the results show good agreement with other models.

Rebiere et al. (2001) proposed two variational models, using different functions for the distribution of the stress field, to show the influence of transverse and longitudinal cracks on the stress distribution and on the elastic property reduction of a cross-ply laminate. In their analysis the crack surface is assumed to be plane and only thin laminates are considered.

Tounsi et al. (2005) used Hashin's (1985) variational model to assess the effect of temperature and moisture on the reduction of longitudinal Young's modulus in cross-ply laminates with transverse cracking. The results show that the hygrothermal environment has a significant effect on the relative reduction of longitudinal Young's modulus at the higher crack density. In contrast, the sensitivity of the hygrothermal effects on the Poisson's ratio becomes weaker.

Li and Lim (2005) developed variational principles for generalised plane strain problems and applied them to the stress analysis of transversely cracked laminates and effective elastic properties of unidirectionally fibre-reinforced composites. Both the total potential energy and the total complementary potential energy principles were well formulated and presented. The expression of the total complementary potential energy is revealed for the first time in the literature.

2.2.1.3. Approximate Elasticity Solutions

Im (1990) investigated the stress transfer in composite laminates with transverse cracks by using the Lekhnitskii's (1963) stress potentials for generalised plane strain deformation. An eigenfunction series solution was constructed by satisfying the boundary conditions near crack surfaces and the interface. The conditions on the other boundaries are satisfied approximately by truncated series terms in the least square method. In general, the number of truncated terms strongly depends on the

geometry and boundary conditions. Furthermore this investigation is limited to symmetric cross-ply laminates.

McCartney (1992; 1996) and McCartney and Pierse (1997a; 1997b) developed a series of stress transfer theories for predicting the stress and displacement distributions in a cross-ply laminate or a general symmetric laminate containing ply cracks in a single ply group, under in-plane biaxial loading or bending. The out-of-plane shear stresses were assumed to be linear functions of the through-thickness coordinate in each layer. A system of ordinary differential equations were derived by satisfying exactly the equilibrium equations, the stress-strain relations and four compatibility equations (strain-displacement relations), as well as satisfying the remaining two compatibility equations in an averaging way. The stress and displacement solutions were then obtained by solving the ordinary differential equations numerically. The stress-free conditions at the crack surfaces can be satisfied exactly, but the displacement boundary conditions for the uncracked layers are specified in an averaging way. In order to reduce such an approximation, the ply refinement technique was recommended of subdividing each ply in the laminate by a set of n elemental layers having the same thickness and properties. It is expected that a highly accurate prediction for a stiffness reduction due to ply cracking can be made by conducting a well-fine ply subdivision (Zhang and Herrmann, 1998).

Abdelrahman and Nayfeh (1999) presented a simple approximate elasticity model to study the stress transfer and stiffness reduction in orthogonally cracked laminates. Using approximate distributions for some of the field variables which automatically satisfy symmetry and interface conditions, the behaviour of the three dimensional laminate is described by two coupled partial differential equations. Once the stress free crack surface boundary conditions are imposed and the stress field components are obtained. Expressions for the reduction in the residual Young's modulus and shear modulus from crack initiation to crack saturation were derived from the stress field solutions.

The aforementioned semi-analytical method (Zhang *et al.*, 2006a; 2006b) was used not only to evaluate stress singularities in the vicinity of free edges, but also to study stress transfer near transverse cracks in cross-ply laminates. In addition, by using the

constitutive equations of laminates in the Classical Laminate Theory and the stress analysis, the thermoelastic property degradation induced by transverse cracking was predicted in Zhang et al. (2006a).

2.2.1.4. Laminate Plate Theories

Apart from the shear lag analysis, Zhang and Herrmann (1998) employed the first-order shear deformation laminate theory to evaluate the stress and displacement fields within the ECM laminates. In comparison with the shear lag analysis, the laminate plate theory solutions satisfy the equilibrium equations more accurately and satisfy the continuity conditions of both displacements and stresses at the interfaces between sub-layers exactly. The method was used to predict stiffness degradations in symmetric laminates containing a cracked mid-layer. Furthermore Zhang and Herrmann (1999) extended this method to model the stiffness degradation induced by multilayer intralaminar cracking in general symmetric composite laminates.

Whitney (2000) used a stress based laminate plate theory to model each ply of a bidirectional laminate. The model considers the effect of transverse shear and normal stresses. All nine independent effective elastic constants of cracked cross-ply laminates were determined. Whitney (2001) proposed a global/local model to determine the effective thermoelastic constants of balanced angle-ply laminates with transverse cracking. The global model is a displacement based, higher order laminated plate theory, while the local model is a stress based plate theory.

2.2.1.5. Finite Element Methods

Yuan and Selek (1993) developed a singular hybrid finite element model to study the stress singularity and stiffness reduction in symmetric composite laminates with transverse cracking. Formulation of the problem is based upon the method of eigenfunction expansion and Lekhnitskii's complex variable potentials for generalised plane strain deformation. For numerical analysis, a singular hybrid element was formulated on the basis of the variational principle of a modified hybrid functional to account for the crack tip singularities. The singular hybrid element model exhibited very good prediction of the stress field, especially in the singular

domain near the transverse cracks where conventional finite element method failed to model the stress distribution accurately.

Li et al. (1994) presented a finite strip method to analyse the stress fields and stiffness reduction of transversely cracked laminates. The approach is based on a generalised plane strain approach and can be used to study general lay-up laminates under general loading. This approach is similar to the displacement based finite element method with discretisation only in the thickness direction. Therefore it could be integrated with a displacement-based analysis of damaged laminated structures. In their numerical results only symmetric laminates were analysed.

Leblond et al. (1996) applied finite-element analyses to the investigation of transverse cracking in cross-ply laminates. Stress and strain distributions were obtained for a given damage state and applied load by using 2D and 3D elements for the case where the cracks cross the full specimen width. Eight-node elements with linear interpolation of displacement were used in 3D investigation. A plane strain state associated with four-node elements was considered in 2D investigations. The results obtained in 2D and 3D investigations do not show any significant differences.

Tong et al. (1997b) simulated the occurrence of cracks in quasi-isotropic laminates by using generalised plane-strain finite element models, which includes the effect of finite strain in the infinite length direction. The loss of stiffness due to matrix cracking was predicted and detailed stress distributions were examined. The interlaminar shear stress close to the crack tip, influenced by the singularity, was discarded in the numerical results.

In order to validate their variational models, Rebiere et al. (2001) also proposed a three-dimensional finite element method to study the stress transfer and stiffness loss. An 8 nodal volume anisotropic element was used with linear interpolation. For a more detailed study of the stress field, the mesh is improved in the vicinity of crack planes and interfaces. However the FEM can not give a distribution of interlaminar shear stress in good agreement with the variational methods.

The state space finite element method (Ye *et al.*, 2004) mentioned in Section 2.1.3 can also provide excellent approximations to the stress singularities in the vicinity of localised stress-free surfaces, e.g., transverse ply cracks. A numerical comparison was made between their new results and those of McCartney and Pierse (1997a) to validate the solution of ply cracking problem.

A review of various stress-distribution models for the analysis of composite laminates with transverse ply cracks has been made in the preceding discussions. Shear lag analysis is considered as the simplest and most commonly used model, however it sometimes can not predict an accurate stress field and has limited application in general cases. On the contrary, the later appeared methods, i.e. the variational approach, the approximate elasticity solution, the laminate plate theory and finite element method, are more complicated but a highly accurate prediction can be obtained. However, almost none of the existing models can handle composite laminates with general lay-ups and stacking sequences.

2.2.2. Property Degradation due to Transverse Cracking

An immediate effect of transverse cracking is to cause a degradation of thermoelastic constants. The effective thermoelastic properties of cracked composite laminates have been estimated as functions of transverse crack density by various approaches. These can be classified in two groups by the method of formulating constitutive relations of the cracked laminate. The first approach is to evaluate the stress distribution in a representative volume element (RVE) between neighbouring cracks and deduce the relationship between the applied loads and laminate overall response. The stress distribution will satisfy the boundary conditions and equilibrium equations near the crack surfaces. The second approach is to evaluate the locally averaged constitutive properties from a damaged local volume so that the effect of the internal damage is reflected in the constitutive equations rather than boundary conditions (Han and Hahn, 1989).

2.2.2.1. Stress Analysis Based Models

In the stress analysis based models, the stress and displacement field in a representative volume element (RVE) between two neighbouring cracks is first

evaluated by a stress transfer model. Then the overall deformation and applied load or the average strains and stresses of the RVE can be calculated. By using the effective constitutive equations or stress strain relations of a cracked laminate, the effective thermoelastic constants can finally be determined. In this procedure, stress analysis is a prerequisite to predict effective thermoelastic properties and determines the accuracy of the prediction. According to the method of evaluating stress and displacement distribution, the stress analysis based models can be further classified as the shear lag analysis, the variational approach, the approximate elasticity solution, the laminate plate theory and finite element method, which have been reviewed in Section 2.2.1.

2.2.2.2. Local Damaged Methods

Continuum damage mechanics (CDM) lays its foundation on basic thermodynamics by introducing a set of independent internal state variables describing the state of damage. The continuum damage models require certain material constants, to be determined experimentally, in addition to the usual elastic moduli of the undamaged composite. The additional constants may be interpreted as the additional basic material characteristics needed for the description of the material response in a wider frame (Talreja *et al.*, 1992). Beginning with Talreja (1985) who developed stiffness-transverse cracking relationships using a continuum damage model, Talreja (1986) considered two modes of damage: the matrix cracking and delamination. Relationships between the overall stiffness properties and the intensity of damage in the individual modes were determined. Talreja (1992) reported the results of an experimental investigation and used the continuum damage model to analyse the test data. Since the model accounts for the effect of cracks on the composite stiffness through certain material constants, it provides a means for distinguishing between the matrices of different toughness by the resulting values of the constants. Allen et al. (1987a; 1987b) also proposed a continuum mechanics model to predict the stiffness loss in composite laminates. The model was specialised for the case of matrix cracks in symmetric cross-ply laminates. As well as Talreja's theory, the approach depends on the damage state which has to be determined experimentally.

Although the continuum damage approaches allow, in principle, the treatment of matrix cracking in off-axis plies of any orientation. However, certain material coefficients are usually to be determined experimentally for each laminate configuration considered. To avoid this practical limitation, therefore some combination theories were proposed. Tay and Lim (1996) developed a computer algorithm which combined CDM and FEM to predict stiffness loss in cross-ply laminates. The finite element method was used to determine the effect of damage accumulation on the internal state variables. Tay and Lim (1996) extended the theory to the analysis of transverse cracks in more general symmetric laminates. Talreja (1996) proposed a synergistic damage mechanics approach, which utilises micromechanics results in a continuum damage mechanics formulation, and illustrated its use in describing deformational response of $[\pm\theta/90°_2]_s$ laminates. Varna et al. (2001) used the synergistic approach to predict stiffness reduction of $[\pm\theta/90_4]_s$ laminates under longitudinal tensile loading. The constraint of θ plies on transverse cracks in 90° plies is represented by a crack-opening displacement (COD) parameter in the CDM model and is expressed in terms of the ply properties and ply thickness ratios on the basis of a finite-element calculation.

2.2.3. Initiation and Propagation of Transverse Cracking

The ultimate failure of a composite laminate follows the occurrence of transverse cracking, longitudinal cracking, delamination, and fibre breaking. Transverse cracking is usually the most common damage mode observed in composite materials. The initiation and propagation of transverse cracks in composite laminates have been studied in the last few decades. These extensive investigations consist of experimental and analytical studies.

2.2.3.1. Experimental Studies

Garrett and Bailey (1977), Parvizi et al. (1978), Bailey et al. (1979) and Bailey and Parvizi (1981) are amongst the earliest researchers who carried out extensive experiments to observe transverse cracks. They found that the cracks formed in a direction parallel to the transverse reinforcement and the thickness of the 90° plies affects the entire cracking process. At large inner-ply thicknesses the specimens

showed uniform transverse cracking, and at very low inner-ply thicknesses this transverse cracking could be suppressed completely prior to total specimen failure.

Flaggs and Kural (1982) presented the results of an experimental study which confirmed that the constrained transverse cracking phenomena observed in 90° ply of uniaxially loaded $[0°/90°]_s$ composite laminates was also exhibited by the more general $[\theta/90°]_s$ class of composite laminates. Experiments showed that by increasing the stiffness of neighbouring laminae or, alternatively, by decreasing the thickness of the 90° laminae, greatly enhanced in situ transverse matrix strengths could be obtained, which would not have been predicted by the traditional stress (or strain) failure criteria.

Takeda and Ogihara (1994) investigated the effects of temperature on the fracture process in CFRP cross-ply laminates. The transverse crack density was measured at room temperature and 80°C. Thermal residual strains which had important effects on the failure process were measured by the ply separation method.

Nairn and Hu (1992), Liu and Nairn (1992) and Nairn et al. (1993) did a series of experiments to record the crack density as a function of applied load. Some interesting results were concluded. For all laminates, the characteristic cracking curve has no cracks until some onset stress that corresponds to the initiation of cracking. After the initial crack, the crack density typically increases very rapidly. At high crack density, the cracking slows down and approaches a saturation damage state. The onset stress decreases as the thickness of the 90° plies increases. On continued loading, however, the situation reverses–thinner 90° ply groups eventually develop more cracks than thicker 90° ply groups. In other words, the saturation crack density is inversely related to the thickness of the 90° plies. However the transverse cracking properties of a laminate are not just a property of the thickness of the 90° plies. The properties also depend on the thickness and mechanical properties of the supporting plies (Nairn, 2000).

Tong et al. (1997a) reported an experimental study on matrix crack growth behaviour in cross-ply $[0°/90°]_s$ and quasi-isotropic $[0°/90°/-45°/+45°]_s$ GRP laminates.

Although the initiation strains for the two laminates are similar, the transverse crack accumulation processes differ significantly. Reductions in elastic properties due to transverse cracking in quasi-isotropic laminates were less significant than those in cross-ply laminates.

Joffe and Varna (1999) carried out a tensile test to investigate the transverse cracking development in Glass Fibre (GF)/Epoxy (EP) laminates with lay-up $[\pm\theta/90°_4]_s$, θ=0°, 15° ,30°, 40°. For these four lay-ups, the first transverse cracks appeared at approximately the same strain level, while with the increasing fibre orientation angle, the crack density decreased. Varna et al. (1999) studied damage in off-axis plies of composite laminates by examining the configuration $[0°/\pm\theta_4/0°_{1/2}]_s$ with θ=25°, 40°, 55°, 70° and 90°. It was found that for the values of θ=55°, 70° and 90°, where the stress in the off-axis plies normal to the fibres is tensile, ply cracks along fibre directions initiate and increase in number, while for other θ values, no ply cracks were found at any axial tensile load until failure. The axial Young's modulus and Poisson's ratio were, however, found to change with the applied load.

Yokozeki et al. (2002) studied the damage process of transverse cracks in cross-ply and quasi-isotropic CFRP laminates under static loading. In the case of cross-ply laminates simultaneous growth of edge crack density and widthwise propagation could be observed. However, in quasi-isotropic CFRP laminates, widthwise propagation of edge cracks is suppressed until the higher strain level is attained, after edge crack densities saturate. Yokozeki et al. (2005) investigated crack accumulation in multiple plies of $[0/\theta_2/90°]_s$ laminates (θ=30°, 45° and 60°). The experimental results indicate that intersecting angle between the contiguous cracked plies (i.e. 90° and θ-ply) has significant effects on the process of θ-ply crack formation. When the intersecting angle is small, micro-formed cracks are observed before propagation in the fibre direction as the cases of θ= 45° and 60°. However, developed cracks mainly form in the cases of large intersecting angles.

Most experimental investigations show that the first damage mode is usually transverse cracking. Both the thickness of 90° layers and stiffness of constrained layers affect the initiation and propagation of transverse cracks. The onset stress

decreases as the thickness of the 90° plies increases or the stiffness of neighbouring layers decreases. Two particular states can characterise this damage mode: its initiation or occurrence of the first transverse crack on the one hand and the saturation state when no more transverse crack can be created on the other hand. The saturation crack density is inversely proportional to the thickness of the 90° plies.

2.2.3.2. Analytical Studies

Most early work on transverse cracking assumed that cracks form when the stress or strain reaches the transverse strength of the ply material. More recent work employed energy methods based on fracture mechanics to evaluate matrix cracking. According to the cracking propagation criteria, the analytical studies consist of the strength based approach and the energy based approach. Among the strength based models are some statistical strength methods to account for the variations in material strength.

(1) Strength Based Approach

A common method for designing with composites to avoid failures is strength based theory. In strength based theory, it is assumed that the new cracks form when the maximum stress or strain reaches the strength of those plies. Furthermore, it is usually assumed that the ply cracking stress or strain can be measured from experiments.

Garrett and Bailey (1977) assumed that the transverse ply has a unique breaking strain, ε_{tu}, and strength σ_{tu}. If a stress is applied in a direction parallel to the longitudinal plies, the transverse ply will fail at a stress σ_{tu}. Using the same strength criteria, Parvizi and Bailey (1978) reported more detailed studies for a glass fibre reinforced epoxy composite. Leblond et al. (1996) studied the multiplication of transverse cracks as a function of the applied stress in cross-ply laminates. The crack development is assumed to be controlled by the fracture stress in the 90° plies.

However the strength based theory usually can not provide a good prediction of transverse cracking because the stresses or strains in the transverse plies at the onset of matrix cracking are not constant between laminates with different lay-ups. In other words, there is no strength based models that can be used to predict transverse

cracking process unless the ply strength properties are treated as in situ properties that depend on laminate configurations.

In fact, the strength of a ply varies from place to place throughout a composite laminate. Uniform ply strength is just an ideal state and does not match the real strength distribution. For this reason there are a few attempts to use statistical models, which account for the variations of strength in composite laminates, to predict progression of transverse cracking. Manders et al. (1983) considered a Weibull distribution of the strength along the 90° layer. The Weibull parameters (shape and scale parameters) of the 90° ply were obtained by measuring crack space. Fukunaga et al. (1984a; 1984b) derived formulae for determining first cracking, subsequent multiple cracking and ultimate fracture by the statistical approach. Peters (1984) found the Weibull parameters from the number of cracks, assuming that the 90° ply consists of a chain of elements with a critical length. Ochiai et al. (1992) presented an operatively equivalent Peters method to estimate Weibull parameters. Berthelot and Corre (2000) used a pseudo-normal distribution to describe the strength distribution in the 90 layer. Sun et al. (2003) adopted Weibull distribution to predict transverse cracking propagation in high temperature composite laminates.

Although the statistical analyses have a better description of the strength distribution in laminates than the conventional strength methods, they still require an individual test programme for each stacking sequence of a laminate and therefore the practical applications of this method are limited.

(2) Energy Based Approach

Due to the drawbacks and limitations of strength based methods, the majority of recent work used energy methods based on fracture mechanics to predict transverse cracking. Most energy models use a representative volume element (RVE) to predict next crack formation when the energy released due to crack formation reaches the critical strain energy release rate G_c. For the same type of laminates with different configurations, the value of G_c almost keeps constant, it can therefore predict results for a wide variety of laminates from a single value of G_c.

Parvizi et al. (1978) demonstrated that a simple shear lag analysis used in conjunction with the Griffith energy criterion can be used to accurately predict matrix cracking. Flaggs (1985) made use of a strain energy release rate fracture criteria in conjunction with an approximate two-dimensional shear-lag model to predict tensile matrix failure. Wang et al (1985) employed the energy release rate method of classical fracture mechanics to model various matrix crack interactions. Dvorak and Laws (1987) investigated the first ply failure using a critical energy release rate criteria and later Laws and Dvorak (1988) presented a model for progressive transverse cracking based on statistical fracture mechanics. Nairn (1989; 2000), Liu and Nairn, (1992) and Nairn and Hu (1992) carried out a series of study on the matrix cracking on the basis of a finite fracture mechanics. Zhang et al. (1992) and Fan and Zhang (1993) proposed the equivalent constraint model (ECM) in which the energy release rate due to transverse ply cracking, incorporating residual thermal stresses, is derived. McCartney (1998; 2002; 2004; 2005) investigated ply crack development in a variety of lay-ups, from cross-ply to general symmetric laminates, subjected to axial extension or mixed mode loading. Smith and Ogin (1999) calculated the applied bending moment at transverse crack onset under flexural loading using a fracture mechanics approach. Gudmundson and Alpman (2000) evaluated the experimental observations of crack initiation and growth in an off-axis loaded tensile specimen by developing the FE model and approximate formulae for energy release rates. Joffe et al. (2001) used a crack-closure technique to calculate the energy release caused by cracking. A Monte-Carlo simulation in incremental strain-controlled loading is used to model the transverse cracking process. The 90° layer is divided in to a large number of elements and a critical energy release rate *Gc* is assigned to each element according to Weibull distribution. Yokozeki el al. (2002) employed energy release rate to investigate crack initiation and propagation across the specimen width. Energy release rates associated with crack propagation in the width direction are calculated using three-dimensional FEA. Subsequently Yokozeki et al. (2005) used the same method to study microcracking behaviours induced by matrix cracks in adjacent ply. Lim and Li (2005) calculated energy release rates for transverse cracking and delamination under the generalised plane strain condition. By applying the minimum strain energy density criterion to a non-linear FE analysis, Sirivedin et al. (2006) predicted matrix crack propagation in continuous-carbon fibre/epoxy composites.

In summary, the energy based analysis can correlate most experimental results in extensive composite laminates with different materials properties and lay-ups. The energy release rate was verified to be a very good material parameter which characterises matrix cracking propagation.

2.3. Summary

In this chapter, the investigations on two types of material discontinuities in composite materials, free edges and transverse cracks, are reviewed. For the free edge effects, investigators focused their work on evaluating the stress singularities in the vicinity of free edges. These include analytical, numerical or semi-analytical methods. For transverse cracking problem, the issues about stress transfer, property degradation and transverse crack propagation are extensively reviewed. The stress transfer is a prerequisite to predict property degradation or transverse crack propagation. As a result, an accurate stress analysis is essential to assess the damage of composite laminates. Some remarks about the existing stress transfer approaches and transverse cracking propagation methods are also made.

Chapter 3. Approaches and Modelling

In this chapter, a brief introduction of approaches and modelling used in the thesis is provided. Further details can be found in Ye (2002), Lekhnitskii (1963), Kollár and Springer (2003), Adolfsson and Gudmundson (1997), and Kanninen and Popelar (1985). The applications of these theories to the stress transfer, the property degradation and the transverse cracking propagation of composite laminates will be presented in subsequent chapters.

3.1. State Space Method and Application to Stress Analysis

The term 'state space' is often used in connection with linear control systems where the principal concern is the relationship between inputs (or source) and outputs (or responses). In practice, these systems may be electrical, hydraulic, mechanical, pneumatic, thermal, or a mixture of these. For example, the state of a continuous system can best be represented by a single-input, single-output, linear electrical net work whose structure is known. The input to, and the output of, the network are both functions of time. Since the network is known, complete knowledge of the input over a time interval is sometimes sufficient to determine the output over the same time interval (Ye, 2002).

For three-dimensional analyses of composite laminates, the use of state equations has many advantages. For example, in a laminate, if the displacements and transverse stresses at the top surface of the laminate as are taken the initial state of the system, after introducing boundary conditions, the displacements and stresses at the bottom surface of the plate may be found and the displacements and stresses at an arbitrary interface of the laminate can be traced as 'the past history of the system' (Ye, 2002).

The concept of state space and solutions of state variable equations or state equations will be briefly introduced in the following. This method is fundamentally important to the stress analysis parts of the thesis. The theories presented herein have been

discussed in Ye (2002) and DeRusso *et al.* (1998), where rigorous mathematical proofs of these theories are provided.

3.1.1. Concept of State and State Variables

Consider a mechanical system in Fig. 3.1. The corresponding elements are a spring, a damper, a mass and a force.

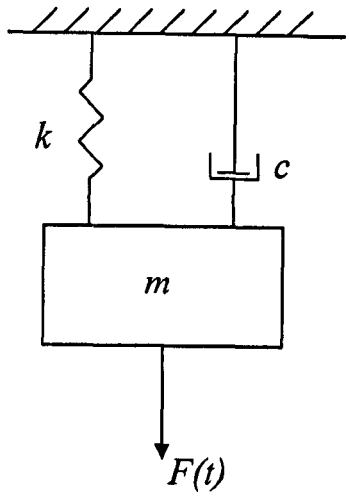

Fig. 3.1 A spring-damper-mass system

By means of Newton's second law, the mathematical model which describes the motion of the system are given by

$$m\ddot{x}(t) + c\dot{x}(t) + kx(t) = F(t) \tag{3.1}$$

where the dots designate time derivatives; t denotes time. The three constant coefficients m, c and k represent, respectively, mass, damping constant and force constant of spring. $F(t)$ is the force at time t. In order to determine the future position $x(t)$ of the mass, a prerequisite is the position and velocity of the mass at an arbitrary time instant t_0.

By letting

$$\begin{aligned} x_1(t) &= x(t) \\ x_2(t) &= \dot{x}(t) \end{aligned} \tag{3.2}$$

The second order linear differential Eq. (3.1) can be converted to the following matrix form

$$\frac{d}{dt}\begin{Bmatrix} x_1(t) \\ x_2(t) \end{Bmatrix} = \begin{bmatrix} 0 & 1 \\ -\frac{k}{m} & -\frac{c}{m} \end{bmatrix} \begin{Bmatrix} x_1(t) \\ x_2(t) \end{Bmatrix} + \begin{Bmatrix} 0 \\ F(t) \end{Bmatrix} \tag{3.3}$$

Eq. (3.3) is a first-order linear differential equation system. The equation governs the behaviour of the state of the system and is called the state variable equation or state equation of the system. The column vector containing $x_1(t)$ and $x_2(t)$ is called the state vector. Each component of the vector is called a state variable, i.e. the position $x_1(t)$ and velocity $x_2(t)$ are two state variables of the spring-mass-damper system in Fig. 3.1.

The notion of a system is rather broad, and is not restricted to simple mechanical systems. In general all these systems can be described by a similar mathematical form. In analogy with Eq. (3.3), the definition of a general form of the state space equation can be expressed as follows

$$\{\dot{\mathbf{x}}(t)\} = [\mathbf{A}]\{\mathbf{x}(t)\} + [\mathbf{B}]\{\mathbf{u}(t)\} \tag{3.4}$$

where the column vector $\{\mathbf{x}(t)\}$ is the state vector of the system and it consists of a set of elements $x_1(t)$, $x_2(t)$,..., $x_n(t)$. [**A**] is an $n \times n$ constant matrix called the coefficient matrix or system matrix in the literature. [**B**] is an $n \times 1$ column vector. $\{\mathbf{u}(t)\}$ is the input of the system. As long as the state of the system at time t_0, $\{\mathbf{x}(t_0)\}$,together with the input $\{\mathbf{u}(t)\}$ are known, the output of the system is uniquely determined for $t \geq t_0$.

Eq. (3.4) is called a linear time-invariant system since the system is characterised by two matrices, [**A**] and [**B**], which are independent of time. The solution of Eq. (3.4) will be discussed in the following section.

3.1.2. Solutions for a Linear Time-invariant System

If the dimension of Eq. (3.4) is one, i.e. a scalar differential equation

$$\dot{x}(t) = ax(t) + bu(t) \tag{3.5}$$

where a and b are constant. Based on the classical solution method of a linear differential equation, the solution of Eq. (3.5) can be written as

$$x(t) = e^{at}x(0) + e^{at}\int_0^t e^{-a\tau}bu(t)d\tau \tag{3.6}$$

where t_0=0 is assumed. In analogy with the scalar case, the solution of Eq. (3.4) can be written as

$$\{\mathbf{x}(t)\} = e^{[A]t}\{\mathbf{x}(0)\} + e^{[A]t}\int_0^t e^{-[A]\tau}[\mathbf{B}]\{\mathbf{u}(\tau)\}d\tau \tag{3.7}$$

or

$$\{\mathbf{x}(t)\} = e^{[A]t}\{\mathbf{x}(0)\} + \int_0^t e^{[A](t-\tau)}[\mathbf{B}]\{\mathbf{u}(\tau)\}d\tau \tag{3.8}$$

Eq. (3.8) is the complete solution of Eq. (3.4). The matrix exponential $e^{[A]t}$ is called transition matrix, transfer matrix or fundamental matrix in the literature. The calculation of $e^{[A]t}$ can be found in Moler and Van Loan (1978; 2003) and Ye (2002).

3.1.3. Application of State Equation to Stress Analysis

From Section 3.1.1, it has been seen that the mechanical behaviour of the spring-damper-mass system shown in Figure 3.1 can be described by a state equation of time co-ordinate *t*. The state variables of the equation are the displacement and its derivative with respect to *t*. In analogy with this, the stress state of an elastic body in a three-dimensional space can also be described by a state equation with respect to one of the three orthogonal co-ordinates, e.g. the *z* coordinate in the rectangular co-ordinate system. The state vector, therefore, may include displacements and stresses with respect to the *z* co-ordinate. The state equation of this form has been used to solve shell problems (see Soldatos and Hadjigeorgiou, 1990; Fan and Ye, 1990a, b). Since the state vector contains the derivatives of displacements with respect to *z*, it is natural to convert these derivatives to relative strains and then stresses. In consequence, the displacements and the stresses relative to the *z*-direction may also be used as the state variables in the state vector. In the case of a plate bending problem, for instance, if the *z*-direction is taken as the transverse direction, the state vector will contain three displacements of the plate and the three transverse stresses (Fan and Ye, 1990a, b). It is also possible to construct the state equation in other different forms, for example, in the one used by Tarn and Wang (2001), where the transverse stresses in the state vector are all multiplied by the transverse co-ordinate (Ye, 2002).

At the beginning of the last decade, Soldatos and Hadjigeorgiou (1990) and Fan and Ye (1990a; 1990b) started applying the state space method systematically to the solutions of various plates and shells composed of laminated composite materials. Employing the same method, Ye and Soldatos (1994a) developed a detailed, three-dimensional stress and displacement analysis of transversely loaded, laminated complete hollow cylinders and open cylindrical panels having a symmetric or an antisymmetric cross-ply lay-up.

The volume of research publications in this area has increased significantly over the last few years. Khdeir and Reddy (1990; 1997) used state variable equation method for the solution of two-dimensional plate bending problems. Wang *et al.*(2000) investigated stress decay in laminates due to edge effects through a state space formulation. Tarn (2002a; 2002b; 2002c) formulated a series of state space equations for rectilinear anisotropy, cylindrical anisotropy and piezothemoelasticity. Chen *et al.*(2003) and Chen and Kang Yong (2004) developed exact solutions of cross-ply and angle-ply laminates with interfacial damage via the state space method.

An application of the state space method to evaluate stress singularities near free edges and transverse cracks in general cross-ply and angle-ply composite laminates has been developed by Zhang et al. (2006b; Submission) as a part of his PhD project and will be presented in Chapters 4 and 5.

3.2. Generalised Plane Strain Deformation

3.2.1. Introduction of Generalised Plane Strain Deformation

There are circumstances in an anisotropic elastic body when the stresses and strains do not vary in a certain direction. This direction is designated by the y-direction in a Cartesian x-y-z coordinate system. Although the stresses and strains do not vary along y, they may vary in planes perpendicular to the y-axis. This condition is referred to as generalised plane strain condition.

An isotropic body under such conditions would experience plane deformation: the x-z planes of the cross section remain plane and perpendicular to the y axis, the out-of-plane shear strain γ_{xy} and γ_{yz} are zero. In a body made of an anisotropic material these

planes do not necessarily remain plane and these out-of-plane shear strains are not necessarily zero. We can only assert that all components of stresses and strains will not depend on y. The deformation of such a body which corresponds to plane deformation in an isotropic body is called generalised plane deformation. When the generalised plane strain condition exists, the three-dimensional analysis simplifies considerably.

In the following, the equilibrium equations, and the stress-strain relationships of an anisotropic material are presented when the generalised plane strain conditions are satisfied.

3.2.2. Formulations of Generalised Plane Strain Deformation

Generalised plane strain deformation requires that the strains do not vary along the longitudinal axis y. Thus

$$\begin{aligned} &\frac{\partial \varepsilon_{xx}}{\partial y}=0,\ \frac{\partial \varepsilon_{yy}}{\partial y}=0,\ \frac{\partial \varepsilon_{zz}}{\partial y}=0 \\ &\frac{\partial \varepsilon_{yz}}{\partial y}=0,\ \frac{\partial \varepsilon_{xz}}{\partial y}=0,\ \frac{\partial \varepsilon_{xy}}{\partial y}=0 \end{aligned} \tag{3.9}$$

Since the strain components are independent of y, the stress components are also independent of y, and so

$$\begin{aligned} &\frac{\partial \sigma_{xx}}{\partial y}=0,\ \frac{\partial \sigma_{xz}}{\partial y}=0,\ \frac{\partial \sigma_{zz}}{\partial y}=0 \\ &\frac{\partial \sigma_{xy}}{\partial y}=0,\ \frac{\partial \sigma_{yy}}{\partial y}=0,\ \frac{\partial \sigma_{yz}}{\partial y}=0 \end{aligned} \tag{3.10}$$

Then the equilibrium equations become

$$\begin{aligned} &\frac{\partial \sigma_{xx}}{\partial x}+\frac{\partial \sigma_{xz}}{\partial z}+f_x=0 \\ &\frac{\partial \sigma_{xy}}{\partial x}+\frac{\partial \sigma_{yz}}{\partial z}+f_y=0 \\ &\frac{\partial \sigma_{xz}}{\partial x}+\frac{\partial \sigma_{zz}}{\partial z}+f_z=0 \end{aligned} \tag{3.11}$$

where f_x, f_y, and f_z are the body force per unit volume in the x, y and z directions, respectively. For a generally anisotropic material the stress-strain relationships may be written in partitioned form, as follows

$$\begin{Bmatrix}\sigma_{xx}\\ \sigma_{zz}\\ \sigma_{yz}\\ \sigma_{xz}\\ \sigma_{xy}\end{Bmatrix}=\begin{bmatrix}C'_{11} & C'_{13} & C'_{14} & C'_{15} & C'_{16}\\ C'_{13} & C'_{33} & C'_{34} & C'_{35} & C'_{36}\\ C'_{14} & C'_{34} & C'_{44} & C'_{45} & C'_{46}\\ C'_{15} & C'_{35} & C'_{45} & C'_{55} & C'_{56}\\ C'_{16} & C'_{36} & C'_{46} & C'_{56} & C'_{66}\end{bmatrix}\begin{Bmatrix}\varepsilon_{xx}\\ \varepsilon_{zz}\\ \varepsilon_{yz}\\ \varepsilon_{xz}\\ \varepsilon_{xy}\end{Bmatrix}+\begin{Bmatrix}C'_{12}\\ C'_{23}\\ C'_{24}\\ C'_{25}\\ C'_{26}\end{Bmatrix}\varepsilon_{yy} \tag{3.12}$$

$$\sigma_{yy}=\begin{bmatrix}C'_{12} & C'_{23} & C'_{24} & C'_{25} & C'_{26}\end{bmatrix}\begin{Bmatrix}\varepsilon_{xx}\\ \varepsilon_{zz}\\ \varepsilon_{yz}\\ \varepsilon_{xz}\\ \varepsilon_{xy}\end{Bmatrix}+C'_{22}\varepsilon_{yy} \tag{3.13}$$

where C'_{ij} are the stiffness coefficients that can be expressed in terms of Young's moduli, Poisson's ratios and shear moduli.

3.3. Effective Thermoelastic Properties of Composite Laminates

The effective thermoelastic constants of composite laminates are of great interest in engineering applications. In practice the Classical Laminate Theory (CLT) is usually employed to determine the thermoelastic properties. The Classical Laminate Theory uses the Kirchhoff-Love assumptions, which require that straight lines, perpendicular to the midplane before deformation, remain straight, inextensible and perpendicular to the midplane after deformation.

Fig. 3.2 gives the coordinate system which is used in the Classical Laminate Theory. The *x-y-z* coordinate system is assumed to have its origin on the mid-surface of the plate, and the mid-surface lies in the *x-y* plane. The stress resultants, in-plane forces N_i and moments M_i (per unit length), are also shown in the figure (i=*x, y, xy*).

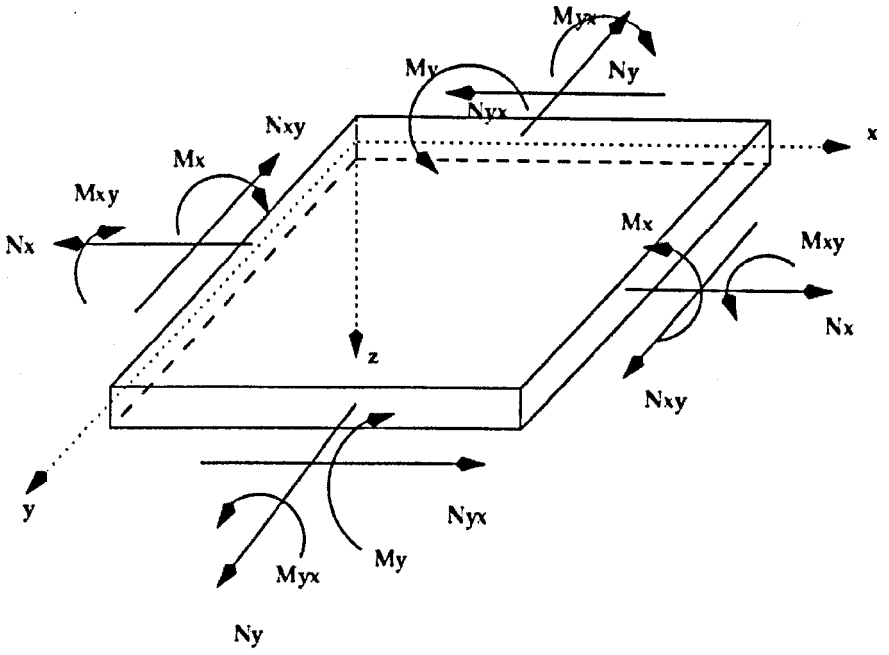

Fig. 3.2 Stress resultants of the loads applied to a composite laminate

3.3.1. Stiffness Matrices of Composite Laminates

For a generally anisotropic plane the relationships between the stress resultants and the overall deformation of the laminate due to applied mechanical and thermal loads follow

$$\begin{Bmatrix}\mathbf{N}\\ \mathbf{M}\end{Bmatrix}=\begin{bmatrix}\mathbf{A} & \mathbf{B}\\ \mathbf{B}^T & \mathbf{D}\end{bmatrix}\left(\begin{Bmatrix}\boldsymbol{\varepsilon}\\ \mathbf{k}\end{Bmatrix}-\{\alpha\}\Delta T\right) \tag{3.14a}$$

where

$$[\mathbf{A}]=\begin{bmatrix}A_{11} & A_{12} & A_{16}\\ A_{12} & A_{22} & A_{26}\\ A_{16} & A_{26} & A_{66}\end{bmatrix},\ [\mathbf{B}]=\begin{bmatrix}B_{11} & B_{12} & B_{16}\\ B_{12} & B_{22} & B_{26}\\ B_{16} & B_{26} & B_{66}\end{bmatrix},\ [\mathbf{D}]=\begin{bmatrix}D_{11} & D_{12} & D_{16}\\ D_{12} & D_{22} & D_{26}\\ D_{16} & D_{26} & D_{66}\end{bmatrix},$$

$$\{N\}=\begin{Bmatrix}N_x\\ N_y\\ N_{xy}\end{Bmatrix},\ \{M\}=\begin{Bmatrix}M_x\\ M_y\\ M_{xy}\end{Bmatrix},\ \{\varepsilon\}=\begin{Bmatrix}\varepsilon_x\\ \varepsilon_y\\ \varepsilon_{xy}\end{Bmatrix},\ \{k\}=\begin{Bmatrix}k_x\\ k_y\\ k_{xy}\end{Bmatrix}, \tag{3.14b}$$

$$\{\alpha\}=[\alpha_1\quad \alpha_2\quad \alpha_3\quad \alpha_4\quad \alpha_5\quad \alpha_6]^T$$

[A], [B], and [D] are the stiffness matrices of the laminate; ε_x^0 and ε_y^0 are the mid-plane strains in the x and y directions respectively; ε_{xy}^0 is the mid-plane shear strain in the x-y plane; k_x and k_y are the bending curvatures experienced by the mid-surface in the x-z and y-z planes, respectively; k_{xy} is the twisting curvature caused by out-of-

plane twisting of the mid-surface; α_i (i=1, 2,..., 6) are effective thermal expansion coefficients of the laminate; and ΔT is a temperature change.

The elements of the stiffness matrices are defined as (i, j=1, 2, 6)

$$A_{ij}=\sum_{k=1}^{N}(Q'_{ij})_k(z_k-z_{k-1}),\ B_{ij}=\frac{1}{2}\sum_{k=1}^{N}(Q'_{ij})_k(z_k^2-z_{k-1}^2),\ D_{ij}=\frac{1}{3}\sum_{k=1}^{N}(Q'_{ij})_k(z_k^3-z_{k-1}^3) \tag{3.14c}$$

where N is the total number of layers in the laminate; z_k, z_{k-1} are the distances from the neutral axial to the two surfaces of the kth ply; and Q'_{ij} are the reduced stiffness constants, which can be expressed by

$$Q'_{ij}=C'_{ij}-\frac{C'_{i3}C'_{j3}}{C'_{33}}\ (i, j=1, 2, 6) \tag{3.14d}$$

where C'_{ij} are stiffness coefficients that can be expressed in terms of Young's moduli, Poisson's ratios, shear moduli and the fibre orientation θ (See Appendix B).

By inverting Eq (3.14), we obtain the strains and curvatures in terms of the in-plane forces, bending moments and thermal loading

$$\begin{Bmatrix}\boldsymbol{\varepsilon}\\ \mathbf{k}\end{Bmatrix}=\begin{bmatrix}\mathbf{a} & \mathbf{b}\\ \mathbf{b}^T & \mathbf{d}\end{bmatrix}\begin{Bmatrix}\mathbf{N}\\ \mathbf{M}\end{Bmatrix}+\{\alpha\}\Delta T \tag{3.15a}$$

where

$$[\mathbf{a}]=\begin{bmatrix}a_{11} & a_{12} & a_{16}\\ a_{12} & a_{22} & a_{26}\\ a_{16} & a_{26} & a_{66}\end{bmatrix},\ [\mathbf{b}]=\begin{bmatrix}b_{11} & b_{12} & b_{16}\\ b_{12} & b_{22} & b_{26}\\ b_{16} & b_{26} & b_{66}\end{bmatrix},\ \text{and}\ [\mathbf{d}]=\begin{bmatrix}d_{11} & d_{12} & d_{16}\\ d_{12} & d_{22} & d_{26}\\ d_{16} & d_{26} & d_{66}\end{bmatrix} \tag{3.15b}$$

are compliance matrices and are related to the [A], [B], and [D] matrices by

$$\begin{bmatrix}a_{11} & a_{12} & a_{16} & b_{11} & b_{12} & b_{16}\\ a_{12} & a_{22} & a_{26} & b_{12} & b_{22} & b_{26}\\ a_{16} & a_{26} & a_{66} & b_{16} & b_{26} & b_{66}\\ b_{11} & b_{21} & b_{61} & d_{11} & d_{12} & d_{16}\\ b_{12} & b_{22} & b_{62} & d_{12} & d_{22} & d_{26}\\ b_{16} & b_{26} & b_{66} & d_{16} & d_{26} & d_{66}\end{bmatrix}=\begin{bmatrix}A_{11} & A_{12} & A_{16} & B_{11} & B_{12} & B_{16}\\ A_{12} & A_{22} & A_{26} & B_{12} & B_{22} & B_{26}\\ A_{16} & A_{26} & A_{66} & B_{16} & B_{26} & B_{66}\\ B_{11} & B_{12} & B_{16} & D_{11} & D_{12} & D_{16}\\ B_{12} & B_{22} & B_{26} & D_{12} & D_{22} & D_{26}\\ B_{16} & B_{26} & B_{66} & D_{16} & D_{26} & D_{66}\end{bmatrix}^{-1} \tag{3.16}$$

3.3.2. Coupling in Composite Laminates

As mentioned before the [A], [B], and [D] matrices represent the stiffness of a laminate and describe the response of the laminate to in-plane forces and moments. In details

- A_{ij} is the in-plane stiffness that relate the in-plane forces N_x, N_y, N_{xy} to the in-plane deformations ε_x^0, ε_y^0, ε_{xy}^0.
- B_{ij} is the in-plane-out-of-plane coupling stiffness that relate the in-plane forces N_x, N_y, N_{xy} to the curvatures k_x, k_y, k_{xy} and the moments M_x, M_y, M_{xy} to the in-plane deformations ε_x^0, ε_y^0, ε_{xy}^0.
- D_{ij} is the bending stiffness that relate the moments M_x, M_y, M_{xy} to the curvatures k_x, k_y, k_{xy}.

Examination of the [A], [B], and [D] matrices shows that different types of couplings may occur as discussed below.

Extension–shear coupling. When the elements A_{16} and A_{26} are not zero, in-plane normal forces N_x and N_y cause shear deformation ε_{xy}^0, and a twist force N_{xy} causes elongations in the x and y directions.

Bending–twist coupling. When the elements D_{16} and D_{26} are not zero, bending moments M_x and M_y cause twist of the laminate k_{xy}, and a twist moment M_{xy} causes curvatures in the x-z and y-z planes.

Extension–twist and bending–shear coupling. When the elements B_{16} and B_{26} are not zero, in-plane normal forces N_x and N_y cause twist k_{xy}, and bending moments M_x, M_y result in shear deformation ε_{xy}^0.

In-plane–out-of-plane coupling. When the elements B_{ij} are not zero, in-plane forces N_x, N_y, and N_{xy} cause out-of-plane deformations (curvatures) of the laminate, and moments M_x, M_y, and M_{xy} cause in-plane deformation in the x-y plane.

The preceding four coupling types are characteristic of composite materials and do not occur in homogeneous isotropic materials (Kollár and Springer, 2003).

3.3.3. Effective Thermoelastic Constants of Composite Laminates

The thermoelastic properties of a laminate are basically expressed in terms of the components of the 6×6 laminate compliances and the 6×1 vector of thermal expansion coefficients. Before give the definitions of these engineering constants, a transformation needs to be applied to ensure that all the compliance coefficients have been normalised to the necessary unit of [length^2/force]. A matrix $[\bar{S}]$ of equivalent laminate compliances is obtained by use of the total laminate thickness H as (Adolfsson and Gudmundson, 1997)

$$[\bar{S}]=\begin{bmatrix} H[\mathbf{a}] & \frac{H^2}{2}[\mathbf{b}] \\ \frac{H^2}{2}[\mathbf{b}]^T & \frac{H^3}{12}[\mathbf{d}] \end{bmatrix}=\begin{bmatrix} [\bar{\mathbf{a}}] & [\bar{\mathbf{b}}] \\ [\bar{\mathbf{b}}]^T & [\bar{\mathbf{d}}] \end{bmatrix} \tag{3.17}$$

Similarly, to let all thermal expansion coefficients have the same unit of [1/temperature], a 6×1 vector of equivalent thermal expansion coefficients $[\bar{\alpha}]$ is introduced as

$$[\bar{\alpha}]=\left[\alpha_1 \quad \alpha_2 \quad \alpha_3 \quad \frac{H}{2}\alpha_4 \quad \frac{H}{2}\alpha_5 \quad \frac{H}{2}\alpha_6\right]^T \tag{3.18}$$

From the compliance matrix $[\bar{S}]$, which is homogeneous with respect to dimension, the extension and shear moduli of the laminate are defined as

$$E_i=\frac{1}{\bar{a}_{ii}},\ i=1, 2, 6. \tag{3.19}$$

The bending and twisting moduli of the laminate are defined as

$$F_i=\frac{1}{\bar{d}_{ii}},\ i=1, 2, 6. \tag{3.20}$$

The extension–extension and extension–shear coupling ratios of the laminate are defined as

$$\nu_{ij}=-\frac{\bar{a}_{ij}}{\bar{a}_{ii}},\ i, j=1, 2, 6.\ i\neq j. \tag{3.21}$$

The bending–bending and bending–twisting coupling ratios of the laminate are defined as

$$\eta_{ij}=-\frac{\bar{d}_{ij}}{\bar{d}_{ii}},\ i, j=1, 2, 6.\ i\neq j. \tag{3.22}$$

The in-plane–out-of-plane coupling ratios of the laminate are defined as

$$\varphi_{ij} = -\frac{\bar{b}_{ij}}{\bar{a}_{ii}} \text{ and } \psi_{ij} = -\frac{\bar{b}_{ij}}{\bar{d}_{jj}},\ i, j=1, 2, 6. \tag{3.23}$$

The thermal expansion coefficients are simply expressed as the components $\bar{\alpha}_i$ (i=1, 2,..., 6) of the vector $[\bar{\alpha}]$.

For symmetric laminates, all the components in the stiffness matrix **[B]** and compliance matrix **[b]** are zero, thus there exists no in-plane–out-of-plane coupling. In this case, the extension and shear moduli E_1, E_2 and E_3 reduce to the ordinary in-plane Young's moduli and shear modulus, respectively.

The above effective thermoelastic constants will be used in Chapter 6 to characterise stiffness degradation due to transverse cracking.

3.4. The Energy Release Rate

Because of the conservative nature of many loadings and the reversible nature of elastic materials, energy principles represent important concepts in the theory of elasticity. These principles have played a fundamental role in the development of many of the concepts in fracture mechanics (Kanninen and Popelar, 1985). Some of the most pertinent principles are reviewed in this section.

3.4.1. Strain Energy and Complementary Strain Energy

The strain energy density is the stored internal energy per unit volume in a body upon which work has been done. If the internal energy is zero in the unstressed state, the strain energy density in the stressed state is

$$\bar{U} = \int \{\sigma\}^T d\{\varepsilon\} \tag{3.24}$$

For a linear elastic material, substituting the stress-strain relationships into Eq. (3.24) and integrating the equation gives the expression

$$\bar{U} = \frac{1}{2}\{\varepsilon\}^T [C]\{\varepsilon\} \tag{3.25}$$

Integration of the strain energy density over a given volume provides the strain energy of the body

$$U = \frac{1}{2}\iiint_V \{\varepsilon\}^T [C]\{\varepsilon\} dV \tag{3.26}$$

The complementary strain energy density is defined by

$$\overline{U}_c = \int \{\varepsilon\}^T d\{\sigma\} \tag{3.27}$$

Following the same procedure as used for strain energy, the complementary strain energy density over a given volume is

$$U_c = \frac{1}{2}\iiint_V \{\sigma\}^T [C]^{-1} \{\sigma\} dV \tag{3.28}$$

For a linear elastic material, the work done by the body forces and tractions acting through the displacements from the unstressed state to the final equilibrium configuration is equal to twice the strain energy or the complementary strain energy of the body.

3.4.2. Total Potential Energy and Total Complementary Potential Energy

The total potential energy Π is defined by the difference of the strain energy U and potential of external forces, i.e.

$$\Pi = U - V \tag{3.29}$$

where V is the potential of the external forces, while prescribed displacements will not contribute to it. The expression of V is

$$V = \sum \overline{F}\delta + \iiint_V \{f\}^T \{u\} dV + \int_{S_\sigma} \{\overline{p}\}^T \{u\} ds \tag{3.30}$$

where on the right-hand side of the equation the first term represents the potential of prescribed concentrated forces $\overline{F}$, the second term is the potential of body forces $\{f\}$, and the third term is the potential of prescribed surface tractions $\{\overline{p}\}$ on the boundary S_σ.

The total complementary potential energy Γ is defined by the difference of the complementary strain energy U_c and the potential of prescribed displacements

$$\Gamma = U_c - V_c \tag{3.31}$$

where V_e is the potential of the external displacements, while prescribed forces will not contribute to it. The expression of V_e is

$$V_e = \int_{S_u} \{\bar{u}\}^T \{p\} ds \tag{3.32}$$

where $\{\bar{u}\}$ is the prescribed displacement fields on the boundary S_u, and $\{p\}$ is the reaction on S_u.

3.4.3. The Energy Release Rate

Griffith (1920) approached the fracture of an ideally brittle material from a thermodynamic viewpoint. He postulated that during an increment of crack extension dA there can be no change in the total energy E composed of the sum of the total potential energy of deformation Π and the surface energy S; that is,

$$dE = d\Pi + dS = 0 \tag{3.33}$$

The surface energy S is the potential energy of the surface of the crack. The equation states that when a crack is able to propagate enough to fracture a material, the gain in the surface energy is equal to the loss of total potential energy

Irwin (1957) proposed an energy approach for fracture that is essentially equivalent to the Griffith model, while Irwin's approach is more convenient for solving engineering problems. The energy release rate G is defined by

$$G = -\frac{d\Pi}{dA} \tag{3.34}$$

G is the rate of change in the total potential energy within the crack area A. Since G is obtained from the derivative of a potential, it is also called the crack extension force or the crack driving force (Anderson, 2005).

In general for an elastic body the sum of the total potential energy and the total complementary potential energy Π vanishes (Lim and Li, 2005). Thus, G can also be expressed as

$$G = \frac{d\Gamma}{dA}. \tag{3.35}$$

Chapter 4. Free Edge and Transverse Cracking Effects in Cross-ply Laminates

4.1. Introduction

In cross-ply laminates fibres are only in the 0° and 90° directions. The cross-ply profile is one of the important profiles that are used to characterise composite material properties. The stacking sequence of composite laminates may be symmetric or nonsymmetric. For most designs of composite laminates, symmetric lay-ups about the middle-plane are often desirable in order to avoid the coupling effects between in-plane and out-of-plane loading. However, many practical applications require nonsymmetric laminates to specifically achieve the design requirements, e.g. the use of nonsymmetric laminates in a wind blade to produce a twisty and smooth shape and to reduce the buckling phenomena. Relatively less attention has been addressed to the analysis of interlaminar stresses in nonsymmetric laminates in the literature. Also little work has been done on the thermal stress problem associated with residual stresses resulting from manufacture at high temperature, although interlaminar thermal stresses may be more significant than the stresses due to mechanical loading.

In this chapter, a semi-analytical method is presented to evaluate the interlaminar stress singularities near free edges and transverse cracks in general cross-ply laminates subjected to biaxial extension, bending or/and thermal loading. The method is based on a state space representation of the three dimensional equations in elasticity and applied to generalised plane strain deformation and, therefore, the stress analysis can be simplified as a quasi-three-dimensional problem.

First a state space equation is developed for the free edge effect in a single orthotropic lamina. By establishing a recursive relationship between the state vectors on the upper and lower surfaces of an interface, the state space equation can then be extended to a multi-layer cross-ply laminate. After introducing the boundary conditions for free edges or transverse cracks, all the displacement and stress

components can finally be obtained. The applications of the method are demonstrated by numerical solutions and comparisons are made with other models.

4.2. Theoretical Modelling of Cross-ply Laminates

4.2.1. Stresses in an Orthotropic Lamina

Consider a single-layer lamina with constant thickness h, width L and infinite length in the Cartesian x-y-z coordinate system (Fig. 4.1). The displacements in the x, y and z directions are denoted by u, v and w, respectively. Suppose that the plate is subjected to a uniaxial tension by the application of a constant longitudinal strain ε_0 in the y direction and a uniform temperature variation, ΔT. The plate is made of a linearly elastic orthotropic material whose material axes of orthotropy coincide with the axes of the adopted co-ordinate system.

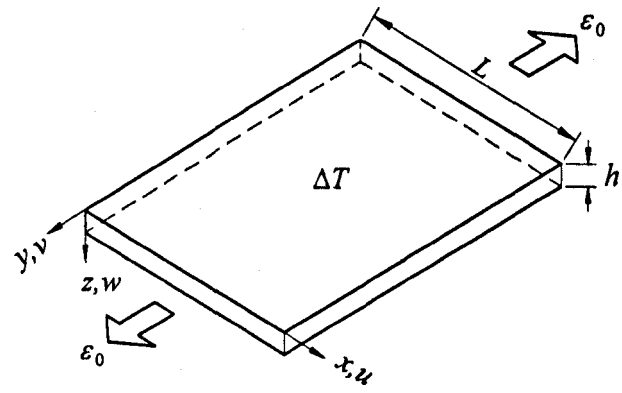

Fig. 4.1 Nomenclature of a single-layered lamina subjected to a uniaxial extension and uniform thermal loading.

(a) Stress-strain relations

The basic constitutive equation for thermo-elastic stress analysis is (Herakovich, 1998)

$$\{\sigma\} = [C](\{\varepsilon\} - \{\varepsilon^T\}) \tag{4.1}$$

Here, the matrices $[C]$, $\{\varepsilon\}$ and $\{\varepsilon^T\}$ are stiffness matrix, mechanical strains and thermal strains, respectively; for a linearly elastic orthotropic material,

$$[C]=\begin{bmatrix} C_{11} & C_{12} & C_{13} & 0 & 0 & 0 \\ C_{12} & C_{22} & C_{23} & 0 & 0 & 0 \\ C_{13} & C_{23} & C_{33} & 0 & 0 & 0 \\ 0 & 0 & 0 & C_{44} & 0 & 0 \\ 0 & 0 & 0 & 0 & C_{55} & 0 \\ 0 & 0 & 0 & 0 & 0 & C_{66} \end{bmatrix} \tag{4.2}$$

where the C_{ij} are stiffness coefficients that can be expressed in terms of elastic moduli, shear moduli and Poisson's ratios (See Appendix A for further details).

$$\{\varepsilon\}=[\varepsilon_{xx} \quad \varepsilon_{yy} \quad \varepsilon_{zz} \quad \varepsilon_{yz} \quad \varepsilon_{xz} \quad \varepsilon_{xy}]^{T} \tag{4.3}$$

$$\{\varepsilon^{T}\}=\{\alpha\}\Delta T \tag{4.4}$$

$$\{\alpha\}=[\alpha_x \quad \alpha_y \quad \alpha_z \quad 0 \quad 0 \quad 0]^{T} \tag{4.5}$$

where α_x, α_y and α_z are the coefficients of thermal expansion relative to the x, y, z directions, respectively.

(b) Equilibrium equations

$$\begin{cases} \dfrac{\partial \sigma_{xx}}{\partial x}+\dfrac{\partial \sigma_{xy}}{\partial y}+\dfrac{\partial \sigma_{xz}}{\partial z}=0 \\ \dfrac{\partial \sigma_{xy}}{\partial x}+\dfrac{\partial \sigma_{yy}}{\partial y}+\dfrac{\partial \sigma_{yz}}{\partial z}=0 \\ \dfrac{\partial \sigma_{xz}}{\partial x}+\dfrac{\partial \sigma_{yz}}{\partial y}+\dfrac{\partial \sigma_{zz}}{\partial z}=0 \end{cases} \tag{4.6}$$

(c) Strain-displacement relations

$$\begin{cases} \varepsilon_{xx}=\dfrac{\partial u}{\partial x}, & \varepsilon_{yy}=\dfrac{\partial v}{\partial y}, & \varepsilon_{zz}=\dfrac{\partial w}{\partial z} \\ \varepsilon_{yz}=\dfrac{\partial w}{\partial y}+\dfrac{\partial v}{\partial z}, & \varepsilon_{xz}=\dfrac{\partial u}{\partial z}+\dfrac{\partial w}{\partial x}, & \varepsilon_{xy}=\dfrac{\partial u}{\partial y}+\dfrac{\partial v}{\partial x} \end{cases} \tag{4.7}$$

Because the plate is subjected to a uniform extension ε_0 in the y direction, it follows that

$$\begin{aligned} \varepsilon_{yy}&=\frac{\partial v}{\partial y}=\varepsilon_0 \\ \varepsilon_{yz}&=\frac{\partial w}{\partial y}+\frac{\partial v}{\partial z}=0 \\ \varepsilon_{xy}&=\frac{\partial u}{\partial y}+\frac{\partial v}{\partial x}=0 \end{aligned} \tag{4.8}$$

As a result, we can conclude from Eqs. (4.1), (4.7) and (4.8) that $\sigma_{yz}= \sigma_{xy}=0$ and the other six variables, u, w, σ_{xz}, σ_{zz}, σ_{xx}, σ_{yy}, are all independent of y. The stress analysis is then restricted to a generalised plane strain problem.

To facilitate the following deduction process, let

$$\begin{aligned} &\alpha = \partial/\partial x\,,\ C_1 = -C_{13}/C_{33}\,, C_2 = C_{11} - C_{13}^2/C_{33}\,, \\ &C_3 = C_{12} - C_{13}C_{23}/C_{33}\,, C_4 = C_{22} - C_{23}^2/C_{33}\,, \\ &C_5 = -C_{23}/C_{33}\,,\ C_7 = 1/C_{33}\,,\ C_8 = 1/C_{55} \end{aligned} \tag{4.9}$$

From the third equation of Eq. (4.1) and Eq.(4.7), the following relation is obtained

$$\frac{\partial w}{\partial z} = C_1\alpha\, u + C_7\sigma_{zz} + C_5\varepsilon_0 - (C_1\alpha_x + C_5\alpha_y - \alpha_z)\Delta T \tag{4.10}$$

Substituting Eq. (4.10) into the first equation of Eq. (4.1) yields

$$\sigma_{xx} = C_2\alpha u - C_1\sigma_{zz} + C_3\varepsilon_o - (C_2\alpha_x + C_3\alpha_y)\Delta T \tag{4.11}$$

Inserting Eq.(4.11) into the first and third equations of Eq.(4.6) and considering Eq. (4.10) along with the fifth equation of Eq.(4.1), we can obtain the following first order non-homogenous partial differential equation system

$$\frac{\partial}{\partial z}\begin{Bmatrix} u \\ w \\ \sigma_{xz} \\ \sigma_{zz} \end{Bmatrix} = \begin{bmatrix} 0 & -\alpha & C_8 & 0 \\ C_1\alpha & 0 & 0 & C_7 \\ -C_2\alpha^2 & 0 & 0 & C_1\alpha \\ 0 & 0 & -\alpha & 0 \end{bmatrix}\begin{Bmatrix} u \\ w \\ \sigma_{xz} \\ \sigma_{zz} \end{Bmatrix} + \begin{Bmatrix} 0 \\ C_5\varepsilon_0 - (C_1\alpha_x + C_5\alpha_y - \alpha_z)\Delta T \\ 0 \\ 0 \end{Bmatrix} \tag{4.12}$$

Assuming that the displacement in the x direction u can be expressed as

$$u(x,z) = \bar{u}(x,z) + U^{(0)}(z)\left(1 - \frac{2x}{L}\right) \tag{4.13}$$

where $\bar{u}(x,z)$ and $U^{(0)}(z)$ are two unknown displacement functions that can be determined by imposing boundary conditions. The introduction of the second term is to ensure that the non-zero displacements at free edges can be satisfied. In this method, $U^{(0)}(z)$ is the main unknown function. The following derivations will focus on the determination of the unknown functions.

Introducing Eq. (4.13) into Eq. (4.12) yields

$$\frac{\partial}{\partial z}\{\mathbf{F}\} = [\mathbf{G}]\{\mathbf{F}\} + \{\mathbf{B}\} \tag{4.14a}$$

where

$$\{\mathbf{B}\}=\left[-\frac{dU^{(0)}(z)}{dz}\left(1-\frac{2x}{L}\right), C_5\varepsilon_0-(C_1\alpha_x+C_5\alpha_y-\alpha_z)\Delta T-\frac{2C_1}{L}U^{(0)}(z),0,0\right]^T \tag{4.14b}$$

$$\{\mathbf{F}\}=[\bar{u}\ \ w\ \ \sigma_{xz}\ \ \sigma_{zz}]^T \quad . \tag{4.14c}$$

and [G] is the 4×4 matrix shown in Eq. (4.12). For the displacements and stresses in {F}, the following Fourier series expansions are assumed

$$\begin{Bmatrix}\bar{u}\\ w\\ \sigma_{xz}\\ \sigma_{zz}\end{Bmatrix}=\sum_{m=0}^{\infty}\begin{Bmatrix}\bar{U}_m(z)\sin(\xi x)\\ W_m(z)\cos(\xi x)\\ X_m(z)\sin(\xi x)\\ Z_m(z)\cos(\xi x)\end{Bmatrix} \tag{4.15}$$

where, $\xi=m\pi/L$, L is the length of the plate in the x direction. There are two reasons why these particular forms of displacements and stresses are assigned. On the one hand, the boundary conditions can be satisfied automatically. On the other hand, the sinusoidal or cosinoidal term can be eliminated during further derivations. In the case of a uniformly distributed extension and thermal loading, the displacement in the x direction u is zero at $x=L/2$. Hence, the integer m in Eq. (4.15) takes only even numbers, i.e. $m = 0, 2, 4, \ldots$. In addition, from the first equation of Eq. (4.15), the displacement $\bar{u}$ is zero at x=0 and L. At the free edges, the displacement is not necessary to be zero. The second term of Eq. (4.3) was then introduced to satisfy the non-zero displacements at free edges.

Substituting Eq. (4.15) into Eq. (4.14a) and expanding also the x co-ordinate in {B} into a Fourier series, as follows

$$\begin{cases}x=-\dfrac{2L}{\pi}\displaystyle\sum_{m=0}^{\infty}\frac{\cos m\pi}{m}\sin\frac{m\pi x}{L}\\ 1=\dfrac{2}{\pi}\displaystyle\sum_{m=0}^{\infty}\frac{1-\cos m\pi}{m}\sin\frac{m\pi x}{L}\end{cases} \tag{4.16}$$

one has the following non-homogenous state space equation for an arbitrary value of m

$$\frac{d}{dz}\{\mathbf{F}_m(z)\}=[\mathbf{G}_m]\{\mathbf{F}_m(z)\}+\{\mathbf{B}_m(z)\} \tag{4.17a}$$

where

$$\{\mathbf{F}_m(z)\}=[\bar{U}_m(z)\ \ W_m(z)\ \ X_m(z)\ \ Z_m(z)]^T \tag{4.17b}$$

$$[\mathbf{G}_m]=\begin{bmatrix} 0 & \xi & C_8 & 0 \\ C_1\xi & 0 & 0 & C_7 \\ C_2\xi^2 & 0 & 0 & -C_1\xi \\ 0 & 0 & -\xi & 0 \end{bmatrix} \tag{4.17c}$$

$$\{\mathbf{B}_0(z)\}=\left[0, C_5\varepsilon_0-(C_1\alpha_x+C_5\alpha_y-\alpha_z)\Delta T-\frac{2C_1}{L}U^{(0)}(z),0,0\right]^T \tag{4.17d}$$

$$\{\mathbf{B}_m(z)\}=\left[-\frac{2}{m\pi}(1+\cos m\pi)\frac{dU^{(0)}(z)}{dz} \quad 0 \quad 0 \quad 0\right]^T, (m=2,4,\cdots) \tag{4.17e}$$

The solution of Eq.(4.17a) can be written as

$$\{\mathbf{F}_m(z)\}=[\mathbf{D}_m(z)]\{\mathbf{F}_m(0)\}+\{\mathbf{H}_m(z)\} \tag{4.18a}$$

where

$$[\mathbf{D}_m(z)]=e^{[G_m]z},$$

$$\{\mathbf{H}_m(z)\}=\int_0^z e^{[G_m](z-\tau)}\{\mathbf{B}_m(\tau)\}d\tau \qquad (z\in[0,h]) \tag{4.18b}$$

In particular, at $z=h$,

$$\{\mathbf{F}_m(h)\}=[\mathbf{D}_m(h)]\{\mathbf{F}_m(0)\}+\{\mathbf{H}_m(h)\} \tag{4.19}$$

where $[\mathbf{D}_m(h)]$ is called transfer matrix that can be calculated either analytically or numerically. The calculation of the two constant matrices, $[\mathbf{D}_m(h)]$ and $\{\mathbf{H}_m(h)\}$, in Eq. (4.18) can be found from Ye (2002) or Moler and Van Loan (2003). It is worth mentioning that $\{\mathbf{H}_m(h)\}$ still contains unknown functions $U^{(0)}(z)$, which can only be determined by introducing the boundary conditions.

4.2.2. Stresses in a Cross-ply Laminate

Consider an infinite long multi-layered cross-ply laminated plate of thickness H and width L (Fig. 4.2). The plate is subjected to a uniaxial tension by application of a constant longitudinal strain, ε_0, and a uniform temperature variation, ΔT.

In order to find the solution of the problem, we must evaluate first the unknown displacement function, $U^{(0)}(z)$, appearing in Eqs. (4.13) and (4.17). If the fictitious sub-layers of the laminate are all sufficiently thin, it is reasonable to assume that the displacement $U^{(0)}(z)$ within the thin layer is linearly distributed in the z direction, i.e.

$$U_j^{(0)}(z) = U_j^-(1-\frac{z}{h_j}) + U_j^+ \frac{z}{h_j} \qquad z \in [0,\ h_j],\ \ j = 1, 2, \cdots, N, \tag{4.20}$$

where U_j^- and U_j^+ are the values of $U_j^{(0)}(z)$ at the upper and bottom surfaces of the jth thin layer.

For this thick multi-layered laminated plate, we may imagine that it is composed of N fictitious sub-layers, each of which may have different thickness. However, it is assumed that the thickness of all the fictitious sub-layers approach zero uniformly as N approaches infinity. Assuming, in addition, that different sub-layers may be composed of different orthotropic materials, two types of material interfaces are distinguished in the plate; the fictitious interfaces which separate sub-layers with the same material properties and the real ones that separate sub-layers composed of different materials.

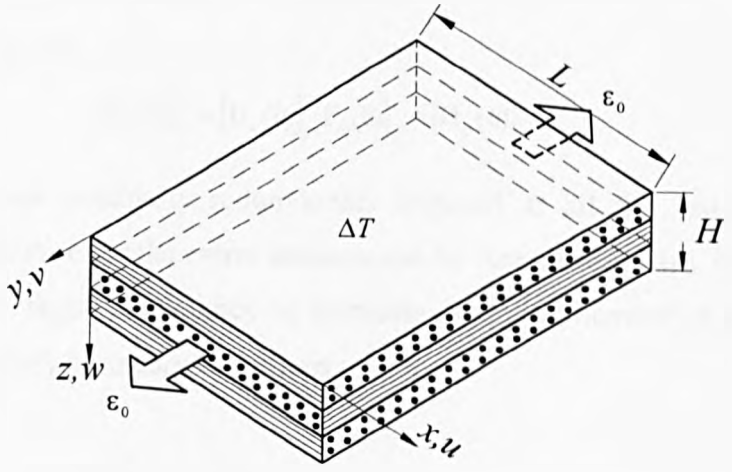

Fig. 4.2 Nomenclature of a cross-ply laminate subjected to a uniaxial tension and uniform thermal loading.

Upon choosing a suitably large value of N, each individual sub-layer becomes sufficiently thin and, as a result, Eqs. (4.17)–(4.19) are considered to be adequate for the solutions of these layers. The state space equation and the form of solution of the jth sub-layer then become

$$\frac{d}{dz}\{\mathbf{F}_m(z)\}_j = [\mathbf{G}_m]_j \{\mathbf{F}_m(z)\}_j + \{\mathbf{B}_m(z)\}_j \tag{4.21}$$

$$\begin{aligned}\{\mathbf{F}_m(z)\}_j &= e^{[\mathbf{G}_m]_j z}\{\mathbf{F}_m(0)\}_j + \int_0^z e^{[\mathbf{G}_m]_j(z-\tau)}\{\mathbf{B}_m(\tau)\}_j d\tau \\ &= [\mathbf{D}_m(z)]_j\{\mathbf{F}_m(0)\}_j + \{\mathbf{H}_m(z)\}_j \qquad (z\in[0,h_j])\end{aligned} \tag{4.22a}$$

where

$$\{\mathbf{F}_m(z)\}_j = [\bar{U}_m(z)\ \ W_m(z)\ \ X_m(z)\ \ Z_m(z)]_j^T \tag{4.22b}$$

$$[\mathbf{G}_m]_j = \begin{bmatrix} 0 & \xi & C_8 & 0 \\ C_1\xi & 0 & 0 & C_7 \\ C_2\xi^2 & 0 & 0 & -C_1\xi \\ 0 & 0 & -\xi & 0 \end{bmatrix}_j \tag{4.22c}$$

$$\{\mathbf{B}_0(z)\}_j = \left[0, C_5\varepsilon_0 - (C_1\alpha_x + C_5\alpha_y - \alpha_z)\Delta T - \frac{2C_1}{L}U^{(0)}(z), 0, 0\right]_j^T \tag{4.22d}$$

$$\{\mathbf{B}_m(z)\}_j = \left[-\frac{2}{m\pi}(1+\cos m\pi)\frac{dU^{(0)}(z)}{dz} \quad 0 \quad 0 \quad 0\right]_j^T, (m=2,4,\cdots) \tag{4.22e}$$

In particular, at $z=h$,

$$\{\mathbf{F}_m(h)\}_j = [\mathbf{D}_m(h)]_j\{\mathbf{F}_m(0)\}_j + \{\mathbf{H}_m(h)\}_j \tag{4.23}$$

With appropriate continuity requirements imposed at all the real and fictitious interfaces, a solution for the entire laminate can be formulated. Also, the solution can be found to the required accuracy by increasing the total number of the thin layers, subjected to satisfy boundary conditions.

Inserting Eq. (4.20) into Eqs. (4.22d) and (4.22e), vector $\{\mathbf{B}_m(z)\}_j$ in Eq. (4.21) can be expressed as

$$\{\mathbf{B}_0(z)\}_j = \left[0, C_5\varepsilon_0 - (C_1\alpha_x + C_5\alpha_y - \alpha_z)\Delta T - \frac{2C_1}{L}\left(U_j^-(1-\frac{z}{h_j}) + U_j^+\frac{z}{h_j}\right), 0, 0\right]_j^T \tag{4.24}$$

$$\{\mathbf{B}_m(z)\}_j = \left[\frac{4}{m\pi}\frac{U_j^- - U_j^+}{h_j} \quad 0 \quad 0 \quad 0\right]_j^T, \ (m=2,4,\cdots) \tag{4.25}$$

By introducing the following continuity conditions at all interfaces, i.e.,

$$\{\mathbf{F}_m(0)\}_{j+1} = \{\mathbf{F}_m(h_j)\}_j \tag{4.26}$$

and then using Eqs.(4.23) and (4.26) recursively, a relationship between the state vectors on the bottom and top surfaces of the plate is established as follows

$$\{\mathbf{F}_m(h_N)\}_N = [\bar{\mathbf{D}}_m]_N \{\mathbf{F}_m(0)\}_1 + \{\bar{\mathbf{H}}_m\} \tag{4.27a}$$

where

$$[\bar{\mathbf{D}}_m]_N = \left(\prod_{j=N}^{1} [\mathbf{D}_m(h_j)]_j\right) \tag{4.27b}$$

$$\{\bar{\mathbf{H}}_m\} = \left(\prod_{j=N}^{2} [\mathbf{D}_m]_j\right)\{\mathbf{H}_m\}_1 + \left(\prod_{j=N}^{3} [\mathbf{D}_m]_j\right)\{\mathbf{H}_m\}_2 + \cdots + \{\mathbf{H}_m\}_N \tag{4.27c}$$

$\{\mathbf{F}_m(0)\}_1$ and $\{\mathbf{F}_m(h_N)\}_N$ are, respectively, the state vectors at the top and bottom surfaces of the laminated plate. Upon using the traction free conditions at the top and bottom surfaces, the following stress conditions are obtained

$$\begin{aligned} [X_m(h_N),\ Z_m(h_N)]_N^{\mathrm{T}} &= (0,\ 0)^{\mathrm{T}} \\ [X_m(0),\ Z_m(0)]_1^{\mathrm{T}} &= (0,\ 0)^{\mathrm{T}} \end{aligned} \tag{4.28}$$

Substituting Eq. (4.28) into Eq. (4.27) yields the following linear algebraic equation system

$$\begin{bmatrix} \bar{D}_{31} & \bar{D}_{32} \\ \bar{D}_{41} & \bar{D}_{42} \end{bmatrix} \begin{Bmatrix} \bar{U}_m \\ W_m \end{Bmatrix}_1 = -\begin{Bmatrix} \bar{H}_{m3} \\ \bar{H}_{m4} \end{Bmatrix} \tag{4.29}$$

where $\bar{D}_{ij}$ and $\bar{H}_{mi}$ are the relevant elements in $[\bar{\mathbf{D}}_m]$ and $\{\bar{\mathbf{H}}_m\}$, respectively.

Eq.(4.29) is a set of linear algebraic equations in terms of the two displacement components, $\bar{U}_m$ and W_m, at the top surface. The free terms of Eq. (4.29), $\bar{H}_{m3}$ and $\bar{H}_{m4}$, contain U_j^- and U_j^+ (j=1, 2,...N), introduced in Eq.(4.20). Because of the continuity of $U^{(0)}(z)$ at the interface between the jth and the (j+1)th sub-layers, the relationships, $U_j^+ = U_{j+1}^-$ (j=1, 2,...N-1), are obtained. Hence, the number of unknown constants is then reduced to (N+1). These constants are determined by introducing appropriate boundary conditions.

4.3. Geometry and Material Discontinuity

4.3.1. Free Edges of a Cross-ply Laminate Subjected to Axial Extension

Typical composite laminates with free edges are shown in Figs. 1.2 and 4.2. The free edge conditions at $x=0, L$ are as follows

$$\sigma_{xz} = \sigma_{xy} = \sigma_{xx} = 0 \tag{4.30}$$

It can be seen from Eqs. (4.8) and (4.15) that $\sigma_{xz} = \sigma_{xy} = 0$ are satisfied automatically along the free edges (x=0, L). The remaining boundary condition to be satisfied at the free edges is $\sigma_{xx} = 0$. In order to impose the condition at the two free edges, we introduce Eq. (4.13) into Eq.(4.11). As a result, the normal stress in the x direction is expressed as follows

$$\sigma_{xx} = C_2\alpha\bar{u} - C_1\sigma_{zz} + C_3\varepsilon_o - (C_2\alpha_x + C_3\alpha_y)\Delta T - C_2\frac{2U^{(0)}}{L} \tag{4.31}$$

After substituting Eq. (4.15) into Eq. (4.31), we obtain for the *jth* sub-layer

$$\sigma_{xx} = \sum_m \left[C_2\xi\bar{U}_m(z) - C_1 Z_m(z)\right]_j \cos\xi x + \left[C_3\varepsilon_0 - (C_2\alpha_x + C_3\alpha_y)\Delta T\right]_j - \left[\frac{2C_2}{L}U^{(0)}(z)\right]_j \tag{4.32}$$

Due to symmetry, we only need to impose the condition at x=0. Thus, from Eq. (4.32), we obtain the following condition

$$\sum_m \left[C_2\xi\bar{U}_m(z) - C_1 Z_m(z)\right]_j + \left[C_3\varepsilon_0 - (C_2\alpha_x + C_3\alpha_y)\Delta T\right]_j - \left[\frac{2C_2}{L}U^{(0)}(z)\right]_j = 0 \tag{4.33}$$

It has been mentioned in the previous section that Eq. (4.29) contains unknown constants U_j^- and U_j^+ (j=1, 2, ..., N). To evaluate for the constants, we first consider the continuity of $U^{(0)}(z)$ at the interface between the jth and the (j+1)th sub-layers. From Eq.(4.20), the following relationship is obtained

$$U_j^+ = U_{j+1}^- \qquad (j = 1, 2, \cdots, N-1) \tag{4.34}$$

Hence, there exist only (N+1) independent unknown constants. In order to evaluate these constants and also the two displacement components of the top surface (see Eq.(4.29)), the traction free condition Eq. (4.33) must be satisfied at the edges of all interfaces, including the fictitious and material interfaces. This can be done by introducing z-coordinates of the interfaces, z_j, into Eq.(4.33) (with z_1=0 and z_{N+1}=H)

$$\begin{cases} \sum_m \left[C_2\xi\bar{U}_m(z_1)-C_1Z_m(z_1)\right]_j+\left[C_3\varepsilon_0-(C_2\alpha_x+C_3\alpha_y)\Delta T\right]_j-\left[\frac{2C_2}{L}U^{(0)}(z_1)\right]_j=0 \\ \sum_m \left[C_2\xi\bar{U}_m(z_2)-C_1Z_m(z_2)\right]_j+\left[C_3\varepsilon_0-(C_2\alpha_x+C_3\alpha_y)\Delta T\right]_j-\left[\frac{2C_2}{L}U^{(0)}(z_2)\right]_j=0 \\ \vdots \\ \sum_m \left[C_2\xi\bar{U}_m(z_j)-C_1Z_m(z_j)\right]_j+\left[C_3\varepsilon_0-(C_2\alpha_x+C_3\alpha_y)\Delta T\right]_j-\left[\frac{2C_2}{L}U^{(0)}(z_j)\right]_j=0 \\ \vdots \\ \sum_m \left[C_2\xi\bar{U}_m(z_{N+1})-C_1Z_m(z_{N+1})\right]_j+\left[C_3\varepsilon_0-(C_2\alpha_x+C_3\alpha_y)\Delta T\right]_j-\left[\frac{2C_2}{L}U^{(0)}(z_{N+1})\right]_j=0 \end{cases} \tag{4.35}$$

This process yields (N+1) independent linear algebraic equations. Along with the two equations from Eq.(4.29), the two displacement components and the (N+1) unknown constants can finally be solved. Once the equation system is solved, all the displacements and stresses can be obtained by substituting the solutions to the iterative Eqs. (4.23) and (4.26).

4.3.2. Transverse Cracks in a Cross-ply Laminate

4.3.2.1. Under In-plane Biaxial Extension and Thermal Loading

When a cross-ply laminate is subjected to biaxial tension and a uniform temperature variation, transverse ply cracks appear parallel to the fibres and across the entire width from edge to edge. For example the $[0°_m/90°_n/0°_s]$ laminate shown in Fig. 4.3 displays an array of periodic cracks in the $90°_n$ layers, where the subscripts denote the number of such layers. Assuming that the distribution of the cracks is equally spaced, a representative element (see Fig. 4.4) can be taken out from two neighbouring cracks to predict the stress and displacement fields. In Fig. 4.4 a global rectangular Cartesian co-ordinate system x-z is chosen for the element.

In order to use the recursive formulations the representative element is further divided into N fictitious sub-layers. Again, each sub-layer may have different thickness and different sub-layers may be composed of different orthotropic materials.

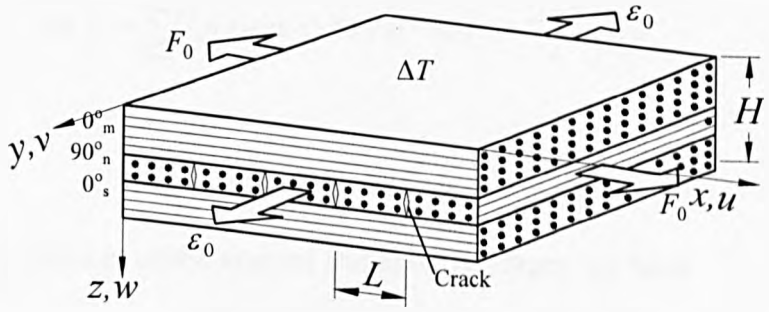

Fig. 4.3 Schematic of a $[0°_m/90°_n/0°_s]$ laminate with an array of transverse ply cracks in $90°_n$ layers.

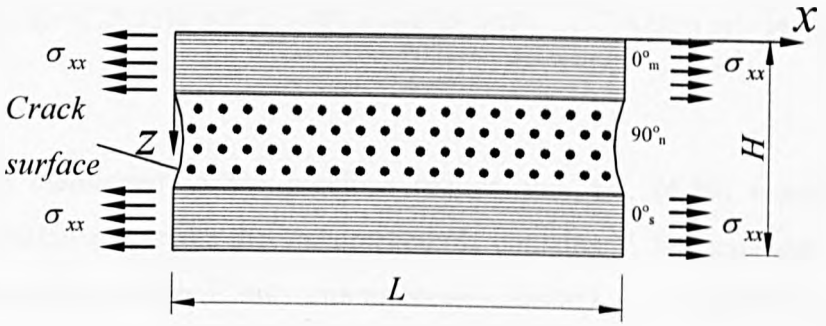

Fig. 4.4 A representative element of a $[0°_m/90°_n/0°_s]$ cracked laminate subjected to in-plane extension and thermal loading.

For the cracked layers at $x=0, L$ the crack surfaces are traction free, i.e.

$$\sigma_{xz} = \sigma_{xy} = \sigma_{xx} = 0 \tag{4.36}$$

From Eqs. (4.36) and (4.30), it is seen that the boundary conditions of transverse cracks are the same as those of free edges. As a result Eq. (4.33) can be used directly to satisfy the crack surface condition.

For the uncracked layers at $x=0, L$, due to the fact that the laminate is subjected to a uniform extension and thermal loading, the longitudinal displacement of an arbitrary jth layer in the x direction remains constant, that is

$$u(0,z) = u_0, \; u(L,z) = -u_0 \tag{4.37}$$

Because of symmetry we only consider the boundary condition at $x=0$. Substituting Eq. (4.36) and $x=0$ into the first equation of Eq. (4.15) and Eq. (4.13) yields

$$u(0,z)=\sum_{m=0}^{\infty}\bar{U}_m(z)\sin(\xi\times 0)+U^{(0)}(z)\left(1-\frac{2\times 0}{L}\right)=u_0 \tag{4.38a}$$

or

$$u(0,z)=U^{(0)}(z)=u_0 \tag{4.38b}$$

From the equilibrium of the internal and external forces, we have

$$\int_H \sigma_{xx}dz=F_0 \tag{4.39}$$

Introducing Eq. (4.32) and x=0 into Eq. (4.39)

$$\int_H\left(\sum_m\left[C_2\xi\bar{U}_m(z)-C_1Z_m(z)\right]_j+\left[C_3\varepsilon_0-(C_2\alpha_x+C_3\alpha_y)\Delta T\right]_j-\left[\frac{2C_2}{L}U^{(0)}(z)\right]_j\right)dz=F_0 \tag{4.40}$$

It has been mentioned in the previous section that Eq. (4.29) contains (N+1) unknown constants. Assume that the cracked ply contains N_c fictitious sub-layers. In the uncracked layers, there is only one unknown constant u_0. In addition to the (N_c-1) unknown constants in the cracked ply, then the number of independent unknown constants is further reduced to N_c in Eq. (4.29). In order to evaluate these constants and also the two displacement components of the top surface (see Eq.(4.29)), where the traction free condition Eq. (4.33) must be satisfied at the crack surfaces of the (N_c-1) interfaces.

$$\begin{cases}\sum_m\left[C_2\xi\bar{U}_m(z_1^c)-C_1Z_m(z_1^c)\right]_j+\left[C_3\varepsilon_0-(C_2\alpha_x+C_3\alpha_y)\Delta T\right]_j-\left[\frac{2C_2}{L}U^{(0)}(z_1^c)\right]_j=0\\ \sum_m\left[C_2\xi\bar{U}_m(z_2^c)-C_1Z_m(z_2^c)\right]_j+\left[C_3\varepsilon_0-(C_2\alpha_x+C_3\alpha_y)\Delta T\right]_j-\left[\frac{2C_2}{L}U^{(0)}(z_2^c)\right]_j=0\\ \vdots\\ \sum_m\left[C_2\xi\bar{U}_m(z_j^c)-C_1Z_m(z_j^c)\right]_j+\left[C_3\varepsilon_0-(C_2\alpha_x+C_3\alpha_y)\Delta T\right]_j-\left[\frac{2C_2}{L}U^{(0)}(z_j^c)\right]_j=0\\ \vdots\\ \sum_m\left[C_2\xi\bar{U}_m(z_{N_c-1}^c)-C_1Z_m(z_{N_c-1}^c)\right]_j+\left[C_3\varepsilon_0-(C_2\alpha_x+C_3\alpha_y)\Delta T\right]_j-\left[\frac{2C_2}{L}U^{(0)}(z_{N_c-1}^c)\right]_j=0\end{cases} \tag{4.41}$$

where z_j^c (j=1, 2, …, N_c-1) denotes the z coordinates of interfaces within the cracked layers. This process yields (N_c-1) independent linear algebraic equations. Along with Eq. (4.40) and the two equations from Eq. (4.29), the two displacement components and the N_c unknown constants can finally be solved. All the displacements and

stresses can be obtained by substituting the solutions to the iterative Eqs. (4.23) and (4.26).

4.3.2.2. Under Out-of-plane Bending

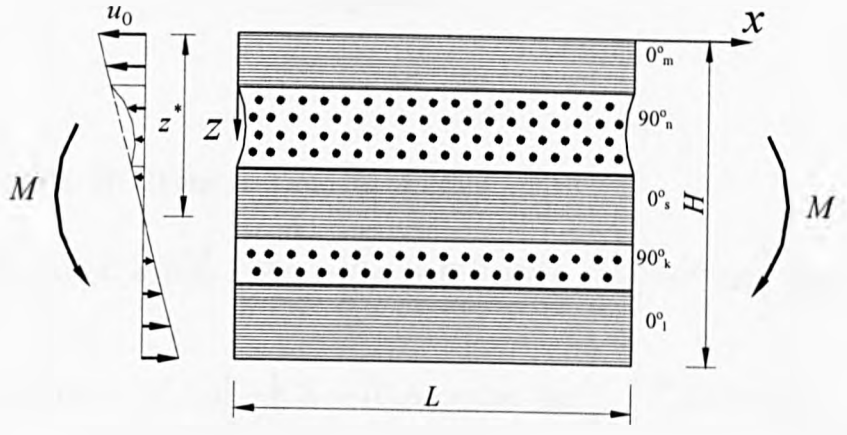

Fig. 4.5 A representative element of a $[0°_m/90°_n/0°_s/90°_k/0°_l]$ cracked laminate subjected to bending.

When a cross-ply laminate is subjected to bending, M, transverse ply cracks often appear in the tensile 90° layers. For example, Fig. 4.5 shows that a representative element taken from a $[0°_m/90°_n/0°_s/90°_k/0°_l]$ laminate under bending displays ply cracks in the upper $90°_n$ layers.

For the cracked layers at $x=0, L$ the crack surfaces are traction free. Hence Eq. (4.33) can be used directly to satisfy the crack surface condition.

For the uncracked layers, the displacement u is assumed to be linear function of the through-thickness z coordinate, i.e.

$$u(0,z) = u_0(1-\frac{z}{z^*}) \tag{4.42}$$

where u_0 is the longitude displacement of the top surface in the x direction and z^* is the z-coordinate of the neutral axial of the cracked laminate. Substituting Eq. (4.42) and x=0 into the first equation of Eq. (4.15) and Eq. (4.13) yields

$$u(0,z) = \sum_{m=0}^{\infty}\overline{U}_m(z)\sin(\xi\times 0) + U^{(0)}(z)\left(1-\frac{2\times 0}{L}\right) = u_0(1-\frac{z}{z^*}) \tag{4.43a}$$

or

$$u(0,z) = U^{(0)}(z) = u_0(1 - \frac{z}{z^*}) \tag{4.43b}$$

For the cracked laminate subjected to pure bending, two equilibrium equations exist at x=0

$$\int_H \sigma_{xx} dz = 0 \tag{4.44a}$$

$$\int_H \sigma_{xx}(z - z^*) dz = M \tag{4.44b}$$

Introducing Eq. (4.32) and x=0 into Eq (4.44)

$$\int_H \left(\sum_m \left[C_2 \xi \bar{U}_m(z) - C_1 Z_m(z) \right]_j + \left[C_3 \varepsilon_0 - (C_2 \alpha_x + C_3 \alpha_y) \Delta T \right]_j - \left[\frac{2C_2}{L} U^{(0)}(z) \right]_j \right) dz = 0 \tag{4.45a}$$

$$\int_H \left(\sum_m \left[C_2 \xi \bar{U}_m(z) - C_1 Z_m(z) \right]_j + \left[C_3 \varepsilon_0 - (C_2 \alpha_x + C_3 \alpha_y) \Delta T \right]_j - \left[\frac{2C_2}{L} U^{(0)}(z) \right]_j \right) (z - z^*) dz = M \tag{4.45b}$$

Once again assume that the upper cracked ply contains N_c fictitious sub-layers. In the uncracked layers, there are two unknown constants: u_0 and z^*. In addition to the (N_c-1) unknown constants in the cracked ply, there exists (N_c +1) unknown constants in Eq. (4.29). In order to evaluate these constants and also the two displacement components of the top surface (see Eq.(4.29)), employing the traction free condition (Eq. (4.33)) at the crack surface yields (N_c-1) independent linear algebraic equations (the same as Eq. (4.41)). Along with Eqs. (4.45a), (4.45b) and the two equations from Eq. (4.29), the two displacement components and the (N_c+1) unknown constants can finally be solved.

4.4. Numerical Results

In what follows several numerical examples of free edge and transverse crack effects are presented for symmetric and nonsymmetric cross-ply laminates subjected to uniform axial extension, thermal loading and/or bending. The convergence study of the stresses in the vicinity of free edges is presented first. The interlaminar stress distributions near free edges and transverse cracks subjected to different loading cases are then presented.

4.4.1. Free Edge Effects

4.4.1.1. Convergence Study

To study the convergence of the stresses near free edges, one simple laminate $[0°/90°]_s$ subjected to a uniform constant axial strain ε_0 is considered. The following elastic stiffnesses are assumed

$$C_{11}=C_{33}=15300N/mm^2,\ C_{22}=140000N/mm^2,$$
$$C_{44}=C_{55}=5900N/mm^2,\ C_{12}=C_{23}=3900N/mm^2, \tag{4.46}$$
$$C_{13}=3300N/mm^2$$

The laminate has a width L, and thickness h, where L=10h. All material layers have equal thickness h/4 and are idealised as homogeneous orthotropic layers. In order to obtain an accurate result near the free edge, the number of terms m included in the Fourier series expansion (see Eq. (4.15)) and the number of layer refinement N must be taken sufficiently large.

Fig. 4.6 and Fig. 4.7 show the convergence of the numerical values of σ_{xz} and σ_{zz} at the 0°/90° interface against different N with m=400 and different m with N=40, respectively. It is seen that the σ_{xz} is noticeably dependent on N and m. It can also be seen that the convergence of σ_{zz} is faster than σ_{xz}. Even for the shear stress σ_{xz}, the difference between m=400 and m=600 is not significant. In the following studies, therefore, results are obtained by taking m=400 and N=40.

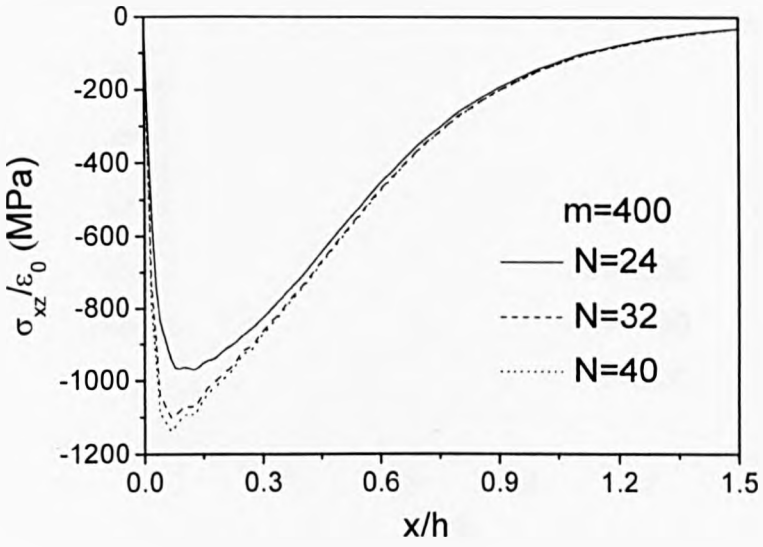

(a) Interlaminar shear stresses

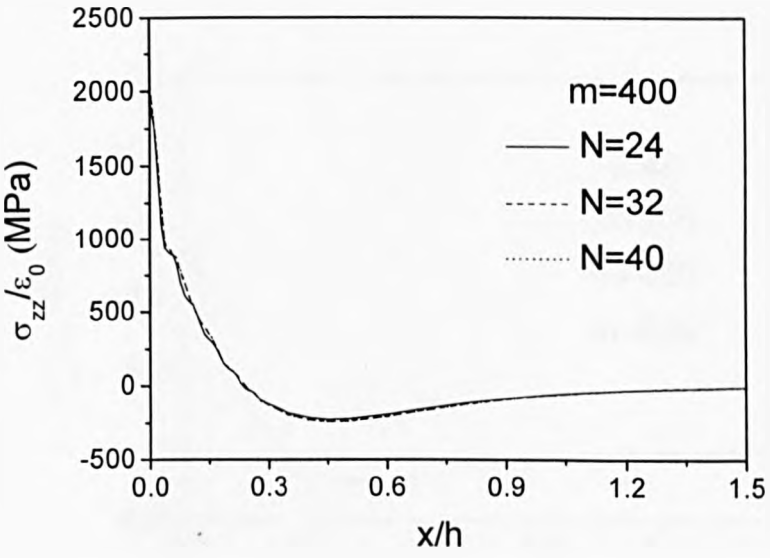

(b) Interlaminar normal stresses

Fig. 4.6 Convergence of interlaminar stresses at $0^o/90^o$ interface in $[0^o/90^o]_s$ laminate under uniform axial strain against different N with m=400.

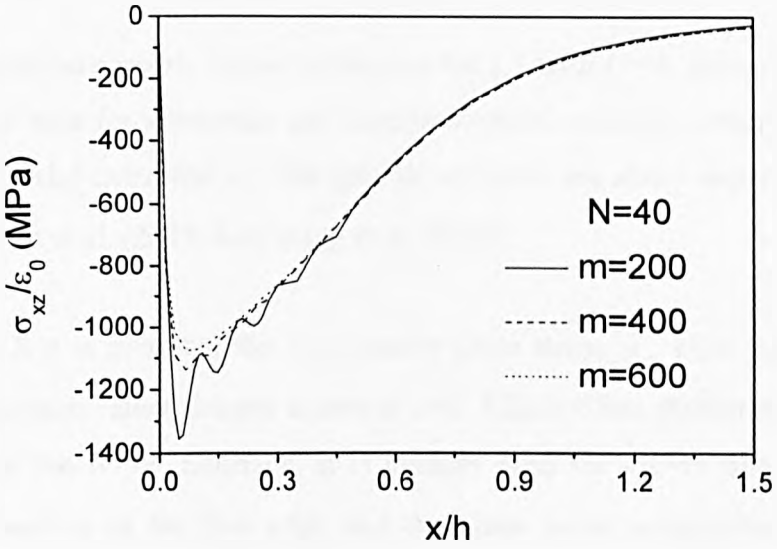

(a) Interlaminar shear stresses

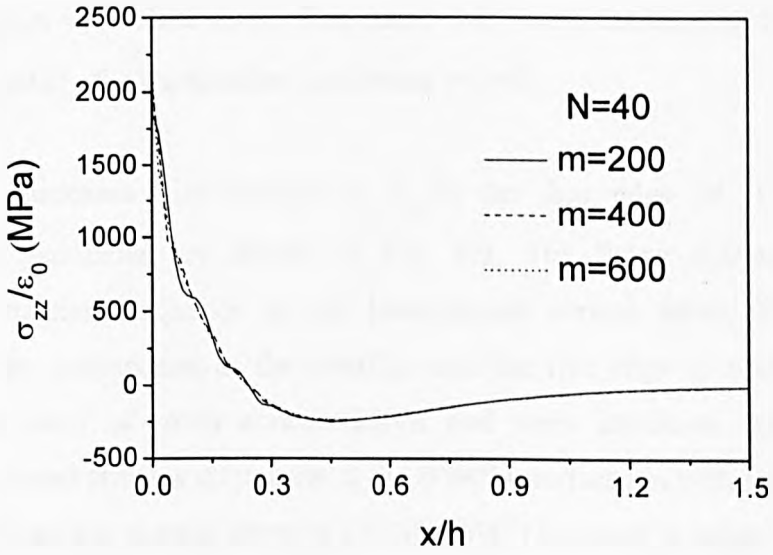

(b) Interlaminar normal stresses

Fig. 4.7 Convergence of interlaminar stresses at $0^o/90^o$ interface in $[0^o/90^o]_s$ laminate under uniform axial strain against different m with N=40.

4.4.1.2. Uniform Axial Extension

Using the material property shown in Section 4.4.1.1 with $L=4h$, numerical examples are presented here for symmetric and nonsymmetrical cross-ply laminates subjected to a uniform axial extension ε_0. The graphic solutions are also compared with those obtained by Ye et al. (2004) and Wang et al. (2000).

From Fig. 4.8 it is seen that the interlaminar shear stress σ_{xz} rises toward the free edge but decreases rather sharply to zero at $x=0$. This is often attributed to a possible singularity at the $0^o/90^o$ interface. It is evident from the curves that σ_{zz} exhibits singular behaviour at the free edge and the plane stress assumption used in the Classical Laminate Theory (CLT) is no more valid here. However, the interlaminar stresses approach to zero after $x>1.5h$. This illuminates that the interlaminar stress disturbance occurs only near the free edge. These results agree well with those of Ye et al. (2004) and Wang et al. (2000), while significant differences are observed for σ_{xz} in the region very close at the free edge. It is worth mentioning that Wang's results do not satisfy the traction free conditions at $x=0$.

The through thickness distributions of σ_{zz} at the free edge of $[0^o/90^o]_s$ and $[0^o/90^o/0^o/90^o]$ laminates are shown in Fig. 4.9. The figure demonstrates the influence of stacking sequence on the interlaminar normal stress. The singular behaviour at the intersection of the interface and the free edge is evident in both curves in the form of stress concentrations and steep gradients. Although the interlaminar normal stresses are tensile at the $0^o/90^o$ interfaces in both laminates, the maximum interlaminar normal stress of $[0^o/90^o/0^o/90^o]$ laminate is larger than that of $[0^o/90^o]_s$. For the nonsymmetric laminate, the interlaminar normal stress is compressive in the lower 0^o layer.

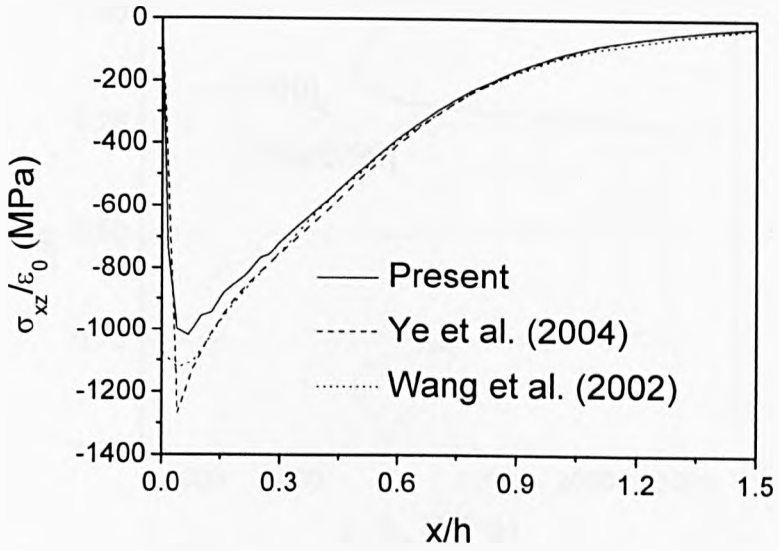

(a) Interlaminar shear stresses

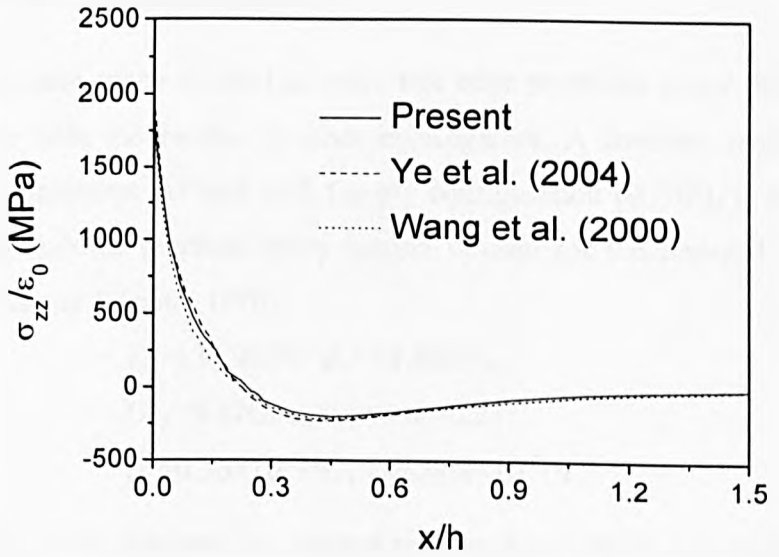

(b) Interlaminar normal stresses

Fig. 4.8 Distribution of interlaminar stresses at the $0^o/90^o$ interface in $[0^o/90^o]_s$ laminate under uniform axial strain.

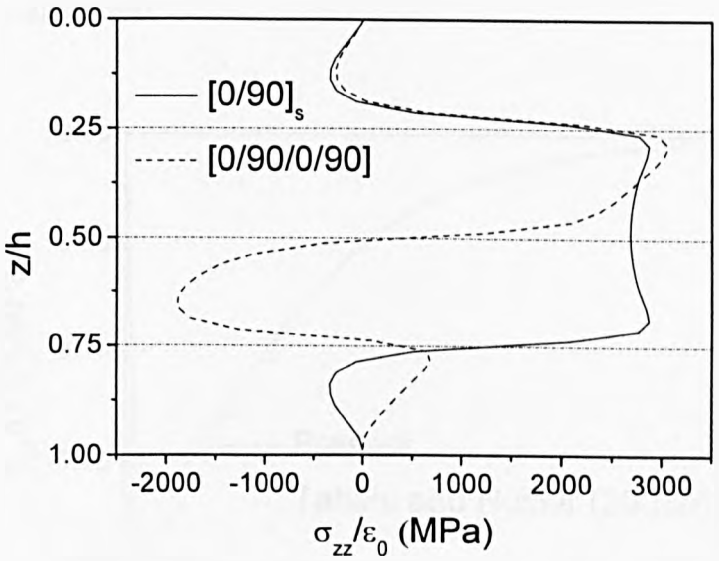

Fig. 4.9 Through the thickness distribution of interlaminar normal stress in $[0^o/90^o]_s$ and $[0^o/90^o/0^o/90^o]$ laminates under uniform axial strain.

4.4.1.3. Uniform Thermal Loading

To apply the state space method to solve free edge problems under thermal loading and compare with the results of other investigators, A laminate under a uniform temperature increment ΔT and with the ply configuration $[90^o/0^o]_s$ is considered. A typical high-modulus graphite/epoxy lamina is used for the material properties as follows (Pipes and Pagano, 1970)

$$\begin{aligned} &E_L=137.9GPa,\ E_T=14.48GPa,\\ &G_{LT}=5.87GPa,\ v_{LT}=v_{TT}=0.21,\\ &\alpha_L=0.36\times10^{-6}/^oC,\ \alpha_T=28.8\times10^{-6}/^oC. \end{aligned} \tag{4.47}$$

The geometry of the laminate is assumed to have the width L, and thickness h, with $L=4h$. Also each of the material layers is of equal thickness $h/4$.

The variations of interlaminar stresses σ_{xz} and σ_{zz} at the $90^o/0^o$ interface are displayed in Fig. 4.10. Except for the region very close to the free edge, the present results of σ_{xz} agree well with those of Tahani and Nosier (2003b). It is to be noted that although Tahani and Nosier's results may be improved by increasing the number

of sub-layers in each lamina, the numerical value of σ_{xz} cannot satisfy the traction free conditions along x=0.

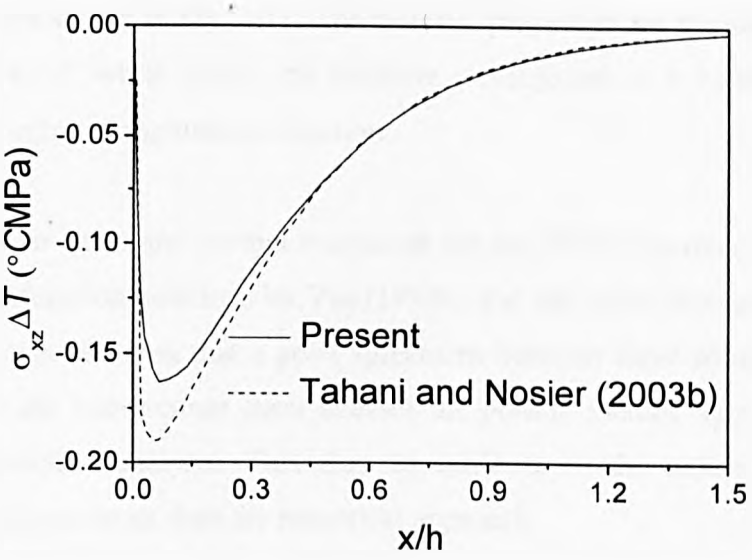

(a) Interlaminar shear stresses

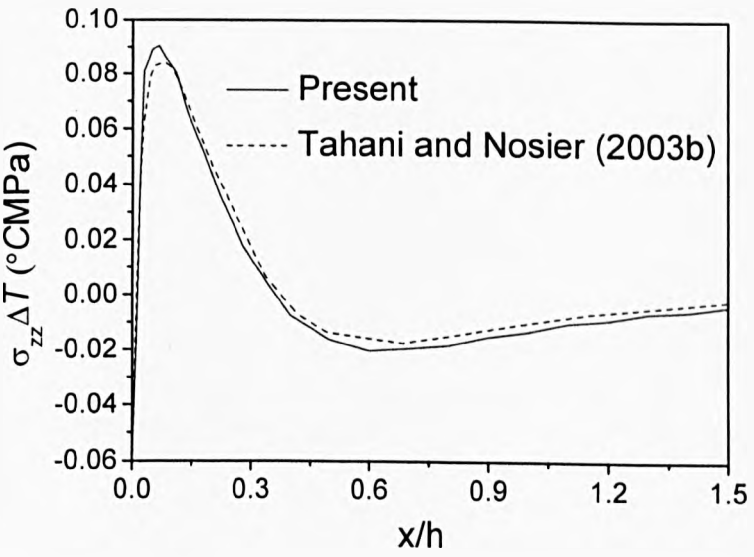

(b) Interlaminar normal stresses

Fig. 4.10 Distribution of interlaminar stresses at the 90°/0° interface in a $[90°/0°]_s$ laminate due to a temperature change.

4.4.1.4. Bending Deformation

In this example, the numerical results of a $[0^o/90^o]_s$ laminate under bending deformation are shown in Fig. 4.11. The material properties are the same as the one in Section 4.4.1.3, while herein the laminate is subjected to a bending curvature $\theta_x=4/h$ in the infinite longitudinal direction.

The interlaminar shear and normal stresses at the top $0^o/90^o$ interface are compared with the eigenfunction solutions by Yin (1994b) and the finite element solutions by Yi (1997). It can bee seen that a good agreement between these solutions has been obtained. For the interlaminar shear stresses the present method agrees better with Yin's eigenfunction analysis. This may be attribute to the nature of analytical methods is more accurate than the numerical approach.

As pointed out by Yin (1994b), the results for the bending deformation is close to that for the uniform axial extension. This may be expected because a bending curvature $\theta_x=4/h$ yields an axial strain $\varepsilon_{yy}=\varepsilon_0=1$ on the top 0^o /90^o interface.

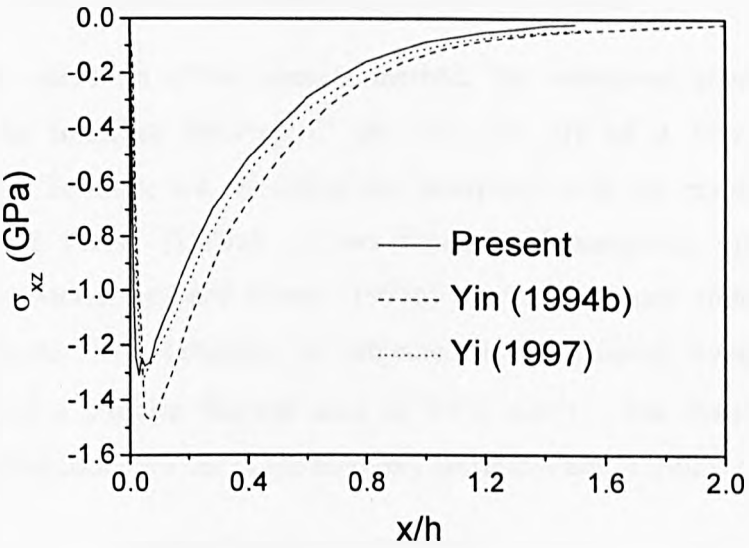

(a) Interlaminar shear stresses

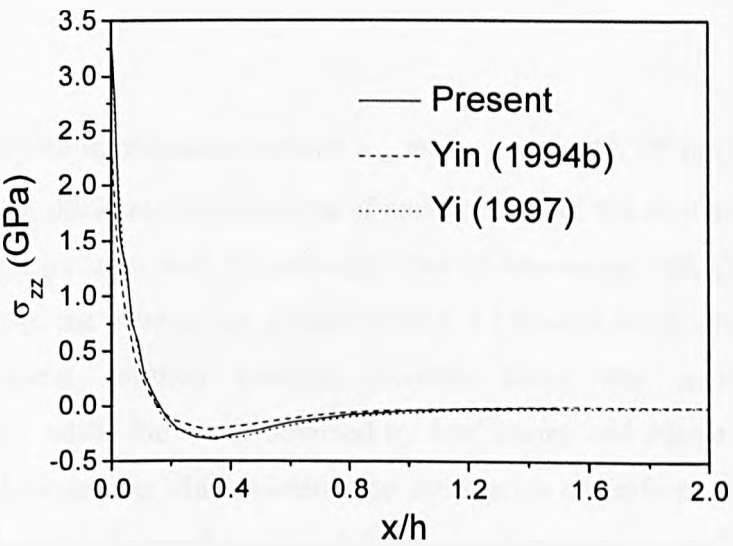

(b) Interlaminar normal stresses

Fig. 4.11 Distribution of interlaminar stresses at the $0^o/90^o$ interface in a $[0^o/90^o]_s$ laminate due to bending deformation in the infinite longitudinal direction.

4.4.2. Transverse Cracking Effects

4.4.2.1. Uniform Axial Extension and Thermal Loading

As a part of validation of the present method, the interfacial shear and normal stresses at the interface between 0° ply and 90° ply of a four ply $[0^\circ/90^\circ]_s$ Graphite/Epoxy laminate are calculated and compared with the results obtained by McCartney and Pierse (1997a). A two-dimensional analytical mode has been established by McCartney and Pierse (1997a) to evaluate stress transfer in such a cracked laminate. The laminate is subjected to a uniaxial average stress of $\sigma = 0.2GPa$, and a uniform thermal load of $\Delta T = -120^\circ C$. The material properties used in the calculations for the graphite/epoxy laminates are as follows

$$\begin{aligned} &E_L=144.78GPa,\ E_T=9.58GPa,\\ &G_{LT}=4.785GPa,\ v_{LT}=v_{TT}=0.31,\\ &\alpha_L=-0.72\times10^{-6}/^\circ C,\ \alpha_T=27\times10^{-6}/^\circ C. \end{aligned} \tag{4.48}$$

The laminate has a crack separation space L=4.0 mm and an equal ply thickness h_{ply}=0.25mm.

Fig. 4.12 shows the interlaminar stresses σ_{xz} and σ_{zz} at the $0^\circ/90^\circ$ interface. Fig. 4.13 presents through thickness distributions of axial stress and the displacement u in the transverse crack plane at $x=0$, respectively. Due to symmetry, only the distributions across top half of the element are plotted. In Fig. 4.13(a) the horizontal displacement from the present solution remains constant along the uncracked surface ($0 \le z/h \le 0.25$), while the result obtained by McCartney and Pierse (1997a) varies slightly near the crack tip which violates the assumption of uniform displacements in uncracked layers. It is seen from Fig. 4.13(b) that McCartney and Pierse's method has difficulty in computing axial stress in the region by showing oscillation near the cracked tip. This difficulty has been overcome by the present approach.

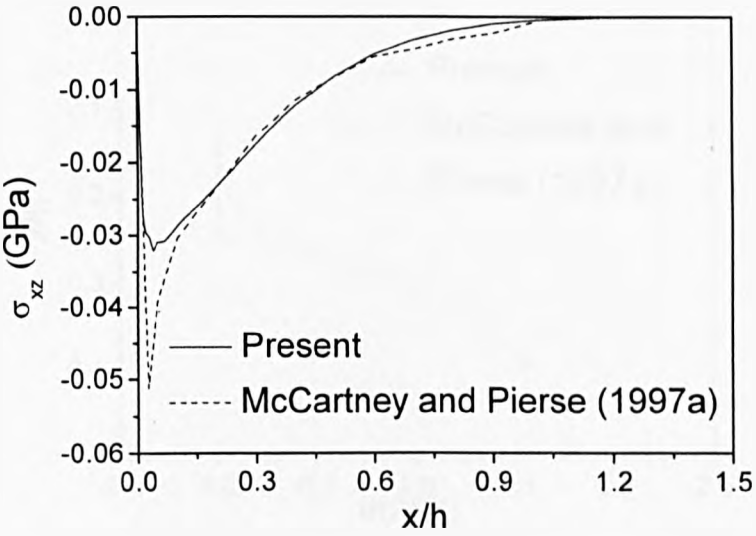

(a) Interlaminar shear stresses

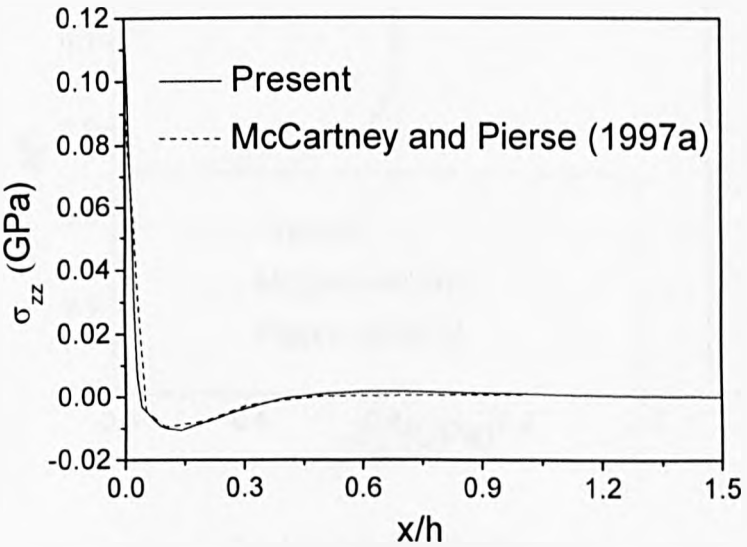

(b) Interlaminar normal stresses

Fig. 4.12 Distribution of interlaminar stresses at the $0^o/90^o$ interface in a $[0^o/90^o]_s$ laminate with transverse cracks under uniform axial strain and thermal loading.

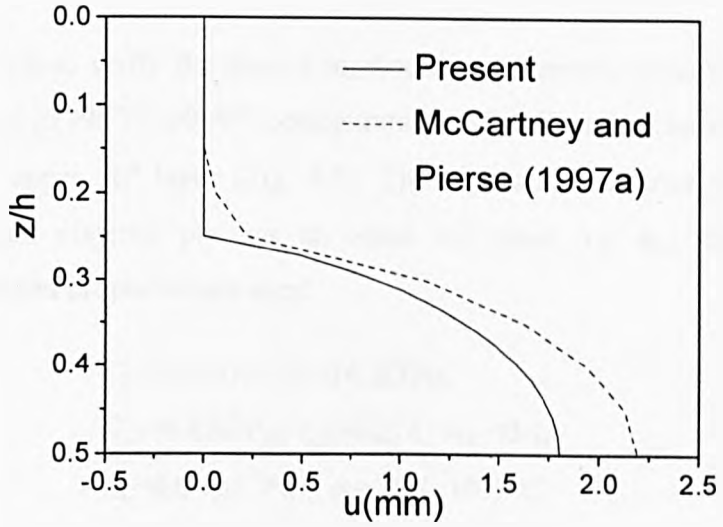

(a) Distribution of the displacement u.

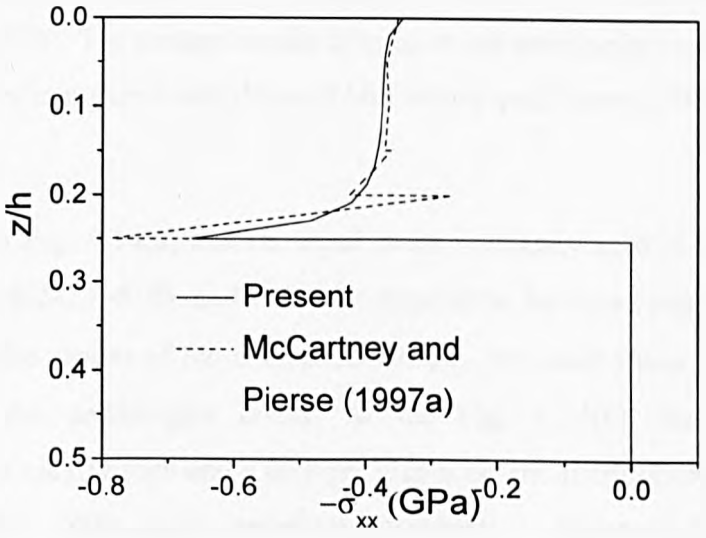

(b) Axial stress distribution

Fig. 4.13 Through thickness distributions of the axial stress and the displacement u in the transverse crack plane at $x=0$ in a $[0^o/90^o]_s$ laminate with transverse cracks under uniform axial strain and thermal loading.

4.4.2.2. Bending and Thermal Loading

Another example to verify the present method is a symmetric cross-ply Glass/Epoxy laminate with a [0°/90°/0°/90°/0°] configuration and uniformly distributed transverse cracks in the upper 90° layer (Fig. 4.5). The separation distance of the cracks is L=1.0mm. Each material ply has an equal thickness, i.e. h_{ply}=0.2mm, and the following material properties are used

$$\begin{aligned} &E_L=45.6GPa,\ E_T=16.2GPa,\\ &G_{LT}=5.83GPa,\ v_{LT}=0.278,\ v_{TT}=0.4,\\ &\alpha_L=8.6\times10^{-6}/°C,\ \alpha_T=26.4\times10^{-6}/°C. \end{aligned} \tag{4.49}$$

A bending moment per unit length of 1.0 KN is applied together with a uniform temperature difference ΔT=-100°C. The moment is applied in such a way that the cracked 90° ply is in tension. This example was previously studied by McCartney and Pierse (1997b). The present results of axial stress and displacement u in the crack plane at $x=0$ are compared with those of McCartney and Pierse (1997b) in Fig 4.14.

It is seen from Fig. 4.14(a) that the axial stress is exactly zero in the region of the crack surface ($0.2<z/h<0.4$), and that there appears to be stress singularities near the crack tips. In the region of the uncracked 90° ply, the axial stress varies linearly as expected in the undamaged layers. In the Fig. 4.14(b), the crack opening displacement is clearly seen and a uniform displacement distribution is shown for the uncracked plies. Once again, excellent agreement is observed between the two methods.

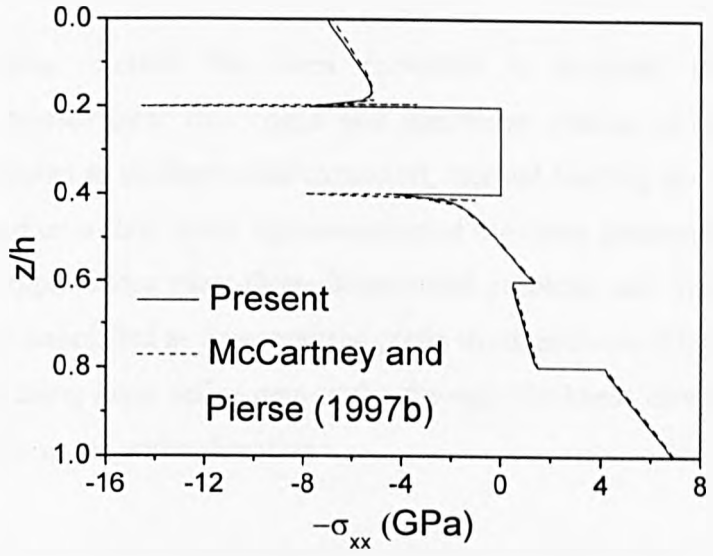

(a) Axial stress distribution

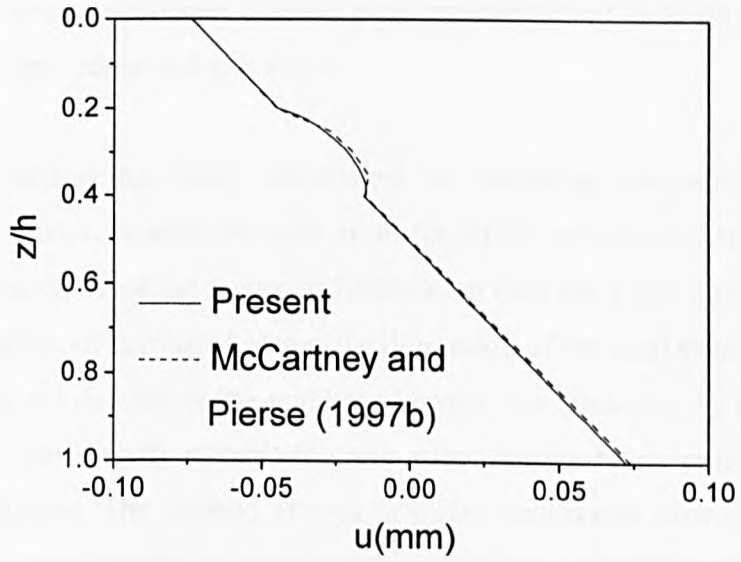

(b) Distribution of the displacement u

Fig. 4.14 Through thickness distributions of axial stress and displacement u in the transverse crack plane at x=0 in a [0°/90°/0°/90°/0°] laminate under bending and thermal loading, with transverse cracks in the upper 90° ply.

4.5. Conclusions

A semi-analytical method has been presented to evaluate three-dimensional interlaminar stresses near free edges and transverse cracks in general cross-ply laminates subjected to uniform axial extension, thermal loading and/or bending. The method is based on a state space representation of the three-dimensional equations of elasticity and applied to a quasi-three-dimensional problem and, therefore, the stress analysis can be simplified as a generalised plane strain problem. Numerical solutions were obtained using layer refinement in the through thickness direction and Fourier series expansion in the width direction.

The applications of the method were shown by numerical examples. The convergence of the new method was assessed with respect to the number of Fourier terms used in expansion as well as layer refinement. It was observed that the numerical results converged very fast. Comparisons have been carried out to validate the method. The present results showed good approximation to stress singularities in the vicinity of free edges and crack tips.

The present method has many advantages in evaluating interlaminar stresses in composite laminates. It takes account of all the stress components and independent material constants. Since the recursive formulation (see Eq. 4.27) was used to derive the state equations of laminated plates, the dimension of the final state equations (see Eq. 4.29) does not depend on the number of layers of a laminate. As a consequence, this method is particularly suitable to solve stress concentration problems of multi-layered composites. The method always provides continuous distributions of both displacements and transverse stresses across interfaces between layers. By this approach, a laminate may be composed of an arbitrary number of orthotropic layers, each of which may have different material property and thickness. As demonstrated in the free edge problem, the model is valid for nonsymmetrical cross-ply laminates. For the case of the cracked laminate under bending, although the layup is symmetric, in fact the geometry is an nonsymmetric profile because the transverse cracks only appears in top 90° layers.

Chapter 5. Free Edge and Transverse Cracking Effects in Angle-ply Laminates

5.1. Introduction

In the Chapter 4, a state space method has been developed successfully to evaluate the interlaminar stress singularities near free edges and transverse cracks in cross-ply laminates. From the viewpoint of computational mechanics, the cross-ply layup is the simplest case because there is no extension-shear coupling in the constitutive equations of a lamina. However in practical applications, the use of composite laminates is not limited to cross-ply profiles, and extensive angle-ply laminates are also being used to in order to meet some specific demands. On the basis of the methodology in the previous Chapter, a more sophisticated state space method will be developed to study the free edge and transverse crack effects in general angle-ply laminates under in-plane and/or thermal loading. Because the extension-shear coupling exists in the angle-ply laminates, the stress components σ_{yz} and σ_{xy} do not vanish and therefore have to be considered in the new formulations. This will increase the complexities in both theoretical and numerical aspects of the model. On the one hand, the displacement and stress expressions need to satisfy the boundary conditions. On the other hand, their Fourier series expansions could be eliminated for further derivations.

In analogy with the cross-ply laminate, a state space equation is first developed for the free edge problem in a single off-axis lamina. By establishing a recursive relationship between the state vectors on the upper and lower surfaces of an interface, the state space equation can then be extended to a multi-layer angle-ply laminate. After introducing the boundary conditions for free edges and transverse cracks, all the displacement and stress components can finally be evaluated. The applications of the method are demonstrated by numerical solutions and comparisons are made with other approaches in the literature.

5.2. Theoretical Modelling of Angle-ply Laminates

5.2.1. Stresses in an Off-axis Lamina

Consider an off-axis lamina (Fig. 5.1) with principal directions (1-2-3) in the global x-y-z coordinate system. The lamina has constant thickness h, width L and infinite length. The displacements in the x, y and z directions are denoted by u, v and w, respectively. Suppose that the lamina is subjected to a uniform temperature change ΔT and a uniform tension by the application of a constant longitudinal strain in the y direction, ε_0. The lamina is made of a homogeneous, monoclinic and linearly elastic material whose principal directions, i.e., fibre direction 1 has an angle of θ to the x axis.

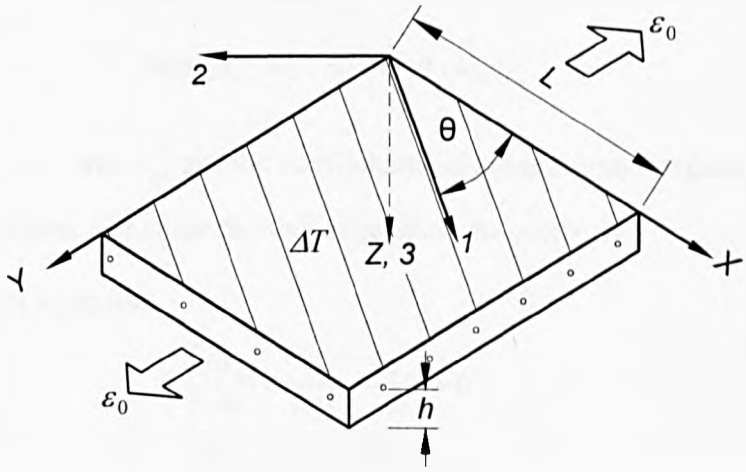

Fig. 5.1 Nomenclature of an off-axis lamina subjected to a uniaxial tension and uniform thermal loading.

(a) Stress-strain relations

The basic constitutive equation for thermo-elastic stress analysis is (Herakovich, 1998)

$$\{\sigma\} = [C'](\{\varepsilon\} - \{\varepsilon^T\}) \tag{5.1}$$

Here, the matrices $[C']$, $\{\varepsilon\}$ and $\{\varepsilon^T\}$ are stiffness matrix, mechanical strains and thermal strains, respectively; for a linearly elastic monoclinic material,

$$[C']=\begin{bmatrix} C'_{11} & C'_{12} & C'_{13} & 0 & 0 & C'_{16} \\ C'_{12} & C'_{22} & C'_{23} & 0 & 0 & C'_{26} \\ C'_{13} & C'_{23} & C'_{33} & 0 & 0 & C'_{36} \\ 0 & 0 & 0 & C'_{44} & C'_{45} & 0 \\ 0 & 0 & 0 & C'_{45} & C'_{55} & 0 \\ C'_{16} & C'_{26} & C'_{36} & 0 & 0 & C'_{66} \end{bmatrix} \tag{5.2}$$

where the C'_{ij} are stiffness coefficients that can be expressed in terms of Young's moduli, Poisson's ratios, shear moduli and the fibre orientation θ (See Appendix B for further details)

$$\{\varepsilon\}=[\varepsilon_{xx} \quad \varepsilon_{yy} \quad \varepsilon_{zz} \quad \varepsilon_{yz} \quad \varepsilon_{xz} \quad \varepsilon_{xy}]^T \tag{5.3}$$

$$\{\varepsilon^T\}=\{\alpha\}\Delta T \tag{5.4}$$

$$\{\alpha\}=[\alpha_x \quad \alpha_y \quad \alpha_z \quad 0 \quad 0 \quad \alpha_{xy}]^T \tag{5.5}$$

where α_x, α_y, α_z and α_{xy} are the coefficients of axial thermal expansion relative to the x, y, z directions and shear thermal expansion, respectively.

(b) Equilibrium equations

$$\begin{cases} \dfrac{\partial \sigma_{xx}}{\partial x}+\dfrac{\partial \sigma_{xy}}{\partial y}+\dfrac{\partial \sigma_{xz}}{\partial z}=0 \\ \dfrac{\partial \sigma_{xy}}{\partial x}+\dfrac{\partial \sigma_{yy}}{\partial y}+\dfrac{\partial \sigma_{yz}}{\partial z}=0 \\ \dfrac{\partial \sigma_{xz}}{\partial x}+\dfrac{\partial \sigma_{yz}}{\partial y}+\dfrac{\partial \sigma_{zz}}{\partial z}=0 \end{cases} \tag{5.6}$$

(c) Strain-displacement relations

$$\begin{cases} \varepsilon_{xx}=\dfrac{\partial u}{\partial x}, & \varepsilon_{yy}=\dfrac{\partial v}{\partial y}, & \varepsilon_{zz}=\dfrac{\partial w}{\partial z} \\ \varepsilon_{yz}=\dfrac{\partial w}{\partial y}+\dfrac{\partial v}{\partial z}, & \varepsilon_{xz}=\dfrac{\partial u}{\partial z}+\dfrac{\partial w}{\partial x}, & \varepsilon_{xy}=\dfrac{\partial u}{\partial y}+\dfrac{\partial v}{\partial x} \end{cases} \tag{5.7}$$

Considering that the lamina is subjecteded to a uniform extension ε_0 in the y direction, it follows that

$$\varepsilon_{yy}=\frac{\partial v}{\partial y}=\varepsilon_0 \tag{5.8}$$

Then the generalised plane strain deformation is assumed such that all components of stress and strain do not depend upon y. Hence Eq. (5.6) reduces to

$$\begin{cases} \dfrac{\partial \sigma_{xx}}{\partial x}+\dfrac{\partial \sigma_{xz}}{\partial z}=0 \\ \dfrac{\partial \sigma_{xy}}{\partial x}+\dfrac{\partial \sigma_{yz}}{\partial z}=0 \\ \dfrac{\partial \sigma_{xz}}{\partial x}+\dfrac{\partial \sigma_{zz}}{\partial z}=0 \end{cases} \tag{5.9}$$

To facilitate the following deduction process, let

$$\begin{aligned} &\alpha=\partial/\partial x,\ C_1=-C'_{13}/C'_{33},\ C_2=C'_{11}-C'^2_{13}/C'_{33}, \\ &C_3=C'_{12}-C'_{13}C'_{23}/C'_{33},\ C_4=C'_{22}-C'^2_{23}/C'_{33},\ C_5=-C'_{23}/C'_{33}, \\ &C_6=-C'_{36}/C'_{33},\ C_7=1/C'_{33},\ C_8=1/C'_{55}, \\ &C_9=C'_{16}-C'_{13}C'_{36}/C'_{33},\ C_{10}=C'_{26}-C'_{23}C'_{36}/C'_{33}, \\ &C_{11}=C'_{45}/\Delta,\ C_{12}=C'_{44}/\Delta,\ C_{13}=C'_{55}/\Delta, \\ &C_{14}=C'_{66}-C'^2_{36}/C'_{33},\ \Delta=C'^2_{45}-C'_{44}C'_{55}, \\ &C_\alpha=(C_1\alpha_x+C_5\alpha_y+C_6\alpha_{xy}-\alpha_z). \end{aligned} \tag{5.10}$$

From the third equation of Eq. (5.1) and Eq. (5.7), the following relation is obtained

$$\frac{\partial w}{\partial z}=C_1\alpha u+C_6\alpha v+C_7\sigma_{zz}+C_5\varepsilon_0-C_\alpha\Delta T \tag{5.11}$$

By substituting Eq. (5.11) into the first, second and sixth equations of Eq. (5.1), the in-plane stresses can be expressed as

$$\begin{Bmatrix}\sigma_{xx}\\ \sigma_{yy}\\ \sigma_{xy}\end{Bmatrix}=\begin{bmatrix}C_2\alpha & C_9\alpha & -C_1\\ C_3\alpha & C_{10}\alpha & -C_5\\ C_9\alpha & C_{14}\alpha & -C_6\end{bmatrix}\begin{Bmatrix}u\\ v\\ \sigma_{zz}\end{Bmatrix}+\begin{Bmatrix}C_3\\ C_4\\ C_{10}\end{Bmatrix}\varepsilon_0-\begin{Bmatrix}C_2\alpha_x+C_3\alpha_y+C_9\alpha_{xy}\\ C_3\alpha_x+C_4\alpha_y+C_{10}\alpha_{xy}\\ C_9\alpha_x+C_{10}\alpha_y+C_{14}\alpha_{xy}\end{Bmatrix}\Delta T \tag{5.12}$$

Inserting Eq. (5.12) into Eq. (5.6) and considering Eq. (5.11) as well as the fourth and fifth equations of Eq. (5.1), the following first order partial differential equation can be obtained

$$\frac{\partial}{\partial z}\begin{Bmatrix}u\\ v\\ w\\ \sigma_{xz}\\ \sigma_{yz}\\ \sigma_{zz}\end{Bmatrix}=\begin{bmatrix}0 & 0 & -\alpha & -C_{12} & C_{11} & 0\\ 0 & 0 & 0 & C_{11} & -C_{13} & 0\\ C_1\alpha & C_6\alpha & 0 & 0 & 0 & C_7\\ -C_2\alpha^2 & -C_9\alpha^2 & 0 & 0 & 0 & C_1\alpha\\ -C_9\alpha^2 & -C_{14}\alpha^2 & 0 & 0 & 0 & C_6\alpha\\ 0 & 0 & 0 & -\alpha & 0 & 0\end{bmatrix}\begin{Bmatrix}u\\ v\\ w\\ \sigma_{xz}\\ \sigma_{yz}\\ \sigma_{zz}\end{Bmatrix}+\begin{Bmatrix}0\\ 0\\ C_5\varepsilon_0-C_\alpha\Delta T\\ 0\\ 0\\ 0\end{Bmatrix} \tag{5.13}$$

Assuming that displacements u, and v can be expressed, respectively, as

$$\begin{cases} u(x,z) = \bar{u}(x,z) + U^{(0)}(z)\left(1-\dfrac{2x}{L}\right) \\ v(x,y,z) = \bar{v}(x,z) + V^{(0)}(z)\left(1-\dfrac{2x}{L}\right) + \varepsilon_0 y \end{cases} \tag{5.14}$$

where $U^{(0)}(z)$ and $V^{(0)}(z)$ are unknown boundary displacements that can be determined by imposing traction free conditions along stress free surfaces (see Section 5.3 the geometry and material discontinuity). Here the displacement function of u is the same as the one for cross-ply laminates. Due to the extension-shear coupling in angle-ply laminates, displacements v, which is constant in cross-ply laminates, varies in the x-z plane. In analogy to $U^{(0)}(z)$, the introduction of $V^{(0)}(z)$ is to satisfy the non-zero boundary displacements in the y direction at free edges.

Introducing Eq. (5.14) into Eq. (5.13) yields

$$\frac{\partial}{\partial z}\{\mathbf{F}\} = [\mathbf{G}]\{\mathbf{F}\} + \{\mathbf{B}\} \tag{5.15a}$$

where

$$\{\mathbf{B}\} = \left[-\frac{dU^{(0)}(z)}{dz}\left(1-\frac{2x}{L}\right), C_5\varepsilon_0 - C_\alpha \Delta T - \frac{2C_1}{L}U^{(0)}(z), 0, 0, 0, 0\right]^T \tag{5.15b}$$

$$\{\mathbf{F}\} = \left[\bar{u}\ \ \bar{v}\ \ w\ \ \sigma_{xz}\ \ \sigma_{yz}\ \ \sigma_{zz}\right]^T \tag{5.15c}$$

and [G] is the 6×6 matrix shown in Eq. (5.13). For the displacements and stresses in {F}, the following Fourier series expansions are assumed

$$\begin{Bmatrix} \bar{u} \\ \bar{v} \\ w \\ \sigma_{xz} \\ \sigma_{yz} \\ \sigma_{zz} \end{Bmatrix} = \sum_{m=0}^{\infty} \begin{Bmatrix} \bar{U}_m(z)\sin(\xi x) \\ \bar{V}_m(z)\sin(\xi x) \\ W_m(z)\cos(\xi x) \\ X_m(z)\sin(\xi x) \\ Y_m(z)\sin(\xi x) \\ Z_m(z)\cos(\xi x) \end{Bmatrix} \tag{5.16}$$

where $\xi = m\pi/L$. The advantage of these particular Fourier series forms is that the sinusoidal and cosinoidal terms can be eliminated when deriving the state space equations. In the case of a uniform extension, the displacement in the x direction u is zero at $x=L/2$. Hence, the integer m in Eq. (5.16) and the remaining formulations takes only even numbers, i.e. $m = 0, 2, 4, \ldots$.

By introducing Eqs. (5.14) and (5.16) into Eq. (5.13) and expanding x and 1 in the polynomial function of Eq. (5.14) into Fourier series, as follows

$$\begin{cases} x = -\dfrac{2L}{\pi}\displaystyle\sum_{m=0}^{\infty}\frac{\cos m\pi}{m}\sin\frac{m\pi x}{L} \\ 1 = \dfrac{2}{\pi}\displaystyle\sum_{m=0}^{\infty}\frac{1-\cos m\pi}{m}\sin\frac{m\pi x}{L} \end{cases} \tag{5.17}$$

the following non-homogenous state space equation for an arbitrary value of m is obtained

$$\frac{d}{dz}\{\mathbf{F}_m(z)\} = [\mathbf{G}_m]\{\mathbf{F}_m(z)\} + \{\mathbf{B}_m(z)\} \tag{5.18a}$$

where

$$\{\mathbf{F}_m(z)\} = \left[\bar{U}_m(z)\ \ \bar{V}_m(z)\ \ W_m(z)\ \ X_m(z)\ \ Y_m(z)\ \ Z_m(z)\right]^T \tag{5.18b}$$

$$[\mathbf{G}_m] = \begin{bmatrix} 0 & 0 & \xi & -C_{12} & C_{11} & 0 \\ 0 & 0 & 0 & C_{11} & -C_{13} & 0 \\ C_1\xi & C_6\xi & 0 & 0 & 0 & C_7 \\ C_2\xi^2 & C_9\xi^2 & 0 & 0 & 0 & -C_1\xi \\ C_9\xi^2 & C_{14}\xi^2 & 0 & 0 & 0 & -C_6\xi \\ 0 & 0 & 0 & -\xi & 0 & 0 \end{bmatrix} \tag{5.18c}$$

$$\{\mathbf{B}_0(z)\} = \left[0,0,C_5\varepsilon_0 - C_\alpha\Delta T - \frac{2C_1}{L}U^{(0)}(z) - \frac{2C_6}{L}V^{(0)}(z),0,0,0\right]^T \tag{5.18d}$$

$$\{\mathbf{B}_m(z)\} = \left[-\frac{2}{m\pi}(1+\cos m\pi)\frac{dU^{(0)}(z)}{dz}, -\frac{2}{m\pi}(1+\cos m\pi)\frac{dV^{(0)}(z)}{dz},0,0,0,0\right]^T \tag{5.18e}$$

The solution of the non-homogenous state space Eq. (5.18a) is

$$\{\mathbf{F}_m(z)\} = [\mathbf{D}_m(z)]\{\mathbf{F}_m(0)\} + \{\mathbf{H}_m(z)\} \tag{5.19a}$$

where

$$[\mathbf{D}_m(z)] = e^{[\mathbf{G}_m]z}\{\mathbf{F}_m(0)\},$$

$$\{\mathbf{H}_m(z)\} = \int_0^z e^{[\mathbf{G}_m](z-\tau)}\{\mathbf{B}_m(\tau)\}d\tau \qquad (z\in[0,h]) \tag{5.19b}$$

In particular, at $z=h$,

$$\{\mathbf{F}_m(h)\} = [\mathbf{D}_m(h)]\{\mathbf{F}_m(0)\} + \{\mathbf{H}_m(h)\} \tag{5.20}$$

where $[\mathbf{D}_m(h)]$ is called transfer matrix that can be calculated either analytically or numerically. The calculation of the two constant matrices, $[\mathbf{D}_m(h)]$ and $\{\mathbf{H}_m(h)\}$, in Eq. (5.19) can be found from Ye (2002) or Moler and Van Loan (2003).

5.2.2. Stresses in an Angle-ply Laminate

Fig. 5.2 shows a multi-layered angle-ply laminate of thickness H, width L and infinite length in the y direction. Again the laminate is subjected to a constant longitudinal strain ε_0 and a uniform thermal loading ΔT. To evaluate the stress transfer in the angle-ply laminate, the similar procedure applied to cross-ply laminates is used again. The solutions of Eq. (5.18) are based on the division of the plate into N fictitious sub-layers, each of which may have different thickness and material properties. Nevertheless, the thickness of all the fictitious sub-layers become very thin and approach zero uniformly if N is assigned to a large value. Assuming that each sub-layer is homogeneous and made of a monoclinic elastic materials, and therefore two types of material interfaces are identified in the plate: the fictitious interfaces which separate the same material layers and the real ones that separate the different material layers.

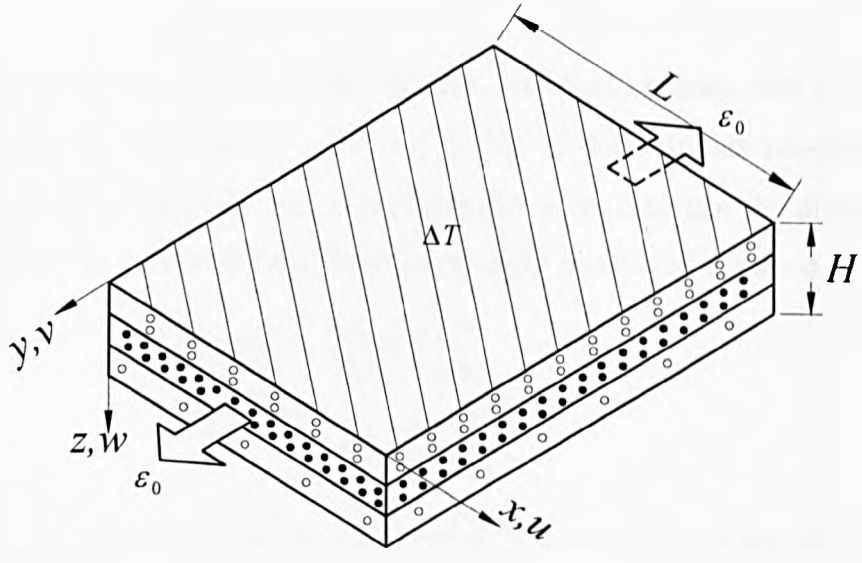

Fig. 5.2 Nomenclature of an anlge-ply laminate subjected to a uniaxial tension and uniform thermal loading.

If a suitably large value of N is assigned, each individual sub-layer becomes sufficiently thin and, consequently, Eqs. (5.18)–(5.20) are considered to be adequate for the solutions of these thin layers. Moreover, the boundary conditions can be satisfied in an approximately continuous way along the thickness of the laminate. The state space equation and the form of solution of an arbitrary sub-layer, e.g., the

jth one whose thickness is h_j, can easily be obtained by replacing h with h_j in Eqs. (5.18)–(5.20). The state space equation of the jth sub-layer then becomes

$$\frac{d}{dz}\{\mathbf{F}_m(z)\}_j = [\mathbf{G}_m]_j \{\mathbf{F}_m(z)\}_j + \{\mathbf{B}_m(z)\}_j \tag{5.21}$$

$$\begin{aligned}\{\mathbf{F}_m(z)\}_j &= e^{[\mathbf{G}_m]_j z}\{\mathbf{F}_m(0)\}_j + \int_0^z e^{[\mathbf{G}_m]_j (z-\tau)}\{\mathbf{B}_m(\tau)\}_j d\tau \\ &= [\mathbf{D}_m(z)]_j \{\mathbf{F}_m(0)\}_j + \{\mathbf{H}_m(z)\}_j \qquad z \in [0, h_j]\end{aligned} \tag{5.22}$$

In particular, at $z=h_j$,

$$\{\mathbf{F}_m(h_j)\}_j = [\mathbf{D}_m(h_j)]_j \{\mathbf{F}_m(0)\}_j + \{\mathbf{H}_m(h_j)\}_j \tag{5.23}$$

After repeating the above process for all individual sub-layers and with appropriate continuity requirements imposed at all the real and fictitious interfaces, a solution for the entire laminate can be formulated. Also, the solution can be found to the required accuracy by increasing the total number of the thin layers, subjected to satisfy boundary conditions.

In order to find the solution of the problem, we must evaluate first the unknown displacements, $U^{(0)}(z)$ and $V^{(0)}(z)$ in Eq. (5.18). If the fictitious sub-layers of the laminate are all sufficiently thin, it is reasonable to assume that the displacements, $U^{(0)}(z)$ and $V^{(0)}(z)$ within the thin layer are linearly distributed in the z direction, i.e.

$$\begin{cases} U_j^{(0)}(z) = U_j^-(1-\dfrac{z}{h_j}) + U_j^+ \dfrac{z}{h_j} \\ V_j^{(0)}(z) = V_j^-(1-\dfrac{z}{h_j}) + V_j^+ \dfrac{z}{h_j} \end{cases}, z \in [0,\ h_j], \tag{5.24}$$

where U_j^-, U_j^+, and V_j^-, V_j^+ are the values of $U_j^{(0)}(z)$ and $V_j^{(0)}(z)$ at the top and bottom surfaces of the jth thin layer, respectively. Inserting Eq. (5.24) into Eqs. (5.18d) and (5.18e), vector $\{\mathbf{B}_m(z)\}_j$ in Eq. (5.21) can be expressed as

$$\begin{aligned}\{\mathbf{B}_0(z)\}_j = [0,0, C_5\varepsilon_0 - C_\alpha \Delta T - \frac{2C_1}{L}\left(U_j^-(1-\frac{z}{h_j}) + U_j^+\frac{z}{h_j}\right) \\ -\frac{2C_6}{L}\left(V_j^-(1-\frac{z}{h_j}) + V_j^+\frac{z}{h_j}\right), 0,0,0]^T\end{aligned}, \quad z \in [0,\ h_j], \tag{5.25a}$$

$$\{\mathbf{B}_m(z)\}_j = \left[\frac{4}{m\pi}\frac{U_j^- - U_j^+}{h_j}, \frac{4}{m\pi}\frac{V_j^- - V_j^+}{h_j}, 0,0,0,0\right]^T, \ (m=2,\ 4,\ 6\ldots). \tag{5.25b}$$

By introducing the following continuity conditions at all interfaces, i.e.,

$$\{\mathbf{F}_m(0)\}_{j+1} = \{\mathbf{F}_m(h_j)\}_j, j=1, 2,\ldots, N\text{-}1, \tag{5.26}$$

and then using Eqs.(5.23) and (5.26) recursively, a relationship between the state vectors on the bottom and top surfaces of the plate is established as follows

$$\{\mathbf{F}_m(h_N)\}_N = [\bar{\mathbf{D}}_m]_N \{\mathbf{F}_m(0)\}_1 + \{\bar{\mathbf{H}}_m\} \tag{5.27a}$$

where

$$[\bar{\mathbf{D}}_m]_N = \left(\prod_{j=N}^{1} [\mathbf{D}_m(h_j)]_j\right) \tag{5.27b}$$

$$\{\bar{\mathbf{H}}_m\} = \left(\prod_{j=N}^{2} [\mathbf{D}_m]_j\right)\{\mathbf{H}_m\}_1 + \left(\prod_{j=N}^{3} [\mathbf{D}_m]_j\right)\{\mathbf{H}_m\}_2 + \cdots + \{\mathbf{H}_m\}_N \tag{5.27c}$$

$\{\mathbf{F}_m(h_N)\}_N$ and $\{\mathbf{F}_m(0)\}_1$ are, respectively, the state vectors at the bottom and top surfaces of the laminated plate. Upon using the traction free conditions at the top and bottom surfaces, the following stress conditions are obtained

$$\begin{cases} [X_m(0) \;\; Y_m(0) \;\; Z_m(0)]^T = [0 \;\; 0 \;\; 0]^T \\ [X_m(h_N) \;\; Y_m(h_N) \;\; Z_m(h_N)]^T_N = [0 \;\; 0 \;\; 0]^T \end{cases} \tag{5.28}$$

Substituting Eq. (5.28) into Eq. (5.27) yields the following linear algebraic equation system

$$\begin{bmatrix} \bar{D}_{41} & \bar{D}_{42} & \bar{D}_{43} \\ \bar{D}_{51} & \bar{D}_{52} & \bar{D}_{53} \\ \bar{D}_{61} & \bar{D}_{62} & \bar{D}_{63} \end{bmatrix} \begin{Bmatrix} \bar{U}_m \\ \bar{V}_m \\ W_m \end{Bmatrix}_1 = -\begin{Bmatrix} \bar{H}_{m4} \\ \bar{H}_{m5} \\ \bar{H}_{m6} \end{Bmatrix} \tag{5.29}$$

where $\bar{D}_{ij}$ and $\bar{H}_{mi}$ are the relevant elements in $[\bar{\mathbf{D}}_m]$ and $\{\bar{\mathbf{H}}_m\}$, respectively.

Eq.(5.29) is a set of linear algebraic equations in terms of the three displacement components, $\bar{U}_m$, $\bar{V}_m$ and W_m, at the top surface. The free terms of Eq. (5.29), $\bar{H}_{m4}$, $\bar{H}_{m5}$ and $\bar{H}_{m6}$, contain $4\times N$ unknown constants, U_j^-, U_j^+, V_j^-, and V_j^+ (j=1, 2,...N), introduced in Eq.(5.24). Because of the continuity of $U^{(0)}(z)$ and $V^{(0)}(z)$ at the interface between the jth and the (j+1)th sub-layers, the relationships, $U_j^+ = U_{j+1}^-$ and $V_j^+ = V_{j+1}^-$ (j=1, 2,...N-1), are obtained. Hence, the number of unknown constants is

then reduced to $2(N+1)$. These constants are determined by introducing appropriate boundary conditions.

5.3. Geometry and Material Discontinuity

5.3.2. Free Edges of an Angle-ply Laminate under Axial Extension

Typical composite laminates with free edges are shown in Fig. 1.2 and Fig. 5.2. The free edge conditions at $x=0, L$ are as follows

$$\sigma_{xz} = \sigma_{xy} = \sigma_{xx} = 0 \tag{5.30}$$

It can be seen from Eqs. (5.16) that $\sigma_{xz} = 0$ is satisfied automatically along the free edges (x=0, L). The remaining boundary condition to be satisfied at the free edges is $\sigma_{xx} = \sigma_{xy} = 0$. In order to impose the condition at the two free edges, we introduce Eqs. (5.14) into Eq.(5.12). As a result, the two in-plane stresses are expressed as follows

$$\begin{cases} \sigma_{xx} = C_2\alpha\bar{u} + C_9\alpha\bar{v} - C_1\sigma_{zz} + C_3\varepsilon_0 - (C_2\alpha_x + C_3\alpha_y + C_9\alpha_{xy})\Delta T \\ -\dfrac{2C_2}{L}U^{(0)}(z) + \dfrac{2C_9}{L}V^{(0)}(z) \\ \sigma_{xy} = C_9\alpha\bar{u} + C_{14}\alpha\bar{v} - C_6\sigma_{zz} + C_{10}\varepsilon_0 - (C_9\alpha_x + C_{10}\alpha_y + C_{14}\alpha_{xy})\Delta T \\ -\dfrac{2C_9}{L}U^{(0)}(z) + \dfrac{2C_{14}}{L}V^{(0)}(z) \end{cases} \tag{5.31}$$

After substituting Eq. (5.16) into Eq. (5.31) and imposing the condition x=0, we obtain for the *jth* sub-layer

$$\begin{cases} \sigma_{xx} = \sum\limits_m \left[C_2\xi\bar{U}_m(z) + C_9\xi\bar{V}_m(z) - C_1Z_m(z)\right]_j \\ +\left[C_3\varepsilon_0 - (C_2\alpha_x + C_3\alpha_y + C_9\alpha_{xy})\Delta T\right]_j - \left[\dfrac{2C_2}{L}U^{(0)}(z) + \dfrac{2C_9}{L}V^{(0)}(z)\right]_j = 0 \\ \sigma_{xy} = \sum\limits_m \left[C_9\xi\bar{U}_m(z) + C_{14}\xi\bar{V}_m(z) - C_6Z_m(z)\right]_j \\ +\left[C_{10}\varepsilon_0 - (C_9\alpha_x + C_{10}\alpha_y + C_{14}\alpha_{xy})\Delta T\right]_j - \left[\dfrac{2C_9}{L}U^{(0)}(z) + \dfrac{2C_{14}}{L}V^{(0)}(z)\right]_j = 0 \end{cases} \tag{5.32}$$

It has been mentioned before that Eq. (5.29) contains $2(N+1)$ unknown constants. In order to evaluate them and also the three displacement components of the top surface (see Eq. (5.29)), the traction free conditions Eq. (5.32) are imposed at the edges of all interfaces, including the fictitious and real material interfaces. This can be done by introducing z-coordinates of the interfaces, z_j, into Eq.(5.32). This process yields

2(N+1) independent linear algebraic equations. Along with the three equations from Eq. (5.29), the three displacement components and the 2(N+1) unknown constants can finally be solved. Once the equation system is solved, all the displacements and stresses can be obtained by substituting the solutions to the state space equations in Section 5.2.2.

5.3.3. Transverse Cracks in an Angle-ply Laminate under In-plane loading

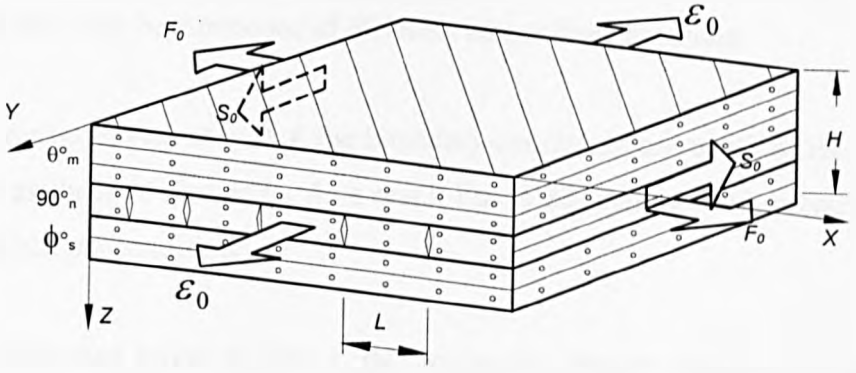

Fig. 5.3 Schematic of a [$\theta°_m$/$90°_n$/$\phi°_s$] laminate with an array of transverse ply cracks in $90°_n$ layers.

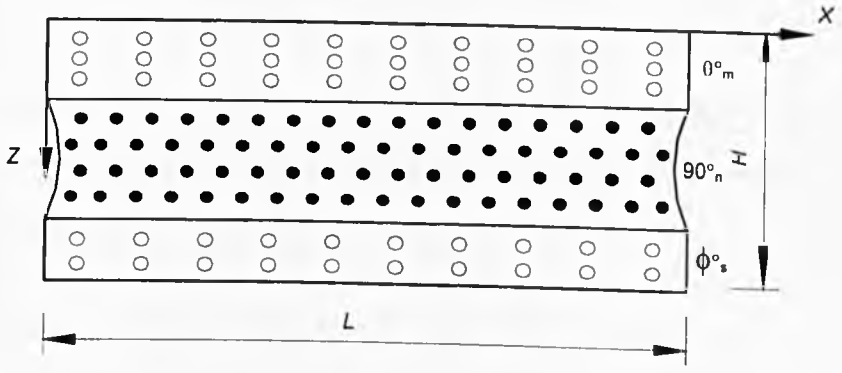

Fig. 5.4 A representative element of a [$\theta°_m$/$90°_n$/$\phi°_s$] laminate with ply cracks in $90°_n$ layers.

When a general angle-ply laminate is subjected to a tension perpendicular to the fibres in the 90° layers, transverse ply cracks appear parallel to the fibres and across the entire width from edge to edge. For example the [$\theta°_m$/$90°_n$/$\phi°_s$] laminate (Fig. 5.3) under uniform biaxial extension, ε_0 and F_0, and shear loading, S_0, displays an array of periodic cracks in the $90°_n$ layers, where the subscripts denote the number of

the real plies within a ply group. It is worth mentioning that the number of separate ply groups may be larger than the number of fibre orientations when the plies having the same fibre orientation are stacked separately in several consecutive ply groups, e.g. 90° plies in the [0°/90°/30°/90°/0°] lay-up. Assuming that the distribution of the cracks is equally spaced, a representative element (Fig. 5.4) can be taken out from two neighbouring cracks to predict the stress and displacement fields.

In order to use the recursive formulations the representative element is further divided into N fictitious sub-layers. Again, each sub-layer may have different thickness and may be composed of different monoclinic materials.

For the cracked layers at x=0, L the boundary conditions are traction free, which are the same as those of free edge. As a result Eq. (5.32) can be used directly to satisfy the crack surface condition.

For the uncracked layers at x=0, L, due to the fact that the laminate is subjected to uniform biaxial extension, shear and thermal loading, the displacements of an arbitrary layer, u and v, remain constant, i.e.

$$\begin{cases} u(0,y,z) = u_0 \\ v(0,y,z) = v_0 \end{cases}, \quad \begin{cases} u(L,y,z) = -u_0 \\ v(L,y,z) = -v_0 \end{cases} \tag{5.33}$$

Due to symmetry, only the boundary conditions at x=0 in the plane of y=0 are considered. Substituting Eq. (5.33) and Eq. (5.16) into Eq. (5.14) yields

$$\begin{cases} u(0,0,z) = \sum_{m=0}^{\infty} \overline{U}_m(z)\sin(\xi \times 0) + U^{(0)}(z)\left(1 - \dfrac{2\times 0}{L}\right) = u_0 \\ v(0,0,z) = \sum_{m=0}^{\infty} \overline{V}_m(z)\sin(\xi \times 0) + V^{(0)}(z)\left(1 - \dfrac{2\times 0}{L}\right) + \varepsilon_0 \times 0 = v_0 \end{cases} \tag{5.34a}$$

or

$$\begin{cases} u(0,0,z) = U^{(0)}(z) = u_0 \\ v(0,0,z) = V^{(0)}(z) = v_0 \end{cases} \tag{5.34b}$$

From the equilibrium of the internal and external forces, the following equation exists

$$\begin{cases} \int_h \sigma_{xx} dz = F_0 \\ \int_h \sigma_{xy} dz = S_0 \end{cases} \tag{5.35a}$$

or

$$\begin{cases} \int_h \left(\sum_m \left[C_2 \xi \bar{U}_m(z) + C_9 \xi \bar{V}_m(z) - C_1 Z_m(z) \right]_j + \left[C_3 \varepsilon_0 - (C_2 \alpha_x + C_3 \alpha_y + C_9 \alpha_{xy}) \Delta T \right]_j \right. \\ \left. - \left[\frac{2C_2}{L} U^{(0)}(z) + \frac{2C_9}{L} V^{(0)}(z) \right]_j \right) dz = F_0 \\ \int_h \left(\sum_m \left[C_9 \xi \bar{U}_m(z) + C_{14} \xi \bar{V}_m(z) - C_6 Z_m(z) \right]_j + \left[C_{10} \varepsilon_0 - (C_9 \alpha_x + C_{10} \alpha_y + C_{14} \alpha_{xy}) \Delta T \right]_j \right. \\ \left. - \left[\frac{2C_9}{L} U^{(0)}(z) + \frac{2C_{14}}{L} V^{(0)}(z) \right]_j \right) dz = S_0 \end{cases} \tag{5.35b}$$

According to Eq. (5.34) u_0 and v_0 are two unknown constants in the uncracked layers. Assume that the cracked ply contains N_c fictitious sub-layers. Then there exist (N_c -1) interfaces which result in 2(N_c -1) unknown constants in the cracked layers. In addition to the two unknown constants in the uncracked layers, there are $2N_c$ independent unknown constants in Eq. (5.29). In order to evaluate these constants and also the three displacement components of the top surface (see Eq. (5.29)), the traction free condition, Eq. (5.32), are imposed at the intersections between the crack surface and the (N_c-1) interfaces. This process yields 2(N_c-1) independent linear algebraic equations. Along with Eq. (5.35) and the three equations from Eq. (5.29), the three displacement components and the $2N_c$ unknown constants can finally be solved.

5.4. Numerical Results

5.4.1. Free Edge Effects

To validate the state space method for angle-ply laminates, a $[+45°/-45°]_s$ graphite-epoxy laminate is first studied. The laminate is subjected to a uniform axial strain ε_0 in the infinite longitudinal direction. The material properties used in the calculations for the graphite/epoxy laminate are as follows

$$E_L=137.9GPa,\ E_T=14.48GPa,$$
$$G_{LT}=G_{TT}=5.87GPa,\ v_{LT}=v_{TT}=0.21, \tag{5.36}$$

The geometry of the laminate is assumed to have the width L, and thickness h, with $L=4h$. Each of the material layers is of equal thickness $h/4$.

The numerical results of this example have been obtained and published by several researchers (Pipes and Pagano, 1970; Wang and Crossman, 1977; Wang and Choi, 1982a, b) in the literature. The present solutions are presented in Fig. 5.5–Fig. 5.11 and have been compared with results in the above publications. No comparisons have been made to σ_{xz} and σ_{xx} because they are not available in these publications.

The distributions of three interlaminar stresses σ_{xz}, σ_{yz} and σ_{zz} at the +45°/-45°are shown in Fig. 5.5–Fig. 5.7. It is evident from the curves that all three interlaminar stresses exhibit singular behaviour near the free edge, however they approach to zero after $x>1.5h$. This confirms that the interlaminar stress disturbance occurs only in the vicinity of the free edge. The results of σ_{zz} and σ_{yz} agree well with those of Wang and Choi (1982b) in Fig. 5.6 and Fig. 5.7, respectively.

Fig. 5.8–Fig. 5.10 illustrate the distributions of three in-plane stresses σ_{xx}, σ_{yy}, and σ_{xy} at the height of $z=h/4$. Among them the present results of σ_{yy} and σ_{xy} are compared with those of Wang and Crossman (1977) and Pipes and Pagano (1970), respectively, in Fig. 5.9 and Fig. 5.10. A higher level of stress concentration is observed from the current results. The disparities between these results are partly due to the fact that the number of sub-layers used in the present analysis is greater than that of the two other works.

In Fig. 5.11 a comparison of the through thickness distribution of displacement v at the free edge is made between present method and Wang and Crossman (1977)'s finite element method. Due to symmetry, only the displacements across the top half of the laminate are plotted. It is seen that Wang and Crossman's result shows small oscillations both above and below the +45°/-45° interface, while the present solution

has no such defect. Apart from the oscillations, the two curves match well with each other.

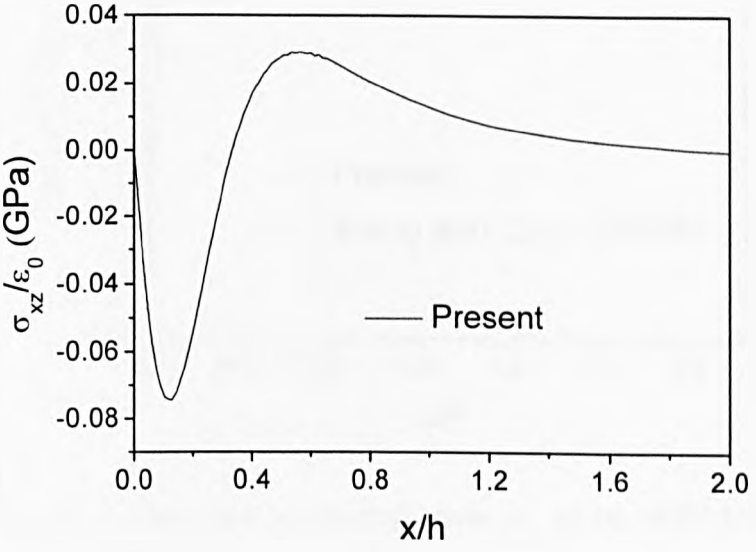

Fig. 5.5 Distribution of interlaminar shear stress σ_{xz} at the +45°/-45° interface in a $[+45°/-45°]_s$ laminate under uniform axial strain.

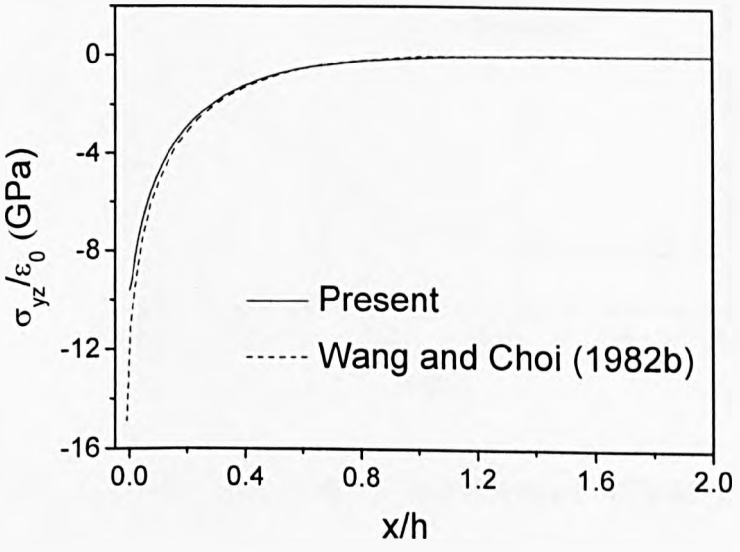

Fig. 5.6 Distribution of interlaminar shear stress σ_{yz} at the +45°/-45° interface in a $[+45°/-45°]_s$ laminate under uniform axial strain.

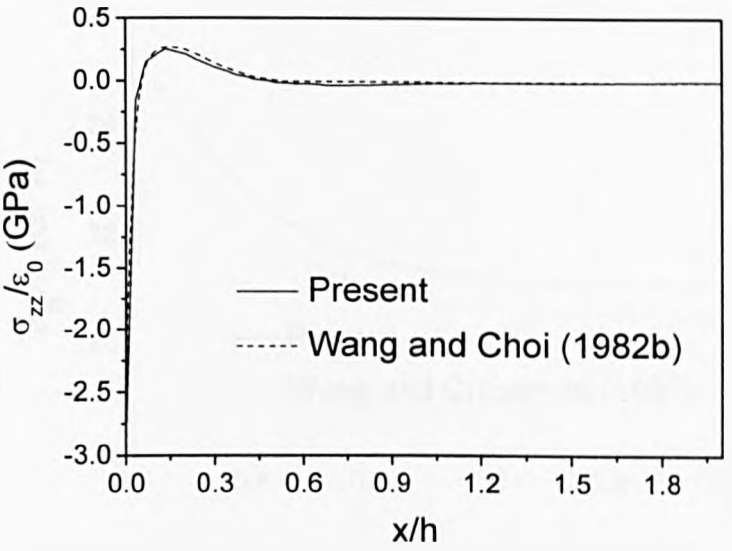

Fig. 5.7 Distribution of interlaminar normal stress σ_{zz} at the +45°/-45° interface in a $[+45°/-45°]_s$ laminate under uniform axial strain.

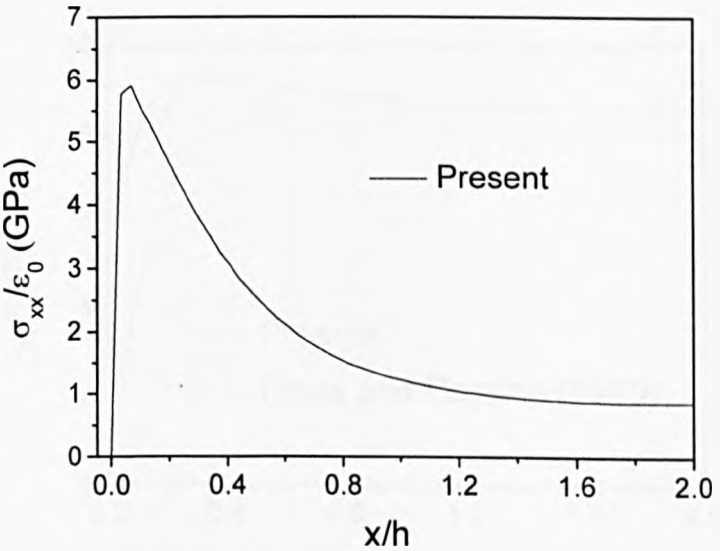

Fig. 5.8 Distribution of the axial stress σ_{xx} at $z=h/4$ in a $[+45°/-45°]_s$ laminate under uniform axial strain.

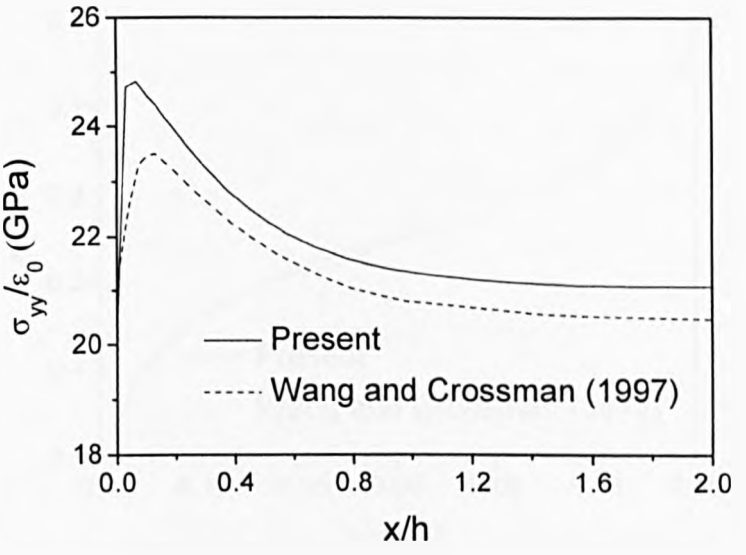

Fig. 5.9 Distribution of the axial stress σ_{yy} at $z=h/4$ in a $[+45°/-45°]_s$ laminate under uniform axial strain.

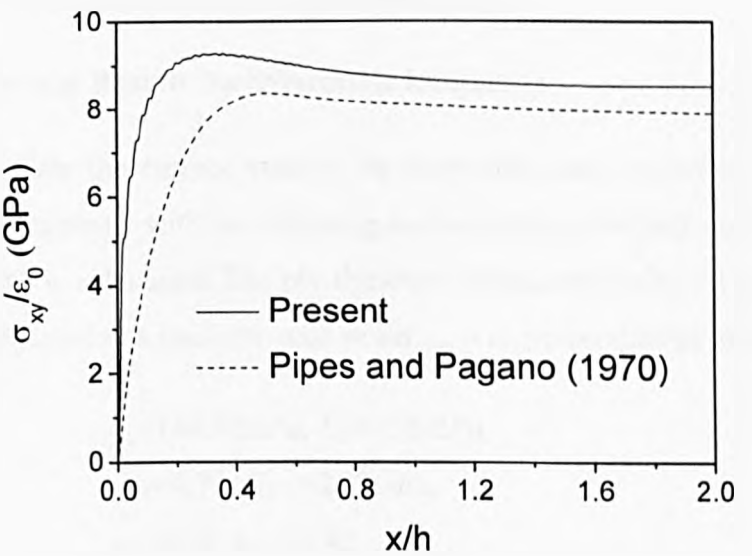

Fig. 5.10 Distribution of the in-plane shear stress σ_{xy} at $z=h/4$ in a $[+45°/-45°]_s$ laminate under uniform axial strain.

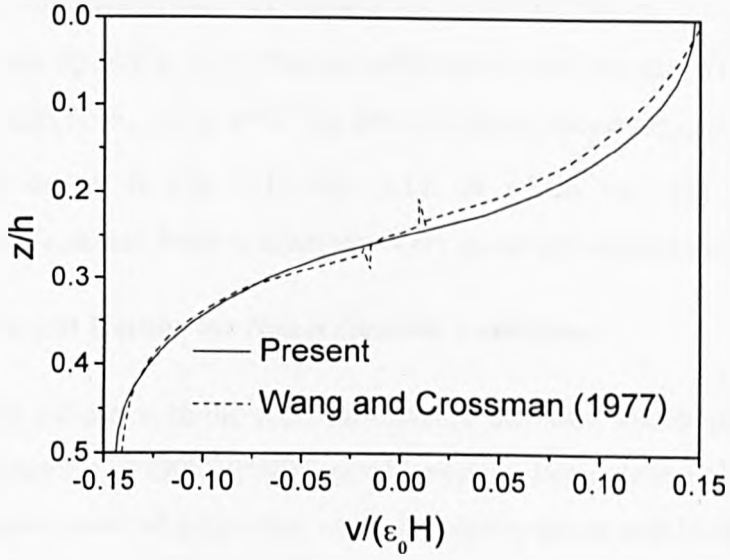

Fig. 5.11 Through thickness distribution of displacement v at the free edge x=0 in a $[+45°/-45°]_s$ laminate under uniform axial strain.

5.4.2. Stress Transfer near Transverse Cracks

5.4.2.1. Numerical Results for Symmetric Laminates

To further validate the current method for transverse crack problems, a $[30°/90°]_s$ graphite/epoxy laminate with the following material properties and a transverse crack separation $L=8h$ is calculated. The ply thickness is assumed to be 0.127 mm and the laminate is subjected to a uniform axial strain $\varepsilon_{xx} = \varepsilon_0$ perpendicular to the 90° plies.

$$\begin{aligned} &E_L=144.78GPa,\ E_T=9.58GPa,\\ &G_{LT}=4.79,\ G_{TT}=3.37GPa,\\ &v_{LT}=0.31,\ v_{TT}=0.42 \end{aligned} \tag{5.37}$$

The present numerical results of six stress components σ_{xz}, σ_{yz}, σ_{zz}, σ_{xx}, σ_{yy}, σ_{xy}, are shown in Fig. 5.12–Fig. 5.17, respectively. Some of present results have been compared with Yuan and Selek (1993)'s finite element solutions. Fig. 5.12–Fig. 5.14 show the distribution of interlaminar shear and normal stresses, σ_{xz}, σ_{yz}, and σ_{zz} along the 30°/90° interface. All these stresses are responsible for the onset of delamination along the interface. Again it is observed that they are highly singular near the crack

tip and vanish in the far field. The present results agree well with those of Yuan and Selek (1993), while significant differences are observed for σ_{xz} in the region very close to the crack tip in Fig. 5.12. This is attribution to the fact that Yuan and Selek's results do not satisfy $\sigma_{xz} = 0$ at x=0. The three in-plane stresses σ_{xx}, σ_{yy}, σ_{xy} along the mid-plane are shown in Fig. 5.15–Fig. 5.17, in which σ_{xx}, and σ_{yy} have been compared with Yuan and Selek's solutions. Very good agreements are observed.

5.4.2.2. Numerical Results for Nonsymmetric Laminates

After the above validation in the symmetric layup, the stress and displacement fields of an nonsymmetric [30°/90°/30°/90°] graphite/epoxy laminate are also investigated by using the same material properties, crack separation space and loading conditions. Generally speaking, the distributions of interlaminar and in-plane stresses in the [30°/90°/30°/90°] laminate have similarly graphic shapes to those in the above symmetric layups. They all exhibit stress singularities near the crack surface and approach to a constant in the far fields. To avoid duplication, these distributions are not presented here. Significant differences are observed in the through thickness distributions because of the effects of different layups.

In order to demonstrate the influence of stacking sequence, the through thickness distributions of interlaminar stresses σ_{yz}, σ_{zz}, axial stress σ_{xx}, and displacement u at x=0 in both the symmetric and nonsymmetric laminates are shown in Fig. 5.18–Fig. 5.21, respectively. The singular behaviour at the interfaces is evident in all figures in the form of stress concentrations or steep gradients. Except σ_{yz} the maximum stresses and displacement of the nonsymmetric laminate are larger than those of the symmetric counterpart. It appears that the local stress concentrations in the anti-symmetric laminate are more sensitive than that in the symmetric case. Moreover, the maximum stresses always occur in the lower 30°/90° interface and the maximum displacement u is found at the bottom surface. In addition, it can be seen from Fig. 5.18 that the interlaminar shear stress σ_{yz} exhibits a very interesting distribution. It vanishes within the uncracked layers, but appears in the cracked layers. On the contrary, the axial stress σ_{xx} (Fig. 5.20) only appears within the uncracked plies and approaches to zero on the crack surfaces.

After the above comparisons in axial extension case, the present method is then applied to study cracked laminates under shear deformation. The numerical results of the above symmetric and nonsymmetric laminates subjected to a uniform shear strain $\varepsilon_{yx} = \gamma_0$ are shown in Fig. 5.22–Fig. 5.31.

The distributions of interlaminar stresses σ_{xz}, σ_{yz}, σ_{zz} and in-plane stresses σ_{xx}, σ_{yy}, σ_{xy} along the top 30°/90° interfaces are shown in Fig. 5.22–Fig. 5.27. Once again, all stresses demonstrate singularities near the crack tip and vanish or approach to a constant in the far fields. There are no much differences in the distributions between nonsymmetric and symmetric laminates. It is also observed that the in-plane shear stress σ_{xy}, is more significant than the other counterparts. The interlaminar shear stress σ_{yz} is even larger than the interlaminar normal stress σ_{zz}.

It is noted that the graphic solutions display oscillations in Fig. 5.22–Fig. 5.27. These oscillations could not be smoothed even using a large value of m. However it does not mean that the present analytical methodology is not suitable to evaluate stress distributions under shear loading. The oscillations may be caused by the present numerical algorithm to calculate the transfer matrix $[\mathbf{D}_m(h)]$ in Eq. (5.19). The built-in Matlab function 'expm' is used in the calculations. It is believed that the oscillation problem can be overcomed by using an appropriate numerical method to compute $[\mathbf{D}_m(h)]$. This is out of scope of the present study and will not be further discussed here.

Fig. 5.28–Fig. 5.31 show the through thickness distributions of interlaminar stresses σ_{yz}, σ_{zz}, the in-plane stress σ_{xy}, and displacement v at x=0. In general the distribution patterns of the stresses under shear deformation are similar to those under extension. Once again, the maximum stresses always occur in the lower 30°/90° interface and the maximum displacement u is found at the bottom surface. The interlaminar shear stress σ_{yz} (Fig. 5.28) vanishes within uncracked layers but appears in the cracked layers. The dominant in-plane shear stress σ_{xy} (Fig. 5.30) only exists in uncracked layers. However it can be seen that the effects of stacking sequence on the maximum stresses and displacement under shearing are not as significant as that observed from

the extension case. The maximum values are very similar between the symmetric and nonsymmetric layups.

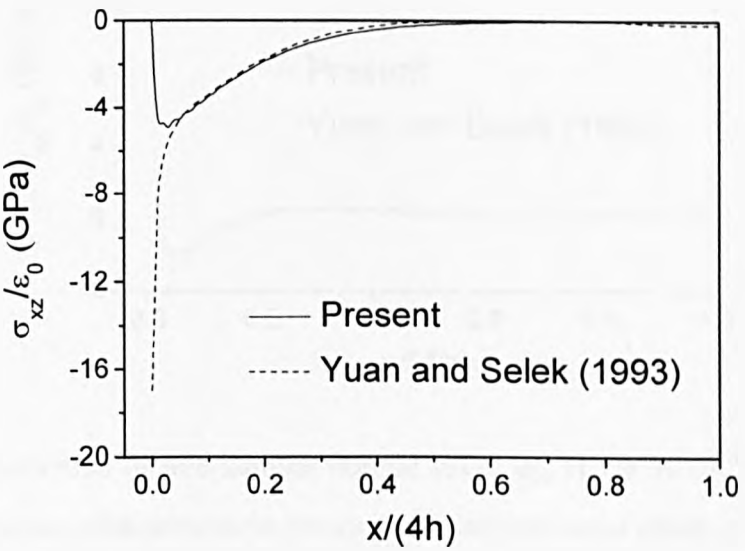

Fig. 5.12 Distribution of interlaminar shear stress σ_{xz} at the 30°/90° interface in a $[30°/90°]_s$ laminate with transverse cracks under uniform axial strain ε_0.

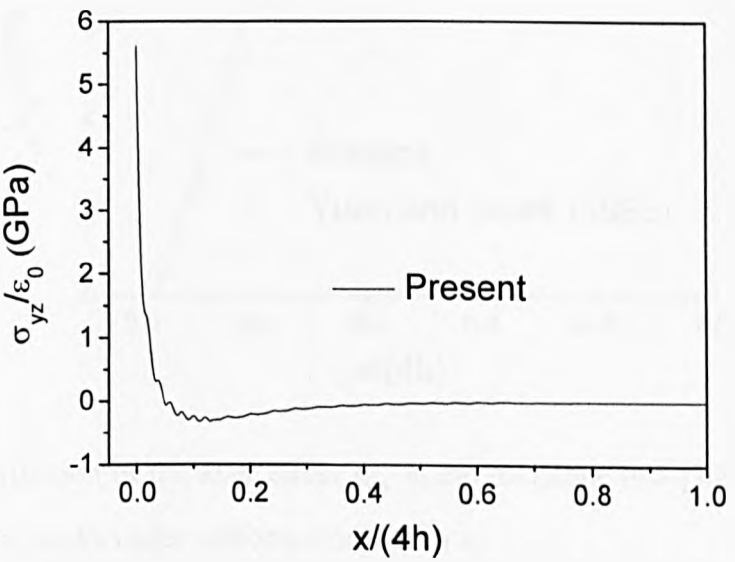

Fig. 5.13 Distribution of interlaminar shear stress σ_{yz} at the 30°/90° interface in a $[30°/90°]_s$ laminate with transverse cracks under uniform axial strain ε_0.

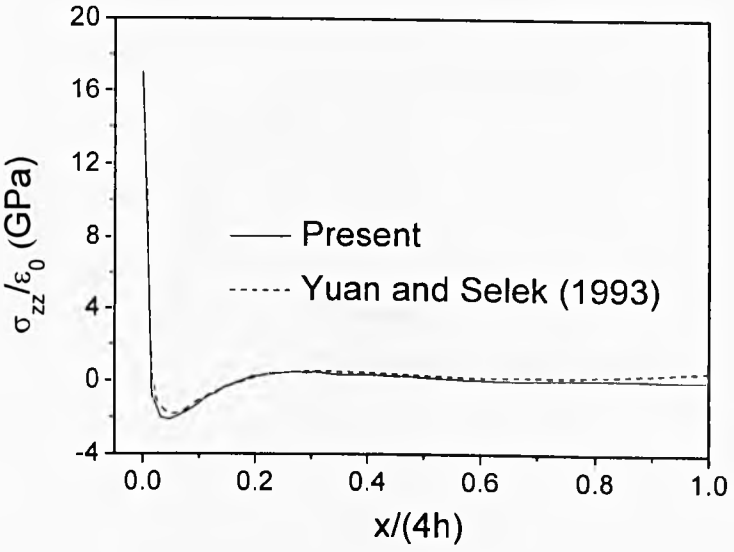

Fig. 5.14 Distribution of interlaminar normal stress σ_{zz} at the 30°/90° interface in a $[30°/90°]_s$ laminate with transverse cracks under uniform axial strain ε_0.

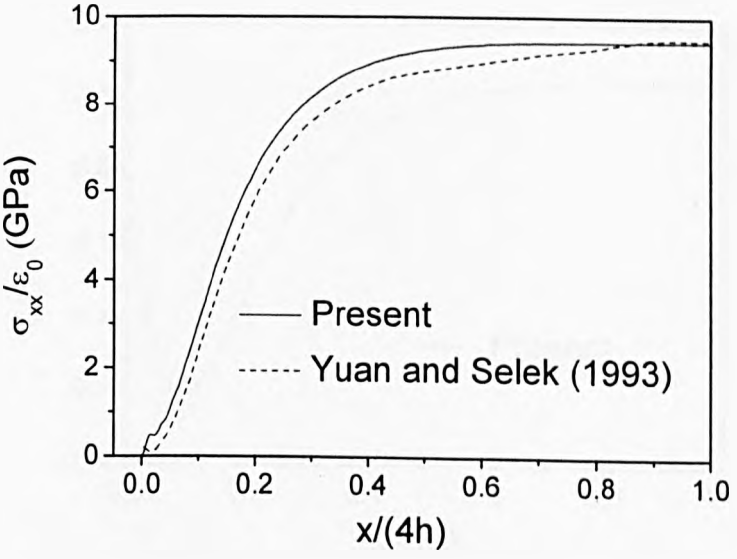

Fig. 5.15 Distribution of the axial stress σ_{xx} at the midplane in a $[30°/90°]_s$ laminate with transverse cracks under uniform axial strain ε_0.

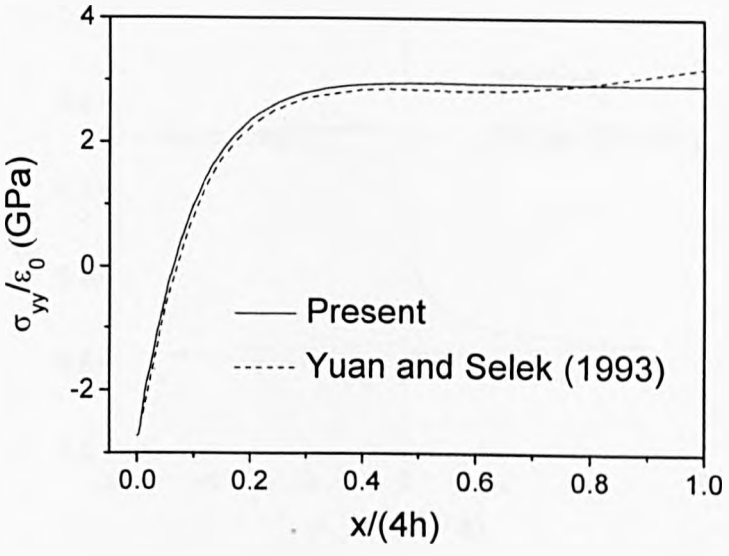

Fig. 5.16 Distribution of the axial stress σ_{yy} at the midplane in a $[30^o/90^o]_s$ laminate with transverse cracks under uniform axial strain ε_0.

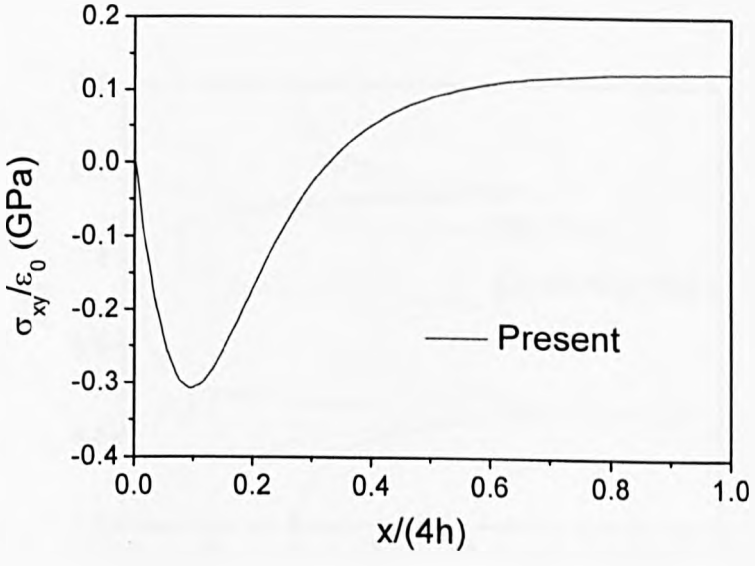

Fig. 5.17 Distribution of the in-plane shear stress σ_{xy} at the midplane in a $[30^o/90^o]_s$ laminate with transverse cracks under uniform axial strain ε_0.

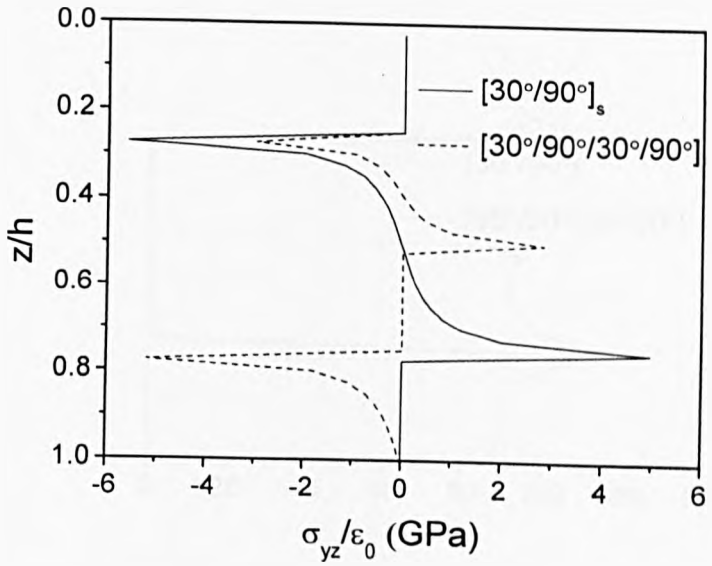

Fig. 5.18 Through thickness distribution of interlaminar shear stress σ_{yz} in the crack plane at x=0 in $[30^o/90^o]_s$ and $[30^o/90^o/30^o/90^o]$ laminates with transverse cracks under uniform axial strain ε_0.

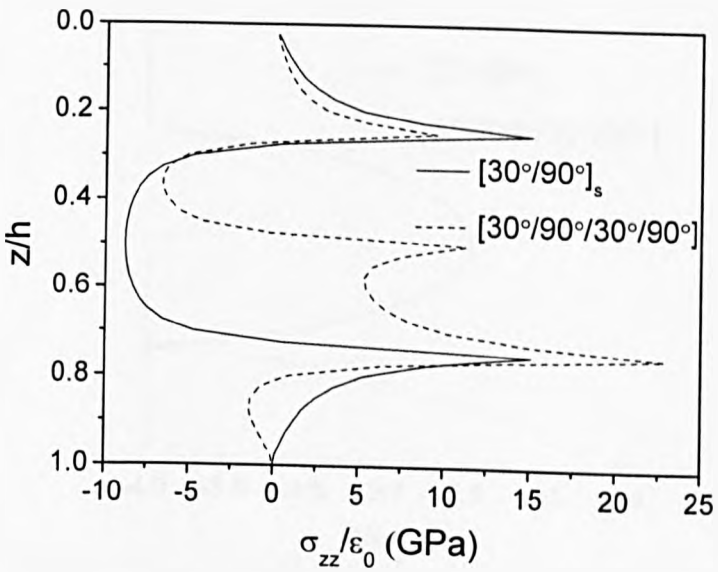

Fig. 5.19 Through thickness distribution of interlaminar normal stress σ_{zz} in the crack plane at x=0 in $[30^o/90^o]_s$ and $[30^o/90^o/30^o/90^o]$ laminates with transverse cracks under uniform axial strain ε_0.

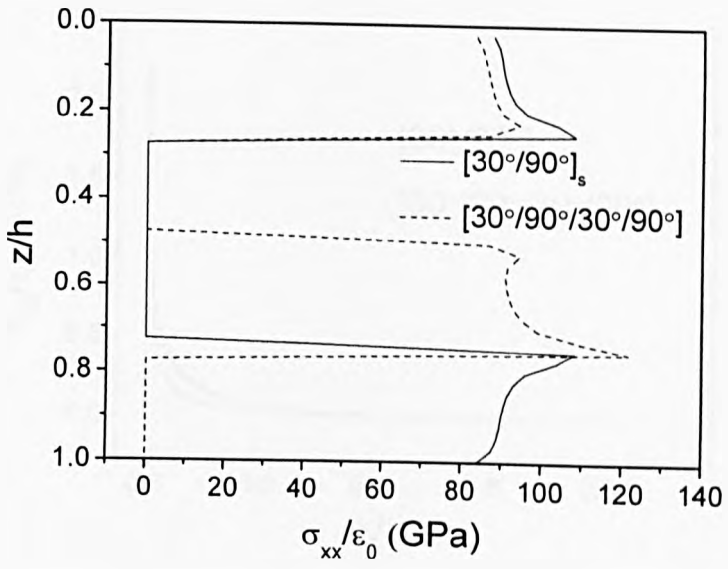

Fig. 5.20 Through thickness distribution of axial stress σ_{xx} in the crack plane at x=0 in $[30^{\circ}/90^{\circ}]_s$ and $[30^{\circ}/90^{\circ}/30^{\circ}/90^{\circ}]$ laminates with transverse cracks under uniform axial strain ε_0.

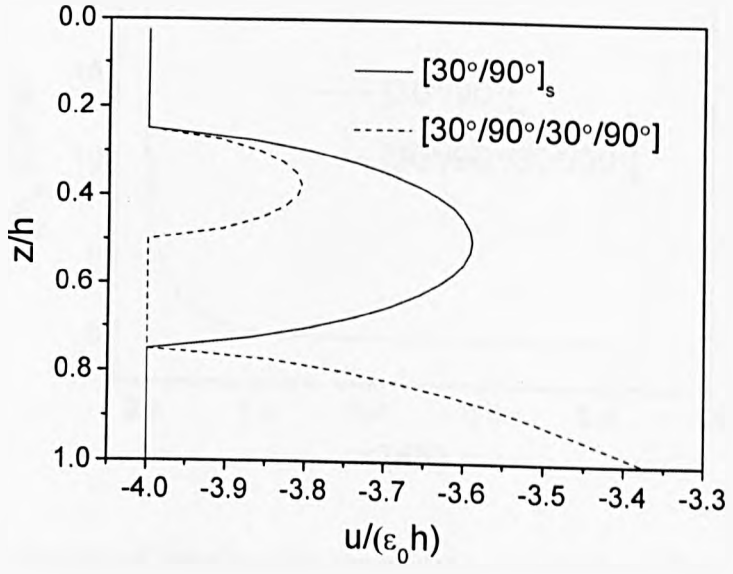

Fig. 5.21 Through thickness distribution of the displacement u in the crack plane at x=0 in $[30^{\circ}/90^{\circ}]_s$ and $[30^{\circ}/90^{\circ}/30^{\circ}/90^{\circ}]$ laminates with transverse cracks under uniform axial strain ε_0.

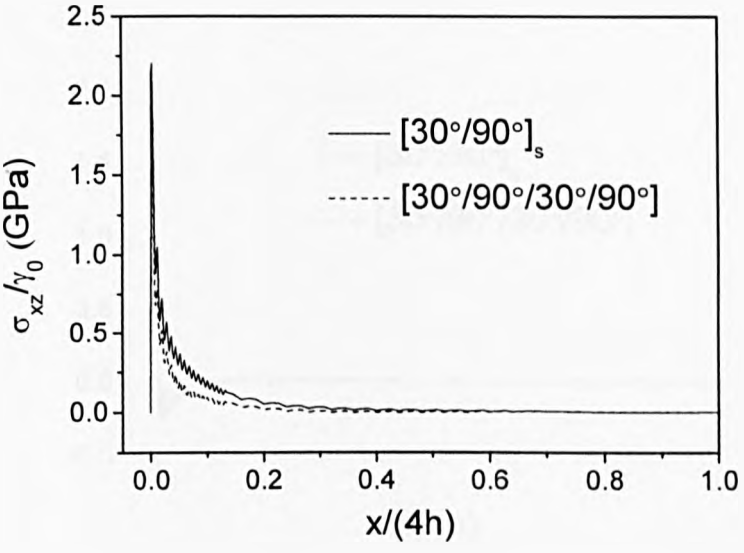

Fig. 5.22 Distribution of interlaminar shear stress σ_{xz} at the 30°/90° interface in a $[30^o/90^o]_s$ laminate with transverse cracks under shear strain γ_0.

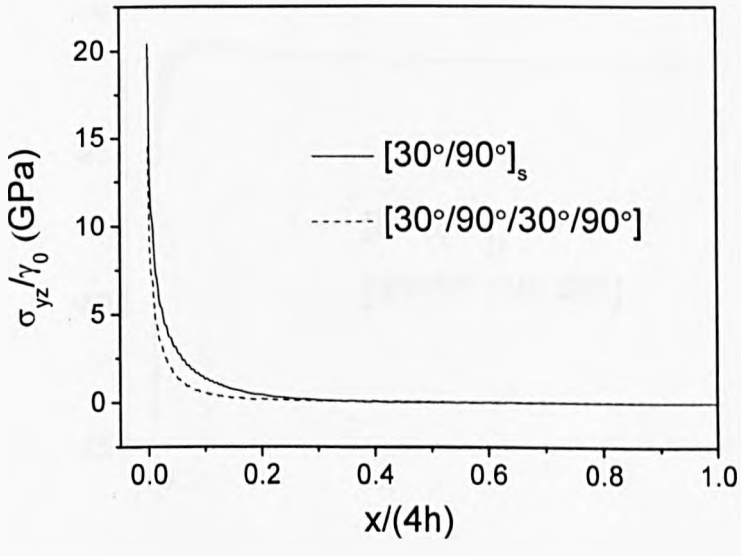

Fig. 5.23 Distribution of interlaminar shear stress σ_{yz} at the 30°/90° interface in a $[30^o/90^o]_s$ laminate with transverse cracks under shear strain γ_0.

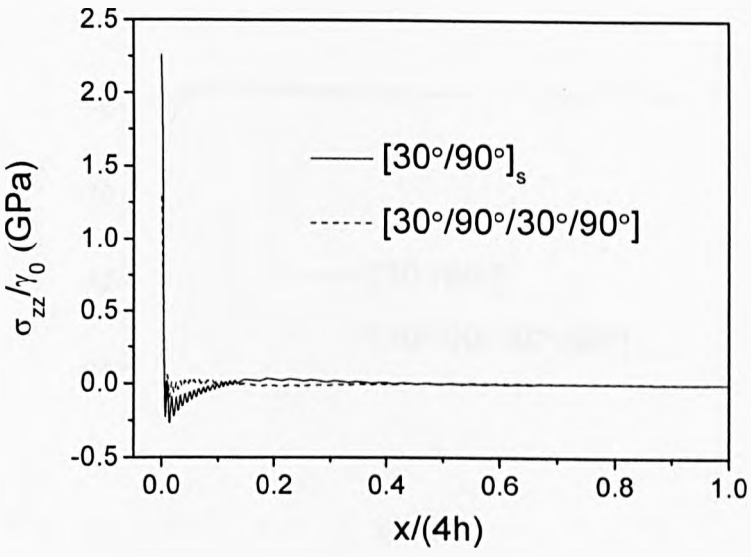

Fig. 5.24 Distribution of interlaminar normal stress σ_{zz} at the 30°/90° interface in a $[30°/90°]_s$ laminate with transverse cracks under shear strain γ_0.

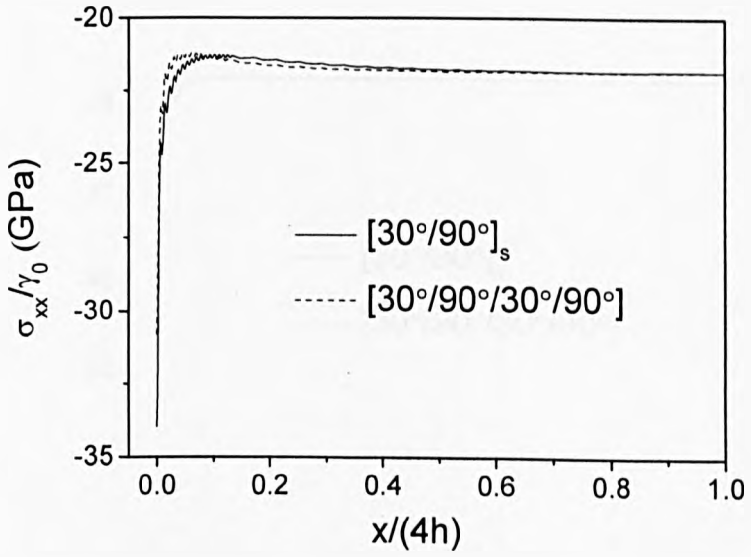

Fig. 5.25 Distribution of axial stress σ_{xx} at the 30°/90° interface in a $[30°/90°]_s$ laminate with transverse cracks under shear strain γ_0.

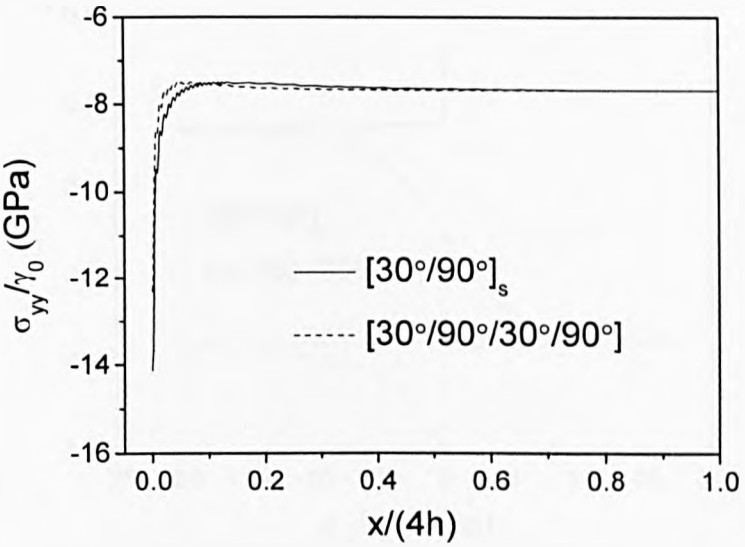

Fig. 5.26 Distribution of axial stress σ_{yy} at the 30°/90° interface in a $[30°/90°]_s$ laminate with transverse cracks under shear strain γ_0.

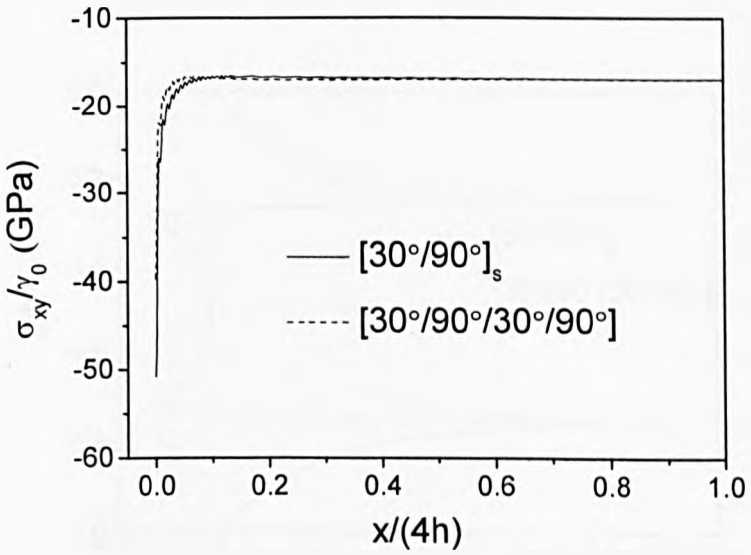

Fig. 5.27 Distribution of in-plane shear stress σ_{xy} at the 30°/90° interface in a $[30°/90°]_s$ laminate with transverse cracks under shear strain γ_0.

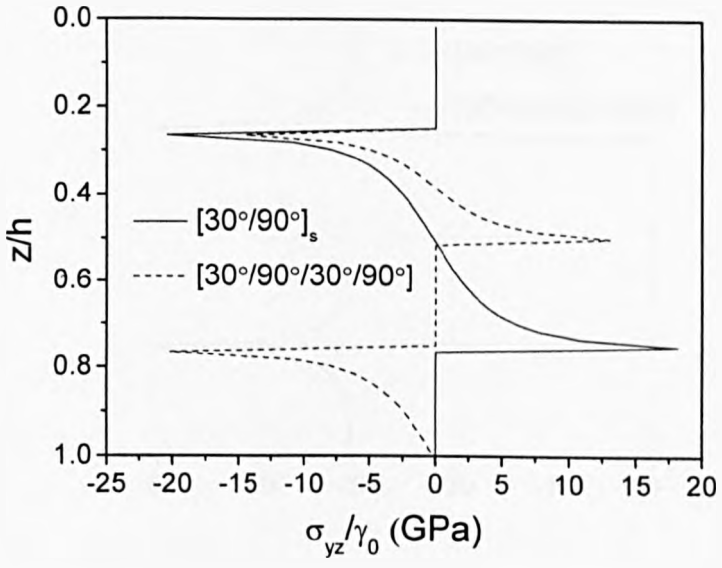

Fig. 5.28 Through thickness distribution of interlaminar shear stress σ_{yz} in the crack plane at x=0 in $[30^{\circ}/90^{\circ}]_s$ and $[30^{\circ}/90^{\circ}/30^{\circ}/90^{\circ}]$ laminates with transverse cracks under uniform shear strain γ_0.

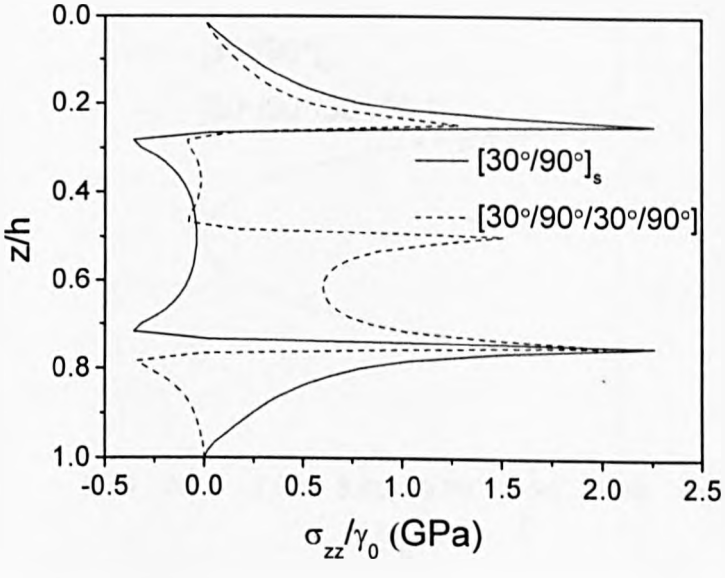

Fig. 5.29 Through thickness distribution of interlaminar normal stress σ_{zz} in the crack plane at x=0 in $[30^{\circ}/90^{\circ}]_s$ and $[30^{\circ}/90^{\circ}/30^{\circ}/90^{\circ}]$ laminates with transverse cracks under uniform shear strain γ_0.

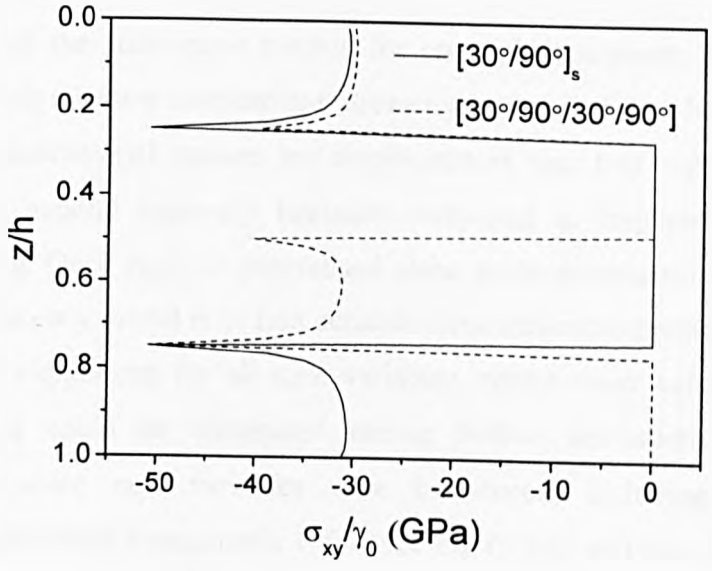

Fig. 5.30 Through thickness distribution of in-plane shear stress σ_{xy} in the crack plane at x=0 in $[30^{\circ}/90^{\circ}]_s$ and $[30^{\circ}/90^{\circ}/30^{\circ}/90^{\circ}]$ laminates with transverse cracks under uniform shear strain γ_0.

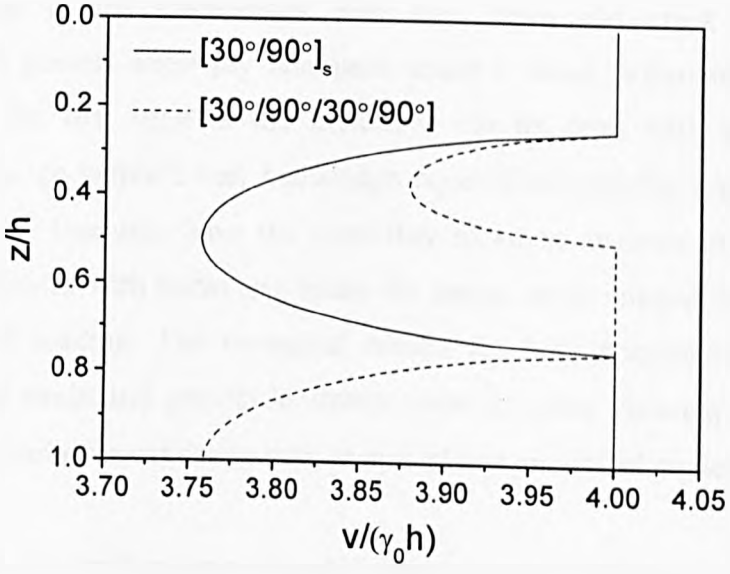

Fig. 5.31 Through thickness distribution of the displacement v in the crack plane at x=0 in $[30^{\circ}/90^{\circ}]_s$ and $[30^{\circ}/90^{\circ}/30^{\circ}/90^{\circ}]$ laminates with transverse cracks under uniform shear strain γ_0.

5.5. Conclusions

On the basis of the state space method for cross-ply composite laminates, a new model, in which all three interlaminar stresses are included, has been developed to predict three-dimensional stresses and displacements near free edges and transverse ply cracks in general angle-ply laminates subjected to in-plane and/or uniform thermal loading. Once again, a generalised plane strain deformation is adopted. The challenge of the new model is to find suitable displacement expressions and in-plane Fourier series expansions for all state variables, which must satisfy the boundary conditions and could be eliminated during further derivations. To meet the requirements, some new variables were introduced, including one unknown boundary displacement components $V^0(z)$ (See Eq. (5.14)) and two state variables $\bar{v}$ and σ_{yz} (See Eq. (5.16)) associated with appropriate Fourier series expansions. Numerical solutions were obtained by using layer refinement in the through thickness direction and Fourier series expansion in the x direction.

Comparisons with other available results were carried out to validate the present predictions. The numerical results for symmetric laminates showed good approximations to the singularities near free edges and crack surfaces. The predictions in general angle-ply laminates under a shear deformation, which are revealed for the first time in the literature, can be dealt with without further difficulties. To the author's best knowledge none of the existing analytical models published in the literature have the capability of stress analysis in nonsymmetric angle-ply laminates with transverse multi-ply cracks under biaxial extension, shear and/or thermal loading. The numerical results for both nonsymmetric laminates under an axial strain and general laminates under in plane shearing can be further used as benchmarks for validating new analytical and numerical models.

Once again by this method, an angle-ply laminate may be composed of an arbitrary number of monoclinic layers and each layer may have different material property and thickness. The method always guarantees continuous distributions of both displacements and interlaminar stresses across interfaces between material layers. Although the new introduced variables increase the complexity of the mathematical model, it is still highly efficient because the dimension of the state space equation is

only 6×6 and the dimension of the final equation (see Eq.5.29) is independent of the number of material layers. Thus, this method is particularly suitable to solve stress concentration problems of multi-layered angle-ply composites.

Because of universality of the new proposed method, it also can be used to analyse cross-ply laminates. For cross-ply laminates, the extension-shear coupling does not exist. Thus the two variables $V^0(z)$ and σ_{yz} will vanish in the present method to calculate cross-ply laminates. This will lead to the same formulations as those introduced in Chapter 4. In fact the state space method for cross-ply laminates can be treated as a special case of the method in this Chapter.

Chapter 6. Thermoelastic Property Degradation due to Transverse Cracking

6.1. Introduction

An immediate effect of transverse cracking is to cause degradation in stiffness and thermal expansion coefficients of composite laminates. In order to design a structure which can tolerate property reduction due to the formation of matrix cracks, the predictions of the effective thermoelastic constants of cracked laminates are of great interest in engineering applications.

In Chapters 4 and 5, the stress and displacement distributions in cross-ply and angle-ply laminates were investigated by using the state space methods. In this Chapter, the effective thermoelastic properties of cracked laminates will be predicted as functions of transverse crack density on the basis of the stress and displacement fields. Because the transverse cracks are assumed to be equally spaced, a representative element between neighbouring cracks can be taken out to evaluate the effective thermoelastic property of the entire laminate. Since the state space method has been verified to provide very accurate stress evaluations, high quality predictions of thermoelastic constants are also expected.

Using the Classical Laminate Theory of undamaged composite laminates, the equivalent stiffness and compliance matrices of cracked laminates are given first. Then the effective stiffness and thermal expansion coefficients of cracked laminates are defined using the compliance matrices. By applying the state space method to some specially prescribed loading cases, the effective thermoelastic constants can then be calculated. Extensive numerical results of the degradations of thermoelastic constants in general cross-ply and symmetric angle-ply laminates are presented. Most of them are compared with solutions of other models and experimental data in the literature. Parts of the work introduced in this Chapter have been published in Zhang et al. (2006a; Accepted).

6.2. Theoretical Formulations

6.2.1. Stiffness Matrices of Cracked Composite Laminates

6.2.1.1. General Laminates

Considering an angle-ply laminate (Fig. 5.3) containing uniform transverse cracks, the response of an element (Fig. 5.4) between neighbouring cracks can represent the deformation of the entire laminate. According to the Classical Laminate Theory introduced in Section 3.3.1, it is assumed that the overall deformation of the cracked laminate and the applied mechanical and thermal loading follow that

$$\begin{Bmatrix} N_x \\ N_y \\ N_{xy} \\ M_x \\ M_y \\ M_{xy} \end{Bmatrix} = \begin{bmatrix} A_{11}^c & A_{12}^c & A_{16}^c & B_{11}^c & B_{12}^c & B_{16}^c \\ A_{12}^c & A_{22}^c & A_{26}^c & B_{12}^c & B_{22}^c & B_{26}^c \\ A_{16}^c & A_{26}^c & A_{36}^c & B_{16}^c & B_{26}^c & B_{66}^c \\ B_{11}^c & B_{12}^c & B_{16}^c & D_{11}^c & D_{12}^c & D_{16}^c \\ B_{12}^c & B_{22}^c & B_{26}^c & D_{12}^c & D_{22}^c & D_{26}^c \\ B_{16}^c & B_{26}^c & B_{66}^c & D_{16}^c & D_{26}^c & D_{36}^c \end{bmatrix} \left(\begin{Bmatrix} \varepsilon_x^0 \\ \varepsilon_y^0 \\ \varepsilon_{xy}^0 \\ k_x \\ k_y \\ k_{xy} \end{Bmatrix} - \begin{Bmatrix} \alpha_1^c \\ \alpha_2^c \\ \alpha_3^c \\ \alpha_4^c \\ \alpha_5^c \\ \alpha_6^c \end{Bmatrix} \Delta T \right) \tag{6.1}$$

where letters with the superscript 'c' indicate properties of laminates with transverse cracks. Then the corresponding compliance matrix of the general cracked laminate is expressed by

$$\begin{bmatrix} [\mathbf{a}^c] & [\mathbf{b}^c] \\ [\mathbf{b}^c]^T & [\mathbf{d}^c] \end{bmatrix} = \begin{bmatrix} [\mathbf{A}^c] & [\mathbf{B}^c] \\ [\mathbf{B}^c]^T & [\mathbf{D}^c] \end{bmatrix}^{-1} \tag{6.2a}$$

where

$$[\mathbf{a}^c] = \begin{bmatrix} a_{11}^c & a_{12}^c & a_{16}^c \\ a_{12}^c & a_{22}^c & a_{26}^c \\ a_{16}^c & a_{26}^c & a_{66}^c \end{bmatrix}, [\mathbf{b}^c] = \begin{bmatrix} b_{11}^c & b_{12}^c & b_{16}^c \\ b_{12}^c & b_{22}^c & b_{26}^c \\ b_{16}^c & b_{26}^c & b_{66}^c \end{bmatrix}, [\mathbf{d}^c] = \begin{bmatrix} d_{11}^c & d_{12}^c & d_{16}^c \\ d_{12}^c & d_{22}^c & d_{26}^c \\ d_{16}^c & d_{26}^c & d_{66}^c \end{bmatrix}$$

$$[\mathbf{A}^c] = \begin{bmatrix} A_{11}^c & A_{12}^c & A_{16}^c \\ A_{12}^c & A_{22}^c & A_{26}^c \\ A_{16}^c & A_{26}^c & A_{66}^c \end{bmatrix}, [\mathbf{B}^c] = \begin{bmatrix} B_{11}^c & B_{12}^c & B_{16}^c \\ B_{12}^c & B_{22}^c & B_{26}^c \\ B_{16}^c & B_{26}^c & B_{66}^c \end{bmatrix}, [\mathbf{D}^c] = \begin{bmatrix} D_{11}^c & D_{12}^c & D_{16}^c \\ D_{12}^c & D_{22}^c & D_{26}^c \\ D_{16}^c & D_{26}^c & D_{66}^c \end{bmatrix} \tag{6.2b}$$

The components of the effective 6×6 laminate compliance matrix as well as the 6×1 vector of thermal expansion coefficients remain to be determined. For certain ply stacking sequences, some of the couplings do not occur and the stiffness and compliance matrices become simpler.

6.2.1.2. General Cross-ply Laminates

In a general cross-ply laminate with transverse cracks, there are no extension-shear, bending-twist, extension-twist and shear-bending couplings. Therefore the stiffness and compliance matrices of such a laminate e.g. $[0°/90°_3]$ become

$$\begin{bmatrix} A_{11}^c & A_{12}^c & 0 & B_{11}^c & B_{12}^c & 0 \\ A_{12}^c & A_{22}^c & 0 & B_{12}^c & B_{22}^c & 0 \\ 0 & 0 & A_{66}^c & 0 & 0 & B_{66}^c \\ B_{11}^c & B_{12}^c & 0 & D_{11}^c & D_{12}^c & 0 \\ B_{12}^c & B_{22}^c & 0 & D_{12}^c & D_{22}^c & 0 \\ 0 & 0 & B_{66}^c & 0 & 0 & D_{66}^c \end{bmatrix} = \begin{bmatrix} a_{11}^c & a_{12}^c & 0 & b_{11}^c & b_{12}^c & 0 \\ a_{12}^c & a_{22}^c & 0 & b_{12}^c & b_{22}^c & 0 \\ 0 & 0 & a_{66}^c & 0 & 0 & b_{66}^c \\ b_{11}^c & b_{12}^c & 0 & d_{11}^c & d_{12}^c & 0 \\ b_{12}^c & b_{22}^c & 0 & d_{12}^c & d_{22}^c & 0 \\ 0 & 0 & b_{66}^c & 0 & 0 & d_{66}^c \end{bmatrix}^{-1} \tag{6.3}$$

6.2.1.3. General Symmetric Laminates

In a general symmetric laminate with transverse cracks, there is no in-plane and out-of-plane coupling. Therefore the stiffness and compliance matrices of such a laminate e.g. $[30°/90°_2]_s$ become

$$\begin{bmatrix} A_{11}^c & A_{12}^c & A_{16}^c & 0 & 0 & 0 \\ A_{12}^c & A_{22}^c & A_{26}^c & 0 & 0 & 0 \\ A_{16}^c & A_{26}^c & A_{66}^c & 0 & 0 & 0 \\ 0 & 0 & 0 & D_{11}^c & D_{12}^c & D_{16}^c \\ 0 & 0 & 0 & D_{12}^c & D_{22}^c & D_{26}^c \\ 0 & 0 & 0 & D_{16}^c & D_{26}^c & D_{66}^c \end{bmatrix} = \begin{bmatrix} a_{11}^c & a_{12}^c & a_{16}^c & 0 & 0 & 0 \\ a_{12}^c & a_{22}^c & a_{26}^c & 0 & 0 & 0 \\ a_{16}^c & a_{26}^c & a_{66}^c & 0 & 0 & 0 \\ 0 & 0 & 0 & d_{11}^c & d_{12}^c & d_{16}^c \\ 0 & 0 & 0 & d_{12}^c & d_{22}^c & d_{26}^c \\ 0 & 0 & 0 & d_{16}^c & d_{26}^c & d_{66}^c \end{bmatrix}^{-1} \tag{6.4}$$

6.2.1.4. Symmetric Cross-ply Laminates

In the case of symmetric cross-ply laminates, the behaviours of general cross-ply and symmetric laminates combine together. Then the stiffness and compliance matrices of such a laminate e.g. $[0°/90°_2]_s$ become

$$\begin{bmatrix} A_{11}^c & A_{12}^c & 0 & 0 & 0 & 0 \\ A_{12}^c & A_{22}^c & 0 & 0 & 0 & 0 \\ 0 & 0 & A_{66}^c & 0 & 0 & 0 \\ 0 & 0 & 0 & D_{11}^c & D_{12}^c & 0 \\ 0 & 0 & 0 & D_{12}^c & D_{22}^c & 0 \\ 0 & 0 & 0 & 0 & 0 & D_{66}^c \end{bmatrix} = \begin{bmatrix} a_{11}^c & a_{12}^c & 0 & 0 & 0 & 0 \\ a_{12}^c & a_{22}^c & 0 & 0 & 0 & 0 \\ 0 & 0 & a_{66}^c & 0 & 0 & 0 \\ 0 & 0 & 0 & d_{11}^c & d_{12}^c & 0 \\ 0 & 0 & 0 & d_{12}^c & d_{22}^c & 0 \\ 0 & 0 & 0 & 0 & 0 & d_{66}^c \end{bmatrix}^{-1} \tag{6.5}$$

6.2.1.5. Antisymmetric Cross-ply Laminates

An antisymmetric cross-ply laminate is that which has an even number of orthotropic layers with principle material directions alternating at 0° or 90° to the laminate axes. For every 0° layer of a given thickness and location, there is a 90° layer of the same thickness and location on the other side of the midplane. The stiffness and compliance matrices of such a laminate e.g. [0°/90°$_2$/0°$_2$/90°] become

$$\begin{bmatrix} A_{11}^c & A_{12}^c & 0 & B_{11}^c & 0 & 0 \\ A_{12}^c & A_{22}^c & 0 & 0 & -B_{11}^c & 0 \\ 0 & 0 & A_{66}^c & 0 & 0 & 0 \\ B_{11}^c & 0 & 0 & D_{11}^c & D_{12}^c & 0 \\ 0 & -B_{11}^c & 0 & D_{12}^c & D_{22}^c & 0 \\ 0 & 0 & 0 & 0 & 0 & D_{66}^c \end{bmatrix} = \begin{bmatrix} a_{11}^c & a_{12}^c & 0 & b_{11}^c & b_{12}^c & 0 \\ a_{12}^c & a_{22}^c & 0 & b_{12}^c & b_{22}^c & 0 \\ 0 & 0 & a_{66}^c & 0 & 0 & 0 \\ b_{11}^c & b_{12}^c & 0 & d_{11}^c & d_{12}^c & 0 \\ b_{12}^c & b_{22}^c & 0 & d_{12}^c & d_{22}^c & 0 \\ 0 & 0 & 0 & 0 & 0 & d_{66}^c \end{bmatrix}^{-1} \tag{6.6}$$

Note that the zero coefficients in stiffness matrix $[\mathbf{B}^c]$ may not have corresponding ones in compliance matrix $[\mathbf{b}^c]$ of such laminates.

6.2.2. Effective Thermoelastic Constants of Cracked Laminates

The effective thermoelastic constants of cracked laminates can be derived by using the definitions for uncracked laminates mentioned in Section 3.3.3. Similarly the thermoelastic properties of a cracked laminate are expressed in terms of the components of the 6×6 laminate compliances and the 6×1 vector of thermal expansion coefficients. A transformation needs to be applied to ensure that all the properties are principally of the same dimension. A matrix $[\bar{\mathbf{S}}^c]$ of equivalent laminate compliances is obtained by use of the total laminate thickness H as

$$[\bar{\mathbf{S}}^c] = \begin{bmatrix} H[\mathbf{a}^c] & \frac{H^2}{2}[\mathbf{b}^c] \\ \frac{H^2}{2}[\mathbf{b}^c]^T & \frac{H^3}{12}[\mathbf{d}^c] \end{bmatrix} = \begin{bmatrix} [\bar{a}^c] & [\bar{b}^c] \\ [\bar{b}^c]^T & [\bar{d}^c] \end{bmatrix} \tag{6.7a}$$

where

$$[\bar{a}^c] = H[\mathbf{a}^c],\ [\bar{b}^c] = \frac{H^2}{2}[\mathbf{b}^c],\ [\bar{d}^c] = \frac{H^3}{12}[\mathbf{d}^c] \tag{6.7b}$$

Similarly, a 6×1 vector of equivalent thermal expansion coefficients $[\bar{\alpha}^c]$ is introduced as

$$[\overline{\alpha}^c] = \left[\alpha_1^c \quad \alpha_2^c \quad \alpha_3^c \quad \frac{H}{2}\alpha_4^c \quad \frac{H}{2}\alpha_5^c \quad \frac{H}{2}\alpha_6^c\right]^T \tag{6.8}$$

From the compliance matrix $[\overline{\mathbf{S}}^c]$, the effective thermoelastic constants of cracked laminates, i.e. effective elastic and shear moduli, effective bending and twisting moduli, effective extension–extension and extension–shear coupling ratios, effective bending–bending and bending–twisting coupling ratios, and in-plane–out-of-plane coupling ratios can be defined as the corresponding Eqs. (3.19-3.23), respectively, for uncracked laminates.

In the present analysis, the effective thermoelastic properties of cracked cross-ply laminates and the effective in-plane thermoelastic constants of symmetric angle-ply laminates will be predicted. The details of these effective properties are introduced as follows.

6.2.2.1. Effective Thermoelastic Constants of Cross-ply Laminates

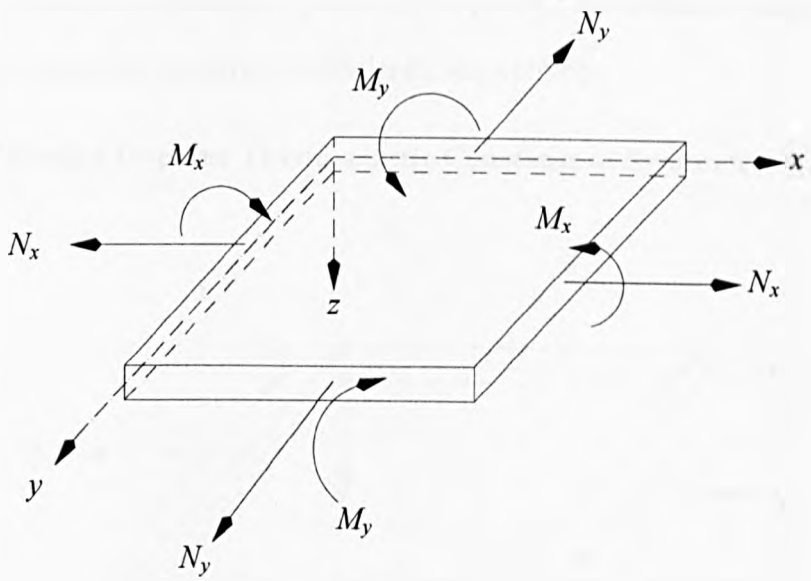

Fig. 6.1 Nomenclature of a cross-ply laminate subjected to in-plane extension and out-of-plane bending.

In a cross-ply laminate with uniform transverse cracks, the extension-shear and bending-twisting couplings vanish (see Eq (6.3)). Considering the laminate is under in-plane extension and out-of-plane bending (Fig. 6.1), the relationship between overall deformation and applied loading of the laminate reduces to

$$\begin{Bmatrix} \varepsilon_x^0 \\ \varepsilon_y^0 \\ k_x \\ k_y \end{Bmatrix} = \begin{bmatrix} a_{11}^c & a_{12}^c & b_{11}^c & b_{12}^c \\ a_{12}^c & a_{22}^c & b_{21}^c & b_{22}^c \\ b_{11}^c & b_{21}^c & d_{11}^c & d_{12}^c \\ b_{12}^c & b_{22}^c & d_{12}^c & d_{22}^c \end{bmatrix} \begin{Bmatrix} N_x \\ N_y \\ M_x \\ M_y \end{Bmatrix} + \begin{Bmatrix} \alpha_1^c \\ \alpha_2^c \\ \alpha_4^c \\ \alpha_5^c \end{Bmatrix} \Delta T \tag{6.9}$$

The engineering constants are defined as

$$\begin{aligned} &E_x^c = \frac{1}{Ha_{11}^c},\ E_y^c = \frac{1}{Ha_{22}^c},\ \nu_{xy}^c = -\frac{a_{12}^c}{a_{11}^c},\ \nu_{yx}^c = -\frac{a_{12}^c}{a_{22}^c}, \\ &F_x^c = \frac{12}{H^3 d_{11}^c},\ F_y^c = \frac{12}{H^3 d_{22}^c},\ \eta_{xy}^c = -\frac{d_{12}^c}{d_{11}^c},\ \eta_{yx}^c = -\frac{d_{12}^c}{d_{22}^c}, \\ &\varphi_{xx}^c = -\frac{Hb_{11}^c}{2a_{11}^c},\ \varphi_{xy}^c = -\frac{Hb_{12}^c}{2a_{11}^c},\ \varphi_{yx}^c = -\frac{Hb_{21}^c}{2a_{22}^c},\ \varphi_{yy}^c = -\frac{Hb_{22}^c}{2a_{22}^c} \\ &\psi_{xx}^c = -\frac{6b_{11}^c}{Hd_{11}^c},\ \psi_{xy}^c = -\frac{6b_{12}^c}{Hd_{11}^c},\ \psi_{yx}^c = -\frac{6b_{21}^c}{Hd_{22}^c},\ \psi_{yy}^c = -\frac{6b_{22}^c}{Hd_{22}^c} \end{aligned} \tag{6.10}$$

where E_x^c and E_y^c are effective Young's moduli; ν_{xy}^c and ν_{xy}^c are effective Poisson's ratios; F_x^c and F_y^c are effective flexural moduli; and η_{xy}^c and η_{yx}^c are effective flexural coupling coefficients; φ_{ij}^c and ψ_{ij}^c (i, j=x, y) are effective extension-flexure and flexure-extension coupling coefficients, respectively.

6.2.2.2. Effective In-plane Thermoelastic Constants of Symmetric Laminates

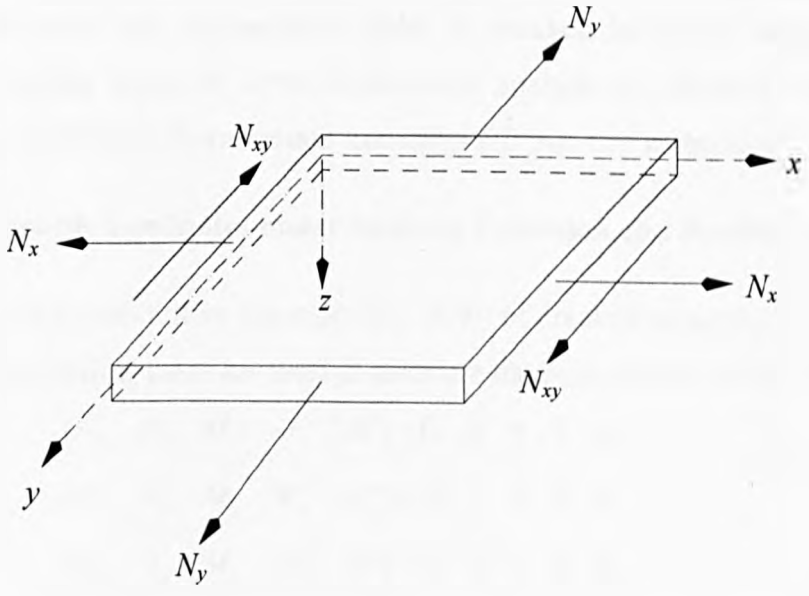

Fig. 6.2 Nomenclature of a symmetric laminate subjected to in-plane loading.

In a symmetric laminate with uniform transverse cracks, there exists no in-plane–out-of-plane coupling. Considering the laminate is subjected to in-plane loading (Fig. 6.2), the in-plane strains are related only to in-plane forces as follows

$$\begin{Bmatrix} \varepsilon_x^0 \\ \varepsilon_y^0 \\ \varepsilon_{xy}^0 \end{Bmatrix} = \begin{bmatrix} a_{11}^c & a_{12}^c & a_{16}^c \\ a_{12}^c & a_{22}^c & a_{26}^c \\ a_{16}^c & a_{26}^c & a_{66}^c \end{bmatrix} \begin{Bmatrix} N_x \\ N_y \\ N_{xy} \end{Bmatrix} + \begin{Bmatrix} \alpha_1^c \\ \alpha_2^c \\ \alpha_3^c \end{Bmatrix} \Delta T \tag{6.11}$$

Analogous to Eq. (6.10), the following relations are obtained

$$\begin{aligned} &E_x^c = \frac{1}{Ha_{11}^c},\ E_y^c = \frac{1}{Ha_{22}^c},\ G_{xy}^c = \frac{1}{Ha_{66}^c} \\ &\nu_{xy}^c = -\frac{a_{12}^c}{a_{11}^c},\ \nu_{yx}^c = -\frac{a_{12}^c}{a_{22}^c},\ \nu_{sx}^c = -\frac{a_{16}^c}{a_{66}^c} \\ &\nu_{xs}^c = -\frac{a_{16}^c}{a_{11}^c},\ \nu_{ys}^c = -\frac{a_{26}^c}{a_{22}^c},\ \nu_{sy}^c = -\frac{a_{26}^c}{a_{66}^c} \end{aligned} \tag{6.12}$$

where G_{xy}^c is the effective shear modulus; and ν_{sx}^c, ν_{xs}^c, ν_{sy}^c, and ν_{ys}^c are effective extension-shear coupling coefficients.

6.2.3. Calculation of Effective Thermoelastic Constants

In order to calculate the effective thermoelastic constants, the related compliances of cracked laminates must be first solved. These compliances can be determined by the solutions of stress and displacement fields in cracked laminates under specially prescribed loading cases. In term of the stress analysis in Chapters 4 and 5, the calculations of effective thermoelastic constants fall into two categories.

6.2.3.1. Cross-ply Laminates under In-plane Extension and Bending

According to the constitutive equation (Eq. (6.9)) of cracked cross-ply laminates, the following five loading cases are used to calculate the compliances in Eq. (6.9).

$$[N_x \quad N_y \quad M_x \quad M_y \quad \Delta T] = [1 \quad 0 \quad 0 \quad 0 \quad 0] \tag{6.13a}$$

$$[N_x \quad N_y \quad M_x \quad M_y \quad \Delta T] = [0 \quad 1 \quad 0 \quad 0 \quad 0] \tag{6.13b}$$

$$[N_x \quad N_y \quad M_x \quad M_y \quad \Delta T] = [0 \quad 0 \quad 1 \quad 0 \quad 0] \tag{6.13c}$$

$$[N_x \quad N_y \quad M_x \quad M_y \quad \Delta T] = [0 \quad 0 \quad 0 \quad 1 \quad 0] \tag{6.13d}$$

$$[N_x \quad N_y \quad M_x \quad M_y \quad \Delta T] = [0 \quad 0 \quad 0 \quad 0 \quad 1] \tag{6.13e}$$

where Eqs. (6.13a), (6.13b), (6.13c), (6.13d), and (6.13e), respectively, represent the loading conditions in which a cracked laminate is subjected to a unit force in the x-direction, a unit force in the y-direction, a unit bending moment in the x-z plane, a unit bending moment in the y-z plane, and a unit uniform temperature increase. The stress analysis of all these loading conditions has been demonstrated by numerical examples in Section 4.4. By using the displacement solutions of the stress analysis, the mid-plane strains and curvatures can be determined by

$$\varepsilon_x^0 = \frac{u(0, H/2)}{L/2} \tag{6.14a}$$

$$\varepsilon_y^0 = \varepsilon_0(H/2) \tag{6.14b}$$

$$k_x = \frac{u(0,H) - u(0,0)}{HL/2} \tag{6.14c}$$

$$k_y = \frac{\varepsilon_0(H) - \varepsilon_0(0)}{H} \tag{6.14d}$$

where the definitions of the displacement u and strain ε_0 can be found in Eqs. (4.13) and (4.8), respectively; H and L are the thickness and width of the laminate (see Fig. 4.2).

Substituting the five sets of prescribed loading Eqs (6.13) into Eq. (6.9), all the compliances and effective thermal expansion coefficients are determined, respectively, as

$$a_{11}^c = \varepsilon_x^0,\ a_{12}^c = \varepsilon_y^0,\ b_{11}^c = k_x,\ b_{12}^c = k_y \tag{6.15a}$$

$$a_{12}^c = \varepsilon_x^0,\ a_{22}^c = \varepsilon_y^0,\ b_{21}^c = k_x,\ b_{22}^c = k_y \tag{6.15b}$$

$$b_{11}^c = \varepsilon_x^0,\ b_{21}^c = \varepsilon_y^0,\ d_{11}^c = k_x,\ d_{12}^c = k_y \tag{6.15c}$$

$$b_{12}^c = \varepsilon_x^0,\ b_{22}^c = \varepsilon_y^0,\ d_{12}^c = k_x,\ d_{22}^c = k_y \tag{6.15d}$$

$$\alpha_1^c = \varepsilon_x^0,\ \alpha_2^c = \varepsilon_y^0,\ \alpha_4^c = k_x,\ \alpha_5^c = k_y \tag{6.15e}$$

Then all the effective engineering constants of cracked cross-ply laminates can be calculated by Eq. (6.10).

6.2.3.2. Symmetric Laminates under In-plane Loading

According to the in-plane constitutive equation (Eq. (6.11)) of cracked symmetric laminates, the following four loading cases are used to calculate the compliances in Eq. (6.11).

$$[N_x \quad N_y \quad N_{xy} \quad \Delta T] = [1 \quad 0 \quad 0 \quad 0] \tag{6.16a}$$

$$[N_x \quad N_y \quad N_{xy} \quad \Delta T] = [0 \quad 1 \quad 0 \quad 0] \tag{6.16b}$$

$$[N_x \quad N_y \quad N_{xy} \quad \Delta T] = [0 \quad 0 \quad 1 \quad 0] \tag{6.16c}$$

$$[N_x \quad N_y \quad N_{xy} \quad \Delta T] = [0 \quad 0 \quad 0 \quad 1] \tag{6.16d}$$

where Eqs. (6.16a), (6.16b), (6.16c), and (6.16d), respectively, represent the loading conditions in which a cracked laminate is subjected to a unit force in the x-direction, a unit force in the y-direction, a unit shear in the x-y plane, and a unit uniform temperature increase. By using the stress analysis in Chapter 5, the displacement fields are obtained and can then be used to calculate the mid-plane strains

$$\varepsilon_x^0 = \frac{u(0, H/2)}{L/2} \tag{6.17a}$$

$$\varepsilon_y^0 = v(L/2, 1, H/2) \tag{6.17b}$$

$$\varepsilon_{xy}^0 = \frac{v(0,0,H)}{L/2} \tag{6.17c}$$

where the expressions of the displacements u and v can be found in Eq. (5.14).

Substituting the four sets of prescribed loading Eqs (6.16) into Eq. (6.11), all the compliances and effective thermal expansion coefficients are determined, respectively, as

$$a_{11}^c = \varepsilon_x^0,\ a_{12}^c = \varepsilon_y^0,\ a_{16}^c = \varepsilon_{xy}^0 \tag{6.18a}$$

$$a_{12}^c = \varepsilon_x^0,\ a_{22}^c = \varepsilon_y^0,\ a_{26}^c = \varepsilon_{xy}^0 \tag{6.18b}$$

$$b_{11}^c = \varepsilon_x^0,\ b_{21}^c = \varepsilon_y^0,\ a_{66}^c = \varepsilon_{xy}^0 \tag{6.18c}$$

$$\alpha_1^c = \varepsilon_x^0,\ \alpha_2^c = \varepsilon_y^0,\ \alpha_3^c = \varepsilon_{xy}^0 \tag{6.18d}$$

Then all the effective in-plane engineering constants of cracked symmetric laminates can be calculated by Eq. (6.12).

6.3. Numerical Results

6.3.1. Cross-ply Laminates

The method proposed above is illustrated by numerical examples. The material properties and dimensions used in this section are given in Table 6.1. To enable comparisons to be made with the results available in the literature, the thermoelastic constants of the damaged laminates are normalised by the stiffness of the undamaged laminates which is indicated by a superscript '°' and plotted with respect to the transverse crack density.

Table 6.1 Material properties and dimensions

	Material 6.1	Material 6.2	Material 6.3	Material 6.4
Type	Graphite/epoxy	Glass/epoxy	Glass/epoxy	Graphite/epoxy
E_L	144.78 GPa	41.7 GPa	45.6 GPa	132.0 GPa
E_T	9.58 GPa	13.0 GPa	16.2 GPa	10.8 GPa
ν_{LT}	0.31	0.30	0.278	0.24
ν_{TT}	0.55	0.42	0.4	0.4
G_{LT}	4.785 GPa	3.4 GPa	5.83 GPa	5.7 GPa
G_{TT}	3.090 GPa	4.58 GPa	5.83 GPa	5.7 GPa
α_1	-0.72×10^{-6}/°C		8.6×10^{-6}/°C	-0.11×10^{-6}/°C
α_2	27.0×10^{-6}/°C		26.4×10^{-6}/°C	27.2×10^{-6}/°C
H_{ply}	0.127 mm	0.203 mm	0.25 mm	0.14 mm

6.3.1.1. Symmetric Cross-ply Laminates

Numerical examples are first presented for symmetric cross-ply laminates containing transverse cracks. Using the Material 6.1, Material 6.2, and Material 6.3 in Table 6.1, the effective Young's modulus and the effective Poisson's ratio as a function of crack density have been predicted in a $[0°/90°]_s$ graphite/epoxy laminate, a $[0°/90°_3]_s$ graphite/epoxy laminate, and a $[0°/90°_3]_s$ glass/epoxy laminate, respectively. These numerical results are plotted in Fig. 6.3–Fig. 6.8.

To validate the present predictions, some of the present solutions are compared with other numerical and experimental results subjected to availability. These comparisons are shown in Fig. 6.3, Fig. 6.5, Fig. 6.7, and Fig. 6.8. Among these results, McCartney et al.(2000) assumed a generalised plane strain deformation as well. Yuan and Selek (1993) employed a finite element method. Groves et al. (1987) and Reifsnider and Highsmith (1982) used experimental methods. In general the present predictions agree well with these analytical or experimental results, while in Fig. 6.7 for large values of crack density the analytical solutions overestimate the axial stiffness. This is because the analytical models consider only pure transverse cracking damage and other forms of damage such as fiber matrix interfacial sliding that may effect the laminate stiffness during testing are neglected (McCartney *et al.*, 2000).

Using the Material 6.4 in Table 6.1, the degradation of the flexural modulus has been calculated as a function of crack density for a glass/epoxy laminate of the type $[0°/90°_2/0°/90°_2/0°]$. The result is compared with that of McCartney and Pierse (1997b) in Fig. 6.9. The transverse cracks were assumed to be uniformly distributed in only one of the $90°_2$ layers in the tension zone. This takes account of the crack closing-up effect in the compression zone. An excellent agreement is obtained between the present solution and McCartney and Pierse (1997b)'s prediction.

The changes in the effective thermal expansion coefficients (TEC) of $[0°/90°]_s$, $[0°_2/90°_2]_s$ and $[0°/90°_3]_s$ graphite/epoxy laminates are predicted. The laminates are made of the Material 6.1 in Table 6.1. Fig. 6.10 shows excellent agreements between the present solutions and Lim and Hong (1989)'s finite element results.

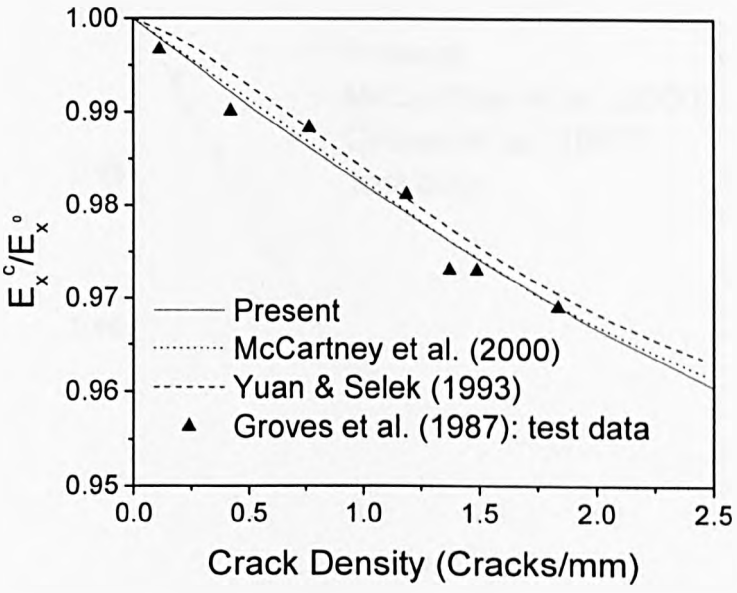

Fig. 6.3 Dependence of the normalised Young's modulus on the crack density in a $[0°/90°]_s$ graphite/epoxy laminate with transverse cracks.

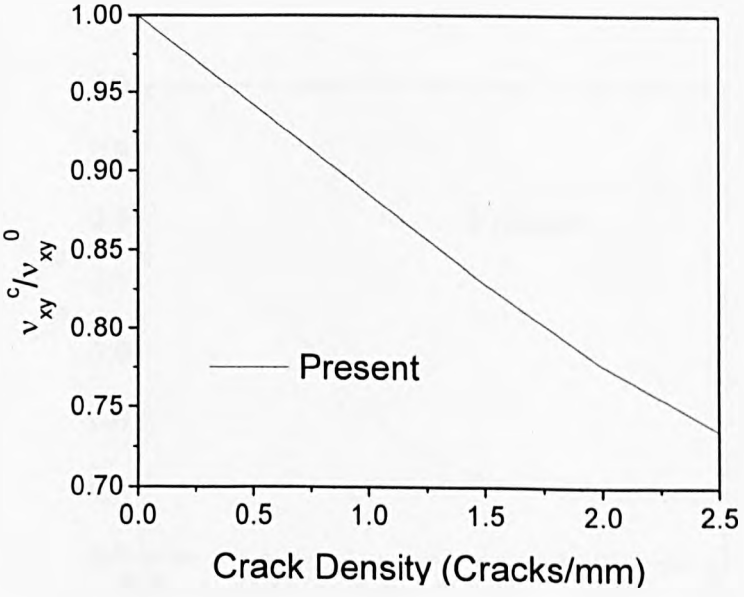

Fig. 6.4 Dependence of the normalised Poisson's ratio on the crack density in a $[0°/90°]_s$ graphite/epoxy laminate with transverse cracks.

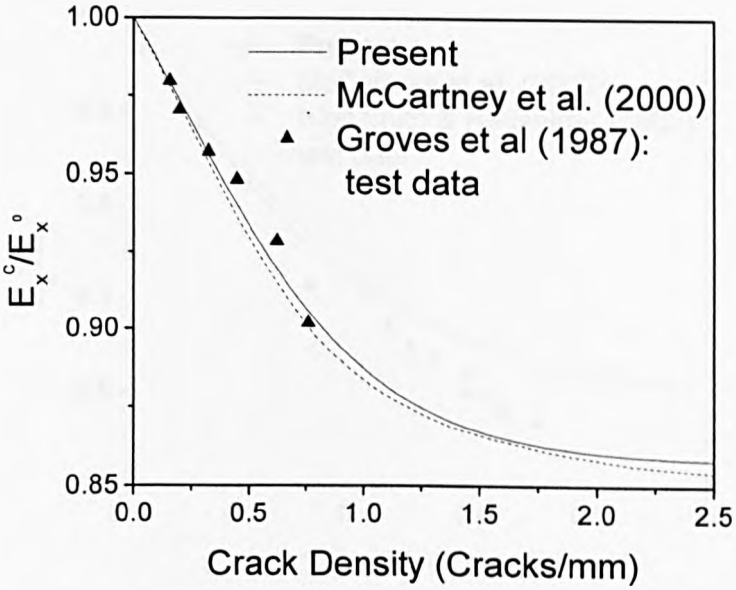

Fig. 6.5 Dependence of the normalised Young's modulus on the crack density in a $[0°/90°_3]_s$ graphite/epoxy laminate with transverse cracks.

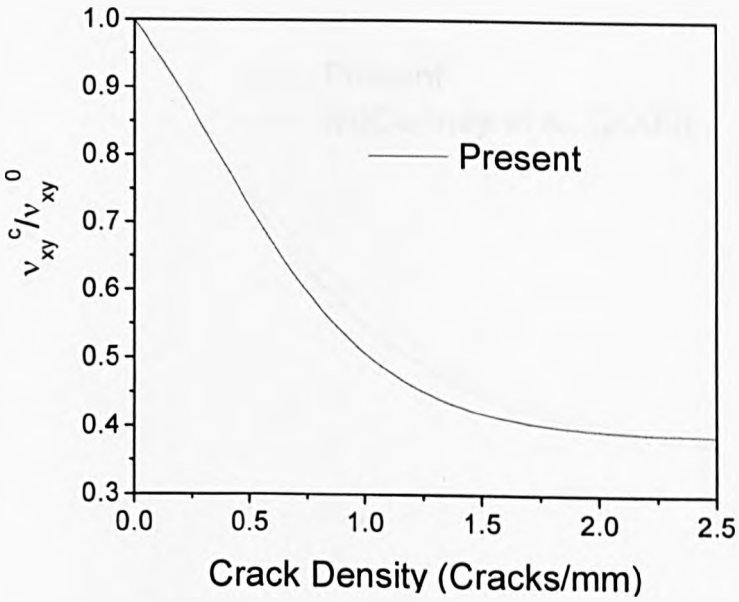

Fig. 6.6 Dependence of the normalised Poisson's ratio on the crack density in a $[0°/90°_3]_s$ graphite/epoxy laminate with transverse cracks.

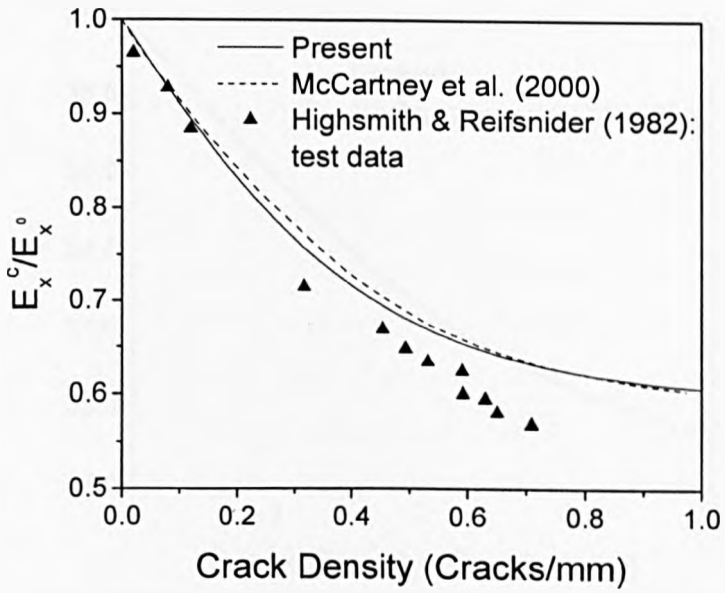

Fig. 6.7 Dependence of the normalised Young's modulus on the crack density in a $[0°/90°_3]_s$ glass/epoxy laminate with transverse cracks.

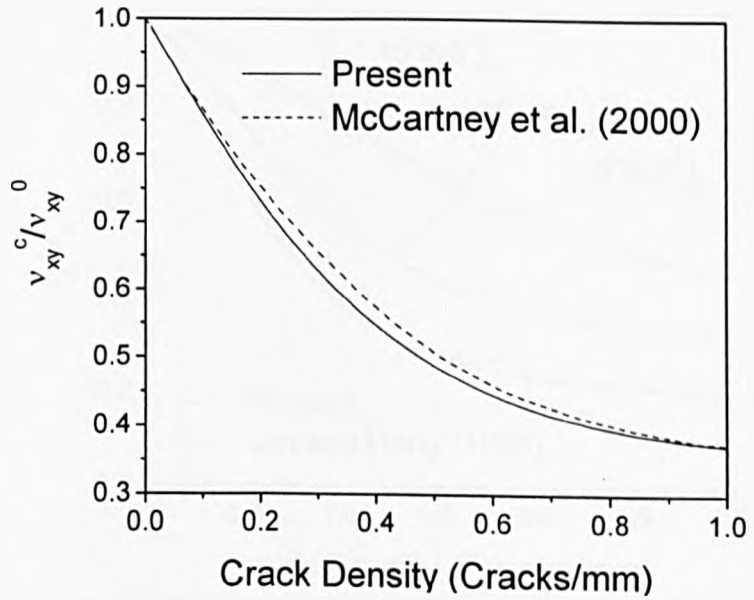

Fig. 6.8 Dependence of the normalised Poisson's ratio on the crack density in a $[0°/90°_3]_s$ glass/epoxy laminate with transverse cracks.

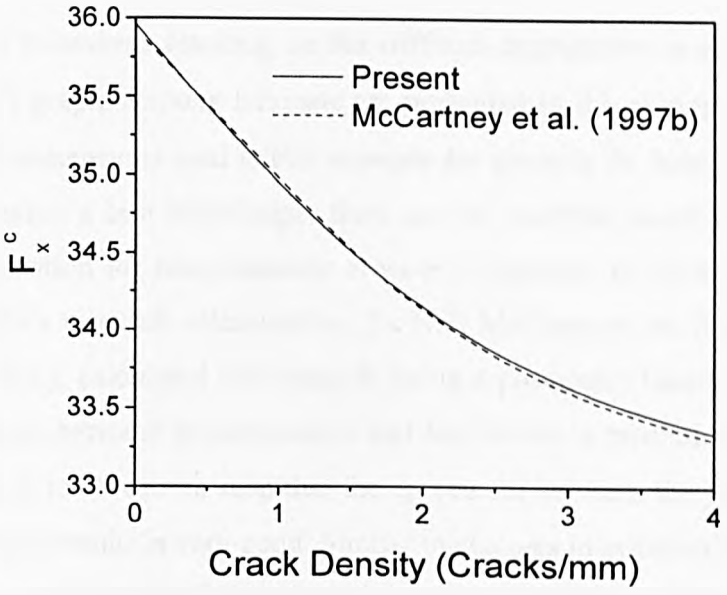

Fig. 6.9 Dependence of the flexural modulus on the crack density in a $[0°/90°_2/0°/90°_2/0°]$ glass/epoxy laminate with transverse cracks.

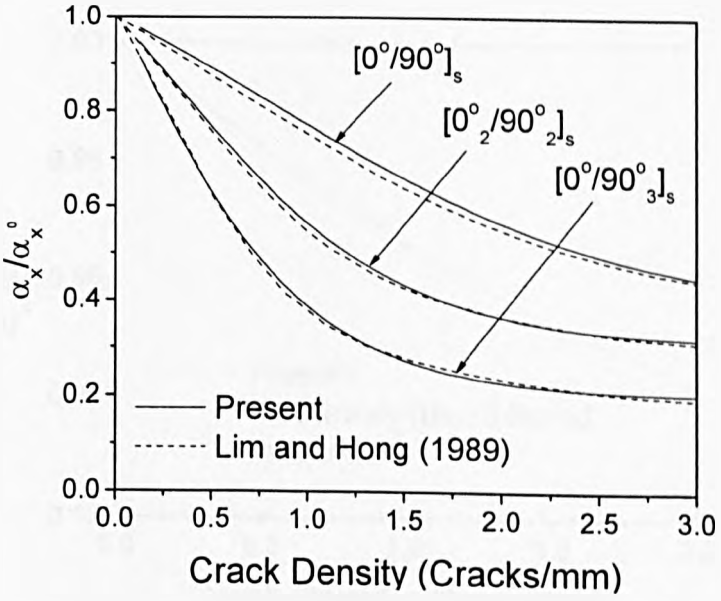

Fig. 6.10 Dependence of the normalised flexural modulus on the crack density in symmetric graphite/epoxy laminates with transverse cracks.

6.3.1.2. Nonsymmetric Cross-ply Laminates

The effects of transverse cracking on the stiffness degradation in an nonsymmetric [0°/90°/0°/90°] graphite/epoxy laminate are presented in this example. The material properties and dimensions used in this example are given in the Material 6.1 of Table 6.1. To the author's best knowledge, there are no available results of stress-based stiffness degradation for nonsymmetric cross-ply laminates in existing publications. Through Dr Ye's research collaboration, Dr Neil McCartney, the National Physical Laboratory (NPL), calculated this example using a physically based damage model. The comparisons between present results and McCartney's predictions are shown in Fig. 6.11–Fig. 6.15. It can be seen that the agreement between the present solutions and McCartney's results is very good. Similar to changes in symmetric laminates, the effective Young's modulus, Poisson's ratio, flexural modulus, and flexural coupling coefficient show obvious degradations in Fig. 6.11–Fig. 6.14, respectively. The nonsymmetric layup characterise its difference in the non-vanishing extension-flexure coupling coefficient in Fig. 6.15. On the contrary to other properties, the extension-flexure coupling coefficient ascends with the increase of crack density.

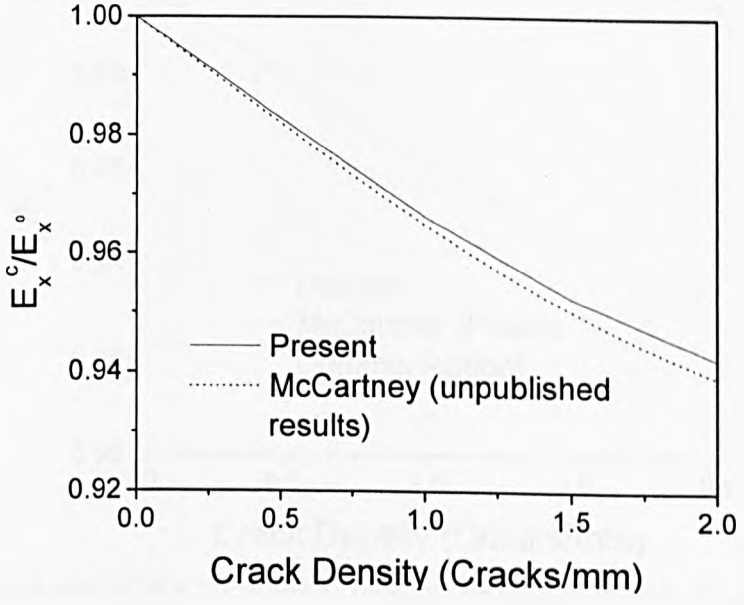

Fig. 6.11 Dependence of the normalised Young's modulus on the crack density in a [0°/90°/0°/90°] graphite/epoxy laminate with transverse cracks.

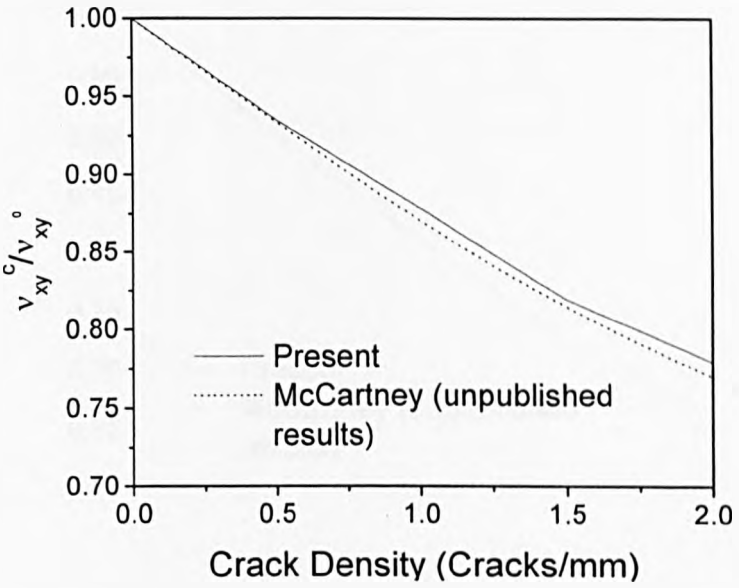

Fig. 6.12 Dependence of the normalised Poisson's ratio on the crack density in a [0°/90°/0°/90°] graphite/epoxy laminate with transverse cracks.

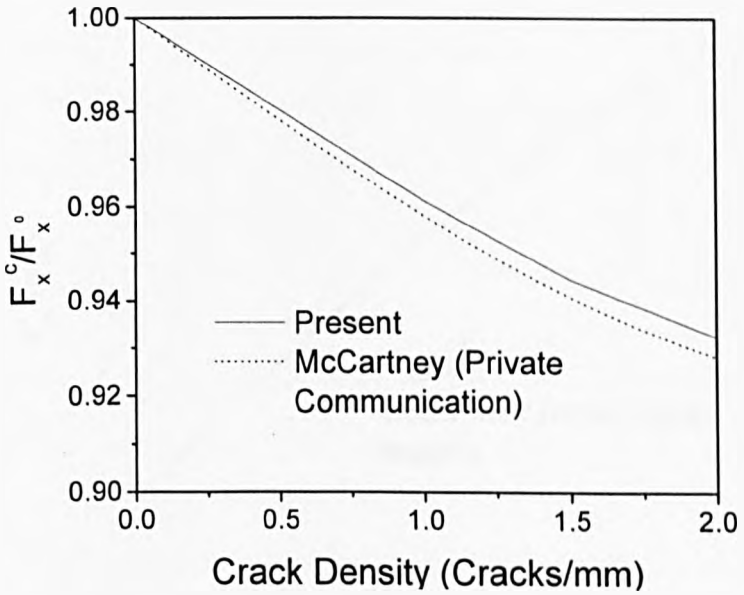

Fig. 6.13 Dependence of the normalised flexural modulus on the crack density in a [0°/90°/0°/90°] graphite/epoxy laminate with transverse cracks.

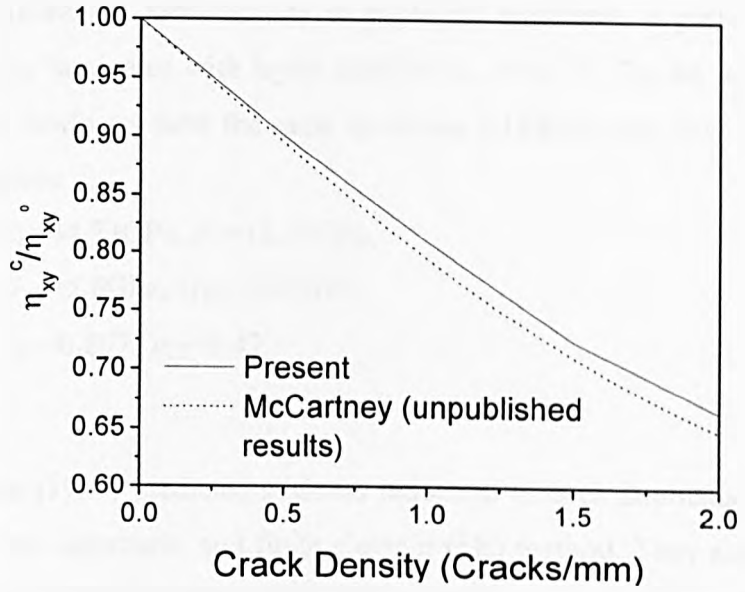

Fig. 6.14 Dependence of the normalised flexural coupling coefficient on the crack density in a [0°/90°/0°/90°] graphite/epoxy laminate with transverse cracks.

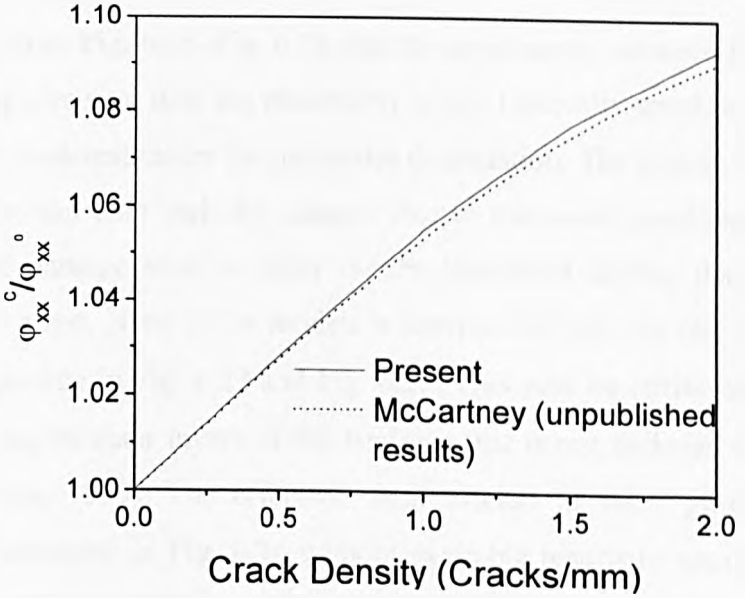

Fig. 6.15 Dependence of the normalised extension-flexure coupling coefficient on the crack density in a [0°/90°/0°/90°] graphite/epoxy laminate with transverse cracks.

6.3.2. Symmetric Angle-ply Laminates

In order to validate the methodology in angle-ply laminates, a group of balanced glass fiber/epoxy laminates with layup $[\pm\theta°/90°_4]_s$, θ=0, 15, 30, 40, are considered. All plies of the laminates have the same thickness 0.144mm, and have the following material properties.

$$\begin{aligned} &E_L=44.73\text{GPa}, E_T=12.76\text{GPa},\\ &G_{LT}=5.8\text{GPa}, G_{TT}=4.49\text{GPa},\\ &\nu_{LT}=0.297, \nu_{TT}=0.42. \end{aligned} \tag{6.19}$$

Joffe and Varna (1999) predicted stiffness reduction of such laminates by shear lag model, variational approach, and finite element (FE) method. They also carried out experiments to measure changes of the effective Young's moduli and the effective Poisson's ratios. Fig. 6.16–Fig. 6.23 show the results of present method, shear lag-2 model, FE analysis and experiment data. For the purpose of comparison, the effective thermoelastic constants of the damaged laminates are normalized by those of the undamaged ones that are indicated by a superscript '°'.

It can be seen from Fig. 6.16–Fig. 6.21 that the agreements between the theoretical models and experimental data are reasonably good. Generally speaking, the present method slightly underestimates the properties degradation. The reason for this is that the analytical model only includes damage due to transverse cracking and ignores other forms of damage such as fiber matrix interfacial sliding that reduces the stiffness during a test. None of the models is comparable with the test results for the $[\pm40°/90°_4]_s$ laminate in Fig. 6.22 and Fig. 6.23. This may be attributed to the early damage occurring in outer layers of the laminate that is not included in the models (Joffe and Varna, 1999). The effective shear moduli of these glass fiber/epoxy laminates are presented in Fig. 6.24 without available results to compare with. As indicated in the figure, there is a descending tendency for shear moduli reduction with the increase of fiber orientation.

McCartney (1996; 2000) derived various inter-relationships for the thermoelastic constants of cracked and uncracked general symmetric laminates. It is expected that

high quality results will obey these relationships. In order to further validate the present method, the numerical solutions of the above four symmetric glass fiber/epoxy laminates with lay-up $[\pm\theta°/90°_4]_s$, θ=0, 15, 30, 40, are tested by the following inter-relationship (McCartney, 2000).

$$\frac{\dfrac{\nu_{xy}^0}{E_x^0}-\dfrac{\nu_{xy}^c(\rho)}{E_x^c(\rho)}}{\dfrac{1}{E_x^c(\rho)}-\dfrac{1}{E_x^0}}=k \tag{6.20}$$

where ρ represents the crack density; k is a laminate constant that is independent of the crack density ρ. The expression of k is

$$k=\frac{E_x^0}{E_y^0}\frac{\nu_{LT}-\nu_{xy}\dfrac{E_y^0}{E_x^0}}{1-\nu_{xy}\nu_{LT}} \tag{6.21}$$

Eqs. (6.20) and (6.21) can be found as Eqs. (115) and (116) in McCartney (2000).

Table 6.2 Inter-relationship test results

		Crack density (cracks/mm)							
		0	0.0625	0.125	0.25	0.375	0.5	0.625	0.75
$[\pm0°/90°_4]_s$ k=0.07857	E_x (GPa)	19.317	18.458	17.935	17.094	16.336	15.646	15.052	14.581
	ν_{xy}	0.0907	0.0831	0.0785	0.0711	0.0645	0.0584	0.0532	0.0490
	Eq. (6.20)[a]	N/A	0.0790	0.0790	0.0790	0.0790	0.0790	0.0790	0.0790
	Error (%)[b]	N/A	0.62%	0.62%	0.62%	0.62%	0.62%	0.62%	0.62%
$[\pm15°/90°_4]_s$ k=0.05481	E_x (GPa)	18.118	17.255	16.725	15.881	15.127	14.445	13.860	13.397
	ν_{xy}	0.1041	0.0965	0.0918	0.0844	0.0778	0.0718	0.0666	0.0626
	Eq. (6.20)[a]	N/A	0.05521	0.05520	0.05520	0.05520	0.05520	0.05520	0.05520
	Error (%)[b]	N/A	0.74%	0.73%	0.73%	0.73%	0.73%	0.72%	0.72%
$[\pm30°/90°_4]_s$ k=0.003412	E_x (GPa)	15.240	15.233	14.358	13.803	12.947	12.204	11.543	10.981
	ν_{xy}	0.1286	0.1286	0.1210	0.1162	0.1088	0.1023	0.0966	0.0917
	Eq. (6.20)[a]	N/A	0.00342	0.00342	0.00343	0.00343	0.00343	0.00343	0.00343
	Error (%)[b]	N/A	0.48%	0.50%	0.55%	0.57%	0.58%	0.60%	0.62%
$[\pm40°/90°_4]_s$ k=-0.024389	E_x (GPa)	13.227	12.314	11.731	10.860	10.121	9.477	8.934	8.505
	ν_{xy}	0.1356	0.1279	0.1231	0.1157	0.1095	0.1041	0.0996	0.0960
	Eq. (6.20)[a]	N/A	-0.02463	-0.02463	-0.02464	-0.02464	-0.02464	-0.02464	-0.02464
	Error (%)[b]	N/A	1.01%	1.02%	1.03%	1.03%	1.04%	1.05%	1.06%

[a] The left side value of Eq. (6.20). [b] Error (%)=(The left side value of Eq (6.20)-k)/k.

The effective Young's moduli, the effective Poisson's rations and the inter-relationship test results of all the four lay-ups are listed in Table 6.2. It is found that the present predictions satisfy the inter-relationship within a very small error.

A quasi-isotropic carbon fiber reinforced epoxy $[-45°/45°/0°/90°]_s$ laminate is considered by McCartney (1996). The thermoelastic constants for a unidirectional ply are

$$\begin{aligned} &E_L=136.6\text{GPa}, E_T=9.79\text{GPa}, \\ &G_{LT}=6.474\text{GPa}, G_{TT}=3.364\text{GPa}, \\ &\nu_{LT}=0.286, \nu_{TT}=0.455. \end{aligned} \tag{6.22}$$

Each ply has the thickness 0.125mm. McCartney (1996) calculated the stiffness degradation with ply refinement parameter (n=1-5). It was considered that the number of sub-layers (n=5) in each ply appear to converge sufficiently to provide an accurate prediction. In consequence McCartney (1996)'s predictions by using ply refinement parameter (n=5) are adopted in this and the following examples. The effective Young's modulus, Poisson's ratio and shear modulus as a function of crack density are plotted in Fig. 6.25–Fig. 6.27, respectively. As seen from the figures, the present results are always smaller than the values of the effective elastic constants predicted by McCartney (1996) in low crack densities but almost very close to McCartney (1996)'s predictions towards high crack densities. In general, the collation between the results of these two methods is very good.

McCartney (1996) also calculated the effective thermoelastic constant degradations of an unbalanced glass/epoxy laminate $[30°/90°]_s$ with ply cracks in 90° plies. The ply thickness is 0.25mm and the material properties are as follows

$$\begin{aligned} &E_L=45.6\text{GPa}, E_T=16.2\text{GPa}, G_{LT}=5.83\text{GPa}, \\ &G_{TT}=5.786\text{GPa}, \nu_{LT}=0.297, \nu_{TT}=0.42, \\ &\alpha_L=8.6\times10^{-6}/°\text{C}, \alpha_T=26.4\times10^{-6}/°\text{C}. \end{aligned} \tag{6.23}$$

For an unbalanced symmetric laminate, there exists a tension-shear coupling. Fig. 6.28–Fig. 6.31 show the comparisons of the stiffness reductions, including the effective Young's modulus, Poisson's ratio, shear modulus, and tension-shear coupling coefficient. Fig. 6.32 and Fig. 6.33 show the results of the effective axial

and shear thermal expansion coefficient, respectively. It is seen that except the shear thermal expansion coefficient α_3 all the effective thermoelastic constants decrease with an increasing crack density. Very good agreements are observed between the present results and McCartney (1996)'s predictions. Both McCartney's and the present models assumed a generalised plane strain deformation. A significant difference between the two models is that the present solution matched the boundary displacement conditions of the uncracked layers exactly while McCartney's solution only satisfied those in an average sense.

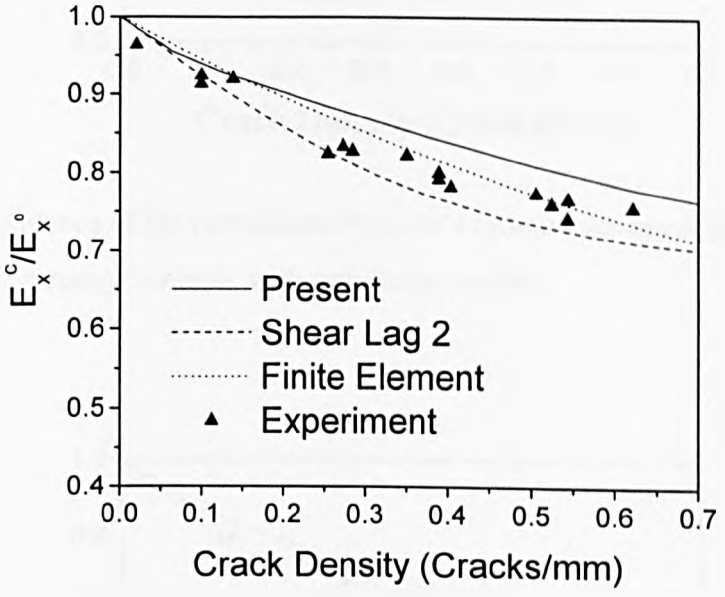

Fig. 6.16 Dependence of the normalised Young's modulus on the crack density in a $[\pm 0°/90°_4]_s$ glass/epoxy laminate with transverse cracks.

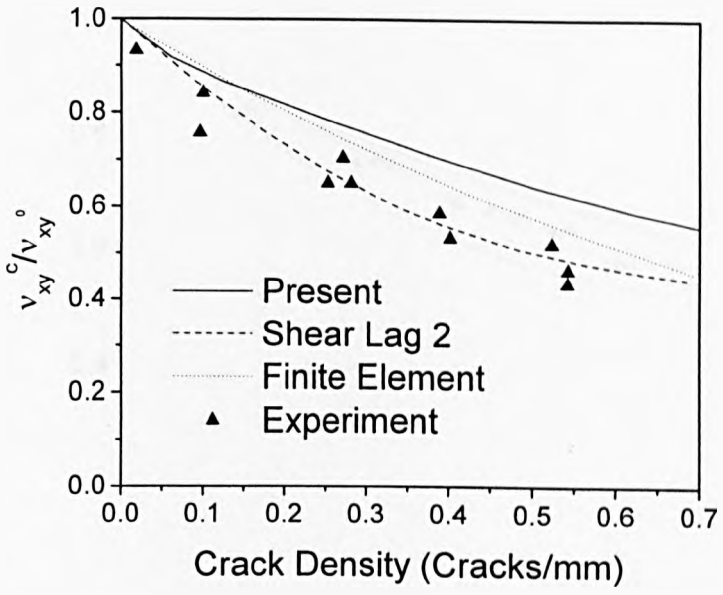

Fig. 6.17 Dependence of the normalised Poisson's ratio on the crack density in a $[\pm 0°/90°_4]_s$ glass/epoxy laminate with transverse cracks.

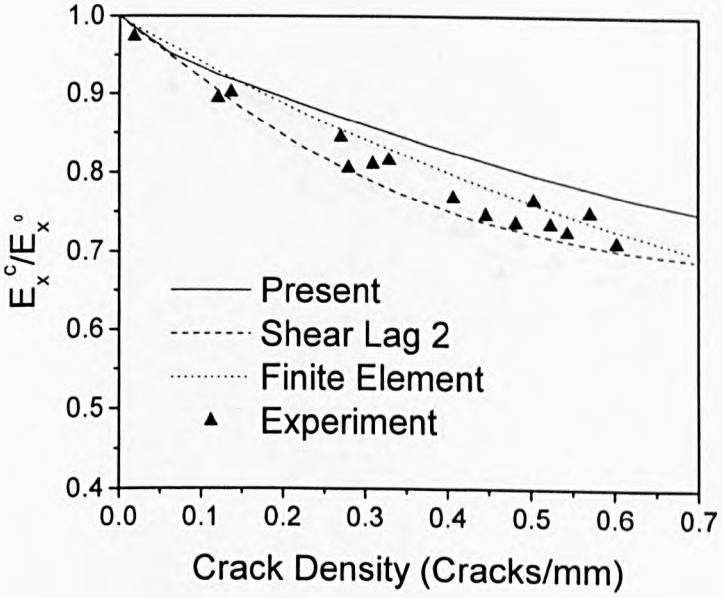

Fig. 6.18 Dependence of the normalised Young's modulus on the crack density in a $[\pm 15°/90°_4]_s$ glass/epoxy laminate with transverse cracks.

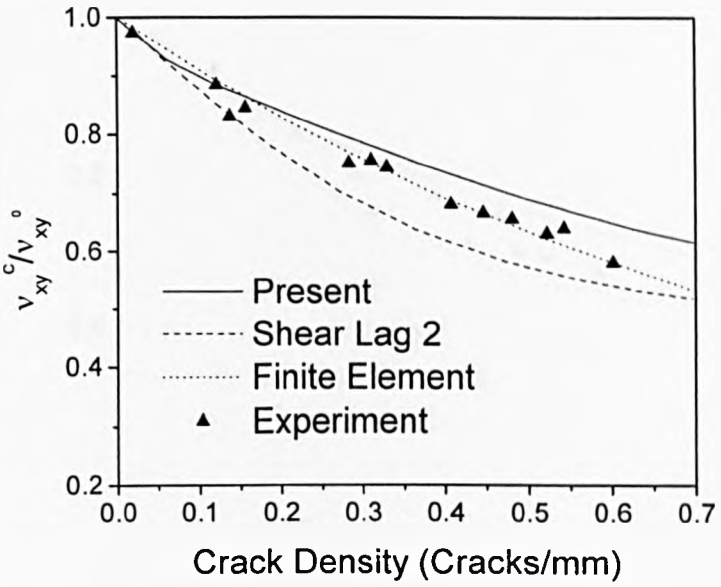

Fig. 6.19 Dependence of the normalised Poisson's ratio on the crack density in a $[\pm 15°/90°_4]_s$ glass/epoxy laminate with transverse cracks.

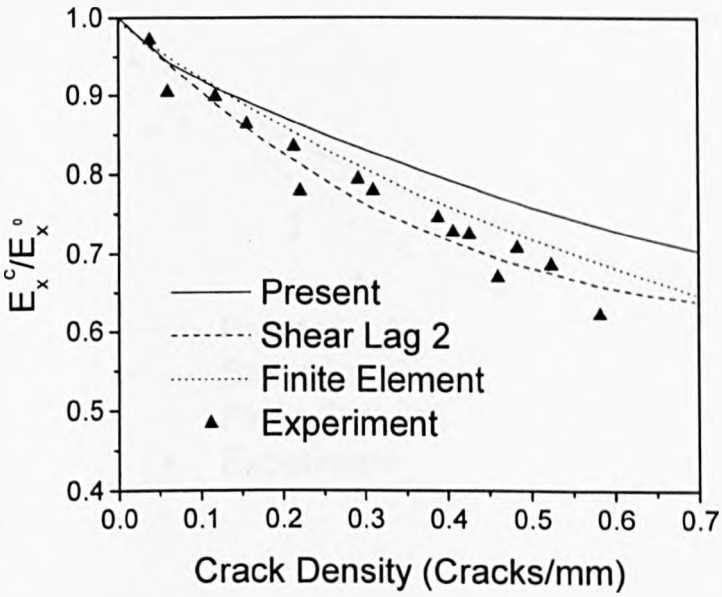

Fig. 6.20 Dependence of the normalised Young's modulus on the crack density in a $[\pm 30°/90°_4]_s$ glass/epoxy laminate with transverse cracks.

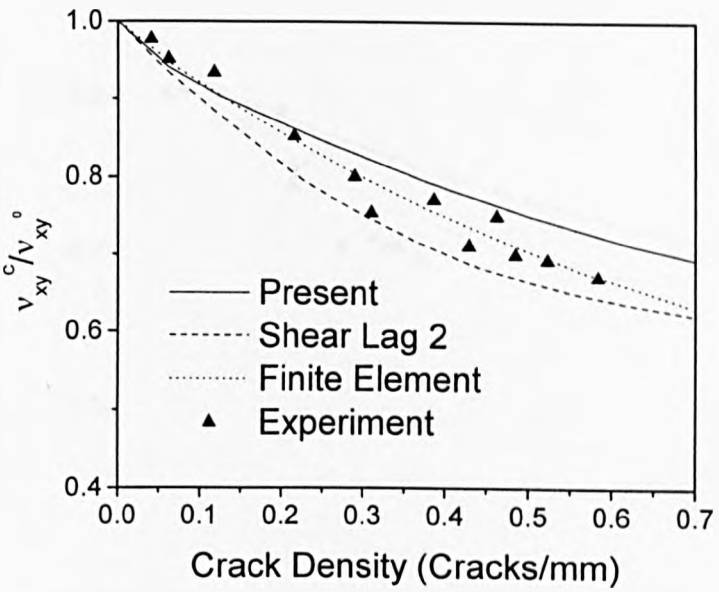

Fig. 6.21 Dependence of the normalised Poisson's ratio on the crack density in a $[\pm 30°/90°_4]_s$ glass/epoxy laminate with transverse cracks.

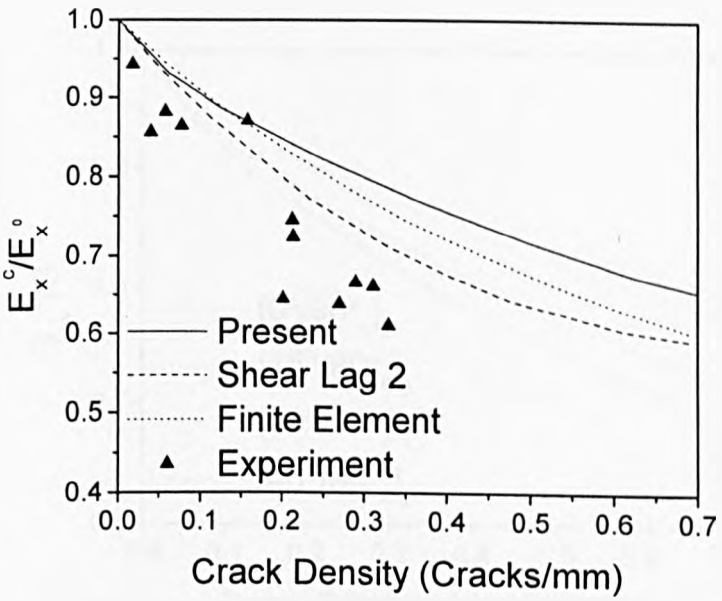

Fig. 6.22 Dependence of the normalised Young's modulus on the crack density in a $[\pm 40°/90°_4]_s$ glass/epoxy laminate with transverse cracks.

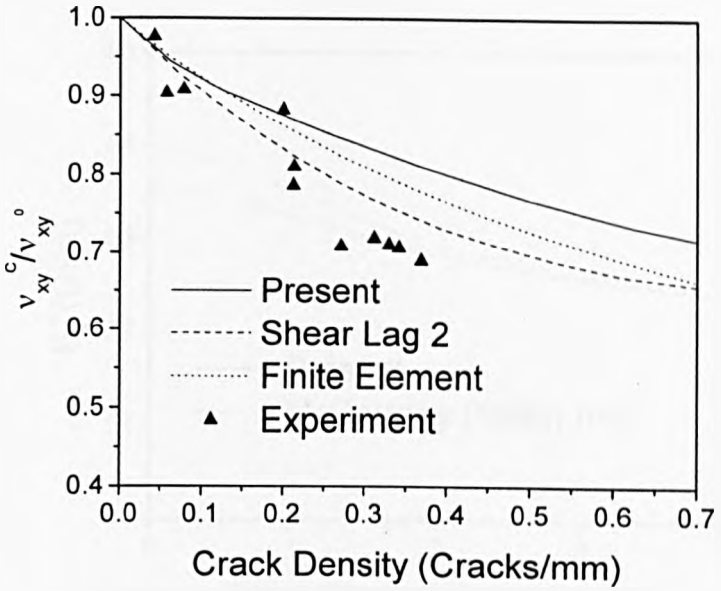

Fig. 6.23 Dependence of the normalised Poisson's ratio on the crack density in a $[\pm 40°/90°_4]_s$ glass/epoxy laminate with transverse cracks.

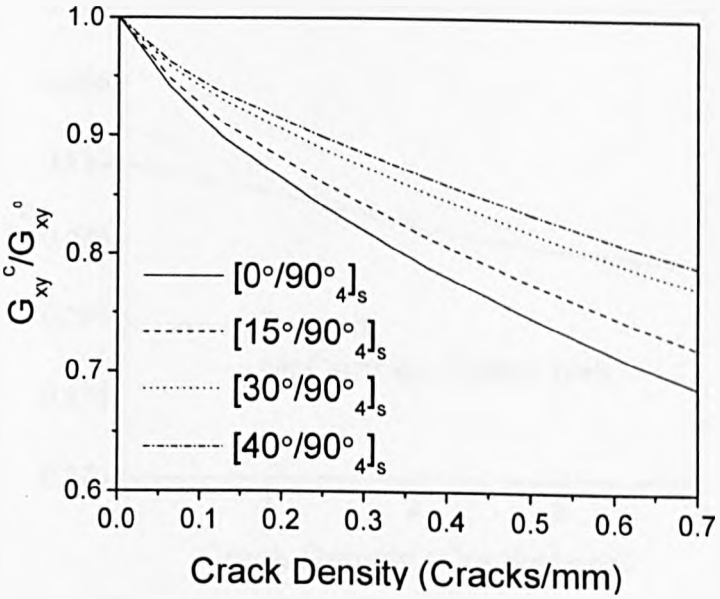

Fig. 6.24 Dependence of the normalised shear moduli on the crack density in a group of glass/epoxy laminates with transverse cracks.

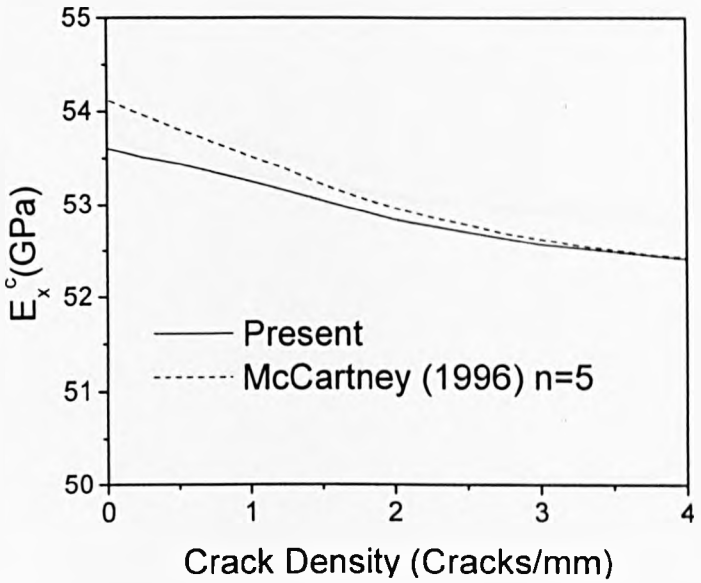

Fig. 6.25 Dependence of the effective Young's modulus on the crack density in a $[-45°/+45°/0°/90°]_s$ carbon/epoxy laminate with transverse cracks.

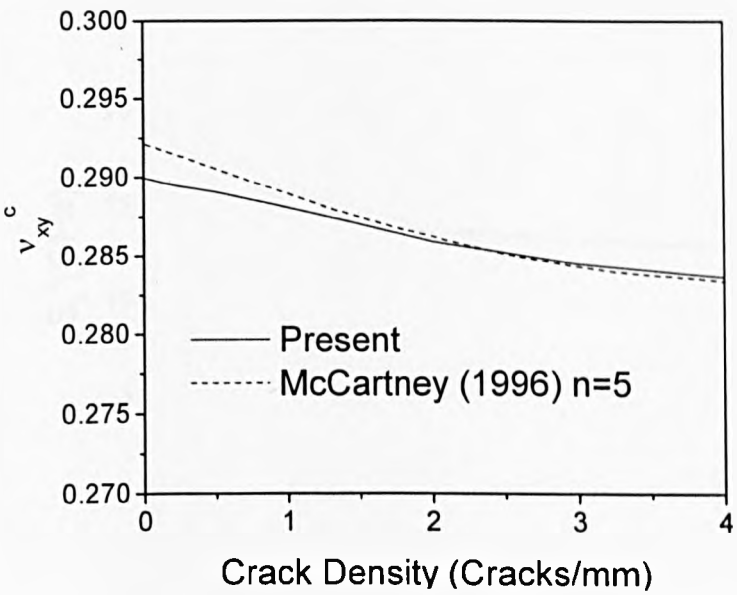

Fig. 6.26 Dependence of the effective Poisson's ratio on the crack density in a $[-45°/+45°/0°/90°]_s$ carbon/epoxy laminate with transverse cracks.

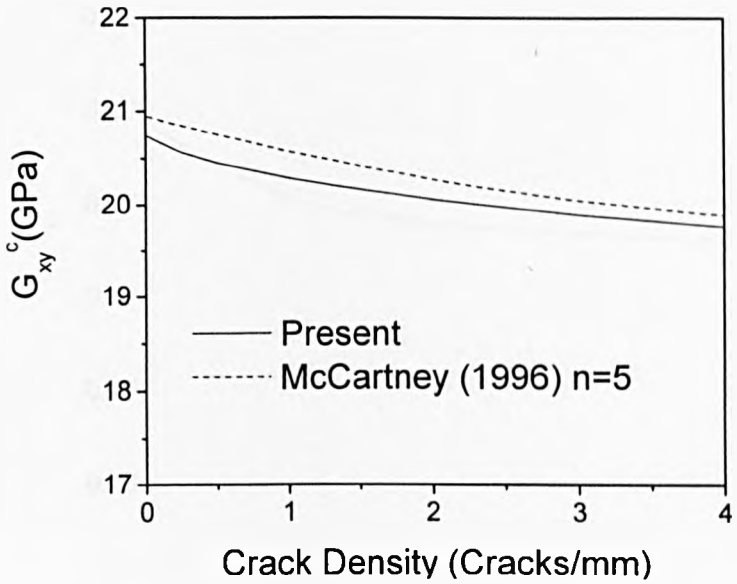

Fig. 6.27 Dependence of the effective shear modulus on the crack density in a $[-45°/+45°/0°/90°]_s$ carbon/epoxy laminate with transverse cracks.

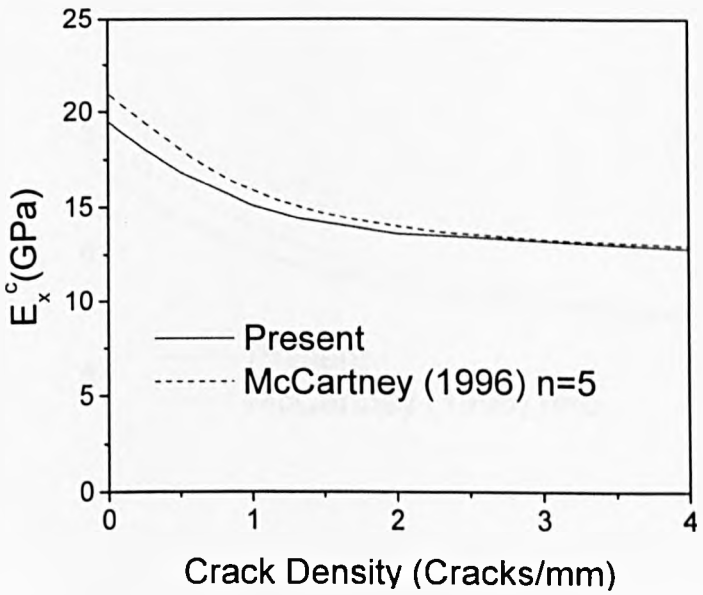

Fig. 6.28 Dependence of the effective Young's modulus on the crack density in a $[30°/90°]_s$ glass/epoxy laminate with transverse cracks.

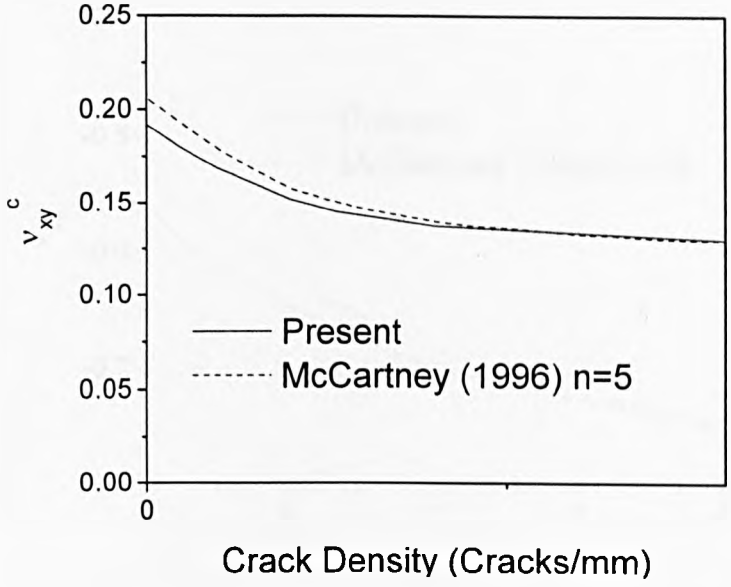

Fig. 6.29 Dependence of the effective Poisson's ratio on the crack density in a $[30°/90°]_s$ glass/epoxy laminate with transverse cracks.

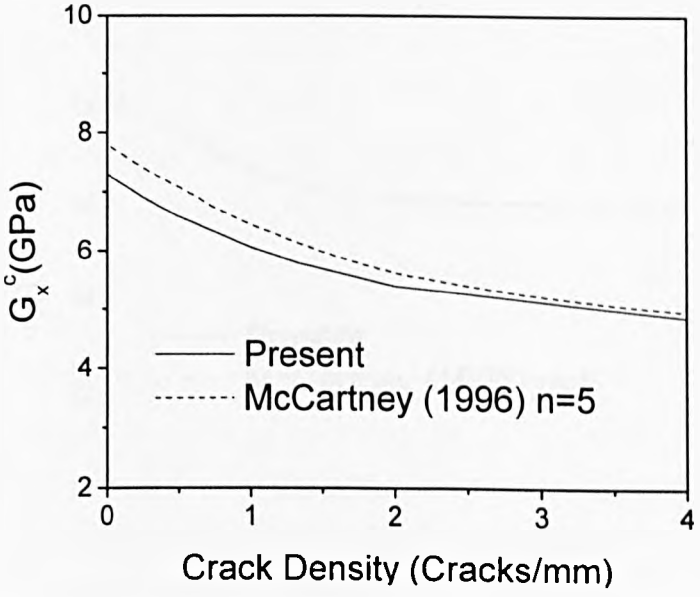

Fig. 6.30 Dependence of the effective shear modulus on the crack density in a $[30°/90°]_s$ glass/epoxy laminate with transverse cracks.

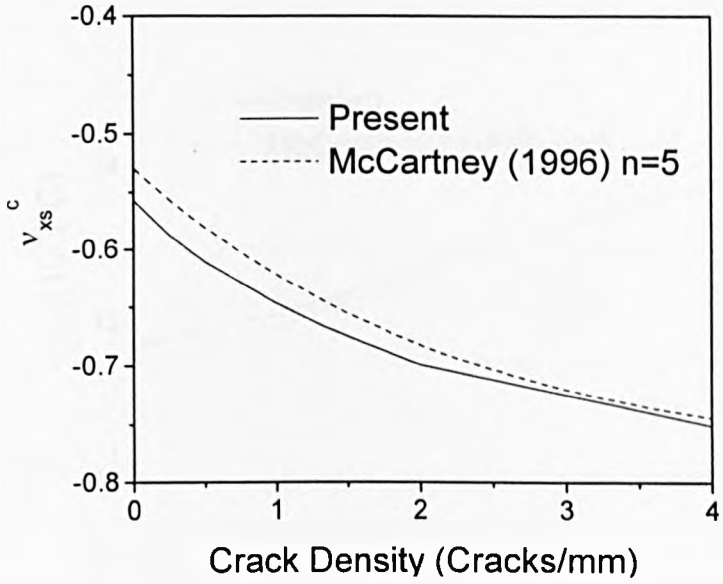

Fig. 6.31 Dependence of the effective extension-shear coupling coefficient on the crack density in a $[30°/90°]_s$ glass/epoxy laminate with transverse cracks.

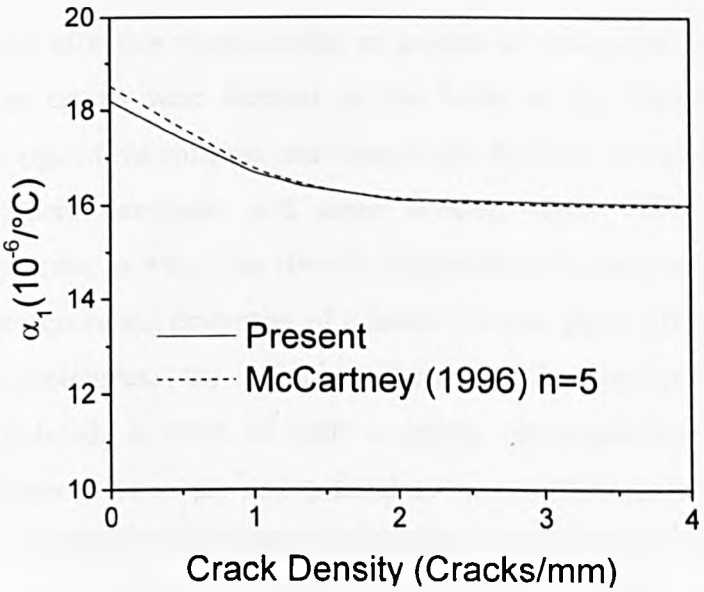

Fig. 6.32 Dependence of the effective axial thermal expansion coefficient on the crack density in a $[30°/90°]_s$ glass/epoxy laminate with transverse cracks.

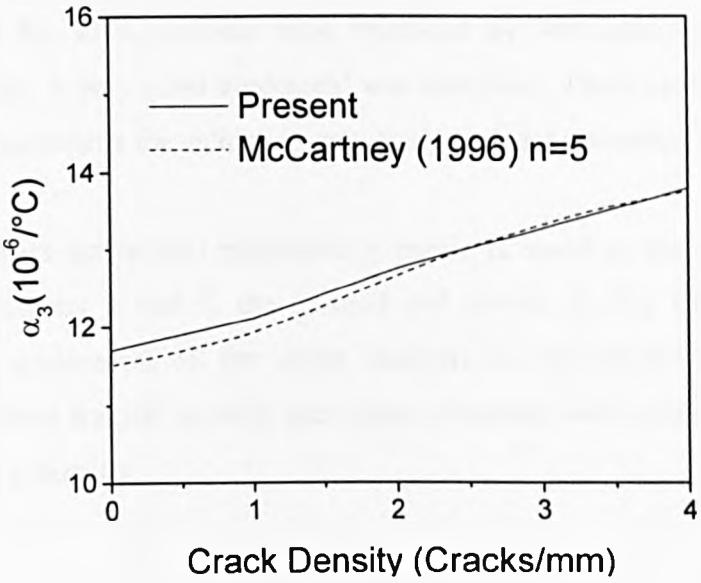

Fig. 6.33 Dependence of the effective shear thermal expansion coefficient on the crack density in a $[30°/90°]_s$ glass/epoxy laminate with transverse cracks.

6.4. Conclusions

In this Chapter, the effective thermoelastic properties of composite laminates with uniform transverse cracks were derived on the basis of the Classical Laminate Theory. First, the equivalent stiffness and compliance matrices of cracked laminates were given in general laminates and some selected cases. This is, in fact, a homogenisation process, in which the effective properties of a cracked laminate were smoothed into the equivalent properties of a homogeneous plate. Then by using the corresponding compliances, the effective thermoelastic constants of cracked laminates were defined. In term of their coupling characteristics, the effective engineering constants in cross-ply and general symmetric laminates were given in detail. Finally, the effective thermoelastic constants were determined by solving the stress and displacement distributions in cracked laminates under some specially designed loading conditions. Numerical results were also presented and most of them were compared with available solutions of other models or experimental data.

It can be seen from the numerical validations that the proposed method provides accurate predictions of stiffness degradation in cracked cross-ply and symmetric

laminates. Although the stiffness degradation due to transverse cracking in nonsymmetric cross-ply laminates has no published data available to date, the present solutions for such laminate were validated by McCartney's unpublished results. Once again, a very good agreement was observed. These results, therefore, can be used as benchmarks for validating new analytical and numerical methods.

Because the stiffness determined methodology herein is based on the stress analysis introduced in Chapters 4 and 5, the method and results in this Chapter can be regarded as an application of the stress analysis in the engineering practice. Meanwhile, the stress transfer models, state space methods, were also verified by the current examples indirectly.

Chapter 7. Propagation of Transverse Cracking in Laminates

7.1. Introduction

Transverse cracking has long been recognised as an important damage mechanism in composite laminates. The initiation and propagation of transverse cracking has been studied extensively in the past few decades. In this chapter, an energy method based on fracture mechanics, combined with the aforementioned stress analysis, is used to predict the development of transverse cracks in both symmetric and nonsymmetric laminates. Further to an application of the stress transfer model in predicting stiffness degradation in the engineering practice, this is another one in evaluating transverse crack multiplication.

The stress transfer models in Chapters 4 and 5 fall into two categories: cross-ply and angle-ply laminates. Since the stress analysis of cross-ply laminates can be regarded as one special case of angle-ply laminates, the theoretical formulations in this chapter are only derived for angle-ply laminates. However it covers all the aspects of cross-ply laminates.

Firstly formulations of the total complementary potential energy of a representative element between two neighbouring transverse cracks are derived. Then the energy release rate during the transverse crack propagation is given in an idealised crack state. By introducing the crack propagation criterion, the crack density as a function of applied average stress can then be predicted. In the end the proposed method is demonstrated by numerical examples and is validated by other results and experimental data.

7.2. Theoretical Formulations based on Fracture Mechanics

In Section 3.4, some fundamental principles in fracture mechanics have been introduced. Herein these principles are used to predict transverse crack propagation in composite materials.

7.2.1. The Total Complementary Potential Energy of a Representative Element

Fig. 5.4 shows a representative element which is taken out from two neighbouring cracks in a $[\theta°_m/90°_n/\phi°_s]$ composite laminates. The stress analysis has been carried out on this idealised element in Chapter 5, where the laminate is assumed to consist of N fictitious sub-layers. The complementary strain energy U_c of this representative element is

$$U_c = \sum_{j=1}^{N} U_c^j \tag{7.1}$$

where the superscript 'j' means the jth sub-layer and U_c^j is the complementary strain energy of the jth sub-layer of the representative element. Using the stresses obtained in Chapter 5, U_c^j per unit length in the y direction can be obtained by Eq. (3.28) as

$$U_c^j = \frac{1}{2}\int_0^{h_j}\int_0^{L}\left[\{\sigma\}^T[C']^{-1}\{\sigma\} + \Delta T\{\alpha\}^T\{\sigma\}\right]_j dxdz \tag{7.2a}$$

where

$$\{\sigma\} = [\sigma_{xx} \quad \sigma_{xy} \quad \sigma_{xz} \quad \sigma_{yz} \quad \sigma_{zz} \quad \sigma_{xy}]^T \tag{7.2b}$$

$$\{\alpha\} = [\alpha_x \quad \alpha_y \quad \alpha_z \quad 0 \quad 0 \quad \alpha_{xy}]^T \tag{7.2c}$$

the matrix $[C']$ is stiffness matrix (See Appendix B) and ΔT is the change in temperature.

Consider the laminate is under a uniformly prescribed strain ε_0 in the y direction. The potential of the prescribed strain ε_0 can be obtained by Eq. (3.32)

$$V_c = \sum_{j=1}^{N} V_c^j \tag{7.3}$$

$$= \sum_{j=1}^{N} \int_0^{h_j} \int_0^{L} \left[\{\bar{u}\}^T \{P\} \right]_j dxdz$$

$$= \sum_{j=1}^{N} \int_0^{h_j} \int_0^{L} \left[\varepsilon_0 \sigma_{yy} \right]_j dxdz$$

Then the total complementary potential energy of this representative element is given as the difference of the complementary strain energy U_c and the potential of prescribed displacements V_c (See Eq. (3.36)).

$$\Gamma = U_c - V_c$$

$$= \sum_{j=1}^{N} \int_0^{h_j} \int_0^{L} \left[\frac{1}{2} \left(\{\sigma\}^T [C']^{-1} \{\sigma\} + \Delta T \{\alpha\}^T \{\sigma\} \right) - \varepsilon_0 \sigma_{yy} \right]_j dxdz \tag{7.4}$$

It can be noted that the last term in Eq. (7.4) is the difference between a generalised plane strain and a plane strain problem.

7.2.2. The Energy Release Rate due to Transverse Cracking

The energy release rate is a well established crack propagation criterion in fracture mechanics. It is used to predict the transverse cracking development in the present study. The energy release rate G can be calculated either by the total potential energy or by the total complementary potential energy, i.e. Eqs. (3.34) and (3.35). The later will be used in the present study.

Consider a composite laminate is subjected to external loading and there are a large number of transverse cracks in the 90° layers. The entire length of the laminate is L_e and the thickness of cracked layers is H_c. Fig. 7.1 shows the propagation process of the transverse cracks from state (a) to state (b), which is then idealised into state (c). In state (a), it is assumed that there exist k uniformly spaced transverse cracks in the laminate. Therefore the crack density in this state is

$$\rho_k = \frac{k}{L_e} \tag{7.5}$$

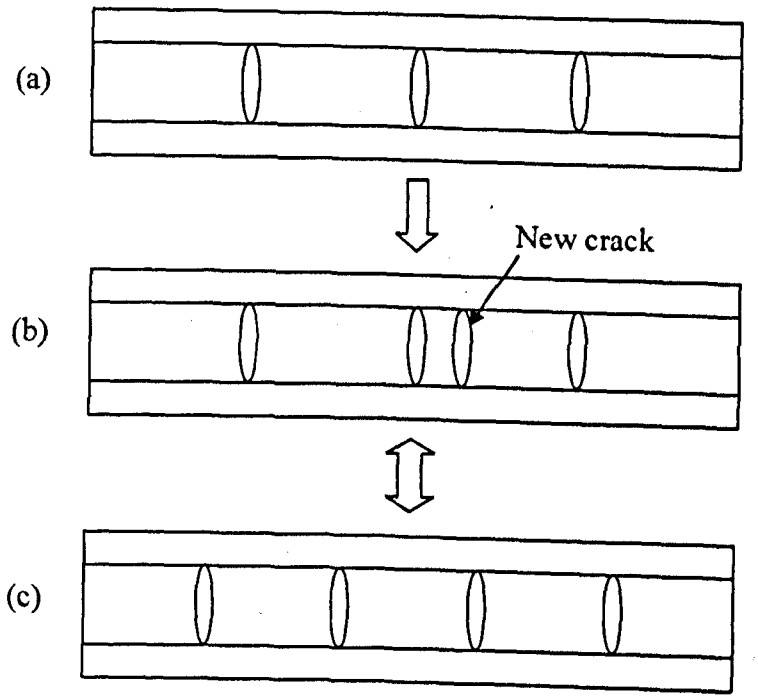

Fig. 7.1 Nomenclature of the propagation process of transverse cracks and the idealised uniform distribution state.

With the changes of external loading, a new transverse crack forms and the state (a) turns to state (b). The number of the transverse cracks increases from k to $(k+1)$. In order to simplify the analysis, state (b) is idealised to state (c), in which the $(k+1)$ cracks are equally spaced. Then the crack density in state (c) is

$$\rho_{k+1} = \frac{k+1}{L_e} \tag{7.6}$$

During the transverse cracking process, the crack surface area increment is $2H_c$. By Eq. (3.35) the energy release rate from state (a) to state (b) is

$$\begin{aligned} G &= \frac{d\Gamma}{dA} \\ &= \frac{\Gamma(\rho_{k+1}) - \Gamma(\rho_k)}{2H_c} \\ &= \frac{(k+1)\Gamma_r(\rho_{k+1}) - k\Gamma_r(\rho_k)}{2H_c} \\ &= \frac{L_e\rho_{k+1}\Gamma_r(\rho_{k+1}) - L_e\rho_k\Gamma_r(\rho_k)}{2H_c} \end{aligned} \tag{7.7}$$

where $\Gamma(\rho_{k+1})$ and $\Gamma(\rho_k)$ are the total complementary potential energies of the entire laminate at crack densities ρ_{k+1} and ρ_k, respectively; $\Gamma_r(\rho_{k+1})$ and $\Gamma_r(\rho_k)$ are the total complementary potential energies of the representative element at crack densities ρ_{k+1} and ρ_k, respectively.

7.2.3. The Transverse Crack Propagation Criterion

A new crack will form if the energy released due to crack formation reaches the critical energy release rate G_c, i.e.

$$G \geq G_c \tag{7.8}$$

G_c is a material property and has units of energy per unit area. It can be measured by an experiment method.

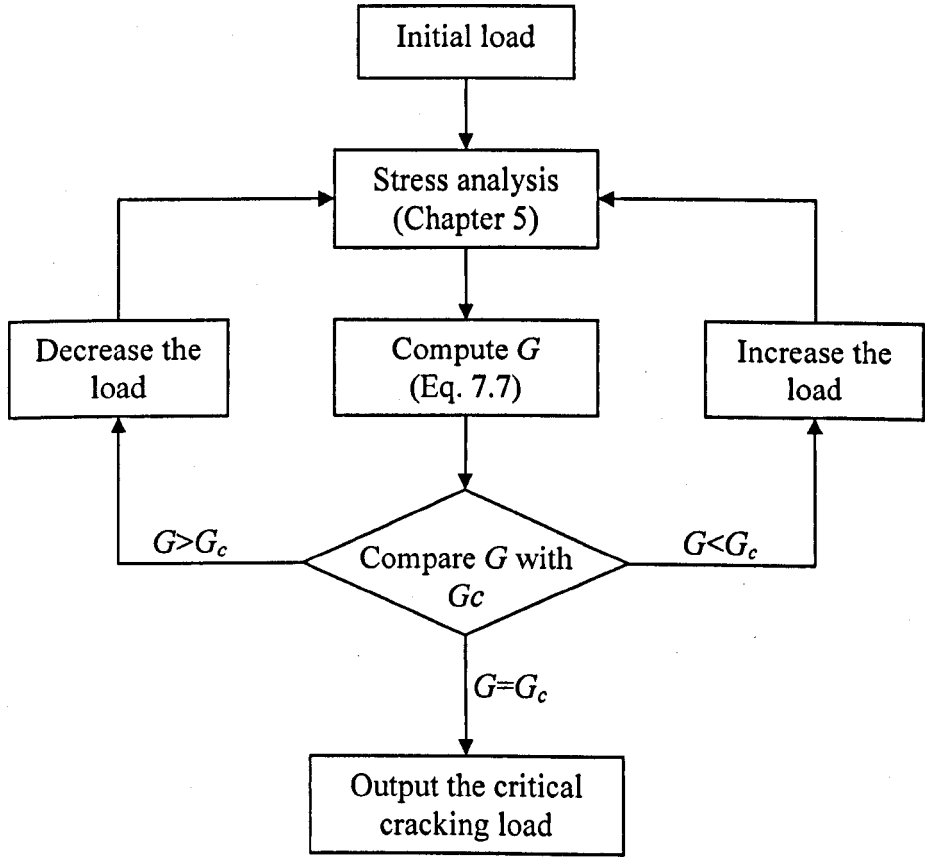

Fig. 7.2 Flowchart of calculating the critical cracking load for a given crack density.

Fig. 7.2 is a flowchart showing how to determine the critical cracking load for a given crack density. First input an initial load to carry out a stress analysis by using the stress transfer model in Chapter 5. Then calculate the energy release rate G of the

laminate by Eq. (7.7) and compare it with G_c. If $G>G_c$, decrease the load value to recalculate the energy release rate until $G=G_c$. If $G<G_c$, increase the load value to recalculate the energy release rate until $G=G_c$. If $G=G_c$, then output the load, i.e. the critical cracking load, for the given crack density.

7.3. Numerical Results

The formulations and criterion proposed above are applied to predict the transverse cracking in composite laminates with different configurations, including symmetric cross-ply laminates, symmetric angle-ply laminates and nonsymmetric laminates. The material properties and dimension of these laminates (Liu and Nairn, 1992; Joffe *et al.*, 2001) are given in Table 7.1. Effects of the residual thermal stresses are included in the analysis. ΔT is the difference between the room temperature and the cure temperature. Table 7.1 also lists the critical energy release rate G_c for each material.

Table 7.1 Material properties and dimensions

	Material 7.1	Material 7.2	Material 7.3	Material 7.4
Type	Fiberite 934/T300	Avimid® K Polymer/IM6	Hercules 3501-6/AS4	Glass/epoxy
E_L	128 GPa	134 GPa	130 GPa	44.73 GPa
E_T	7.2 GPa	9.8 GPa	9.7 GPa	12.76 GPa
ν_{LT}	0.3	0.3	0.3	0.297
ν_{TT}	0.5	0.5	0.5	0.42
G_{LT}	4.0 GPa	5.5 GPa	5.0 GPa	5.8 GPa
G_{TT}	2.4 GPa	3.6 GPa	3.6 GPa	4.49 GPa
α_1	-0.09×10^{-6}/°C	-0.09×10^{-6}/°C	-0.09×10^{-6}/°C	8.6×10^{-6}/°C
α_2	28.8×10^{-6}/°C	28.8×10^{-6}/°C	28.8×10^{-6}/°C	22.1×10^{-6}/°C
ΔT	-125 °C	-225 °C	-125 °C	-105 °C
G_c	690 J/m^2	960 J/m^2	240 J/m^2	610 J/m^2
L_e	50mm	50mm	50mm	50mm
H_{ply}	0.154 mm	0.154 mm	0.154 mm	0.144 mm

7.3.1. Symmetric Laminates under Tension

The crack densities as a function of applied average stresses for symmetric cross-ply laminates are plotted in Fig. 7.3–Fig. 7.8. Herein, the applied average stresses refer to the axial tension per unit length in the x direction divided by the height H of a laminate. The results of Liu and Narin (1992)'s variational method and experimental data are also shown in these figures to validate the present predictions. In general, both present and Liu and Narin (1992)'s results agree well with the experimental data, while the present predictions fit better in low crack densities.

By using Material 7.1, the numerical results of $[0°_2/90°_2]_s$ and $[0°_2/90°_4]_s$ laminates are plotted in Fig. 7.3 and Fig. 7.4, respectively. As can be seen, using a single value of G_c, the predictions of two different layups collate well with the experimental data. This indicates that the critical energy release rate is a material property which characterises transverse crack propagation in composite materials. In addition, the difference between the two laminates lies in the thickness of 90° layers. It can be seen that the cracks formed earlier in the laminate with thicker 90° layers. This indicates that the onset stress is inversely proportional to the thickness of 90° layers. After the initial crack, the crack density increases very rapidly and then gradually slows down in the high crack density.

Fig. 7.5 and Fig. 7.6 show the solutions of $[0°/90°_2]_s$ and $[0°_2/90°_2]_s$ laminates made of Material 7.2. For these two laminates, which have the same thickness of 90° layers, the transverse cracks initiated earlier in the $[0°/90°_2]_s$ laminate. This suggests that the supporting layers restrain transverse cracking process and the onset stress is proportional to the thickness of supporting layers.

The numerical results of two laminates with layups $[0°/90°_2]_s$ and $[0°_2/90°_4]_s$ are shown in Fig. 7.7 and Fig. 7.8 by using Material 7.3. Although the thickness ratio of 0° to 90° layer in the two laminates is the same, the onset stress of transverse cracks is different. The laminate with thicker 90° layers is more prone to the formation of matrix cracks.

The dependence of the crack density on the applied average stress in a series of symmetric angle-ply laminates with layups $[\pm\theta°/90°_4]_s$ (θ=0, 15, 30) are presented in Fig. 7.9–Fig. 7.11. The laminates are made of Material 7.4 in Table 7.1. The present results are compared with Joffe et al. (2001)'s Monte-Carlo simulations and their experimental data. Once again very good agreements are observed in these figures. It can be seen that the cracks initiated earliest in $[\pm30°/90°_4]_s$, then in $[\pm15°/90°_4]_s$, and last in $[\pm0°/90°_4]_s$ laminate. The reason is that the onset stress is enhanced by increasing the stiffness of supporting layers, which constrain cracking process in neighbouring layers.

7.3.2. Nonsymmetric Laminates under Tension

The predictions of transverse crack propagation in two nonsymmetric laminates are carried out. The first laminate is constructed by replacing one set of $90°_4$ layers in the above $[\pm30°/90°_4]_s$ laminate with $0°_4$ layers. Thus the new layup becomes $[\pm30°/90°_4/0°_4/\mp30°]$. The numerical results are shown in Fig. 7.12. In comparison with Fig. 7.11, the onset stress is greatly enhanced. The other laminate has layup [30°/90°/30°/90°] and the material properties of Eq. (5.37), with ΔT=0, G_c=900 J/m^2, and L_e=50mm. Both 90° layers are assumed to have transverse cracks and the crack distributions are identical. Fig. 7.13 shows the crack density as a function of the applied average stress in the laminate. No comparisons have been made in Fig. 7.12 and Fig. 7.13, because the present solutions are believed to be the first ones to predict transverse crack propagation in nonsymmetric laminates. Therefore these results can be used as benchmarks for testing new models.

7.3.3. Laminates under Tension and Shearing

To study the effects of shearing on the transverse cracking, a symmetric and an nonsymmetric cracked laminates under a combination of tension and shearing are analysed by using the material properties of Eq. (5.37). A series of curves are shown in Fig. 7.14 to demonstrate the effects of different shear stresses on the transverse cracking process in the symmetric [30°/90°/90°/30°] laminate under an axial tension. The values of the shear stresses are -100, -50, 0, 50 and 100 MPa. It can be seen that the shear stress has significant effects on the initiation and development of transverse cracks. With the increase of the shear stress, the general trend of the initiation

stresses is enhanced. Moreover, two negative shear stresses make the whole cracking form earlier and they are dangerous in the practical application. On the contrary, two positive shear stresses restrain the transverse cracking and they are safe to the laminate.

A series of graphic results of an nonsymmetric [30°/90°/30°/90°] laminate are shown in Fig. 7.15. As can be seen, the effects of shearing are similar to the symmetric layup. Nevertheless, under the same loading condition the crack initiation stress of the nonsymmetric laminate is slightly larger than that of the symmetric case. This may be because the thickness of single continuous 90° layers in the symmetric laminate is larger than that in nonsymmetric laminate and a thicker 90° layer is more prone to crack formation.

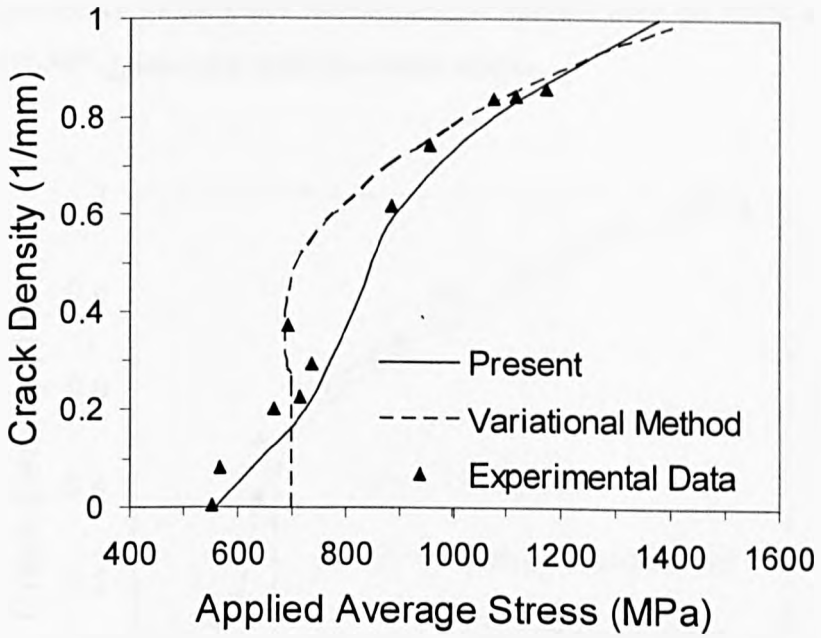

Fig. 7.3 Dependence of the crack density on the applied average stress in a Fiberite 934/T300 $[0°_2/90°_2]_s$ laminate with transverse cracks.

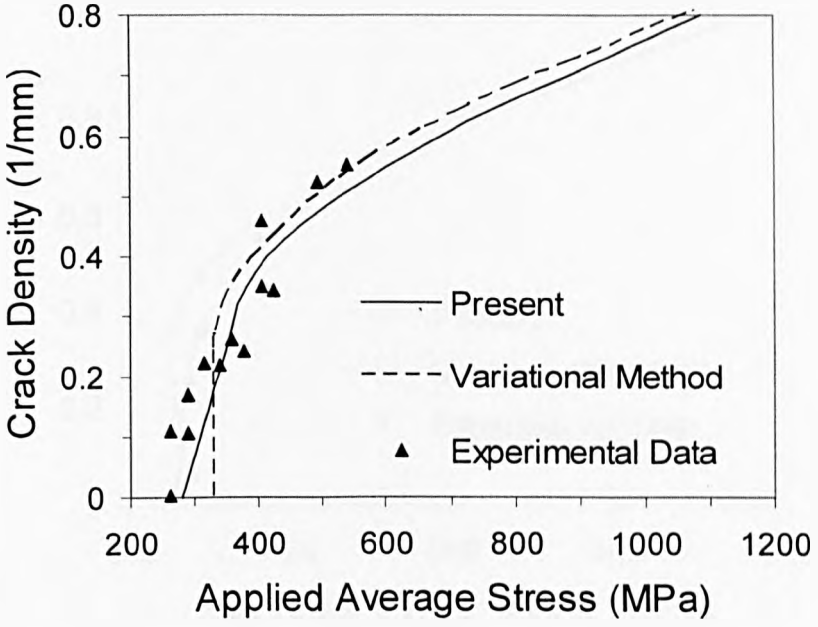

Fig. 7.4 Dependence of the crack density on the applied average stress in a Fiberite 934/T300 $[0°_2/90°_4]_s$ laminate with transverse cracks.

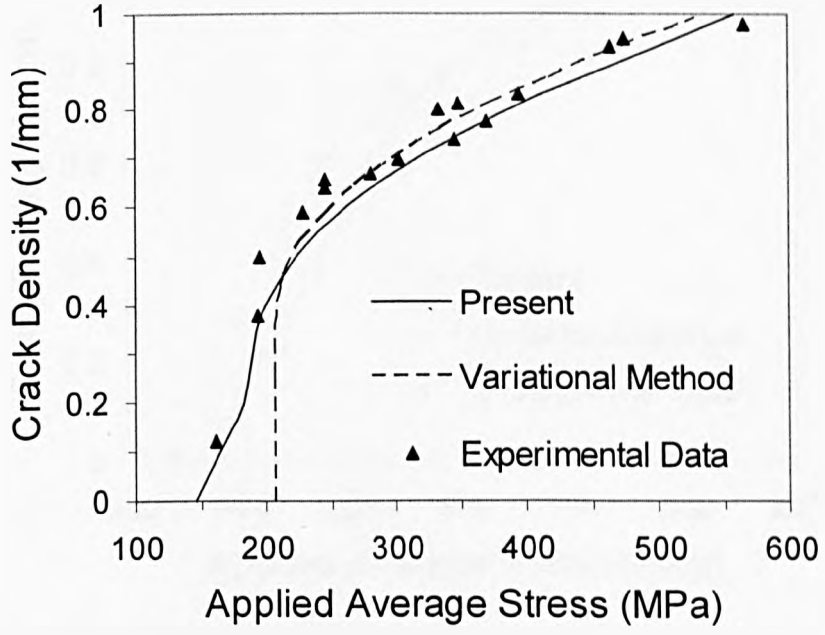

Fig. 7.5 Dependence of the crack density on the applied average stress in a Hercules 3501-6/AS4 $[0°/90°_2]_s$ laminate with transverse cracks.

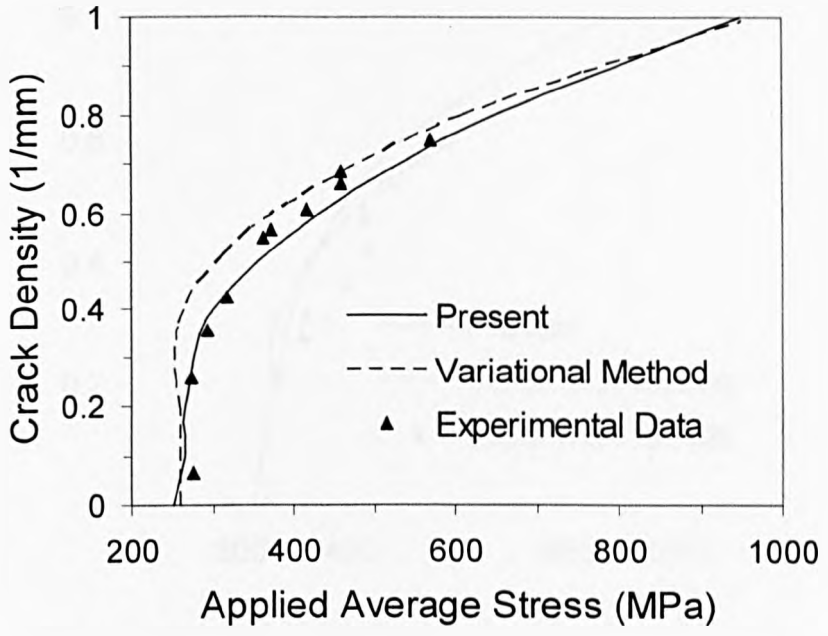

Fig. 7.6 Dependence of the crack density on the applied average stress in a Hercules 3501-6/AS4 $[0°_2/90°_2]_s$ laminate with transverse cracks.

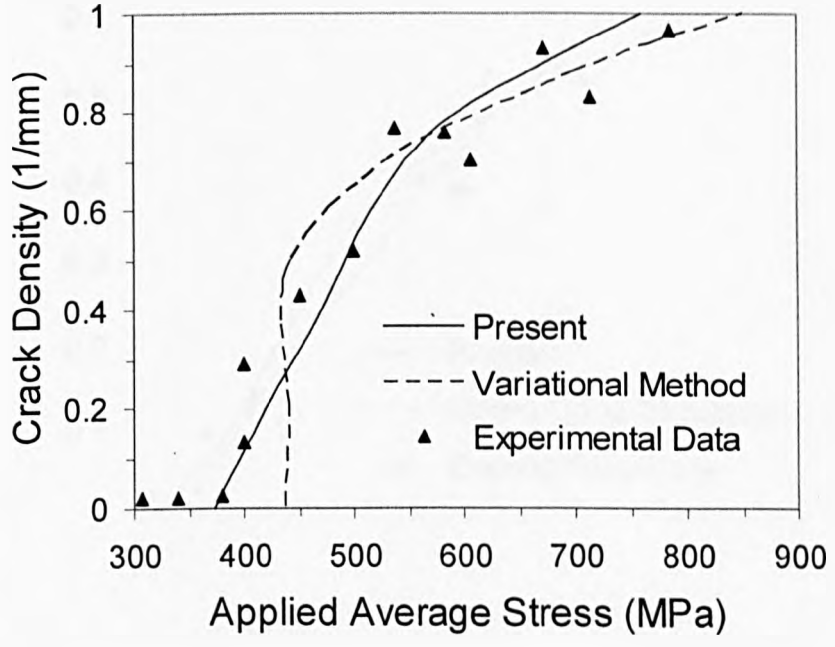

Fig. 7.7 Dependence of the crack density on the applied average stress in a Avimid K Polymer/IM6 $[0°/90°_2]_s$ laminate with transverse cracks.

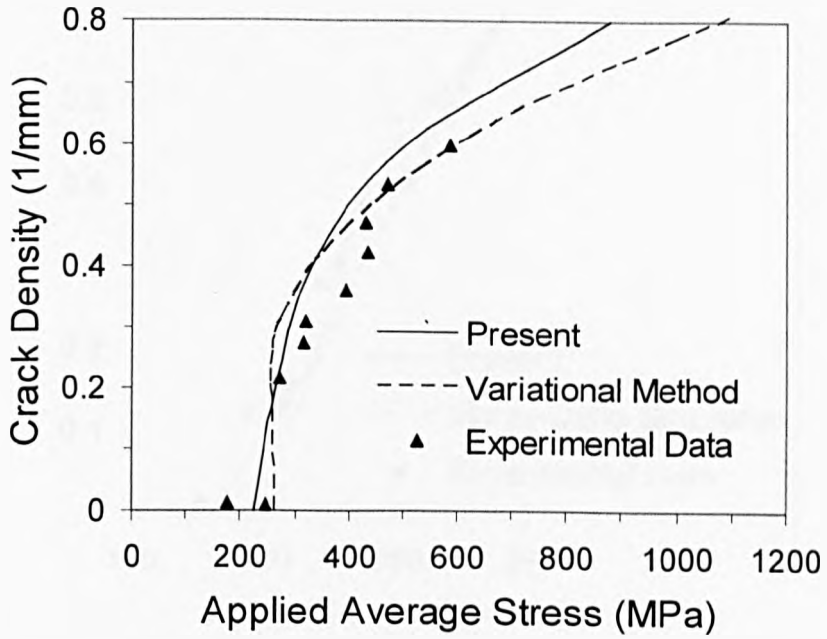

Fig. 7.8 Dependence of the crack density on the applied average stress in a Avimid K Polymer/IM6 $[0°_2/90°_4]_s$ laminate with transverse cracks.

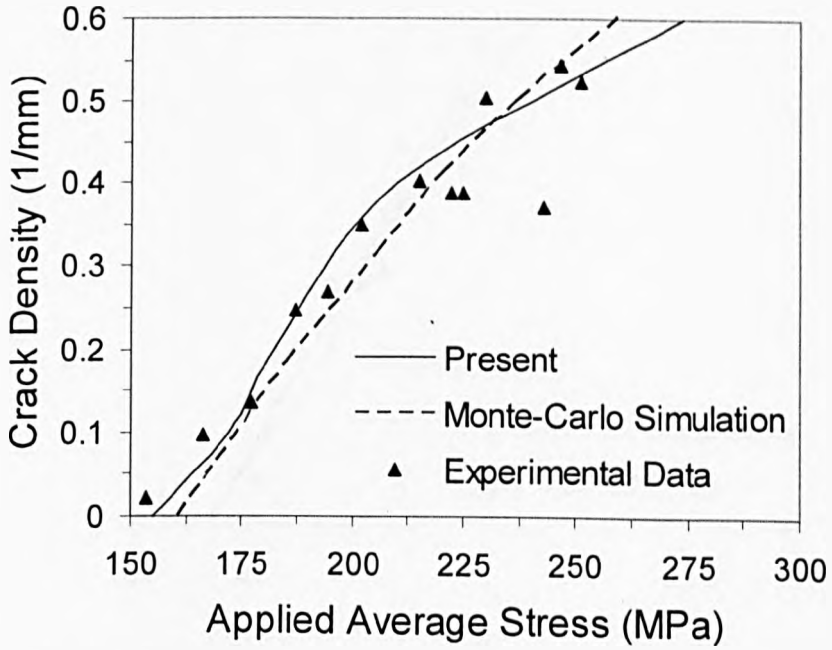

Fig. 7.9 Dependence of the crack density on the applied average stress in a $[0°_2/90°_4]_s$ glass/epoxy laminate with transverse cracks.

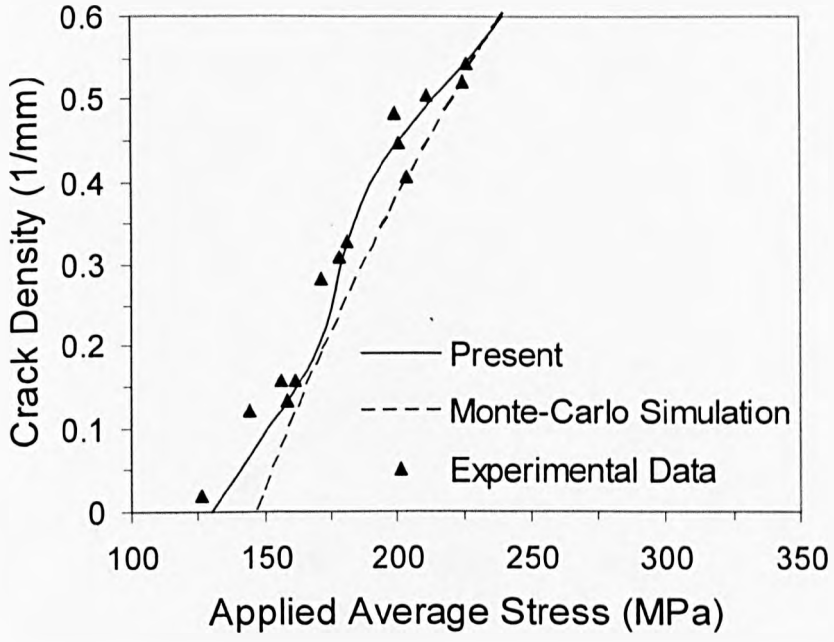

Fig. 7.10 Dependence of the crack density on the applied average stress in a $[\pm 15°/90°_4]_s$ glass/epoxy laminate with transverse cracks.

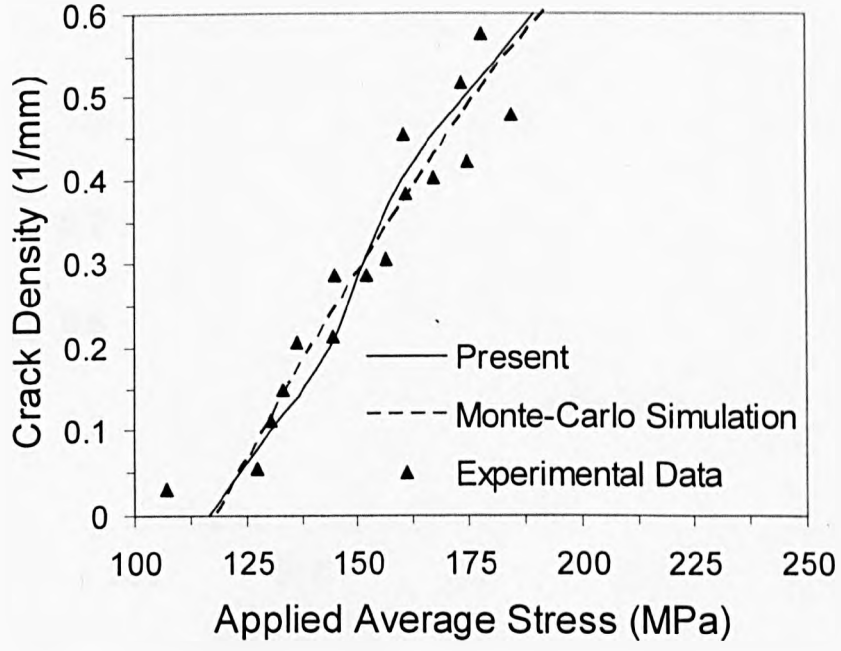

Fig. 7.11 Dependence of the crack density on the applied average stress in a $[\pm 30°/90°_4]_s$ glass/epoxy laminate with transverse cracks.

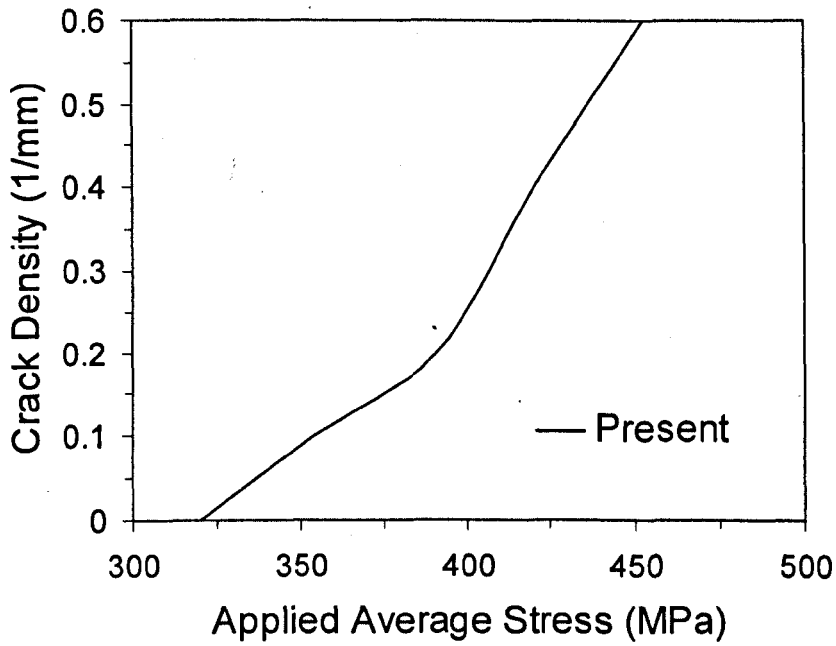

Fig. 7.12 Dependence of the crack density on the applied average stress in an nonsymmetric [±30°/90°$_4$/0°$_4$/∓30°] glass/epoxy laminate with transverse cracks.

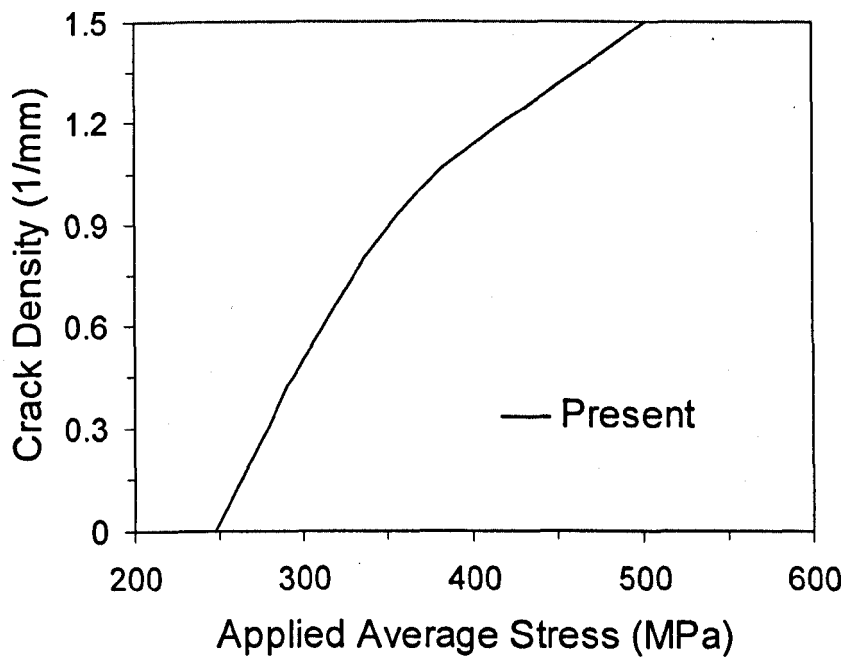

Fig. 7.13 Dependence of the crack density on the applied average stress in an nonsymmetric [30°/90°/30°/90°] graphite/epoxy laminate with transverse cracks.

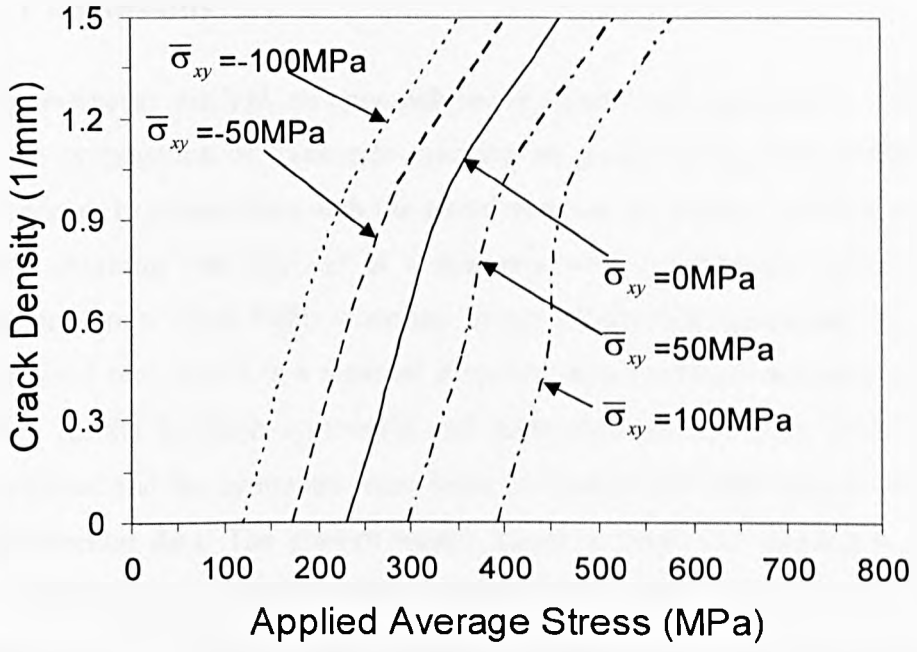

Fig. 7.14 Dependence of the crack density on the applied average stress in a [30°/90°/90°/30°] graphite/epoxy laminate with different shear stresses $\bar{\sigma}_{xy}$.

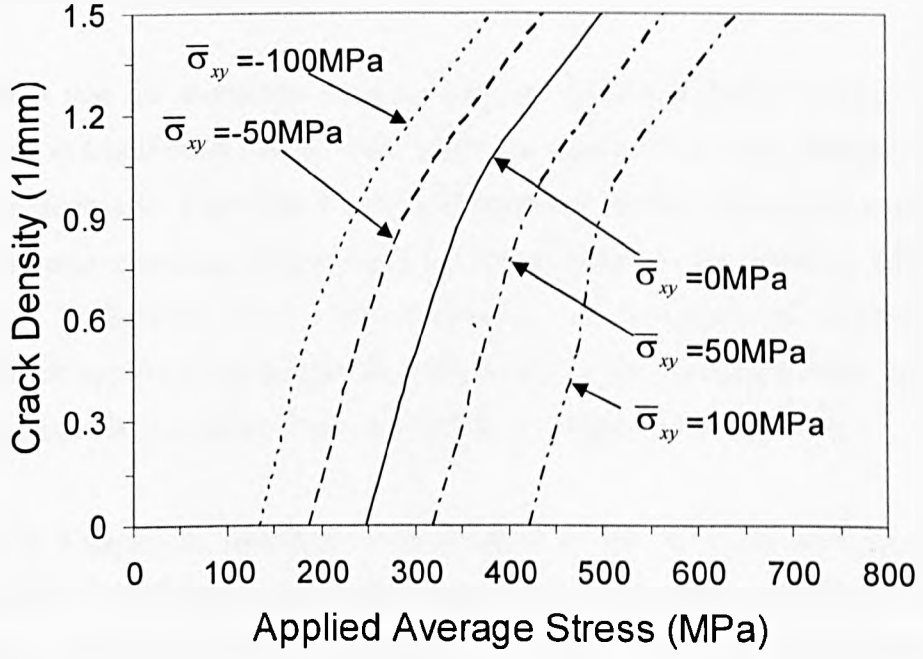

Fig. 7.15 Dependence of the crack density on the applied average stress in an nonsymmetric [30°/90°/30°/90°] graphite/epoxy laminate with different shear stresses $\bar{\sigma}_{xy}$.

7.4. Conclusions

By using an energy method, an approach based on the state space stress analysis to predict the propagation of transverse cracking in general composite laminates has been proposed. In conjunction with the stress analysis, the energy release rate due to transverse cracking was derived in a laminate with an idealised uniform crack distribution. A new crack forms when the energy release rate approaches the critical energy release rate, which is a material property characterising transverse cracking. Numerical results for both symmetric and nonsymmetric laminates under tension were presented and the symmetric ones were compared with other numerical results and experimental data. The present energy based method was verified to provide good predictions of transverse crack propagation. The transverse cracking in laminates under a combination of tension and shearing is also studied. It is found that shearing has significant effects on the cracking process. With regard to the transverse cracking in nonsymmetric laminates and the effects of shearing, there are no published results to date. As a result, the present solutions can serve as benchmarks to test new theories and methods.

It is noted that the transverse cracking process was simplified as a crack density increment in a uniformly spaced state, while the nature of the crack multiplication in reality is stochastic. Therefore, a statistical approach should be resorted to modelling the transverse cracking. Some statistical approaches to the problem have been reviewed in Section 2.2.3. The integration of computational methods and probabilistic approach can predict the uncertainties in the cracking process, but it will not be pursued in this thesis. This topic is left as a suggested future work.

Further to Chapter 6, which is an application of the stress analysis in stiffness degradation, this Chapter is another application of the stress transfer model in predicating transverse cracking propagation. Again the state space method was indirectly verified to be a highly accurate method.

Chapter 8. Conclusions and Future Work

The objectives of the current work were to develop a new analytical model to evaluate the stress distributions near free edges and transverse cracks, to assess the degradation of thermoelastic properties due to transverse cracking, and to predict the propagation of transverse cracking in composite laminates. The main achievements and results of the work are now summarised, and areas needing future work are suggested.

8.1. Summary of Work Presented

In the present work the following main points have been presented:

- **A Stress Transfer Model for General Cross-ply Laminates**

A semi-analytical method, the state space method, was developed to evaluate the stress distributions near free edges and transverse cracks. The method is based on a state space representation of elasticity under a generalised plane strain condition. The approach is capable of calculating interlaminar stress singularities in general cross-ply laminates subjected to uniform axial extension, bending and/or thermal loading. Numerical results were obtained by using layer refinement technique in the through thickness direction and Fourier series expansion in the width direction. The present solutions showed good approximation to interlaminar stress singularities in the vicinity of free edge and transverse cracks. Although this stress transfer model is only a preliminary step to develop a sophisticated model for angle-ply laminates, the results for nonsymmetric cross-ply laminates are even difficult to obtain by many other methods.

- **A Stress Transfer Model for General Angle-ply Laminates**

Further to the state space method for cross-ply composite laminates, a more sophisticated stress transfer model was developed for general angle-ply laminates under in-plane and/or thermal loading. In this new model, the stress components σ_{yz} and σ_{xy}, which vanished in cross-ply laminates, was included to reflect the stress

state in angle-ply laminates. Again, the model is based on a generalised plane strain condition. In order to find suitable displacement expressions and Fourier series expansions, which have to satisfy the boundary conditions and also could be eliminated during further derivations, some new variables were introduced. Because of universality of the method, it also can be used to analyse cross-ply laminates. In fact, the state space method for cross-ply laminates can be regarded as a special case of the method for angle-ply cases.

Numerical results were obtained by using the same layer refinement as in cross-ply laminates. Through comparisons with other results in symmetric angle-ply laminates, the present method was validated to provide an accurate stress analysis. In addition, the current state space method is not restricted to the symmetric layup and meanwhile can consider in-plane shear loading. The numerical results for nonsymmetric angle-ply laminates under in-plane extension and those for general angle-ply laminates under shear deformation were all revealed for the first time in the literature. Therefore, these results can be served as benchmarks for testing new models and this is an important contribution of the present work.

The application of the state space method to evaluate interlaminar stresses in composite laminates has many advantages. Firstly, it takes account of all the stress components and independent material constants. Secondly, the method always guarantees continuous distributions of both displacements and interlaminar stresses across interfaces between material layers. Thirdly, the method is highly efficient because the dimension of the final equations (see Eqs.4.29 and 5.29) is independent of the number of material layers. Thus, this method is particularly suitable to evaluate stress singularities in laminates with a large number of layers. Lastly, by this method, a laminate may be composed of an arbitrary number of monoclinic layers and each layer may have different material property and thickness.

- **Thermoelastic Property Degradation due to Transverse Cracking**

As a practical application of the stress analysis, the effective thermoelastic property degradation due to transverse cracking was assessed on the basis of the Classical Laminate Theory. The constitutive equations for a cracked laminate were assumed to have the same form as those of an undamaged laminate. In fact, this is a process to

homogenise a cracked laminate to a homogeneous plate. In term of their coupling characteristics, the effective thermoelastic constants of cross-ply and general symmetric laminates were defined by the compliance matrices and the compliance coefficients were calculated by the stress analysis of some specially designed loading conditions.

Numerical examples were presented in cross-ply and symmetric angle-ply laminates. Through comparisons with results of other models or experimental data, the present method was validated to provide accurate predictions of thermoelastic property degradation. It is noted that the numerical results for nonsymmetric cross-ply laminates were compared with McCartney's solutions via private communication and no such results in the published literature can be found. Therefore, it is also one of the contributions of the present work.

- **Propagation of Transverse Cracking**

As another practical application of stress transfer model, the propagation of transverse cracking was predicted by using an energy method. The energy release rate due to transverse cracking was derived under idealised crack states, in which the crack density increased uniformly. A new crack form when the energy release rate reaches a critical value with the increment of the applied load. Then the applied load at the critical state is the one triggers crack propagation. The method was demonstrated by numerical results and those of symmetric laminates were compared with available results and experimental data. The predictions of transverse cracking for nonsymmetric laminates under tension and the numerical results considering a combination of tension and shearing are new in the literature and they are the third contribution of this thesis.

8.2. Suggestions for Future Work

The thesis has developed a semi-analytical method to evaluate the stress transfer near free edges and transverse cracks, and has applied the stress analysis to assess stiffness degradation due to transverse cracking and to predict propagation of transverse cracking in composite laminates. However, there still exists room for future work, which is discussed as follows.

- **Stress analysis under triaxial loading and twisting**

The present stress analysis considers the laminate subjected to in-plane loading, bending and/or thermal loading, while the through-thickness loading and twisting are not included. Both loading cases can be considered by describing the boundary conditions properly. The through-thickness loading can be introduced by imposing the traction conditions at the top and bottom surfaces. The twisting moment is a resultant of the in-plane shear stress and distance, thus by giving the shear stress a suitable distribution in the crack plane, the twisting moment could be obtained by integrating the product of the shear stress and distance. After adding these two loading cases to the present work, most practical loading conditions are covered.

- **Stress Analysis of Laminated Cylindrical Shells**

The present state space method can be extended to evaluate stress transfer near free edges and circumferential cracks in laminated cylindrical shells. Because the geometry of cylindrical shells is more complex than that of plates, the radial coordinates will be introduced to the coefficient matrix [G] to reflect the shape effects. As a result the state space equation turns from the present linear time-invariant system into a linear time-varying system, which is considered more difficult to solve. However, a successive approximation method (Soldatos and Hadjigeorgiou, 1990) can be used to solve the time-varying system.

- **Stiffness degradation in nonsymmetric angle-ply laminates.**

In this thesis, the assessment of thermoelastic property degradation due to transverse cracking is limited to cross-ply and symmetric angle-ply laminates. The nonsymmetric angle-ply laminates are out of the scope of the present study. The reason is that the present stress analysis for angle-ply laminates does not consider bending and twisting conditions, so that the in-plane and out-of-plane coupling coefficients in the compliance matrix can not be determined. If the stress analysis under bending and twisting is provided, the stiffness degradation in nonsymmetric angle-ply laminates can be calculated following the similar procedure in Chapter 6.

- **Stiffness degradation in the through thickness direction.**

In the present study, the constitutive equations of laminates in the Classical Laminate Theory were used to assess the stiffness degradation due to transverse cracking.

Because of the restrictions of the Classical Laminate Theory, only the in-plane stiffness can be determined. The present stress analysis is three dimensional, it is capable of evaluating the through thickness stress and displacement components. Therefore, if a three dimensional relationship between the overall deformations and the applied loading is used, the stiffness degradation in the through thickness direction can then be determined.

- **Statistical model to predict the transverse cracking**

It has been noted in Chapter 7 that the transverse cracking process was assumed to be a crack density increment in an idealised uniform state. However the transverse cracks usually initiate at the flaws of composite materials. Since in reality the distribution of these flaws is stochastic, therefore a statistical approach is typically used to model the nondeterministic progressive transverse cracking. The integration of the present energy based method and a statistical approach is able to predict the uncertainties during the transverse cracking process.

- **Ply cracking in multiple orientations**

The present stress transfer model was developed for transverse cracking that occurs in a single orientation. In order that the present method has opportunities for much wider practical applications, so that ply cracking in any plies of the laminate should be modelled. Extending the current state space method to evaluate stress transfer in laminates with ply cracking in multiple orientations will have mathematical difficulties when describing the complex geometry and boundary conditions. However by using a homogenisation approach, it is feasible to predict the effective thermoelastic properties and stress-strain behaviour in such a laminate. The method will involve homogenising the effective properties of each cracked layer into an equivalent homogeneous ply having the same properties. The present stress analysis can be used to predict the equivalent properties of each discretely cracked layer. Then the entire properties of the damaged laminate will be determined by an undamaged laminate analysis.

- **Effects of delamination**

The present work focuses on the study of intralaminar material discontinuities, i.e. free edges and transverse cracks. Delamination is an interlaminar material discontinuity which often occurs at free edges and crack tips. The state space method

can be extended to investigate the delamination problem by employing a general spring-layer model, which has been adopted by Chen et al. (2003) to analyse a simply supported, cross-ply laminate with bonding imperfections. The general spring-layer model will introduce an interfacial transfer matrix to the present state space equation. This will not bring too much computational complexes and the present solution procedure can be followed to study the stress field near delamination.

References

Abdelrahman W G and Nayfeh A H 1999 Stress transfer and stiffness reduction in orthogonally cracked laminates *Mechanics of Materials* **31** 303-16

Adolfsson E and Gudmundson P 1997 Thermoelastic properties in combined bending and extension of thin composite laminates with transverse matrix cracks *International Journal of Solids and Structures* **34** 2035

Allen D H, Harris C E and Groves S E 1987a A thermomechanical constitutive theory for elastic composites with distributed damage. I. Theoretical development *International Journal of Solids and Structures* **23** 1301-18

Allen D H, Harris C E and Groves S E 1987b A thermomechanical constitutive theory for elastic composites with distributed damage. II. Application to matrix cracking in laminated composites *International Journal of Solids and Structures* **23** 1319-38

Altus E, Rotem A and Shmueli M 1980 Free edge effect in angle ply laminates-a new three dimensional finite difference solution *Journal of Composite Materials* **14** 21

Amrutharaj G S, Lam K Y and Cotterell B 1996 Delaminations at the free edge of a composite laminate *Composites Part B:Engineering* **27** 475

Anderson T L 2005 *Fracture Mechanics: Fundamentals and Applications* (Boca Roton: CRC Press)

Bailey J E, Curtis P T and Parvizi A 1979 On the transverse cracking and longitudinal splitting behaviour of glass and carbon fibre reinforced epoxy cross ply laminates and the effect of Poisson and thermally generated strain *Proceedings of the Royal Society of London, Series A (Mathematical and Physical Sciences)* **366** 599-623

Bailey J E and Parvizi A 1981 On fiber debonding effects and the mechanism of tranverse-ply failure in cross-ply laminates of glass fiber/thermoset composites *Journal of Materials Science* **16** 649-59

Bauld N R, Jr., Goree J G and Tzeng L S 1985 A comparison of finite-difference and finite-element methods for calculating free edge stresses in composites *Computers and Structures* **20** 897

Becker W 1993 Closed-form solution for the free-edge effect in cross-ply laminates *Composite Structures* **26** 39

Becker W 1994 Closed-form analysis of the free edge effect in angle-ply laminates *Transactions of the ASME. Journal of Applied Mechanics* **61** 209

Berthelot J M 1997 Analysis of the transverse cracking of cross-ply laminates: a generalized approach *Journal of Composite Materials* **31** 1780

Berthelot J M and Le Corre J F 2000 Statistical analysis of the progression of transverse cracking and delamination in cross-ply laminates *Composites Science and Technology* **60** 2659-69

Berthelot J M, Leblond P, El Mahi A and Le Corre J F 1996 Transverse cracking of cross-ply laminates: Part 1. Analysis *Composites - Part A: Applied Science and Manufacturing* **27** 989

Bhaskar K, Varadan T K and Jacob C 2000 Free-edge Stresses in Laminated Cylindrical Shells due to Axisymmetric Transverse Loads *Journal of the Aeronautical Society of India* **52** 26-38

Carreira R P, Caron J F and Diaz Diaz A 2002 Model of multilayered materials for interface stresses estimation and validation by finite element calculations *Mechanics of Materials* **34** 217

Chen W-H and Huang T-F 1989 Three dimensional interlaminar stress analysis at free edges of composite laminate *Computers and Structures* **32** 1275

Chen W Q, Cai J B and Ye G R 2003 Exact solutions of cross-ply laminates with bonding imperfections *AIAA Journal* **41** 2244-50

Chen W Q and Kang Yong L 2004 Three-dimensional exact analysis of angle-ply laminates in cylindrical bending with interfacial damage via state-space method *Composite Structures* **64** 275-83

Cho M and Kim H S 2000 Iterative free-edge stress analysis of composite laminates under extension, bending, twisting and thermal loadings *International Journal of Solids and Structures* **37** 435

Cho M and Rhee S Y 2004 Optimization of laminates with free edges under bounded uncertainty subject to extension, bending and twisting *International Journal of Solids and Structures* **41** 227-45

Cho M and Yoon J-Y 1999 Free-edge interlaminar stress analysis of composite laminates by extended Kantorovich method *AIAA Journal* **37** 656

Davet J L and Destuynder P 1986 Free-edge stress concentration in composite laminates: a boundary layer approach *Computer Methods in Applied Mechanics and Engineering* **59** 129

DeRusso P M, Roy R J, Close C M and Desrochers A A 1998 *State Variables for Engineers* (New York: John Wiley & Sons, Inc.)

Diaz Diaz A, Caron J-F and Carreira R P 2002 Software application for evaluating interfacial stresses in inelastic symmetrical laminates with free edges *Composite Structures* **58** 195

Dong S B and Goetschel D B 1982 Edge effects in laminated composite plates *Transactions of the ASME. Journal of Applied Mechanics* **49** 129

Dvorak G J and Laws N 1987 Analysis of progressive matrix cracking in composite laminates. II. First ply failure *Journal of Composite Materials* **21** 309-29

Fan J and Ye J 1990a An exact solution for the statics and dynamics of laminated thick plates with orthotropic layers *International Journal of Solids and Structures* **26** 655-62

Fan J and Ye J 1990b A series solution of the exact equation for thick orthotropic plates *International Journal of Solids and Structures* **26** 773-8

Fan J and Zhang J 1993 In-situ damage evolution and micro/macro transition for laminated composites *Composites Science and Technology* **47** 107

Flaggs D L 1985 Prediction of tensile matrix failure in composite laminates *Journal of Composite Materials* **19** 29

Flaggs D L and Kural M H 1982 Experimental determination of the in situ transverse lamina strength in graphite/epoxy laminates *Journal of Composite Materials* **16** 103-16

Flanagan G 1994 An efficient stress function approximation for the free-edge stresses in laminates *International Journal of Solids and Structures* **31** 941

Fukunaga H, Chou T-W, Peters P W M and Schulte K 1984a Probabilistic failure strength analyses of graphite/epoxy cross-ply laminates *Journal of Composite Materials* **18** 339-56

Fukunaga H, Chou T-W, Schulte K and Peters P W M 1984b Probabilistic initial failure strength of hybrid and non-hybrid laminates *Journal of Materials Science* **19** 3546-53

Garrett K W and Bailey J E 1977 Multiple transverse fracture in 90° cross-ply laminates of a glass fibre-reinforced polyester *Journal of Materials Science* **12** 157

Gaudenzi P, Mannini A and Carbonaro R 1998 Multi-layer higher-order finite elements for the analysis of free-edge stresses in composite laminates *International Journal for Numerical Methods in Engineering* **41** 851

Griffith A A 1920 The phenomena of rupture and flow in solids *Philosophical Transactions of the Royal Society of London* **221** 163-98

Groves S E, Hams C, Highsmith A L, Allen D H and Norvell R G 1987 An experimental and analytical treatment of matrix cracking in cross-ply laminates *Experimental Mechanics* **27** 73-9

Gudmundson P and Alpman J 2000 Initiation and growth criteria for transverse matrix cracks in composite laminates *Composites Science and Technology* **60** 185

Gudmundson P and Zang W 1993 An analytic model for thermoelastic properties of composite laminates containing transverse matrix cracks *International Journal of Solids and Structures* **30** 3211

Han Y M and Hahn H T 1989 Ply cracking and property degradations of symmetric balanced laminates under general in-plane loading *Composites Science and Technology* **35** 377

Hashin Z 1985 Analysis of cracked laminates: a variatinoal approach *Mechanics of Materials* **4** 121

Hashin Z 1988 Thermal expansion coefficients of cracked laminates *Composites Science and Technology* **31** 247

Herakovich C T 1976 On thermal edge effects in composite laminates *International Journal of Mechanical Sciences* **18** 129

Herakovich C T 1989 *Handbook of Composites, Structure and Design,* ed C T Herakovich and Y M Tarnopol'SKII (Amsterdam: Elsevier) p 189

Herakovich C T 1998 *Mechanics of Fibrous Composites* (New York: John Wiley & Sons, Inc.)

Herakovich C T and Bargner H W, Jr. 1980 Finite element stress analysis of a notched coupon specimen for in-plane shear behaviour of composites *Composites* **11** 149

Herakovich C T, Nagarkar A and O'Brien D A 1979 Failure analysis of composite laminaes with free edges *TRRL Supplementary Report (Transport and Road Research Laboratory, Great Britain)* 53

Herakovich C T and O'Brien D A 1979 Failure analysis of an idealized composite damage zone. In: *Advanced Composites: Design and Applications*: Nat. Bur. Stand., Washington, DC, USA) p 242

Hirai I, Wang B P and Pilkey W D 1984 Efficient zooming method for finite element analysis *International Journal for Numerical Methods in Engineering* **20** 1671

Hsu P W and Herakovich C T 1977 Edge effects in angle-ply composite laminates *Journal of Composite Materials* **11** 422

Icardi U and Bertetto A M 1995 An evaluation of the influence of geometry and of material properties at free edges and at corners of composite laminates *Computers and Structures* **57** 555

Im S 1990 Asymptotic stress field around a crack normal to the ply-interface of an anisotropic composite laminate *International Journal of Solids and Structures* **26** 111

Irwin G R 1957 Analysis of stresses and strains near end of crack traversing plate *American Society of Mechanical Engineers -- Transactions -- Journal of Applied Mechanics* **24** 361-4

Isakson G and Levy A 1971 Finite-element analysis of interlaminar shear in fibrous composites *Journal of Composite Materials* **5** 273

Joffe R, Krasnikovs A and Varna J 2001 COD-based simulation of transverse cracking and stiffness reduction in $[S/90_n]_s$ laminates *Composites Science and Technology* **61** 637-56

Joffe R and Varna J 1999 Analytical modeling of stiffness reduction in symmetric and balanced laminates due to cracks in 90° layers *Composites Science and Technology* **59** 1641

Kanninen M F and Popelar C H 1985 *Advanced Fracture Mechanics* (Oxford: Oxford University Press)

Kant T and Swaminathan K 2000 Estimation of transverse/interlaminar stresses in laminated composites - a selective review and survey of current developments *Composite Structures* **49** 65

Kashtalyan M and Soutis C 2000 Stiffness degradation in cross-ply laminates damaged by transverse cracking and splitting *Composites - Part A: Applied Science and Manufacturing* **31** 335

Kassapoglou C and Lagace P A 1986 An efficient method for the calculation of interlaminar stresses in composite materials *Transactions of the ASME. Journal of Applied Mechanics* **53** 744

Kassapoglou C and Lagace P A 1987 Closed form solutions for the interlaminar stress field in angle-ply and cross-ply laminates *Journal of Composite Materials* **21** 292

Khdeir A A and Reddy J N 1990 Influence of edge conditions on the modal characteristics of cross-ply laminated shells *Computers and Structures* **34** 817-26

Khdeir A A and Reddy J N 1997 An exact solution for the bending of thin and thick cross-ply laminated beams *Composite Structures* **37** 195-203

Kim H S, Cho M and Kim G-I 2000 Free-edge strength analysis in composite laminates by the extended Kantorovich method *Composite Structures* **49** 229

Kim J Y and Hong C S 1991 Three-dimensional finite element analysis of interlaminar stresses in thick composite laminates *Computers and Structures* **40** 1395

Kim T and Atluri S N 1994 Interlaminar stresses in composite laminates under out-of-plane shear/bending *AIAA Journal* **32** 1700

Kollár L P and Springer G S 2003 *Mechanics of Composite Structures* (Cambridge: Cambridge University Press)

Krishna Murty A V and Hari Kumar H K 1989 Modelling of symmetric laminates under extension *Composite Structures* **11** 15

Laws N and Dvorak G J 1988 Progressive transverse cracking in composite laminates *Journal of Composite Materials* **22** 900-16

Leblond P, El Mahi A and Berthelot J M 1996 2D and 3D numerical models of transverse cracking in cross-ply laminates *Composites Science and Technology* **56** 793

Lee J W and Daniel I M 1990 Progressive transverse cracking of crossply composite laminates *Journal of Composite Materials* **24** 1225-43

Lekhnitskii S G 1963 *Theory of elasticity of an anisotropic elastic body* (San Francisco: Holden Day)

Lessard L B, Schmidt A S and Shokrieh M M 1996 Three-dimensional stress analysis of free-edge effects in a simple composite cross-ply laminate *International Journal of Solids and Structures* **33** 2243

Li S, Reid S R and Soden P D 1994 A finite strip analysis of cracked laminates *Mechanics of Materials* **18** 289

Lim S-H and Li S 2005 Energy release rates for transverse cracking and delaminations induced by transverse cracks in laminated composites *Composites Part A (Applied Science and Manufacturing)* **36** 1467-76

Lim S G and Hong C S 1989 Effect of transverse cracks on the thermomechanical properties of cross-ply laminated composites *Composites Science and Technology* **34** 145-62

Lin C-C, Hsu C-Y and Ko C-C 1995 Interlaminar stresses in general laminates with straight free edges *AIAA Journal* **33** 1471

Liu S and Nairn J A 1992 The formation and propagation of matrix microcracks in cross-ply laminates during static loading *Journal of Reinforced Plastics and Composites* **11** 158-78

Manders P W, Chou T W, Jones F R and Rock J W 1983 Statistical analysis of multiple fracture in $0^{\circ}/90^{\circ}/0^{\circ}$ glass fibre/epoxy resin laminates *Journal of Materials Science* **18** 2876-89

Mao K M and Sun C T 1991 Refined global-local finite element analysis method *International Journal for Numerical Methods in Engineering* **32** 29

McCartney L N 1992 Theory of stress transfer in a 0°-90°-0° cross-ply laminate containing a parallel array of transverse cracks *Journal of the Mechanics and Physics of Solids* **40** 27

McCartney L N 1996 Stress transfer mechanics for ply cracks in general symmetric laminates. In: *NPL CMMT(A)50*: (Nat. Phys. Lab., Teddington, UK) p 47

McCartney L N 1998 Predicting transverse crack formation in cross-ply laminates *Composites Science and Technology* **58** 1069-81

McCartney L N 2000 Model to predict effects of triaxial loading on ply cracking in general symmetric laminates *Composites Science and Technology* **60** 2255

McCartney L N 2001 Laminates: Physical and Mechanical Behavior. In: *Encyclopedia of Materials: Science and Technology,* ed R W C K. H. Jürgen Buschow, Merton C. Flemings, Bernard Ilschner (print), Edward J. Kramer, Subhash Mahajan, and Patrick Veyssière (Oxford: Elsevier) p 4383

McCartney L N 2002 Prediction of ply crack formation and failure in laminates *Composites Science and Technology* **62** 1619-31

McCartney L N 2004 Effect of mixed mode loading on ply crack development in laminated composites: theory and application. Nat. Phys. Lab., Teddington, UK) p iv+22

McCartney L N 2005 Energy-based prediction of progressive ply cracking and strength of general symmetric laminates using an homogenisation method *Composites Part A (Applied Science and Manufacturing)* **36** 119-28

McCartney L N and Pierse C 1997a Stress transfer mechanics for multiple ply laminates for axial loading and bending. In: *Proceedings of the 11th International Conference on Composite Materials,* (14-18, July 1997. Gold Coast, Australia)

McCartney L N and Pierse C 1997b Stress transfer mechanics for multiple ply laminates subject to bending. In: *NPL Report CMMT(A) 55*: (Nat. Phys. Lab., Teddington, UK) p 41

McCartney L N, Schoeppner G A and Becker W 2000 Comparison of models for transverse ply cracks in composite laminates. (Anaheim, CA, USA: Elsevier) pp 2347-59

Mittelstedt C and Becker W 2004 Interlaminar stress concentrations in layered structures: part I - a selective literature survey on the free-edge effect since 1967 *Journal of Composite Materials* **38** 1037

Mittelstedt C and Becker W 2006 Fast and reliable analysis of free-edge fields in a thermally loaded composite strip by a layerwise laminate theory *International Journal for Numerical Methods in Engineering* **67** 747-70

Moler C and Van Loan C 1978 Nineteen dubious ways to compute the exponential of a matrix *SIAM Review* **20** 801-36

Moler C and Van Loan C 2003 Nineteen dubious ways to compute the exponential of a matrix, twenty-five years later *SIAM Review* **45** 3-49

Nairn J A 1989 The strain energy release rate of composite microcracking: a variational approach *Journal of Composite Materials* **23** 1106

Nairn J A 2000 *Comprehensive Composite Materials,* ed Z Anthony Kelly and Carl (Oxford: Pergamon) p 403

Nairn J A and Hu S 1992 The formation and effect of outer-ply microcracks in cross-ply laminates: a variational approach *Engineering Fracture Mechanics* **41** 203-21

Nairn J A, Hu S and Bark J S 1993 A critical evaluation of theories for predicting microcracking in composite laminates *Journal of Materials Science* **28** 5099-111

Nguyen V-T and Caron J-F 2006 A new finite element for free edge effect analysis in laminated composites *Computers and Structures* **84** 1538-46

Nosier A and Bahrami A 2006 Free-edge stresses in antisymmetric angle-ply laminates in extension and torsion *International Journal of Solids and Structures* **43** 6800

Ochiai S, Osamura K, Peters P W M and Schulte K 1992 Estimation of the 90° ply strength distribution and shear lag parameter from multiple transverse cracking in graphite-epoxy cross-ply laminates *Materials Science & Engineering A (Structural Materials: Properties, Microstructure and Processing)* **A158** 65-70

Pagano N J 1974 On the calculation of interlaminar normal stress in composite lamiante *Journal of Composite Materials* **8** 65

Pagano N J 1978a Free edge stress fields in composite laminates *International Journal of Solids and Structures* **14** 401

Pagano N J 1978b Stress fields in composite laminates *International Journal of Solids and Structures* **14** 385

Pagano N J and Pipes R B 1971 The influence of stacking sequence on laminate strength *Journal of Composite Materials* **5** 50

Pagano N J and Pipes R B 1973 Some observations on the interlaminar strength of composite laminates *International Journal of Mechanical Sciences* **15** 679

Pagano N J and Soni S R 1983 Global-local laminate variational model *International Journal of Solids and Structures* **19** 207

Parvizi A, Garrett K W and Bailey J E 1978 Constrained cracking in glass fibre-reinforced epoxy cross-ply laminates *Journal of Materials Science* **13** 195-201

Peters P W M 1984 The strength distribution of 90° plies in 0/90/0 graphite-epoxy laminates *Journal of Composite Materials* **18** 545-56

Pipes R B and Pagano N J 1970 Interlaminar stresses in composite laminates under uniform axial extension *Journal of Composite Materials* **4** 538

Praveen G N and Reddy J N 1998 Transverse matrix cracks in cross-ply laminates: stress transfer, stiffness reduction and crack opening profiles *Acta Mechanica* **130** 227

Puppo A H and Evensen H A 1970 Interlaminar shear in laminated composites under generalised plane stress **4** 204

Rebiere J L, Maatallah M N and Gamby D 2001 Initiation and growth of transverse and longitudinal cracks in composite cross-ply laminates *Composite Structures* **53** 173-87

Reddy J N 1987 Generalization of two-dimensional theories of laminated composite plates *Communications in Applied Numerical Methods* **3** 173

Reifsnider K L and Highsmith A 1982 The relationship of stiffness changes in composite laminates to fracutre-related damage mechanisms. (Bethlehem, Pa, USA: Martinus Nijhoff Publ, The Hague, Neth) pp 279-90

Reifsnider K L and Jamison R 1982 Fracture of fatigue-loaded composite laminates *International Journal of Fatigue* **4** 187

Reifsnider K L and Talug A 1980 Analysis of fatigue damage in composite laminates *International Journal of Fatigue* **2** 3

Reissner E 1950 On a variational theorem in elasticity *Journal of Mathematics and Physics* **29** 90

Rose C A and Herakovich C T 1993 An approximate solution for interlaminar stresses in composite laminates *Composites Engineering* **3** 271

Salamon N J 1978 Interlaminar stresses in a layered composite laminate in bending *Fibre Science and Technology* **11** 305

Schapery R A 1969 On characterizatino of nonlinear viscoelastic materials **9** 295-310

Schoeppner G A and Pagano N J 1998 Stress fields and energy release rates in cross-ply laminates *International Journal of Solids and Structures* **35** 1025

Sirivedin S, Fenner D N, Nath R B and Galiotis C 2006 Viscoplastic finite element analysis of matrix crack propagation in model continuous-carbon fibre/epoxy composites *Composites Part A: Applied Science and Manufacturing* **37** 1922-35

Smith P A and Ogin S L 1999 On transverse matrix cracking in cross-ply laminates loaded in simple bending *Composites - Part A: Applied Science and Manufacturing* **30** 1003

Soldatos K P and Hadjigeorgiou V P 1990 Three-dimensional solution of the free vibration problem of homogeneous isotropic cylindrical shells and panels *Journal of Sound and Vibration* **137** 369-84

Spilker R L and Chou S C 1980 Edge effects in symmetric composite laminates: importance of satisfying the traction-free-edge condition *Journal of Composite Materials* **14** 2

Sun Z, Luo J-J and Daniel I M 2003 A novel statistical model for predicting matrix cracking in high temperature polymer composite laminates *Journal of Materials Science* **38** 3029-35

Suvorov A P and Dvorak G J 2001 Optimized fiber prestress for reduction of free edge stresses in composite laminates *International Journal of Solids and Structures* **38** 6751

Tahani M and Nosier A 2003a Edge effects of uniformly loaded cross-ply composite laminates *Materials & Design* **24** 647-58

Tahani M and Nosier A 2003b Free edge stress analysis of general cross-ply composite laminates under extension and thermal loading *Composite Structures* **60** 91-103

Tahani M and Nosier A 2003c Three-dimensional interlaminar stress analysis at free edges of general cross-ply composite laminates *Materials & Design* **24** 121-30

Takeda N and Ogihara S 1994 In situ observation and probabilistic prediction of microscopic failure processes in CFRP cross-ply laminates *Composites Science and Technology* **52** 183-95

Talreja R 1985 Transverse cracking and stiffness reduction in composite laminates *Journal of Composite Materials* **19** 355

Talreja R 1986 Stiffness properties of composite laminates with matrix cracking and interior delamination. (Haifa, Israel) p 751

Talreja R 1996 *Progress in durability analysis of composite systems,* ed A Cardon, *et al.* (Rotterdam: A.A. Balkema) pp 117-29

Talreja R, Yalvac S, Yats L D and Wetters D G 1992 Transverse cracking and stiffness reduction in cross ply laminates of different matrix toughness *Journal of Composite Materials* **26** 1644-63

Tang S 1975 A boundary layer theory. I. Laminated composites in plane stress *Journal of Composite Materials* **9** 33

Tang S and Levy A 1975 A boundary layer theory. II. Extension of laminated finite strip *Journal of Composite Materials* **9** 42

Tarn J-Q 2002a A state space formalism for anisotropic elasticity Part I: Rectilinear anistropy *International Journal of Solids and Structures* **39** 5143-55

Tarn J-Q 2002b A state space formalism for anisotropic elasticity. Part II: Cylindrical anisotropy *International Journal of Solids and Structures* **39** 5157-72

Tarn J-Q 2002c A state space formalism for piezothermoelasticity *International Journal of Solids and Structures* **39** 5173-84

Tarn J Q and Wang Y M 2001 Laminated composite tubes under extension, torsion, bending, shearing and pressuring: A state space approach *International Journal of Solids and Structures* **38** 9053-75

Tay T E and Lim E H 1996 Analysis of composite laminates with transverse cracks *Composite Structures* **34** 419-26

Thompson D M and Griffin O H J 1990 2-D to 3-D global/local finite element analysis of cross-ply composite laminates *Journal of Reinforced Plastics and Composites* **9** 492-502

Tong J, Guild F J, Ogin S L and Smith P A 1997a On matrix crack growth in quasi-isotropic laminates - I. Experimental investigation *Composites Science and Technology* **57** 1527

Tong J, Guild F J, Ogin S L and Smith P A 1997b On matrix crack growth in quasi-isotropic laminates - II. Finite element analysis *Composites Science and Technology* **57** 1537

Tounsi A, Amara K H and Benzair A 2005 Transverse cracking and elastic properties reduction in hygrothermal aged cross-ply laminates *Materials Science & Engineering A (Structural Materials: Properties, Microstructure and Processing)* **396** 369-75

Valisetty R R and Rehfield L W 1985 New ply model for interlaminar stress analysis. (Pittsburgh, PA, USA: ASTM, Philadelphia, PA, USA) p 52

Varna J and Berglund L 1991 Multiple transverse cracking and stiffness reduction in cross-ply laminates *Journal of Composites Technology and Research* **13** 97

Varna J and Berglund L A 1994 Thermo-elastic properties of composite laminates with transverse cracks *Journal of Composites Technology and Research* **16** 77

Varna J, Joffe R, Akshantala N V and Talreja R 1999 Damage in composite laminates with off-axis plies *Composites Science and Technology* **59** 2139-47

Varna J, Joffe R and Talreja R 2001 A synergistic damage-mechanics analysis of transverse cracking $[\pm\theta/90_4]_s$ laminates *Composites Science and Technology* **61** 657-65

Wang A S D and Crossman F W 1977 Some new results on edge effect in symmetric composite laminates *Journal of Composite Materials* **11** 92

Wang A S D and Crossman F W 1978 Calculation of edge stresses in multi-layer laminates by sub-structuring *Journal of Composite Materials* **12** 76

Wang A S D, Kishore N N and Li C A 1985 Crack development in graphite-epoxy cross-ply laminates under uniaxial tension *Composites Science and Technology* **24** 1

Wang S S and Choi I 1982a Boundary-layer effects in composite laminates. I. Free-edge stress singularities *Transactions of the ASME. Journal of Applied Mechanics* **49** 541

Wang S S and Choi I 1982b Boundary-layer effects in composite laminates. II. Free-edge stress solutions and basic characteristics *Transactions of the ASME. Journal of Applied Mechanics* **49** 549

Wang Y-M, Tarn J-Q and Hsu C-K 2000 State space approach for stress decay in laminates *International Journal of Solids and Structures* **37** 3535-53

Wanthal S P and Yang H T Y 1991 Three-dimensional finite element formulations for laminated plates *Journal of Reinforced Plastics and Composites* **10** 330

Webber J P H and Morton S K 1993 An analytical solution for the thermal stresses at the free edges of laminated plates *Composites Science and Technology* **46** 175

Whitcomb J D, Raju I S and Goree J G 1982 Reliability of the finite element method for calculating free edge stresses in composite laminates *Computers and Structures* **15** 23

Whitcomb J D and Woo K 1993a Application of iterative global/local finite-element analysis. Part 1: linear analysis *Communications in Numerical Methods in Engineering* **9** 745

Whitcomb J D and Woo K 1993b Application of iterative global/local finite-element analysis. Part 2: geometrically non-linear analysis *Communications in Numerical Methods in Engineering* **9** 757

Whitney J M 2000 Effective elastic constants of bidirectional laminates containing transverse ply cracks *Journal of Composite Materials* **34** 954

Whitney J M 2001 Effective thermo-elastic constants of angle-ply laminates containing 90 degree ply cracks *Journal of Composite Materials* **35** 1373

Xu L-Y 1995 Influence of stacking sequence on the transverse matrix cracking in continuous fiber crossply laminates *Journal of Composite Materials* **29** 1337

Yang H T Y and He C C 1994 Three-dimensional finite element analysis of free edge stresses and delamination of composite laminates *Journal of Composite Materials* **28** 1394

Ye J 2001a Decay rate of edge effects in cross-ply-laminated hollow cylinders *International Journal of Mechanical Sciences* **43** 455-70

Ye J 2001b Edge effects in angle-ply laminated hollow cylinders *Composite Structures* **52** 247-53

Ye J 2002 *Laminated Composite Plates and shells: 3D Modelling* (London: Springer)

Ye J and Soldatos K P 1994a Three-dimensional stress analysis of orthotropic and cross-ply laminated hollow cylinders and cylindrical panels *Computer Methods in Applied Mechanics and Engineering* **117** 331-51

Ye J and Soldatos K P 1994b Three-dimensional vibration of laminated cylinders and cylindrical panels with symmetric or antisymmetric cross-ply lay-up *Composites Engineering* **4** 429-44

Ye J and Soldatos K P 1995 Three-dimensional buckling analysis of laminated composite hollow cylinders and cylindrical panels *International Journal of Solids and Structures* **32** 1949-62

Ye J and Soldatos K P 1996 Three-dimensional vibration of laminated composite plates and cylindrical panels with arbitrarily located lateral surfaces point supports *International Journal of Mechanical Sciences* **38** 271-81

Ye J Q and Sheng H Y 2003 Free-edge effect in cross-ply laminated hollow cylinders subjected to axisymmetric transverse loads *International Journal of Mechanical Sciences* **45** 1309-26

Ye J Q, Sheng H Y and Qin Q H 2004 A state space finite element for laminated composites with free edges and subjected to transverse and in-plane loads *Computers & Structures* **82** 1131-41

Ye J Q and Soldatos K P 1997 Three-dimensional vibrations of cross-ply laminated hollow cylinders with clamped edge boundaries *Journal of Vibration and Acoustics, Transactions of the ASME* **119** 317-23

Yi S 1997 Finite element analysis of free edge stresses in non-linear viscoelastic composites under uniaxial extension, bending and twisting loadings *International Journal for Numerical Methods in Engineering* **40** 4225-38

Yi S, Ahmad M F and Hilton H H 1998 Nonlinear viscoelastic stress singularities near free edges of unsymmetrically laminated composites *International Journal of Solids and Structures* **35** 3221

Yin W L 1994a Free-edge effects in anisotropic laminates under extension bending and twisting, part I; A stress-function-based variational approach *Journal of Applied Mechanics, Transactions ASME* **61** 410

Yin W L 1994b Free-edge effects in anisotropic laminates under extension, bending, and twisting, part II: eigenfunction analysis and the results for symmetric laminates *Journal of Applied Mechanics, Transactions ASME* **61** 416

Yin W L 1994c Simple solutions of the free-edge stresses in composite laminates under thermal and mechanical loads *Journal of Composite Materials* **28** 573

Yin W L 1997 Effect of temperature gradient on the free-edge interlaminar stresses in multi-layered structures *Journal of Composite Materials* **31** 2460

Yokozeki T, Aoki T and Ishikawa T 2002 Transverse crack propagation in the specimen width direction of CFRP laminates under static tensile loadings *Journal of Composite Materials* **36** 2085

Yokozeki T, Aoki T and Ishikawa T 2005 Consecutive matrix cracking in contiguous plies of composite laminates *International Journal of Solids and Structures* **42** 2785

Yuan F G and Selek M C 1993 Transverse cracking and stiffness reduction in composite laminates *Journal of Reinforced Plastics and Composites* **12** 987

Zhang C and Yeh H-Y 1998 A variational approach for straight edge effect stresses in laminated composites *Composite Structures* **43** 243

Zhang D, Ye J and Lam D 2006a Ply cracking and stiffness degradation in cross-ply laminates under biaxial extension, bending and thermal loading *Composite Structures* **75** 121-31

Zhang D, Ye J and Lam D Submission Free-edge and Ply Cracking Effect in Angle-ply Laminated Composites subjected to In-plane Loads *Journal of Engineering Mechanics, Transactions ASCE*

Zhang D, Ye J and Sheng H Y 2006b Free-edge and ply cracking effect in cross-ply laminated composites under uniform extension and thermal loading *Composite Structures* **76** 314-25

Zhang D, Ye J Q and Lam D Accepted Properties degradation induced by transverse cracks in general symmetric laminates *International Journal of Solids and Structures*

Zhang J, Fan J and Soutis C 1992 Analysis of multiple matrix cracking in $[\pm\theta_m/90_n]_s$ composite laminates. 1. In-plane stiffness properties *Composites* **23** 291

Zhang J and Herrmann K P 1998 Application of the laminate plate theory to the analysis of symmetric laminates containing a cracked mid-layer *Computational Materials Science* **13** 195

Zhang J and Herrmann K P 1999 Stiffness degradation induced by multilayer intralaminar cracking in composite laminates *Composites - Part A: Applied Science and Manufacturing* **30** 683

Appendices

Appendix A. Stiffness Coefficients of an Orthotropic Lamina

In Eq. (4.2), the stiffness coefficients C_{ij} can be expressed by the engineering constants as follows

$$C_{11} = \frac{1-\nu_{23}\nu_{32}}{E_2 E_3 \Delta} \tag{A.1}$$

$$C_{12} = \frac{\nu_{21}+\nu_{31}\nu_{23}}{E_2 E_3 \Delta} = \frac{\nu_{12}+\nu_{32}\nu_{13}}{E_1 E_3 \Delta} \tag{A.2}$$

$$C_{13} = \frac{\nu_{31}+\nu_{21}\nu_{32}}{E_2 E_3 \Delta} = \frac{\nu_{13}+\nu_{12}\nu_{23}}{E_1 E_2 \Delta} \tag{A.3}$$

$$C_{22} = \frac{1-\nu_{13}\nu_{31}}{E_1 E_3 \Delta} \tag{A.4}$$

$$C_{23} = \frac{\nu_{32}+\nu_{12}\nu_{31}}{E_1 E_3 \Delta} = \frac{\nu_{23}+\nu_{21}\nu_{13}}{E_1 E_2 \Delta} \tag{A.5}$$

$$C_{33} = \frac{1-\nu_{12}\nu_{21}}{E_1 E_2 \Delta} \tag{A.6}$$

$$C_{44} = G_{23} \tag{A.7}$$

$$C_{55} = G_{13} \tag{A.8}$$

$$C_{66} = G_{12} \tag{A.9}$$

$$\Delta = \frac{1-\nu_{12}\nu_{21}-\nu_{23}\nu_{32}-\nu_{31}\nu_{13}-2\nu_{21}\nu_{32}\nu_{13}}{E_1 E_2 E_3} \tag{A.10}$$

where E_1, E_2 and E_3 denote the orthotropic moduli of an lamina relative to the x, y, and z directions, respectively; G_{23}, G_{13} and G_{12} are the orthotropic shear moduli in the y-z, x-z and x-y planes, respectively; v_{ij} is the Poisson's ratio for strain in the j direction when stressed in the i direction.

Appendix B. Stiffness Coefficients of an Off-axis Lamina

In Eq. (5.2), the stiffness coefficients of an off-axis lamina (Fig. 5.1) whose fibre direction makes an angle θ with the x direction can be expressed as

$$C'_{11} = C_{11}\cos^4\theta + C_{22}\sin^4\theta + 2(C_{12} + 2C_{66})\sin^2\theta\cos^2\theta \tag{B.1}$$

$$C'_{12} = (C_{11} + C_{22} - 4C_{66})\sin^2\theta\cos^2\theta + C_{12}(\sin^4\theta + \cos^4\theta) \tag{B.2}$$

$$C'_{13} = C_{13}\cos^2\theta + C_{23}\sin^2\theta \tag{B.3}$$

$$C'_{16} = (C_{11} - C_{12} - 2C_{66})\sin\theta\cos^3\theta + (C_{12} - C_{22} + 2C_{66})\sin^3\theta\cos\theta \tag{B.4}$$

$$C'_{22} = C_{11}\sin^4\theta + 2(C_{12} + 2C_{66})\sin^2\theta\cos^2\theta + C_{22}\cos^4\theta \tag{B.5}$$

$$C'_{23} = C_{13}\sin^2\theta + C_{23}\cos^2\theta \tag{B.6}$$

$$C'_{26} = (C_{11} - C_{12} - 2C_{66})\sin^3\theta\cos\theta + (C_{12} - C_{22} + 2C_{66})\sin\theta\cos^3\theta \tag{B.7}$$

$$C'_{36} = (C_{13} - C_{23})\sin\theta\cos\theta \tag{B.8}$$

$$C'_{44} = C_{44}\cos^2\theta + C_{55}\sin^2\theta \tag{B.9}$$

$$C'_{45} = (C_{55} - C_{44})\sin\theta\cos\theta \tag{B.10}$$

$$C'_{55} = C_{44}\sin^2\theta + C_{55}\cos^2\theta \tag{B.11}$$

$$C'_{66} = (C_{11} + C_{22} - 2(C_{12} + C_{66}))\sin^2\theta\cos^2\theta + C_{66}(\sin^4\theta + \cos^4\theta) \tag{B.12}$$

Appendix C. List of My Publications

Zhang D, Ye J and Lam D 2006a Ply cracking and stiffness degradation in cross-ply laminates under biaxial extension, bending and thermal loading *Composite Structures* **75** 121-31

Zhang D, Ye J and Sheng H Y 2006b Free-edge and ply cracking effect in cross-ply laminated composites under uniform extension and thermal loading *Composite Structures* **76** 314-25

Zhang D, Ye J and Lam D Submission Free-edge and Ply Cracking Effect in Angle-ply Laminated Composites subjected to In-plane Loads *Journal of Engineering Mechanics, Transactions ASCE*

Zhang D, Ye J Q and Lam D Accepted Properties degradation induced by transverse cracks in general symmetric laminates *International Journal of Solids and Structures*